Fabrication and Characterisation of Degradable Biosynthetic Hydrogels for Cell Encapsulation: Development of A New Method for Protein Incorporation

by

Khoon S. Lim

A Thesis submitted for the Degree of Doctor of Philosophy

Graduate School of Biomedical Engineering

University of New South Wales

March 2014

PLEASE TYPE

THE UNIVERSITY OF NEW SOUTH WALES
Thesis/Dissertation Sheet

Surname or Family name: LIM

First name: Shen Khoon Other name/s:

Abbreviation for degree as given in the University calendar: PhD

School: Graduate School of Biomedical Engineering Faculty: Engineering

Title: Fabrication and characterisation of degradable biosynthetic hydrogels for cell encapsulation: Development of a new method for protein incorporation.

Abstract 350 words maximum: (PLEASE TYPE)

Biosynthetic hydrogels which have tailorable physical properties as well as the desired biological attributes to support cellular interaction have emerged as potential biomaterials for cell encapsulation. These hydrogels are normally fabricated by incorporating biological polymers into a synthetic hydrogel network. However, long term use of these matrices requires the biological molecules to be covalently bound into the network. This stable integration can be achieved by chemically modifying the biological polymer with short linear polymer chains, such as poly(ethylene glycol) (PEG), or functional moieties like acrylate and methacrylates. However, these chemical functionalisation processes may impose degradation and denaturation of the biological molecules, as well as disrupting the bioactive side groups that are required for cellular interactions.

Therefore, the overall aim of this research is to covalently incorporate biological molecules into synthetic hydrogels without the need of prior chemical modification. A visible light polymerisation system consisting of ruthenium and persulphate that was previously shown to crosslink proteins through their phenolic residues was employed. It was shown that by grafting phenolic containing moieties, such as tyramine onto poly(vinyl alcohol) (PVA-Tyr), the resultant PVA-Tyr was able to be crosslinked in a similar manner to proteins using the ruthenium/persulphate system. The physical properties of the hydrogels were tailorable through varying the nominal macromer concentration. Non-chemically modified gelatin was successfully covalently integrated into the PVA-Tyr hydrogels, without affecting the base characteristics (mass loss, swelling and degradation profile) of PVA-Tyr, but also retained the bioactivity to support cells in 2D culture (fibroblasts, endothelial, Schwann cells).

Fibroblasts were also encapsulated inside the PVA-Tyr gels, where it was showed that the presence of the antioxidative protein, sericin was needed to ensure survival of the cells during the photoencapsulation process. However, both sericin and gelatin were required synergistically to facilitate long-term 3D cell growth, proliferation and function. The encapsulated cells were able to form clusters and interconnected networks, as well as remained metabolically active after 21 days in culture. This work has demonstrated a novel method to covalently incorporate proteins in their native state into synthetic hydrogels.

Declaration relating to disposition of project thesis/dissertation

I hereby grant to the University of New South Wales or its agents the right to archive and to make available my thesis or dissertation in whole or in part in the University libraries in all forms of media, now or here after known, subject to the provisions of the Copyright Act 1968. I retain all property rights, such as patent rights. I also retain the right to use in future works (such as articles or books) all or part of this thesis or dissertation.

I also authorise University Microfilms to use the 350 word abstract of my thesis in Dissertation Abstracts International (this is applicable to doctoral theses only).

Signature

Witness

03/07/14

Date

The University recognises that there may be exceptional circumstances requiring restrictions on copying or conditions on use. Requests for restriction for a period of up to 2 years must be made in writing. Requests for a longer period of restriction may be considered in exceptional circumstances and require the approval of the Dean of Graduate Research.

FOR OFFICE USE ONLY Date of completion of requirements for Award:

THIS SHEET IS TO BE GLUED TO THE INSIDE FRONT COVER OF THE THESIS

ORIGINALITY STATEMENT

'I hereby declare that this submission is my own work and to the best of my knowledge it contains no materials previously published or written by another person, or substantial proportions of material which have been accepted for the award of any other degree or diploma at UNSW or any other educational institution, except where due acknowledgement is made in the thesis. Any contribution made to the research by others, with whom I have worked at UNSW or elsewhere, is explicitly acknowledged in the thesis. I also declare that the intellectual content of this thesis is the product of my own work, except to the extent that assistance from others in the project's design and conception or in style, presentation and linguistic expression is acknowledged.'

Signed 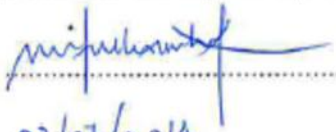

Date 03/07/2014

COPYRIGHT STATEMENT

'I hereby grant the University of New South Wales or its agents the right to archive and to make available my thesis or dissertation in whole or part in the University libraries in all forms of media, now or here after known, subject to the provisions of the Copyright Act 1968. I retain all proprietary rights, such as patent rights. I also retain the right to use in future works (such as articles or books) all or part of this thesis or dissertation.
I also authorise University Microfilms to use the 350 word abstract of my thesis in Dissertation Abstract International (this is applicable to doctoral theses only).
I have either used no substantial portions of copyright material in my thesis or I have obtained permission to use copyright material; where permission has not been granted I have applied/will apply for a partial restriction of the digital copy of my thesis or dissertation.'

Signed 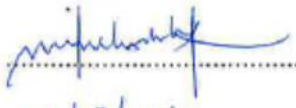

Date 03/07/2014

AUTHENTICITY STATEMENT

'I certify that the Library deposit digital copy is a direct equivalent of the final officially approved version of my thesis. No emendation of content has occurred and if there are any minor variations in formatting, they are the result of the conversion to digital format.'

Signed 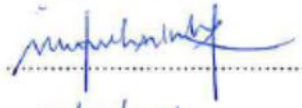

Date 03/07/2014

Abstract

Biosynthetic hydrogels which have tailorable physical properties as well as the desired biological attributes to support cellular interaction have emerged as potential biomaterials for cell encapsulation. These hydrogels are normally fabricated by incorporating biological molecules into a synthetic hydrogel network. However, long term use of these matrices requires the biological molecules to be covalently bound into the network. This stable integration can be achieved by chemically modifying the biological molecules with short linear polymer chains, such as poly(ethylene glycol) (PEG), or functional moieties like acrylate and methacrylates. However, these chemical functionalisation processes may impose degradation and denaturation of the biological molecules, as well as disrupting the bioactive side groups that are required for cellular interactions.

Therefore, the overall aim of this research is to covalently incorporate biological molecules into synthetic hydrogels without the need of prior chemical modification. A visible light polymerisation system consisting of ruthenium and persulphate that was previously shown to crosslink proteins through their phenolic residues was employed. It was shown that by grafting phenolic containing moieties, such as tyramine onto poly(vinyl alcohol) (PVA-Tyr), the resultant PVA-Tyr was able to be crosslinked in a similar manner to proteins using the ruthenium/persulphate system. The physical properties of the hydrogels were tailorable through varying the nominal macromer concentration. Non-chemically modified gelatin was successfully covalently integrated into the PVA-Tyr hydrogels, without affecting the base characteristics (mass loss,

swelling and degradation profile) of PVA-Tyr, but also retained the bioactivity to support cells in 2D culture (fibroblasts, endothelial, Schwann cells).

Fibroblasts were also encapsulated inside the PVA-Tyr gels, where it was showed that the presence of the antioxidative protein, sericin was needed to ensure survival of the cells during the photoencapsulation process. However, both sericin and gelatin were required synergistically to facilitate long-term 3D cell growth, proliferation and function. The encapsulated cells were able to form clusters and interconnected networks, as well as remained metabolically active after 21 days in culture.

This work has demonstrated a novel method to covalently incorporate proteins in their native state into synthetic hydrogels. The resultant PVA-Tyr/protein biosynthetic hydrogels showed great promise as tissue engineering matrices.

Acknowledgements

I wish to dedicate this thesis to my **father**, for his constant support and endless encouragements that have always kept me going in finishing this journey. I wish I could share the joy of completing this thesis with him, and may his soul rest in peace. To my **mother**, thanks for always being there for me as my listener whenever I seek to vent my frustrations. My **uncle (peh deh)** and **aunt (peh nin)**, thanks for the unconditional support that helped paved my way to complete this thesis. Not to forget my lovely **siblings (and siblings in law)**, and **cousins**, who not only took good care of me, but also brought dozens of beloved **nephews and nieces** into my life. Thank you to my supervisor, **Penny Martens** for her guidance and encouragement, especially during (many) moments when I think this PhD journey will never end. I would also like to thank my co-supervisor, **Laura Poole-Warren** for all the fruitful discussions and good advices. All the GSBME members and ex-members: **Yogi, Helene, Jenny, Cara, Eman, Naat, Bonny, Josef, Rylie, Bill, MoonSun, Johnson, Brooke, Sally, Adry, Steve, Liyuan, Aaron, Rachelle, Wenqi, Cherry, Kain, Chris**, and **Anthony**, thanks for all the "SHORT" coffee breaks that kept my sanity throughout this journey. My friends: **Macy, Lin, Angie, Wei** and **Lita**, thanks for hanging out with me whenever and wherever. I would not have made it without you guys. Lastly, thanks to everyone who helped me in making this thesis a reality.

"一切有为法，如梦幻泡影；如露亦如电，应作如是观"

"All phenomena are like a dream, an illusion, a bubble and a shadow;
Like dew or a flash of lightning; Thus we shall perceive them"

List of Publications

Journal Publications

1. **Lim, K. S.**; Alves, M.-H.; Poole-Warren, L. A.; Martens, P. J. *Covalent incorporation of non-chemically modified gelatin into degradable PVA-tyramine hydrogels*. Biomaterials, 2013.34(29): p. 7097-7105;
2. **Lim, K. S.**; Kundu, J.; Reeves, A.; Poole-Warren, L. A.; Kundu, S. C.; Martens, P. J. *The influence of silkworm species on cellular interactions with novel PVA-silk sericin hydrogels.* Macromolecular Biosciences, 2012. **12**(3): p.322-332
3. Cheong, G. L. M.; **Lim, K. S.**; Jakubowicz, A.; Martens, P.; Poole-Warren, L., Green, R. A. *Conductive hydrogels with tailored bioactivity for implantable electrode coatings*. Acta Biomaterialia, 2014. **10**:p.1216-1226
4. Peterson, M. B.; Le-Masurier, S. P.; **Lim**, **K. S.**; Hook, J. M.; Martens, P. J.; Granville, A. M. *Incorporation of 5-Hydroxyindazole into the Self-Polymerization of Dopamine for Novel Copolymer Synthesis*. Macromolecular Rapid Communications, 2013. **35**:291-297

Conference Proceeding

1. Green, R. A.; **Lim, K. S**.; Henderson, W.; Hassarati, R.; Martens, P.; Poole-Warren, L. A.; Lovell, N. Living electrodes: *Tissue engineering the neural interface*. Proceedings of the 35th Annual International Conference of the IEEE Engineering in Medicine and Biology Society. 2013. Osaka, Japan.

Conference Presentations

1. **Lim, K. S.**, Alves, M.-H., Ramaswamy, Y., Poole-Warren, L., Martens, P. *Combination of sericin and gelatin facilitates cellular function in novel degradable PVA-phenol hydrogels.* 22nd Annual Conference of the Australasian Society for Biomaterials and Tissue Engineering. 2013. Adelaide, Australia

2. **Lim, K. S.**, Alves, M.-H., Ramaswamy, Y., Poole-Warren, L., Martens, P.. *Covalent incorporation of unmodified, native proteins into synthetic hydrogels for cell encapsulation*. 3rd International Nanomedicine Conference. 2012. Sydney, Australia

3. **Lim, K. S.**, Alves, M.-H., Ramaswamy, Y., Poole-Warren, L., Martens, P. *Visible light photopolymerization system: A novel approach to fabricate PVA hydrogels*. 3rd World Congress on Medical Physics and Biomedical Engineering. 2012. Beijing, China

4. **Lim, K. S.**, Alves, M.-H., Ramaswamy, Y., Poole-Warren, L., Martens, P. *Covalent incorporation of unmodified, natrive proteins into synthetic hydrogels*. 9th World Biomaterials Congress. 2012. Chengdu, China

5. **Lim, K. S.**, Alves, M.-H., Ramaswamy, Y., Poole-Warren, L., Martens, P. *Exploration of a visible light initiating system for co-polymerising bio-synthetic hydrogels*. 3rd International Congress on Biohydrogels. 2011. Florence, Italy

6. **Lim, K. S.**, Alves, M.-H., Ramaswamy, Y., Poole-Warren, L., Martens, P. *Visible light intiatiated crosslinking for integration of unmodified proteins into synthetic hydrogel networks*. 25th European Conference on Biomaterials. 2013. Madrid, Spain.

7. Poole-Warren, L., **Lim, K. S.**, Young, C., Cheng, J., Nafea, E., Martens, P. *Biosynthetic hydrogel cell encapsulation systems*. 7th International Conference on Materials for Advanced Technologies. 2013. Singapore

8. Poole-Warren, L., Martens, P., Goding, J., **Lim, K. S.**, Lovell, N., Green, R. *Tissue engineered electrodes for improved neural tissue communication*. TERMIS AP Annual Conference. 2013. Shanghai & Wuzhen, China.

9. Martens, P., **Lim, K. S.**, Alves, M.-H., Poole-Warren, L. *Characterisation of degradable PVA-Tyramine hydrogels for tissue engineering applications*. 12th International Conference on Frontiers of Polymers and Advanced Materials. 2013. Auckland, New Zealand.

Table of contents

List of Figures

List of Table

Chapter 1

Introduction

1.1. Research motive

Biosynthetic hydrogels are potential biomaterials as cell encapsulation matrices. However, current approaches for stable integration of biological molecules into synthetic hydrogel networks require chemical modification processes that may cause denaturation and degradation of the biological molecule, thus affecting its bioactivity. Therefore, this thesis focuses on evaluating the feasibility of covalent incorporation of biological molecules into a synthetic polymer network without the need of prior chemical modification.

Tissue engineering (TE) aims to regenerate, repair and replace dysfunctional or deceased tissue/organ and is an attractive solution to the current issues faced with organ transplantation [1, 2]. Most research strategies for engineering a functional tissue involve the encapsulation of cells within an artificial structure (i.e., TE scaffold) that supports 3D cellular function. It is hypothesised that the encapsulated cells are able to secrete extracellular matrix (ECM) and remodel the artificial environment to form regenerated tissue that is structurally and biochemically similar to native *in vivo* tissues. It has been previously proposed in the literature that the ideal scaffold should be able to provide structural and mechanical support to the encapsulated cells, as well as having the required biofunctionality to induce cell growth, proliferation and ECM secretion within the 3D network [2]. Moreover, the degradation rate of the scaffold should also match the rate of ECM secretion from cells to ensure formation of engineered tissue with similar functionality as native *in vivo* tissues [1]. Although several biomaterials have emerged as potential TE scaffolds, no scaffolds to date have successfully facilitated the formation of functional tissues that can be used to replace a deceased organ. Therefore, the focus of this thesis is

to develop and characterise a new material in an attempt to fulfil the design criteria of an ideal cell encapsulation scaffold.

Hydrogels, which are a class of polymers that are capable of absorbing water, have arose as potential candidates for cell encapsulation matrices due to their similarity to the native ECM surrounding cells in the body [3]. Moreover, this highly hydrated environment was also reported to allow good permeability and diffusion of nutrients and oxygen through the network to the encapsulated cells, as well as waste products released from the cells to the environment [3]. A number of parameters such as macromer cytocompatibility, crosslinking process, physical and mechanical properties, as well as the hydrogel's degradation rate are to be accounted for in selecting the suitable material to fabricate hydrogels for cell encapsulation purposes. It has been previously reported that both natural and synthetic polymers have been employed to fabricate hydrogels that may satisfy these design considerations [2].

Hydrogels fabricated from naturally occurring polymers, such as the ECM proteins and glycosaminoglycans, often have good biological attributes that can promote cellular interactions with the hydrogels. However, they are usually mechanically weak and chemically unstable when used *in vivo* [4]. Moreover, the variations between each batch of natural polymers also lead to inconsistency in sample preparations [1]. On the other hand, hydrogels made from synthetic polymers are advantageous due to the consistent structural composition and high mechano-chemical stability *in vivo*. Other advantages of synthetic hydrogels include tailorable physical and mechanical properties, as well as degradation rate [5]. However, synthetic polymers lack biological recognition sites which are vital

for cellular processes such as proliferation and differentiation. Hence, biosynthetic hydrogels which are fabricated from using synthetic polymers as a platform to tailor the bulk physical properties of the hydrogel, and then combined with biological molecules to impart biofunctionality, have been proposed to address this problem.

To date, several biological molecules such as polysaccharides, proteins, peptides and growth factors have been integrated into synthetic hydrogels to promote cell viability, growth and proliferation within the gel. This incorporation can be done by physically blending the biological molecules into the synthetic hydrogels, or covalently co-polymerising the biological and synthetic polymers. However, physically blending leads to leaching of the biologics in a short period of time leading to rapid loss in the biosynthetic hydrogel's bioactivity [6]. Therefore, in order to maintain the bioactivity of the gels over a longer period of time, the biological molecules are preferred to be covalently crosslinked within the synthetic hydrogel network.

In the literature, the two most common methods used to fabricate covalent biosynthetic hydrogels are the Michael-type addition and photopolymerisation. Both of these techniques require chemically grafting functional moieties such as thiols, acrylates, methacrylates and vinyl sulfones, or linear synthetic polymers such as poly(ethylene glycol) onto the biological molecule, to allow co-polymerisation with the synthetic polymer [7-10]. However, these chemical modification processes may induce denaturation and degradation of the biological molecules [7, 8, 11]. Moreover, the functional groups grafted may also disrupt the original side groups on the biological

molecules that are required for bioactivity [7, 12]. Therefore, there is a need to develop a system where biological molecules can be covalently incorporated into synthetic hydrogels without the need of chemical modification.

1.2. Aims of thesis

The focus of this thesis was to investigate a new method for the covalent incorporation of native biological molecules into synthetic hydrogels. This focus addresses the hypothesis that non-chemically modified biological molecules such as proteins, growth factors and cytokines can be co-polymerised with synthetic hydrogels using a crosslinking system that has only been traditionally applied to protein-protein crosslinking. Proteins are chosen as the model for biological molecules in this thesis. In addition, the retention of the biological activity of the proteins will be verified and the ability of the resultant biosynthetic hydrogels to promote survival and function of encapsulated cells will be investigated. For this purpose, poly(vinyl alcohol) was chosen as the synthetic base and the proteins gelatin and sericin were chosen as the biological molecules. The overall objectives of the thesis were to:

1. Synthesise a phenolated PVA system that can be crosslinked via a similar mechanism used for native protein-protein crosslinking.

2. Covalently incorporate non-chemically modified proteins into the PVA hydrogel and evaluate that the base characteristics of the base PVA network, as well as the biofunctionality of the incorporated proteins are not affected.

3. Evaluate the feasibility of encapsulating cells into the PVA/protein hydrogels as well as assessing the cell viability, growth and function post encapsulation.

These objectives were addressed through specific aims throughout the thesis, as described below:

The literature regarding the design consideration of using hydrogels as cell encapsulation matrices, as well as methods to incorporate biological molecules into synthetic hydrogels is reviewed in Chapter 2, highlighting the current issues in chemically modifying biological molecules.

Chapter 3 reports on fabricating PVA hydrogels using a photopolymerisation system (ruthenium/persulphate) that has only been traditionally applied to crosslink native proteins. The aim was to synthesise PVA with functional phenol moieties that can covalently crosslink with tyrosine groups on native proteins using the ruthenium/persulphate system.

Chapter 4 is focused on understanding the degradation behaviour of the fabricated PVA hydrogels. The aim was to establish the mechanism behind the hydrogel's degradation, as well as tailoring their degradation profile and mechanics.

In Chapter 5, studies in which non-chemically modified gelatin was incorporated into the PVA hydrogels are reported. The aim was to assess the effect of gelatin incorporation on the base characteristics of the PVA hydrogels. The biofunctionality of the PVA/gelatin hydrogels was also evaluated through 2D cell adhesion and 3D cell encapsulation studies.

Chapter 6 reports on incorporating antioxidants into the PVA hydrogels with the aim to protect the cells from radical damage during the photoencapsulation

process. The long term survival, proliferation and function of the encapsulated cells were studied.

Finally, Chapter 7 presents the conclusions from the thesis and makes recommendations for future work

Chapter 2

Literature Review

2.1. Introduction

Organ and tissue transplantation is often the only possible solution for patients suffering from end stage organ damage and failure. However, there are significant issues with the availability and compatibility of donated organs. It has been reported that 1 patient is added to the organ transplantation waiting list every 10 minutes in Australia, and the average waiting period is between 6 months to 4 years [13]. As a result, tissue engineering (TE) has been proposed as a solution to the problems faced with organ donation. Tissue engineering aims to repair or regenerate tissues in the laboratory to replace dysfunctional and/or damaged organs. To achieve this, cells are grown in artificial structures known as TE scaffolds that can either be directly implanted into specific sites to stimulate *in vivo* tissue repair and regeneration; or cultured *in vitro* for a period of time until the cells differentiate into targeted tissues and are then implanted; or just cultured *in vitro* without being implanted to produce model tissues that can be used for drug screening [14]. In the past, several biomaterial scaffolds have emerged as potential candidates for TE matrices. However, despite the potential, there has yet to be success with engineering a functional tissue to replace a damaged or non-functioning organ.

This chapter aims to address important requirements for fabricating tissue engineering matrices, with a specific focus on hydrogels. Different classes of hydrogels and their subsequent advantages and disadvantages as cell encapsulation matrices will be discussed. Comparison will also be done on various methods that have previously been used to encapsulate cells within the hydrogels. Moreover, different techniques applied to improve the hydrogels'

ability to support cellular functions and tissue growth within the gel will also be reviewed.

2.2. Hydrogels for cell encapsulation

Hydrogels are defined as hydrophilic polymeric networks which are capable of absorbing water in the amount from 10% to a thousand times their dry weight [1, 2, 15, 16]. It was previously described that the highly hydrated environment is similar to the native extracellular matrix (ECM) [9, 17, 18]. The aqueous environment has been speculated to provide good transport of nutrients to the cells and waste product from cells [1, 5, 16, 19, 20]. Moreover, drugs and other biological molecules such as peptides, proteins and oligonucleotides can be co-encapsulated with cells, and protected from immune reactions [19, 21-24]. Various hydrogel fabrication methods reported in the literature such as photolithography and microfluidics allow production of samples of controlled size and shape [2, 22, 25]. The overarching aim is to encapsulate the cells within the gel matrix, and induce secretion of ECM when the hydrogel degrades (Figure 2.1) [1]. It is desired that the newly formed tissue is similar to native tissues in terms of structure and biochemical aspects, and can function properly *in vivo*. In order to achieve this goal, a number of systems and strategies have been employed to design the ideal hydrogel matrix for tissue engineering applications. A number of design considerations that dictate the suitability of the materials as cell encapsulation matrices will be discussed in the following sections.

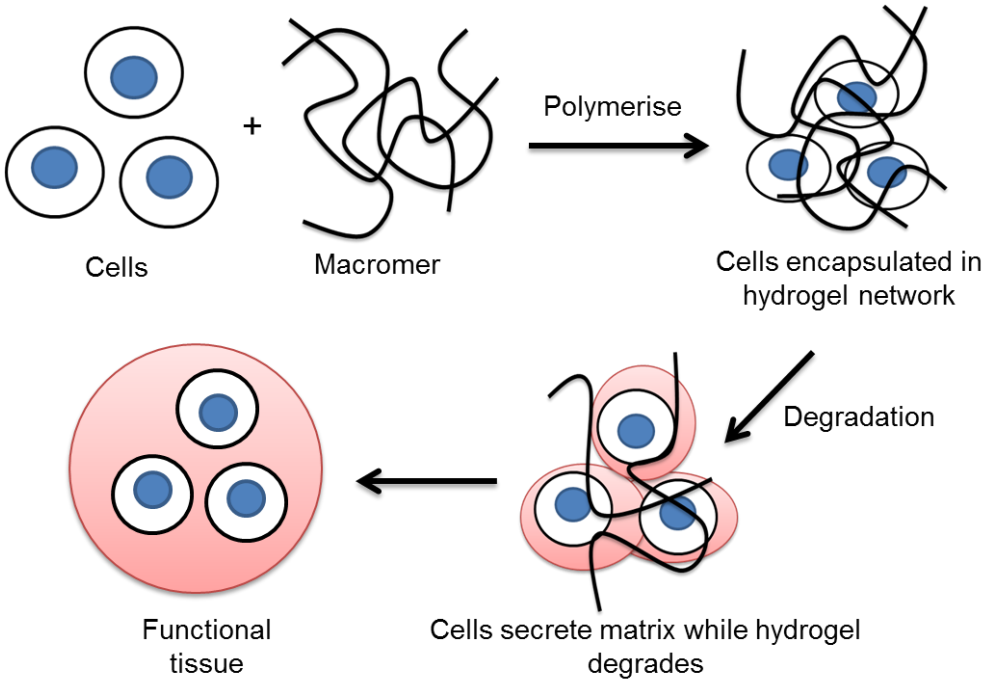

Figure 2.1: Overall scenario of tissue formation in cells encapsulated hydrogels (adapted from [1]).

2.2.1. Macromer cytocompatibility and biocompatibility

For many TE applications, cells are suspended in a macromer solution prior to encapsulation. Therefore, the macromers should be soluble in cell compatible aqueous solutions with appropriate pH and osmolality to prevent cell lysis [1]. The size of the macromers is also an important consideration, as previous studies have shown that low molecular weight macromers (<3kDa) are generally cytotoxic [26, 27]. Biocompatibility, which is defined as the ability of the material to perform with an appropriate host response in a specific situation is also a key consideration in the selection of materials used to fabricate the hydrogels. The gels must not cause any toxicity issues to the host tissue *in vivo* post implantation.

2.2.1. Hydrogel crosslinking methods

The crosslinking methods used to fabricate the hydrogels must also be carefully selected to not impose detrimental effects on the cells. Over the years, a variety of techniques have been developed to enable successful cell encapsulation into hydrogels. Depending on the nature of the bonds formed between the polymer chains, hydrogels can be classified as either physical or covalent gels. This section will focus on the different methods used for physical and covalent hydrogel fabrication, as well as the advantages and disadvantages of the derived techniques specifically related to cell encapsulation.

2.2.1.1. Physical hydrogels

Physicalhydrogels have either molecular entanglements, ionic or hydrogen bonds holding the network together. A common example is the crosslinking of alginate using divalent cations such as Ca^{2+} [28]. The interaction between the anionic groups on alginate with the added Ca^{2+} cations leads to ionotropic gelation (Figure 2.2) [29]. The similar principle behind mixing polymers of different charges was further applied for formation of complex coacervate gels (Figure 2.2). The ionic interaction between polyelectrolytes of opposite charges allows the formation of polyion complex gels. An example of this method is the gelation between polyanionic xanthan gum and polycationic chitosan [30, 31]. This crosslinking technique is generally simple and can be done at physiological conditions.

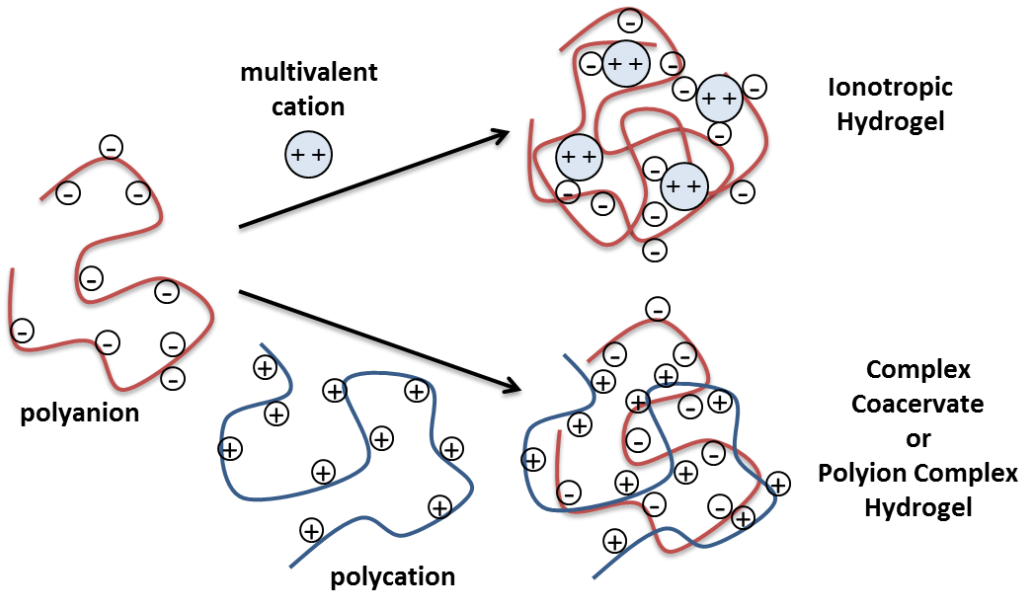

Figure 2.2: Schematic diagram of ionotropic gelation (top) and complex coacervation (bottom) (adapted from [16]).

Physical hydrogels can also be fabricated from formation of hydrogen bonds between polymeric chains during molecular aggregation. For instance, lowering the pH of a carboxylmethylcellulose (CMC) solution was able to induce gelation by promoting establishment of hydrogen bonds between the CMC chains [32, 33]. Similarly, reducing the temperature of gelatin solution beneath 35ºC successfully produced hydrogels due to the formation of hydrogen bonds between the gelatin aggregates [34]. Another method to induce physical crosslinking is freeze-thawing. During this process, gelation happens when microcrystals are introduced into the network over the numerous freeze-thaw cycles. Both poly(vinyl alcohol) (PVA) and xantham gum hydrogels were successfully fabricated using this method [35, 36]. Nevertheless, the freeze-thaw cycles are not cell compatible. Moreover, physical hydrogels in general are associated with weak chemical and mechanical stability due to the reversibility of the bonds formed. Hence, covalent hydrogels where covalent crosslinks

formed in the network are permanent and irreversible have been extensively researched as cell encapsulation matrices.

2.2.1.2. Covalent hydrogels

2.2.1.2.1. Chemical crosslinking

Covalently bound hydrogels can be fabricated through various chemical crosslinking methods. These techniques utilise crosslinking agents that are able to react with functional groups such as carboxyl, hydroxyl and amine on polymers, thus forming covalent crosslinks between the polymer chains. Crosslinking agents that have been reported in the past include aldehyde and epoxide. For instance, PVA (Figure 2.3), chitosan and collagen hydrogels have been fabricated using glutaraldehyde as the crosslinking agent [3, 37-40].

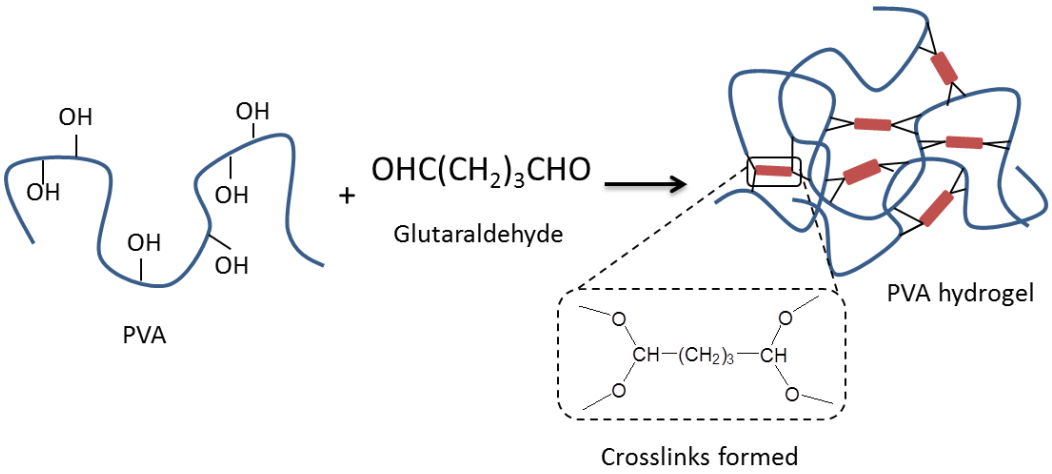

Figure 2.3: Schematic illustration of using glutaraldehyde to chemically crosslink PVA; Inset is the chemical structure of the crosslink formed.

Another example is the usage of epichlorohydrin to crosslink PVA, dextran and chitosan hydrogels [41-43]. However, the main issue with this technique is the toxicity of the chemical crosslinkers [44, 45]. Therefore, other chemical

crosslinking strategies that do not require toxic agents have been explored to encapsulate cells.

2.2.1.2.2. Michael type addition

In recent years, the Michael addition reactions are emerging as an advantageous chemical crosslinking method. The reaction is particularly suitable for preparation of cell laden hydrogels because it occurs in aqueous medium, at room temperature and physiological pH [46]. This system involves the addition of a nucleophile to a carbon-carbon double bond on an alkene [47, 48]. In terms of hydrogels, the addition reaction is often between nucleophilic thiolates and unsaturated ester bonds, where covalent thioether crosslinks are formed [6, 49-51]. However, thiolate nucleophiles normally form in slightly basic conditions (pH = 8.0) that are not suitable for cells. The unsaturated ester bonds reported to form covalent crosslinks with thiol groups in Michael addition reactions are methacrylates, acrylates and vinyl sulfones [6, 10, 52]. Hubbell and co-workers successfully encapsulated cells within hydrogels fabricated from multifunctional poly(ethylene glycol) (PEG) based macromers containing thiol and vinyl sulfone groups (Figure 2.4) [50, 53, 54].

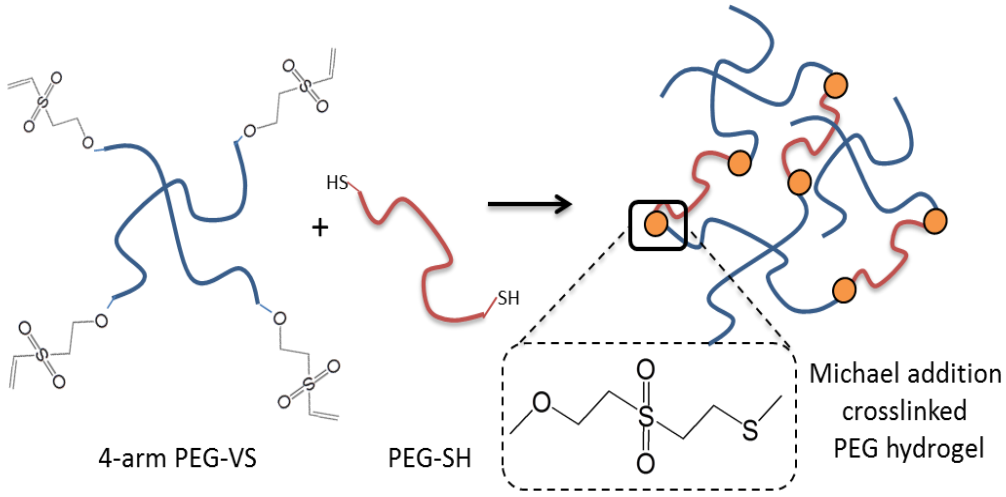

Figure 2.4: Michael-type addition crosslinked PEG hydrogel using 4-arm PEG-vinyl sulfone (PEG-VS) and PEG-thiol (PEG-SH); Inset is the structure of crosslinks formed.

These studies showed that the slightly basic environment and thiolate nucleophiles were not detrimental to cells [52, 55, 56]. Moreover, Lutolf et al. showed that altering the chemistry of groups adjacent to the thiols can increase thiolate nucleophiles formation at neutral pH [51]. Another advantage of this system is the ability to incorporate peptides or polysaccharides containing thiols, as well as degradable linkers into the gels. However, the gelation rates are typically slower compared to other systems, such as radical chain polymerisation. Thiols are also known to be chemically unstable [57]. They can easily dimerize upon contact with oxygen in the air, leading to disulfide bond formation [1, 58, 59].

2.2.1.2.3. Click hydrogels

"Click" reaction has also been developed as a new method to fabricate covalent hydrogels in recent years [57, 60-62]. The most well-known click

chemistry reaction is the Cu(I)-catalysed Huisgen cycloaddition, between an azide and alkyne to form a trizaole [63-65]. The advantages of this reaction include quantitative conversion, high specificity, and lack of side reactions with functional groups of biological molecules [61, 62]. It was also speculated that the distribution of crosslinks formed in "click" hydrogels are more organized [60]. Therefore, better control over the physical properties (mesh size, mechanics and swelling) can be obtained. The kinetics of this "click" reaction are relatively fast under physiological conditions. However, the major drawback of this reaction is the usage of copper (Cu(I)) as a catalyst, which is potentially toxic to cells [66, 67]. Recent advancements have resulted in copper free "click" reactions [68, 69]. One example is the "click" hydrogel formed from PEG tetraazide and polypeptides functionalised with di-fluorinated cyclooctyne (DIFO) moieties [68]. Cells encapsulated in these gels were shown to be viable after 24 hours [68]. However, the DIFO moieties require a multiple-step synthesis and are not commercially available. Another copper free "click" reaction is the formation of hydrazone bond between hydrazide and aldehyde groups. Hyaluronan (HA), dextran and PVA hydrogels have been successfully fabricated using this reaction [57, 62, 70, 71]. The major advantage of this system from a biomedical standpoint is the formation of water as the only by-product. Cell encapsulation studies further confirmed the cytocompatibility of the hydrazone "click" reactions. A study conducted by Alves et al. successfully created PVA gels crosslinked with hydrazone bonds (Figure 2.5), and showed that encapsulated fibroblasts remained viable after 14 days [57]. However, the stability of the hydrazone bonds *in vivo* has yet to be examined.

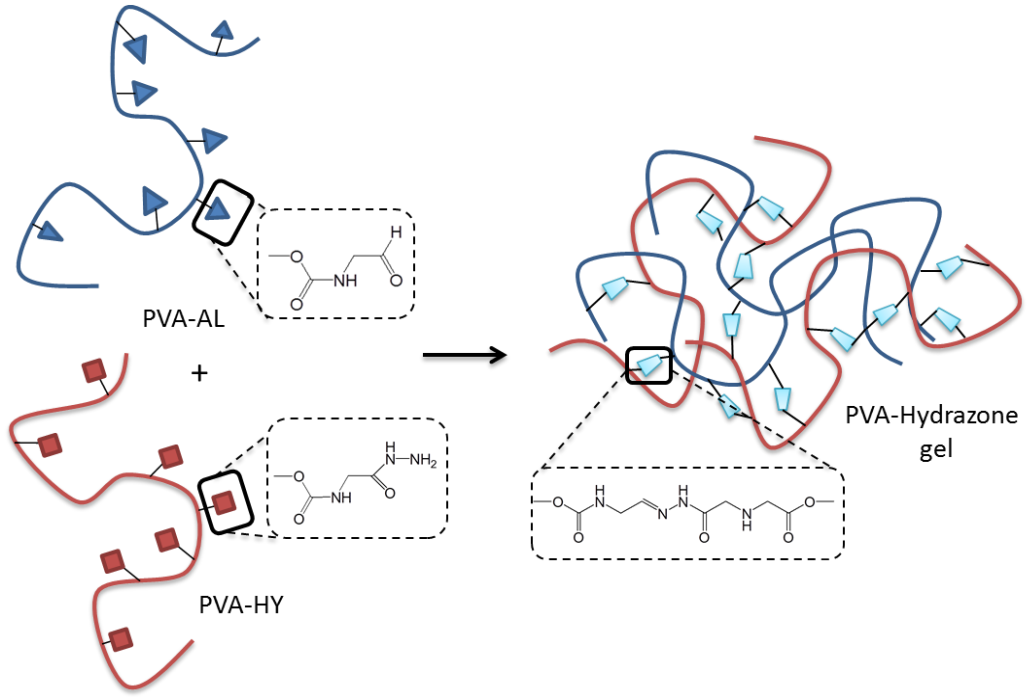

Figure 2.5: Schematic illustration of "click" PVA-Hydrazone hydrogels formed using PVA-Aldehyde (PVA-AL) and PVA-Hydrazide (PVA-HY); Insets are the structure of respective groups (adapted from [57]).

2.2.1.2.2. Radical chain polymerisation

Radical chain polymerisation involves grafting functional vinyl groups such as acrylates, methacrylates and fumarate onto polymer chains to create multifunctional macromers. In the presence of an initiator and under proper initiating conditions, radicals are generated then allowed to propagate through the vinyl groups forming kinetic chains that hold the network together (Figure 2.6).

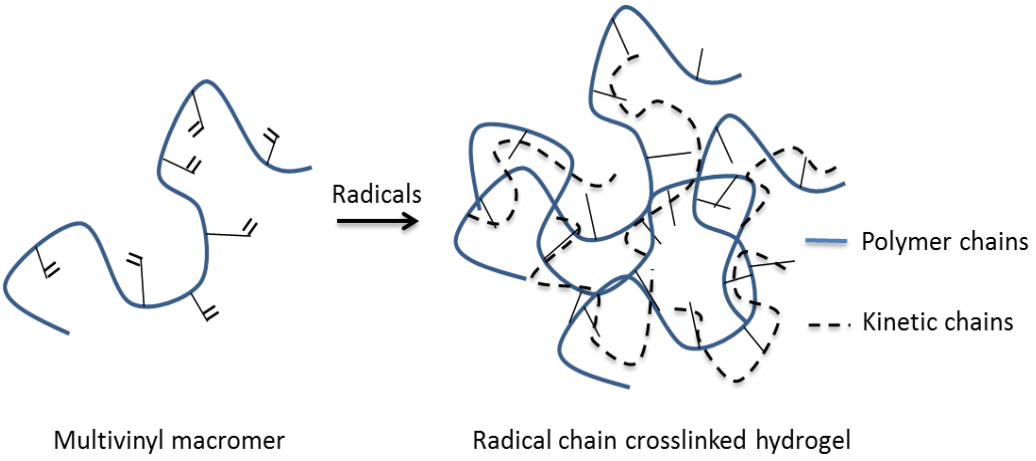

Figure 2.6: Schematic diagram of radical chain polymerisation used to crosslink multivinyl macromers into hydrogels.

However, the initiators used and radicals generated might be toxic to cells. Nicodemus and Bryant stated that the concentration of radicals generated is highly dependent on initiator size, chemistry, concentration, initiating conditions (thermal, redox, photo-polymerisastion) and polymerisation kinetics [1]. Redox-initiating systems typically consist of two components (oxidising and reducing agents) which catalyse free radical generation to initiate polymerisation [72]. The most well-known redox system used to make hydrogels is the ammonium persulfate (APS) and N,N,N',N'-tetramethylethylenediamine (TEMED) reaction, and has been used to fabricated PVA, PEG and chitosan hydrogels [72-75]. Although cells such as bone marrow stem cells and chondrocytes have been successfully encapsulated in these gels [74, 75], there are also controversial reports on the toxicity of this initiating system [73].

On the other hand, photoinitiating systems have been extensively studied to crosslink hydrogels in situ. This system mainly utilises a photoinitiator which decomposes into radicals in the presence of UV (200 - 400nm) or visible light

(400 – 800nm). This type of crosslinking is attractive for encapsulating cells due to being able to be performed at room or physiological temperature with fast curing rates, provision of spatial and temporal control over the polymerisation process, and minimal heat generation [3, 76-78]. However, the photoinitiators used might also be toxic. It was previously reported that the initiator concentration and chemistry influenced cell viability [79-81]. Burdick et al. reported that viability of fibroblasts encapsulated in photopolymerised HA gels decreased with increasing initiator concentration [82]. Williams et al. compared the effect of two kinds of photoinitiators, 2, 2-dimethoxy-2-phenylacetophenone (Irgacure 651) and 2-hydroxy-1-[4-(hydroxyethoxy)phenyl]-2-methyl-1-propanone (Irgacure 2959) in viability of bovine chondrocytes encapsulated in PVA hydrogels [79]. The chondrocytes, macromers and photoinitiators were mixed together then irradiated with UV light for 6 minutes. It was reported that cell survival was higher in samples fabricated using Irgacure 2959, whereas Irgacure 651 was detrimental to cells [79]. In contrary, Mann et al. showed that by reducing the irradiation time, rat aortic smooth muscle cells survived the photo-encapsulation process in PEG hydrogels using the same Irgacure 651 [81]. Regardless, another drawback of this system is the usage of UV light, which has been previously reported to impair the cell cytoskeleton and degrade cell-surface proteins [46]. Hence, visible light initiating polymerisations have been explored as cell encapsulation systems to minimise the effect of UV irradiation. Several visible light photoinitiators such as eosin-Y, triethanolamine and camphorquinone have been reported in the literature [83-85]. Shih and Lin demonstrated that human mesenchymal stem cells (hMSCs) and pancreatic mouse insulinoma cells (MIN6) were successfully encapsulated in PEG thiol-

norbornene hydrogels using eosin-Y as the photoinitiator, and remained viable after 14 days [85] . Overall, although photopolymerisation is a promising technique to encapsulate cells, the initiators and initiating conditions (light intensity and wavelength) must be carefully selected to minimise any adverse effects on cells.

2.2.2. Hydrogel properties

Once the cells are encapsulated in the gels, they should be able to differentiate, migrate, proliferate and secrete native ECM to remodel the artificial environment. However, these cellular functions are highly dependent on the physical and mechanical properties of the gels, as well as their degradation rate.

2.2.2.1. Physical and mechanical properties

Physical and mechanical properties such as mass loss, swelling, diffusion, compressive modulus and mesh size have been previously reported to affect the cell behaviour within the hydrogel. These properties are known to closely relate to the degree of crosslinking of the gel. It was previously demonstrated that an increase in crosslinking density results in gels with higher mechanical strengths, lower swelling capacity and smaller mesh size [6, 82, 86-89]. The hydrogels' physical and mechanical properties can also be tailored depending on the application of the final product. For example, hydrogels designed for cartilage repair must exhibit high compressive moduli due to the stresses exerted on native cartilage. Vilanueva et al. successfully encapsulated chondrocytes in PEG hydrogels of compressive moduli ~900kPa, which is in the range of native cartilage, by varying the crosslinking density [90].

The mesh size (as shown in Figure 2.7) which is a measure of the distance between crosslinks in the hydrogel is also highly influenced by the crosslinking density.

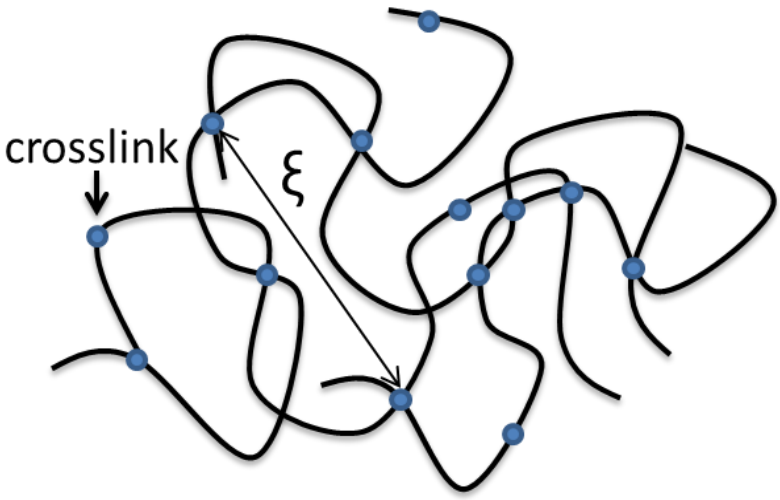

Figure 2.7: Schematic representation of a hydrogel network showing the macromolecular mesh (ξ).

As the crosslinking density increases, the mesh size decreases, forming hydrogels with tighter structure. These tight networks restricts the movement of polymeric chains hence decreases the amount of water uptake into the network. Burdick et al. reported formation of gels with smaller mesh size and lower swelling when the crosslinking density was increased [82]. Zustiak et al. also reported a decrease in the hydrogel swelling with increase in crosslinking density [6]. The mesh size also dictates the permeability of solute and nutrients to the encapsulated cells, as well as diffusion of tissue-specific molecules secreted by the cells [1, 5, 15, 18, 46]. Several studies have demonstrated that the physical and mechanical properties of the gels highly influence the rate and nature of tissue formation in the gels [86, 91, 92]. Hydrogels with high mechanical strength were reported to inhibit the ECM assembly and remodelling [93, 94].

2.2.2.2. Degradation

Another important factor for using hydrogels for tissue regeneration is the degradability of the hydrogels. The hydrogel is required to provide temporary mechanical support for the cells that will eventually be replaced by ECM secreted by the cells. During degradation, the mesh size increases, allowing cells to differentiate, migrate and secrete ECM to remodel the 3D environment for tissue formation. A study done by Cushing et al. showed that with sufficient degradation, hMSCs were able to migrate towards one another to form the cell-cell junctions that are required for osteogenesis [95]. Moreover, it is optimal for the hydrogel to degrade at the same rate as the tissue is regenerating, [1, 96-98]. Rapid degradation will cause the whole scaffold to break down before tissue is regenerated while slow degradation will result in excess ECM accumulation in the pericellular regions [1]. The degradation must also be tailored to allow homogenous addition of secreted ECM molecules to the network [92, 99].

Hydrogels can be either hydrolytically or enzymatically degradable depending on the type of degradable linkages incorporated within the network. Most hydrolytically degradable gels contain ester linkages such as lactic acid, caprolactone, fumarate and phosphoesters [18, 100-106]. Degradation normally occurs immediately upon the ester linkages being exposed to an aqueous environment. On the other hand, enzymatically degradable gels are mostly either fabricated from natural polymers or contain peptides that can be cleaved by proteases [52, 56, 58, 59, 107]. These enzymatically degradable peptides are mostly susceptible to plasmin or matrix metalloproteinases (MMPs) [108, 109]. The typical mass loss profile for a degradable hydrogel is shown in Figure 2.8, where mass loss increases with time until a point where there are not enough

linkages to maintain the hydrogel network, the whole matrix breaks down (reverse gelation) [1].

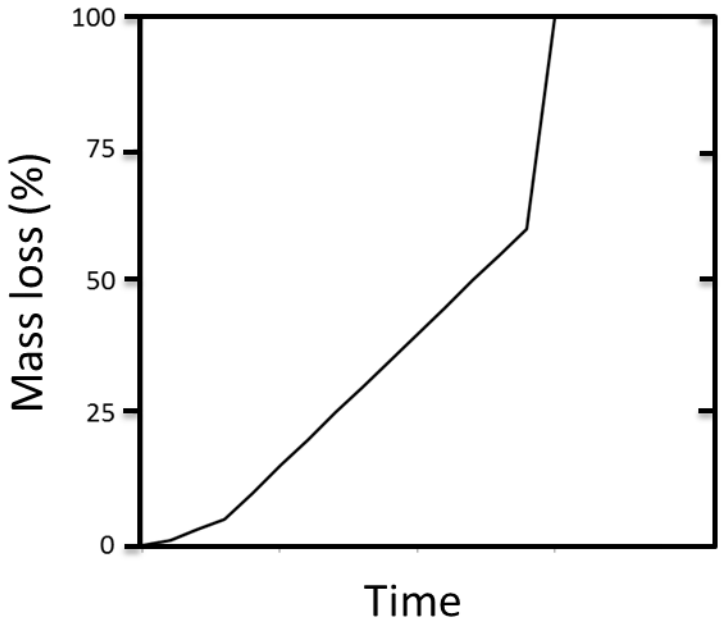

Figure 2.8: Mass loss vs degradation time for a degradable hydrogels (adapted from [1]).

The degradation rate of hydrolytically degradable gels is highly dependent on the amount of crosslinks in the network as well as the structure of the hydrogel. It was reported that varying the macromer concentration, amount of ester linkages, and crosslinking density can subsequently tailor the degradation rate [82, 89, 110, 111]. Moreover, the chemistry of other groups around the ester bonds in the hydrogel can also affect the degradation rate. For example, ester groups of poly(lactic acid) (PLA) were reported to degrade faster than poly(caprolactone) (PCL) [1, 112]. On the other hand, enzymatically degradable hydrogels can be cell mediated where the degradation rate is controlled by the encapsulated cells. For example, hydrogel formed from HA degrades in response to hyaluronidase which is secreted by the cells [58, 59, 107]. Other soluble

molecules in the environment where the hydrogels are incubated in can also influence the degradation kinetics. It was shown that the degradation of PEG-PLA hydrogels was significantly slower in cell culture media compared to phosphate buffered saline [89]. More interestingly, Bryant et al. showed that the presence of cells in the hydrogel slowed the degradation of PEG-PLA hydrogels. Since there are a lot of factors influencing the degradation kinetics of the hydrogels, each system needs to be studied and tailored individually to produce the ideal cell encapsulation scaffold. Table 2.1 below summarises degradable hydrogels that were reported in the literature, as well as cells encapsulated in them and their mode of degradation.

Table 2.1: Biodegradable hydrogels used for cell encapsulation

Macromer used	**Cells encapsulated**	**Degradation mode**	**Ref**
Chitosan grafted with lactid acid and methacrylate	Chondrocytes	Enzymatic (lysozyme) and hydrolytic	[75]
Alginate dialdehyde and gelatin	Hepatocytes	Hydrolytic	[113]
Chitosan-g-azidobenzoic acid and acryloyl-PEG-RGD	Cardiomyocytes	Enzymatic (lysozyme)	[114]
Thiol modified HA and PEG-diacrylate	Fibroblasts, adipocyte stem cells	Enzymatic	[115, 116]
Methacrylated HA	Chondrocytes, fibroblasts	Enzymatic (Hyaluronidase)	[117, 118]

Methacrylated chondroitin sulfate	Chondrocytes	Enzymatic (Chondroitinase)	[119, 120]
Styrenated gelatin	Chondrocytes	Enzymatic	[121]
Acrylated HA and PEG-$(SH)_4$	hMSCs	Enzymatic (Hyaluronidase)	[122]
Fibrinogen-*g*-PEG-acryloyl and PEG diacrylate	Bone marrow stromal cells	Enzymatic (plasmin, MMPs)	[123]
PCL-*b*-PEG-*b*-PCL dimethacrylate	Chondrocytes	Enzymatic (lipase)	[124]
PEG-(poly(glycerol succinic acid methacrylate$_4$))$_2$	Chondrocytes	Hydrolytic	[101]
Poly(lactide-co-ethylene oxide-co-fumarate) and MMP diacrylate	Bone marrow stem cells	Enzymatic (MMPs) and hydrolytic	[125]
PEG-diacrylate and fibrinogen fragments	Bovine aortic smooth muscle cells	Enzymatic	[123]
PVA-Aldehyde and PVA-Hydrazone	Fibroblasts	Hydrolytic	[57]
PEG-diacrylate and MMP degradable peptides	Human umbilical vein endothelial cells (HUVEC)	Enzymatic (MMPs)	[126]
PEG-vinyl sulfone and MMP degradable peptides	Mouse MSCs, embryonic carcinoma cells, smooth muscle cells, fibroblasts	Enzymatic (MMPs)	[127-130]

2.3. Hydrogel materials

In order to satisfy the design considerations outlined above, the materials used to fabricate the hydrogels must be carefully selected. Hydrogels can be made from natural and synthetic polymers. The earliest cell encapsulation systems were based on natural polymers such as alginate and chitosan which are derived from seaweed and crustaceans respectively [131, 132]. These materials have been reported to be structurally similar to the mammalian polysaccharide, but are not commonly found in the body and do not contain cell adhesive sequences or bioactive segments [133]. Therefore, research on cell encapsulation materials has expanded onto mammalian ECM molecules such as hyaluronan (HA), collagen, gelatin and fibrin, which have biologically active groups that can promote cell proliferation, migration and differentiation [1]. However, major issues associated with hydrogels fabricated from ECM molecules are the relatively weak mechanical strength, batch to batch variability, sterilisation difficulties, and immunogenicity [5, 22, 134]. On the other hand, synthetic polymers such as poly(ethylene glycol) (PEG) and poly(vinyl alcohol) (PVA) offer flexibility with synthesis and generally have better reproducibility and chemical stability [22, 134]. These synthetic polymers can be chemically tailored to produce the required properties for a specific application but lack bioactive sites for cellular interactions. Therefore, biosynthetic hydrogels which combine the benefits of synthetic and biological molecules are seen as the more promising materials to fabricate hydrogels for cell encapsulation.

The following sections will discuss the most common natural, synthetic and biosynthetic hydrogels used for cell encapsulation. The advantages and disadvantages of these hydrogels will be reviewed.

2.3.1. Natural hydrogels for cell encapsulation

Alginate, which is extracted from seaweed, is composed of linear polysaccharide block copolymers containing D-mannuronic acid and L-guluronic acid monomers [135]. The most commonly reported alginate hydrogels are based on ionotropic gelation, where the anionic carboxyl groups of alginate interacts with divalent cations in the solution (see section 2.2.1.1.). The first reported case of cell transplantation was published in 1980 by Lim and Sun using alginate-polylysine (PLL) carriers [131]. Since then, human liver carcinoma cells (HepG2), human acute T cells, pancreatic islets and fibroblasts have been successfully encapsulated in these gels [131, 136-138].

Similarly, chitosan which is obtained from partial deacetylation of chitin by alkaline hydrolysis at high temperature, is structurally similar to mammalian polysaccharides, making it attractive as a hydrogel material [135]. It is a linear polysaccharide composed of randomly distributed D-glucosamine and N-acetyl-D-glucosamine units [139]. It can be commercially obtained in low or high degrees of deacetylation, where the latter has higher hydrophobicity which was reported to promote better cell adhesion [140]. The most common sources used to obtain chitosan are the shells of crabs and shrimps. Chitosan itself is cationic and water soluble at mild acid conditions (pH<6) but becomes neutral and hydrophobic at physiological pH. By adding anionic molecules to chitosan solutions, ionotropic gelation leading to the formation of chitosan hydrogels occurs [141, 142]. The physical and swelling properties of these gels can be tailored by varying the concentration of the chitosan or anionic solution [15, 139]. Neonatal cardiomyocytes, chondrocytes and fetal mouse cortical cells have also been encapsulated in chitosan hydrogels [143-145].

The similarities between both alginate and chitosan are their ionic characteristics and feasibility to be crosslinked into hydrogels through ionotropic gelation. As ionotropic gelation happens at physiological conditions without the use of any toxic chemicals, cells encapsulated into these gels often have high viability. However, both alginate and chitosan are not commonly found in the body and do not contain the biological segments required to facilitate long term cell growth and proliferation. Therefore, biological molecules obtained from the ECM such as HA, collagen, gelatin and fibrin have spurred interest as hydrogel materials.

HA is a polysaccharide that can be found in most connective tissues of the body such as skin and cartilage [82, 135, 146]. It is composed of D-glucuronic acid and D-N-acetylglucosamine linked together via glycosidic bonds [135]. Its size ranges from 5000 to 20,000,000Da *in vivo* and can be easily reproduced from microbial fermentation of bacteria. HA has roles in many biological functions such as tissue formation, embryonic development, wound healing and angiogenesis [135, 147-149]. HA gels have encapsulated chondrocytes and development of cartilage tissue was observed within the scaffold [82, 117].

On the other hand, collagen is a protein with more than twenty nine distinct types identified to date. It is highly expressed in connective tissue of animals and is also the most abundant protein in mammals. Being the major component of the ECM, collagen has abundant RGD sequences that are required for cell attachment and migration. It is known to self-assemble into fibrillar structures and has been fabricated into hydrogels using this feature. Chondrocytes and fibroblasts have been successfully encapsulated in this kind of

collagen gel [4, 150]. However, collagen is only soluble in mild acidic conditions which may not be appropriate for hydrogel fabrication in the presence of cells.

Therefore, gelatin, which is a product of collagen hydrolysation, has also been studied as a substitute of collagen. One major advantage of gelatin is its water solubility, which enables cell encapsulation in physiological conditions [151]. Several cells such as human adipose derived stem cells, human umbilical vein endothelial cells, human mesenchymal stem cells, fibroblasts, chondrocytes, dorsal root ganglia and Schwann cells have been successfully encapsulated in gelatin based hydrogels [121, 151-156].

Other proteins that have been highlighted as potential materials for cell encapsulation are fibrin and fibrinogen. Both fibrin and fibrinogen play important roles in blood clotting, fibrinolysis, wound healing and angiogenesis [157]. Fibrin is a fibrous protein formed from fibrinogen and thrombin. Its precursor, fibrinogen exists in high concentration in the blood plasma. Once mixed with the protease thrombin, fibrinogen is converted to fibrin monomers, which then undergo end-to-end polymerisation to form a 3D network [158, 159]. Fibrin gels are attractive as cell encapsulation matrices because they have cell adhesive sequences as well as growth factors binding motifs [158-160]. The physical properties of fibrin gels can be controlled by varying the concentration of fibrinogen or thrombin during the crosslinking process [161]. It has been reported that neonatal cardiomyocytes, carotid artery derived cells, osteoblasts, chondrocytes, endothelial cells, human mesenchymal stem cells and mouse embryonic stem cells have been crosslinked in fibrin hydrogels [162-166].

2.3.1.1. Problems associated with natural hydrogels

Despite the advantages associated with natural hydrogels, there are also significant limitations. The high batch-to-batch variability of natural polymers leads to issues with reproducibility [1]. This is significant for alginate particularly as alginate derived from different sources were reported to have different viscosity and mechanical strength [167]. This phenomenon was believed to be due to the different ratios of mannuronic and guluronic acid in different kinds of alginate [167, 168]. Similarly, batch-to-batch variation was also observed in commercially available alginate and collagen which can potentially affect the performance and reproducibility of the hydrogels fabricated [168, 169].

Natural hydrogels are also generally mechanically weak. Alginate and chitosan hydrogels that are physically crosslinked through ionotropic gelation have been reported to have poor long term stability, due to the reversibility of the crosslinks formed [170, 171]. Similarly, collagen and fibrin gels have also been shown to be mechanically unstable. Both collagen and fibrin gels were reported to shrink and deform when cells are encapsulated within them [4, 150, 160, 166]. Attempts to improve the mechanical rigidity of collagen gels include chemically crosslinking collagen with glutardehyde and carbodiimide [172, 173]. However, the usage of these toxic chemicals is not suitable for cell encapsulation processes especially in the presence of cells. On the other hand, fibrin gels have been reinforced by incorporating other materials such as HA, poly-L-lysine, calcium phosphate and PEG into the gels [165, 174-179].

Collagen, HA and fibrin have been reported to be antigenic [180-182]. It was believed that these natural polymers contain impurities such as endotoxins

and antigenic telopeptides that may cause an immune response when implanted *in vivo* [181, 183-185]. A number of purification techniques have been employed to remove these impurities from the natural polymers. For instance, collagen has been reported to be treated with proteolytic enzymes such as pepsin to cleave the antigenic telopeptides [181, 186-188]. However, enzyme treatment also induces denaturation that may affect the native bioactivity of the protein. Moreover, crosslinking collagen with glutaraldehyde also successfully masked the antigenic sites from interacting with antibodies [189]. Once again, glutaraldehyde is toxic and not suitable for cell encapsulation processes.

2.3.2. Synthetic hydrogels

Synthetic materials have advantages over natural hydrogels, such as reproducibility, tailorable mechanical properties, and control over scaffold architecture and macroscopic features. However, most synthetic polymers require harsh processing conditions, such as usage of organic solvents or high temperature, which are not suitable for cells. Over the past decades, several cell compatible synthetic polymers such as PEG and PVA have been extensively researched for cell encapsulation.

PEG has been widely studied for biomaterials due to advantages such as hydrophilic, non-toxic and resistive to protein adsorption. The PEG structures reported in the literature are either linear or branched, with end hydroxyl groups that can be chemically conjugated with a variety of functional groups (Figure 2.9). Depending on the chemistry of the functional moieties, both degradable and non-degradable PEG hydrogels can be synthesised.

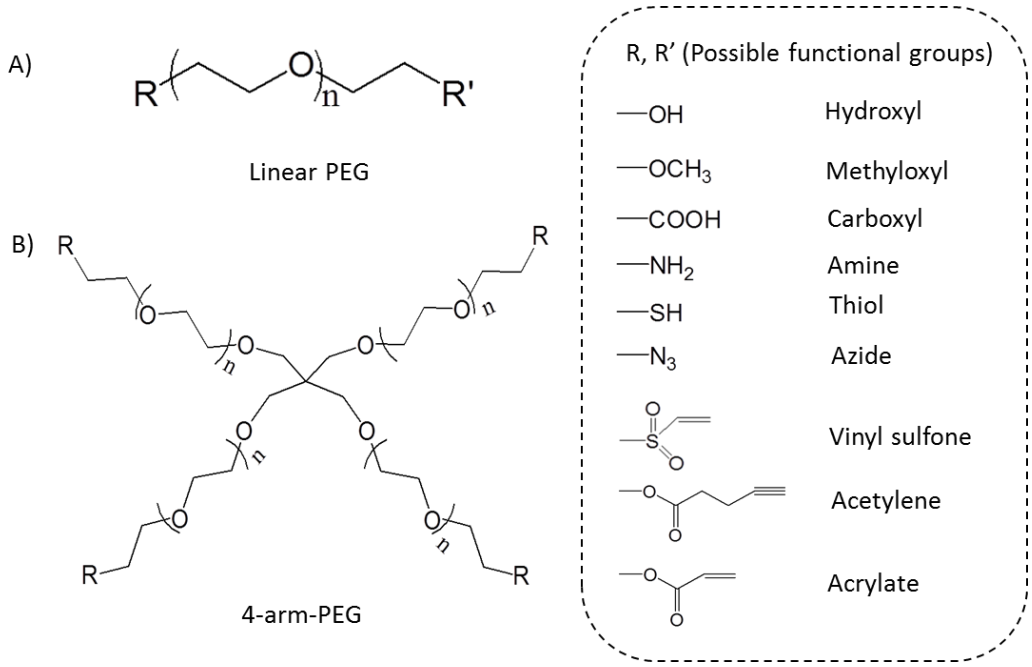

Figure 2.9: Structures of A) linear PEG, B) 4-arm-PEG, and various possible functional end groups reported in the literature (adapted from [190]).

Common approaches to fabricate PEG hydrogels include photopolymerisation of acrylated PEG or Michael-type addition of PEG grafted with vinyl sulfone [50, 86, 112, 191, 192]. One important feature of PEG hydrogels is that the physical and mechanical properties have been shown to be tailorable depending on the macromer concentration and crosslinking density [6, 17, 111, 193]. Chondrocytes, messenchymal stem cells and adipogenic cells have been successfully encapsulated in these PEG gels [194-197].

PVA which has similar chemistry to PEG, has also been employed in several biomedical applications [198]. It can be obtained from hydrolysis of poly(vinyl acetate), where the degree of hydrolysis has an overall effect on its chemical properties, solubility and crystallinity [35, 199]. It is well known for its low toxicity, hydrophilic nature, and the pendant hydroxyl groups that can be easily modified with various functional groups (Figure 2.10) [199-201].

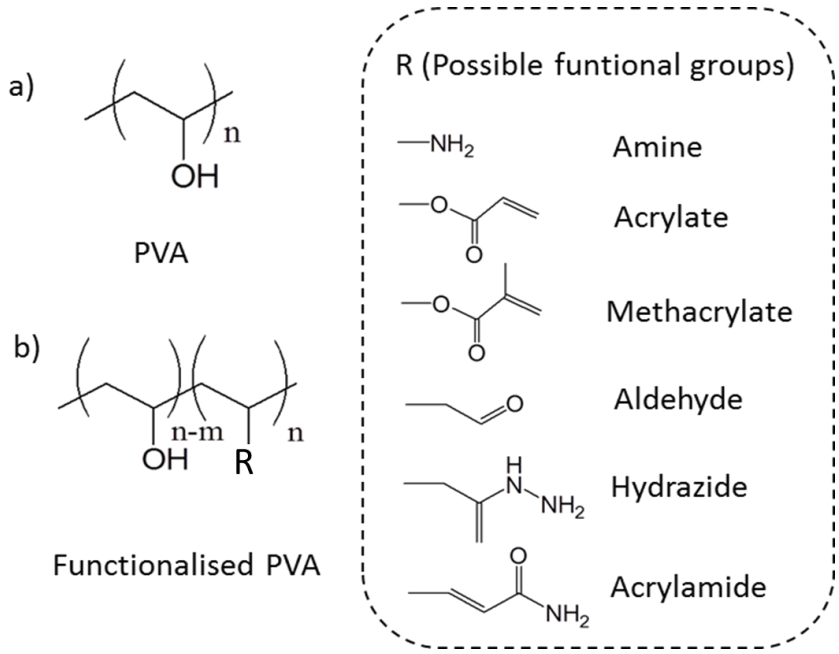

Figure 2.10: Structures of A) PVA, B) Functionalised PVA and the various possible pendant functional groups reported in the literature.

The abundance of hydroxyl groups on the PVA backbone allows for functionalisation of more than one type of functional groups, as well as control over the number of functional moieties grafted onto the polymer backbone [5, 89, 110, 200, 202, 203]. Both degradable and non-degradable PVA gels have been reported in the literature. The physical and mechanical properties of PVA gels can be varied according to the degree of functionalisation, molecular weight and macromer concentration [202-204]. For example, the compressive moduli of PVA hydrogels have been reported to range from 300 kPa to 20 MPa [203, 204]. Chondrocytes and fibroblasts have been successfully encapsulated within PVA gels [22, 57, 205].

Degradable hydrogels based on PEG and PVA have also been formed through their copolymerisation with other synthetic polymers that contain

hydrolytically labile ester bonds such as poly(lactic acid), polycaprolactone, poly(propylene fumarate) and polyphospoester (Figure 2.11). [206-210].

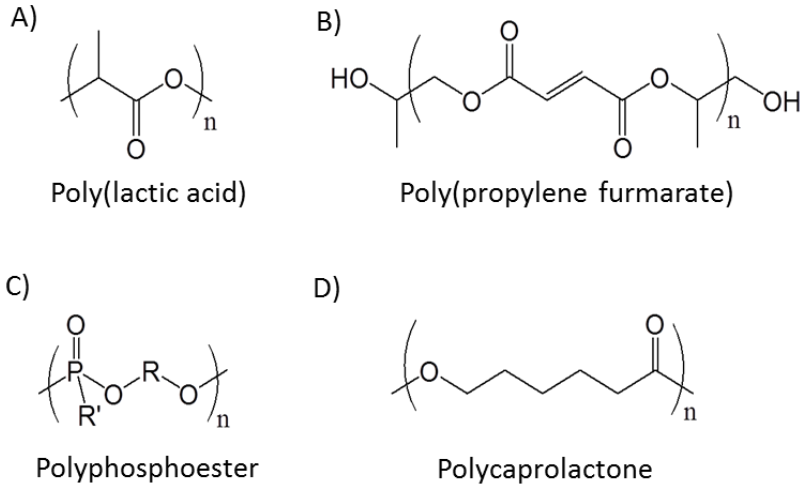

Figure 2.11: Structures of A) Poly(lactic acid), B) Poly(propylene furmarate), C) Polyphosphoester, and D) Polycaprolactone.

2.3.2.1. Disadvantages of synthetic hydrogels

One common problem associated with synthetic hydrogels is the lack of biological recognition sites for cell to attach, migrate and proliferate. Although the fabricated scaffold can be tailored to the desired physical and mechanical properties, the cells encapsulated within them are unable to function and promote tissue formation. Nuttelman et al. showed that the viability of hMSCs encapsulated in photopolymerised PEG hydrogels decrease from 100% viability initially to less than 10% after 4 weeks in osteogenic conditions [195]. Similarly, another study conducted on hMSCs encapsulated in PEG hydrogels also showed that the DNA concentration, which is relative to the total number of cells in the gels, also decreased from 2000 ng/gel to 500 ng/gel over 10 days [211]. The

viability of fibroblasts encapsulated in pure PVA hydrogels was observed to decrease from 95% to 80% over 28 days [134].

While synthetic polymers offer the advantages in terms of good reproducibility, mechanical stability, ease of purification and tailorable physical properties, cells are unable to function in these gels due to the lack of biological recognition sites. Therefore, biosynthetic polymers which combine the advantages of both synthetic and natural polymers, have emerged as better materials for cell encapsulation matrices.

2.3.3. Biosynthetic hydrogels

As mentioned above, synthetic hydrogels have been shown to have desirable physical properties as cell encapsulation matrices. However, these hydrogels do not have the required bioactive segments to facilitate cell function and proliferation. In the body, the ECM provides adhesion sites for cells and binds growth factors to regulate important cell functions to maintain the cell phenotype [55]. Therefore, ECM molecules such as polysaccharide, proteins and growth factors have been incorporated into synthetic hydrogel networks to impart biofunctionality. These biosynthetic hydrogels are designed to have the tailorable physical properties of the base synthetic polymer, as well as the desired biological attributes of the incorporated biological molecules.

Biological molecules can be either physically blended or covalently immobilised into hydrogels. In certain applications such as drug delivery, physical entrapment might be desired. For example, insulin has been physically blended in PEG based hydrogels for treatment of diabetes. The PEG gel has been

reported to protect insulin from proteolytic degradation before it reaches the targeted delivery site, preferentially the colon [206]. However, in terms as cell encapsulation matrices, blending leads to the biological molecule being leached out from the network in a short period of time [6]. Therefore, covalent incorporation of natural polymers into the synthetic network is more preferred for long term applications. This section will focus on the different biological molecules incorporated into synthetic hydrogels and their effect on cellular behaviour.

2.3.3.1. Polysaccharides

The polysaccharide HA has been incorporated into synthetic hydrogels to impart biofunctionality. A study conducted by Kutty et al. showed that fibroblasts encapsulated in PEG hydrogels remained rounded after 14 days [212]. However, when HA was incorporated into the PEG gels, the morphology of the fibroblasts was vastly different, where spreading and interconnected networks were observed [212]. This phenomenon was hypothesised to be due to the role of HA in regulating metastasis and wound healing by binding to cell surface receptors [213]. Jin et al. showed that HA functionalised with thiol groups can be crosslinked with PEG-vinyl sulfone through Michael-type addition. The resultant PEG-HA hydrogel was used to encapsulate chondrocytes, which were shown to secrete glycosaminoglycans and collagen type II in the gel up to 21 days [10]. Using a similar Michael-type addition, acrylated HA has been reacted with thiolated PEG, and the formed hybrid gels have been used to encapsulate mesenchymal stem cells for bone regeneration [122]. In that study, the cells were shown to express osteocalcin and stimulated mature bone formation after 4

weeks of implantation [122]. PEG-HA hydrogels have also been employed to encapsulated fibroblasts, chondrocytes and embryonic carcinoma cells [10, 59, 214].

Another class of polysaccharides known as glycosaminoglycans (GAGs) have also been incorporated into synthetic gels. GAGs are known to have important roles in the ECM such as binding and presenting growth factors to cells. As an approach to engineer cartilage, the GAG chondroitin sulphate (CS), which is an important structural component of this tissue, has been integrated into synthetic cells to regulate the function of encapsulated chondrocytes. Bryant et al. successfully grafted photopolymerisable methacrylate groups onto CS, which was then co-polymerised with methacrylated PVA [215]. The resultant PVA-CS hydrogel was reported to promote viability of encapsulated chondrocytes [215]. Heparin, which is the highly sulphated derivative of the GAG heparan sulphate (HS), has also been studied to improve the biological functions of synthetic hydrogels. It has been reported to be chemically conjugated with thiol groups, then crosslinked with acrylated PEG through Michael-type addition reaction [216]. In another approach, methacrylate groups were conjugated onto heparin to allow co-polymerisation with metharylated PVA [9, 134]. The presence of heparin significantly improved viability of mammalian cells encapsulated within the PVA/heparin gels for a time period of 28 days [134]. In a separate study, heparin immobilised in PEG hydrogels has been shown to direct differentiation of encapsulated mesenchymal stem cells down an osteogenic lineage [96, 217].

2.3.3.2. Proteins and peptides

Proteins such as collagen, laminin and fibrinogen contain cell signalling sequences that are fundamental for cells to facilitate functional activities such as adhesion, differentiation and proliferation. Singh et al. reported the grafting of acrylated PEG onto collagen, followed by photopolymerisation where fibroblasts and endothelial cells were co-encapsulated within these gels [218]. It was observed that the cells were able to form capillary vessel-like networks with hollow lumens in the gel [218]. A similar chemistry was also applied to fibrinogen and laminin, where PEG chains were conjugated onto these proteins [7, 123, 219-222]. The fabricated PEG-laminin gels were shown to promote aggregation of encapsulated nucleus pulposus cells as well as maintain their phenotype [219, 220]. PEG has also be co-polymerised with fibrinogen, and these gels have been used to encapsulate smooth muscle cells and endothelial cells [123]. Both cells were able to migrate and form interconnecting networks within the gel [123]. Photocrosslinked PEG-gelatin gels showed that the addition of gelatin facilitated development of 3D fibroblast cellular networks within the gel [223]. From all of these studies (and other not mentioned here), it is obvious that the incorporation of proteins into synthetic hydrogels significantly improved the cellular function of the gels. The cell-adhesive sequences which are present in these proteins were speculated to be the reason for the improved bioactivity [224-226]. Hence, protein fragments/peptides containing the adhesive domains have also been covalently immobilised in hydrogel networks to promote adhesion, migration and proliferation of encapsulated cells [76, 227, 228]. However, Weber et al. conducted a study where the whole protein laminin and laminin derived cell adhesive IKVAV peptide were incorporated into PEG

hydrogels encapsulated with islets [229]. Interestingly, it was observed that the islets were secreting much more insulin when the whole protein was used [229]. This phenomenon highlights that besides the adhesive sequences of the protein, other domains on the protein, such as growth factor binding sites are required to facilitate overall cellular function [230]. A full review of the use of protein fragments and peptides is available elsewhere, and is outside the scope of this thesis [1, 190].

2.3.3.3. Growth factors

Growth factors which are important biological molecules that provide adequate signalling to cells have also been immobilised in hydrogels. Vascular endothelial growth factor (VEGF) has been reported to be conjugated to PEG, then covalently immobilised in acrylated PEG hydrogels [231]. The presence of VEGF was shown to stimulate tubulogenesis of the encapsulated endothelial cells. Similarly, platelet-derived growth factor (PDGF-BB) and fibroblast growth factor (FGF) have been PEGylated, then crosslinked in PEG hydrogels [232]. In the same study, the presence of the growth factors was shown to increase the migration of encapsulated endothelial cells significantly [232].

2.3.3.4. Issues associated with incorporation of natural molecules

As reviewed above, Michael-type addition and photopolymerisation are the most popular techniques used to covalently co-polymerise natural and synthetic polymers. These approaches often require chemical modification processes, such as conjugation of linear PEG chains (PEGylation), thiols, acrylates/methacrylates and maleimide groups onto the biological molecule

backbone. However, many of these chemical reactions are usually conducted in harsh conditions that have the potential to induce denaturation and degradation of the biological molecules, which leads to loss in functionality.

PEGylation has been applied to a number of biological molecules such as fibrinogen, collagen and albumin with similar reactions conditions. PEGylation of fibrinogen can be done through Michael-type addition of thiols on fibrinogen to acrylated PEG [233]. However, this PEGylation reaction requires the fibrinogen to be degraded. The thiols in native fibrinogen are presented in their oxidised form, which are the disulfide bridges of the protein [233]. Therefore, reducing agent such as Tris(2-carboxyethyl)phosphine (TCEP) are used to reduce the disulfide bonds to thiols, which are then reacted with the acrylates on PEG (Figure 2.12) [12, 233].

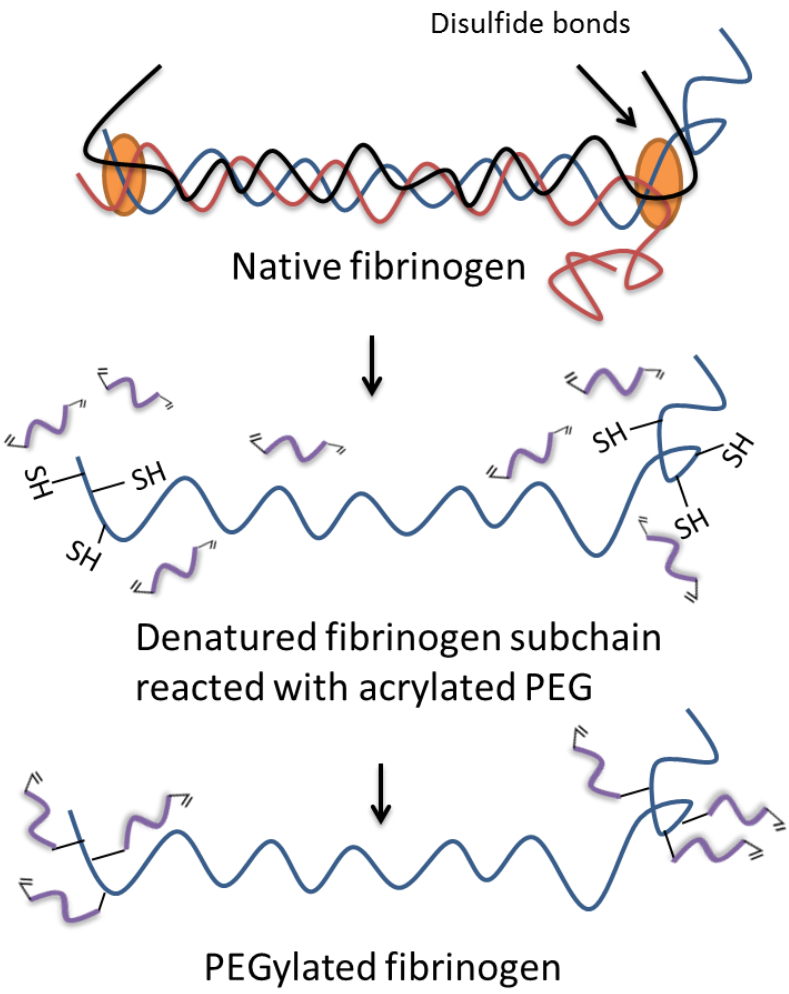

Figure 2.12: Schematic of fibrinogen PEGylation (Adapted from [233])

Similarly, Gonen-Wadmany et al. showed that SDS PAGE smears were observed for PEGylated albumin and collagen, as compared to distinct bands for the non-modified proteins, indicating the occurrence of denaturation and degradation [12]. It was also reported that the reaction conditions to functionalise collagen with methacrylate groups can cause partial denaturation of the collagen, resulting in significant changes in the fibrillar structure [234-236].

Another issue with chemically modifying biological molecules is that the newly conjugated functional groups can physically block or increase steric hindrance around the protein's bioactive side groups, thus interfering with cell-

protein interaction [237]. For example, functional methacrylate and cinnamate groups were attached onto collagen using the conventional carboxyl-amine coupling reaction that targets the protein amine or carboxyl groups [234, 238, 239]. Other protocols used to methacrylate collagen involve chemicals such as methacrylic anhydride and glycidyl acrylate/methacrylate, which also target the amine and carboxyl groups of collagen [235, 236]. As the well-known cell adhesive RGD sequence has both amine and carboxyl side chains [240], there is a high possibility that the functional groups are directly attached onto the RGD sequence, thus affecting its ability to bind to cell surface integrins (Figure 2.13).

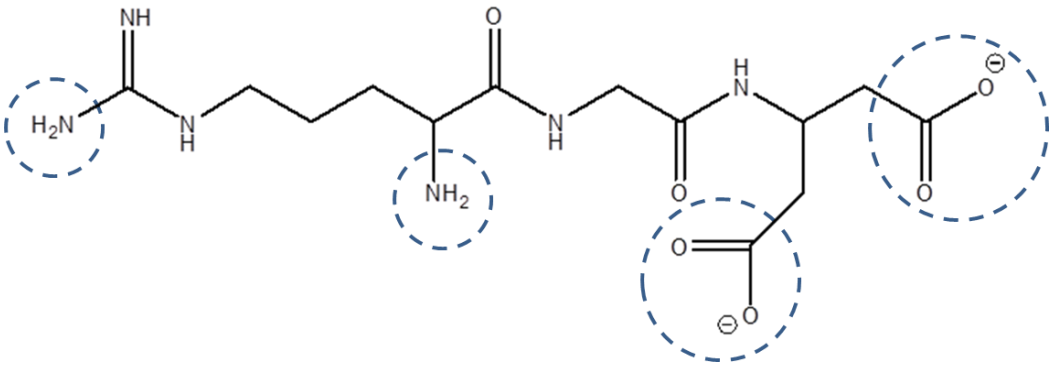

Figure 2.13: Molecular structure of RGD sequence; both amine and carboxyl side groups are highlighted (Adapted from [240]).

Browning et al. also reported that collagen bioactivity retention is heavily influenced by the degree of functionalisation [237]. A decrease in protein functionalisation density resulted in an increase in total amount of endothelial cells adhered onto functionalised collagen hydrogels [237]. Highly functionalised collagen gels facilitated attachment of only ~30 cells/mm^2, whereas ~75 cells/mm^2 were adhered onto lowly functionalised gels after 3 hours of incubation [237]. Conducting similar cell adhesion studies on Streptococcal collagen-like proteins (Scl2-1) revealed that the spreading of the attached

endothelial cells also decreases with increasing level of funtionalisation [237]. It was therefore believed that protein functionalisation/modification can physically block the adhesive segments required for cellular spreading and attachment.

Besides physically hindering the cell adhesive segments, other functional bioactive sites can also be affected following the modification process. Gaudet etl al. reported that attaching methacrylate groups onto collagen significantly impeded its ability to self-assemble [234]. Moreover, mesenchymal stem cells encapsulated in the modified collagen gels had significantly lower cell viability (~70%) compared to the native collagen gels (~95%) [234]. PEGylating fibrinogen was reported to affect its ability to form fibrin clots [7, 241]. Barker et al. showed that conjugating more than six PEG chains onto fibrinogen hindered the protein's clotting characteristics completely [241]. Moreover, the degradation response of PEGylated fibrinogen and native fibrinogen to plasmin is also significantly different. It was also reported that PEGylation significantly affected the cellular interaction with proteins in hydrogels. For example, fibroblasts were able to form lamelliphodia and interconnected networks in unmodified fibrinogen hydrogels after 2 and 6 days respectively [7]. However, at similar time points, the fibroblasts encapsulated in PEGylated fibrinogen gels remained rounded with no formation of interconnected networks [7]. These fibroblasts were also reported to have lower levels of matrix metalloproteinase (MMP) markers (MMP-2 and MMP-9) compared to those entrapped in native fibrinogen gels, suggesting a change in phenotype [7]. Functionalisation of heparin with thiol groups also decreased its antithrombin III binding affinity, which further affects its anti-coagulation properties [8, 11]. A 20% conversion of the carboxyl

groups of heparin to thiol groups resulted in significant loss of its anticoagulant activity [11].

Thus, while biosynthetic hydrogels have emerged as attractive materials for cell encapsulation due to their tailorable physical and mechanical properties, as well as their desired biological attributes to support 3D cellular functions, many issues still remain. In particular, the exact method for the covalent integration of biological molecules into synthetic hydrogels still presents several challenges. As stated above, current methods of biological molecule incorporation often requires varying degree of chemical modification/functionalisation of the biological molecules, and these chemical modification processes can potentially denature, degrade and impede the bioactivity of the biological molecules. Therefore, there is still a need for new approaches that allow covalent incorporation of biological molecules into synthetic hydrogels in their native state.

2.4. Summary

The ideal cell encapsulation scaffold is required to provide temporal support to the cells while they secrete their ECM to form tissue that is structurally, biochemically and functionally similar to the native tissue. Hydrogels are potential candidates as cell encapsulation matrices due to their structural comparability to the native ECM. The hydrogel must consist of cytocompatible macromer, can be crosslinked by means not detrimental to cells, as well as having good physicomechanical properties and tailorable degradation rates to facilitate tissue formation within the scaffold. Biosynthetic hydrogels which have tailorable physical and mechanical properties, as well as the

biofunctionality required for cellular processes, can meet these needs. However, current approaches in incorporating biological molecules into synthetic gels may cause denaturation, degradation and loss of bioactivity of the particular molecule. Therefore, a new system that allows stable integration of biological molecules (e.g., proteins, growth factors and cytokines) within synthetic hydrogels without the need of chemical modification needs to be developed.

The following aims form the basis for the body of work presented on this thesis.

- Investigate the feasibility of incorporating biological molecules (proteins) in their native state into synthetic hydrogels. In this thesis, the base polymer selected is PVA due to the abundance of hydroxyl groups that can be easily modified with other functional moieties. A photocrosslinking system that has only been applied to protein-protein crosslinking was utilised (will be elaborated further in Chapter 3).
- Understanding the effect of incorporating proteins into PVA hydrogels on the physical properties of the fabricated hydrogels, as well as study the effects on protein retention and bioactivity within the gel.
- Evaluate the possibility of encapsulating cells within these biosynthetic hydrogels, and study the effect of protein incorporation on 3D cellular functions.

Chapter 3

Synthesis of Phenolated PVA and Hydrogel Fabrication Using Ruthenium/Persulphate Initiating System

---

The synthesis of PVA-Tyr in this chapter was published in Biomaterials and permission was granted by the publisher for use in this thesis. The concepts and writing of this paper was largely under the control of Lim KS (90% input). The other authors contributed to the analysis and interpretation of the literature and assisted in the development of the arguments.

Paper citation:

Lim KS, Alves MH, Poole-Warren LA, Martens PJ. *Covalent incorporation of non-chemically modified gelatin into degradable PVA-tyramine hydrogels*. Biomaterials. 2013;34:7097-105.

3.1. Introduction

Incorporation of proteins into synthetic hydrogels is known to significantly enhance cellular interactions within the resultant biosynthetic gels [242, 243]. However, long term usage of these hydrogels requires the protein to be covalently crosslinked with the synthetic polymers. This covalent incorporation has been achieved through a number of approaches, such as modification of protein side chains with poly(ethylene glycol) (PEG), and grafting functional reactive groups onto the protein backbone [7, 9, 12, 120, 244]. However, these approaches are often associated with protein degradation, deformation, and loss of functionality [7, 244]. Therefore, new methods are needed to allow co-polymerisation of proteins and synthetic polymers without the need for chemical modification.

Proteins are natural polymers with complex structures, compositions and functions, which play important roles in a variety of biological functions. These roles include catalysing chemical reactions in the body, maintenance of the body tissue, and transporting molecules from one location to another [245, 246]. More importantly, all of these mentioned functions are dependent on the protein's activity and stability in the body, which are tightly associated with protein-protein interactions [247]. In order to study these interactions, several methods have been developed in the past, such as using computational methods, or protein-protein crosslinking reactions [247, 248].

Protein-protein crosslinking is usually a chemical reaction where two or more molecules of a protein are linked together with a covalent bond [247]. Crosslinking between two groups on a single protein could stabilise the tertiary

and quaternary structure of the protein, whereas intermolecular crosslinks between two or more proteins would stabilise the protein-protein interaction sites [249-251]. These crosslinked multi protein complexes have been captured and analysed to identify unknown protein interaction domains [252]. However, due to the complexity of the protein structure, only a small amount of functional groups can be targeted for crosslinking. The most targeted protein side chains are primary amines ($-NH_2$) [250, 251, 253], carboxyls (-COOH) [254, 255], and thiols (-SH) [256-258], which are mostly present in the amino acid residues of the protein. Unfortunately, most of these protein-protein crosslinking processes require toxic chemicals such as formaldehyde, glutaraldehyde, maleimide and methanol [250, 259, 260].

On the other hand, metal catalysed oxidation has also been used to crosslink proteins. Fancy et al. reported on the usage of a transition metal complex, ruthenium (Ru) as photo-redox catalysts to crosslink proteins. Such photo-redox catalysts, which were firstly reported in the 1970's, spurred great interest due to their absorbance in the visible range, as well as their chemical stability in the excited state [261]. In terms of protein-protein crosslinking, the photolysis of Ru^{2+} generated excited Ru^{3+} that could oxidise aromatic residues, such as tyrosine in the protein. The oxidised tyrosine groups were converted to tyrosyl radicals, which were further quenched by forming covalent crosslinks with nearby tyrosine residues (Figure 3.1) [252, 262, 263]. This system has been used to study the interactions between proteins involved in genetic regulation [247, 252].

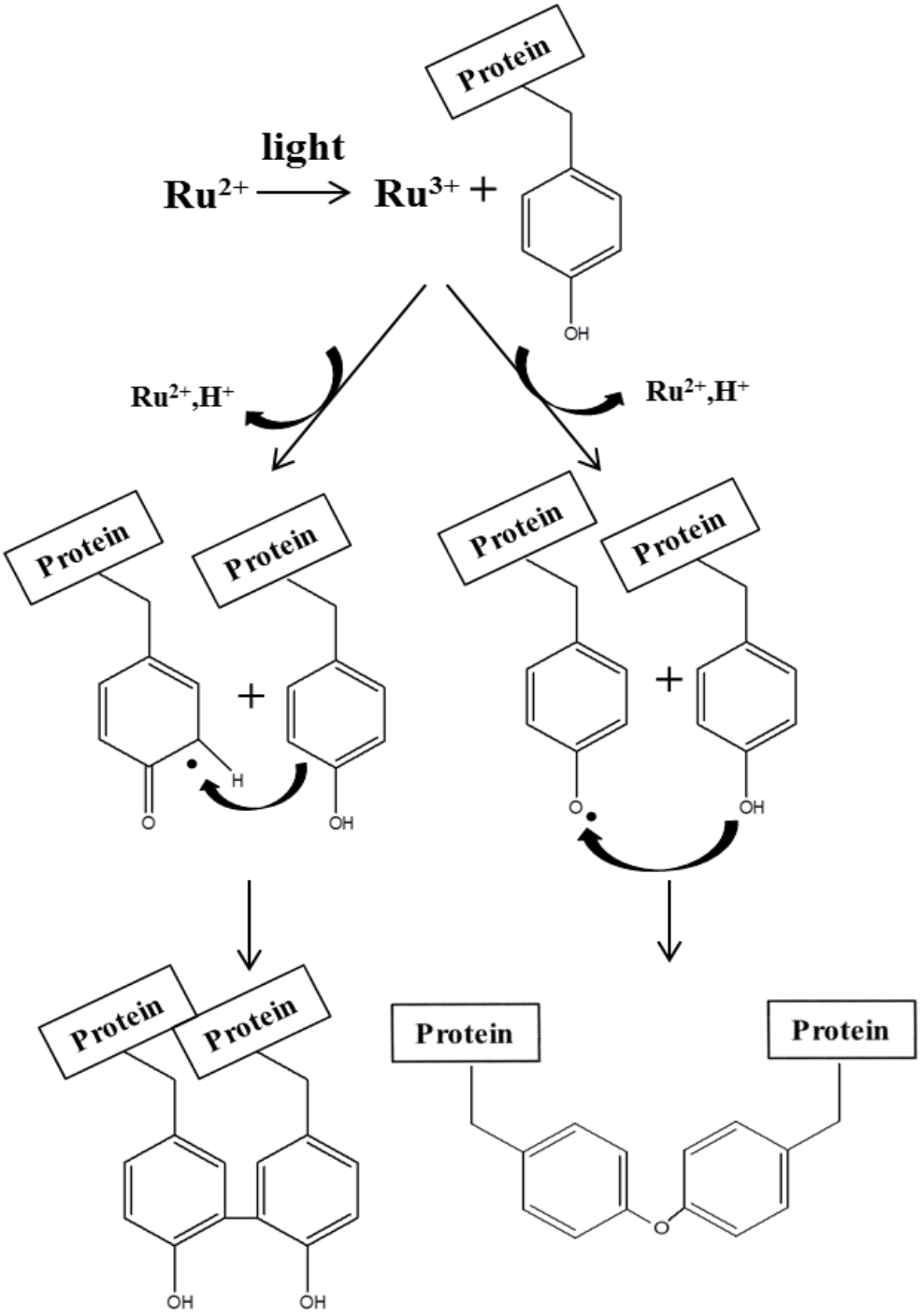

Figure 3.1: Schematic of protein-protein crosslinking using photo-oxidation of Ru (Adapted from [252, 263]).

In recent years, Elvin et al. reported the use of the Ru photo-oxidation system to fabricate protein hydrogels as tissue sealants [254, 264, 265]. Ru used in combination with a potent persulphate electron acceptor, has been shown to

crosslink hydrogels from collagen, fibrinogen, gelatin, resilin and keratin [254, 264, 266-269]. In particular, the resultant gelatin and fibrinogen hydrogels had good elasticity and adhesive properties for sealing gastrointestinal surgical incisions [265, 269]. However, to the best of our knowledge, there have not been any reports in the literature to date on using this initiating system to crosslink synthetic polymers. It was hypothesised in this chapter that functionalisation of synthetic polymers with phenolic moieties will allow the formation of a synthetic hydrogel network using the visible light initiated Ru/persulphate system. In addition, proteins can also be covalently crosslinked into the synthetic hydrogel network through their native tyrosine residues, without any extra chemical modification.

A variety of chemistry has been reported to conjugate phenolic residues onto synthetic polymers. The most common chemistry used is the carboxyl-amine condensation reaction coupling. This reaction requires a carbodiimide reagent to activate the carboxyl groups, forming reactive esters that couple with primary amines. Poly(ethylene glycol) (PEG), poly(ethylene oxide) (PEO) and poly(propylene oxide) (PPO), has been functionalised with phenolic groups using this chemistry [270-272].

Therefore, the aim of this chapter was to examine different chemical routes for the functionalisation of PVA with phenolic moieties using the carboxyl-amine condensation reaction. Furthermore, the feasibility of crosslinking phenolated PVA using the visible light initiated Ru/persulphate system was examined, where different initiator concentrations and irradiation conditions were also investigated.

3.2. Experimental

3.2.1. Materials

Poly(vinyl alcohol) (PVA) (13-23 kDa, 98% hydrolysed), succinic anhydride (SA), triethylamine (TEA), 1,3-Dicyclohexylcarbodiimide (DCC), N-hydroxysuccinimide (NHS), tyramine (Tyr), ammonium persulphate (APS), sodium persulphate (SPS), 1,1-carbonyldiimidazole (CDI), tris(2,2-bipyridyl)dichlororuthenium(II) hexahydrate (Ru(II)bpy_3^{2+}), glycine ethyl ester hydrochloride, hydrazine monohydrate, 4-hydroxybenzoic acid (HBA), deuterium oxide (D_2O), molecular sieves (4Å), Dulbecco's phosphate buffered saline (DPBS), and dialysis tubing (10 kDa molecular weight cut-off) were purchased from Sigma-Aldrich and used as received. Dimethyl sulfoxide (DMSO) was bought from Ajax Chemicals and was dried over 4 Å molecular sieves. Hydrogel disc moulds were made from silicone sheets (Silastic®Sheeting, reinforced medical grade silicone rubber, Dow Corning).

3.2.2. Synthesis of phenolated PVA

Two chemical synthesis routes were considered to conjugate phenol groups onto PVA (Figure 3.2). The targeted phenolation was 2% (7 phenol groups per PVA backbone).

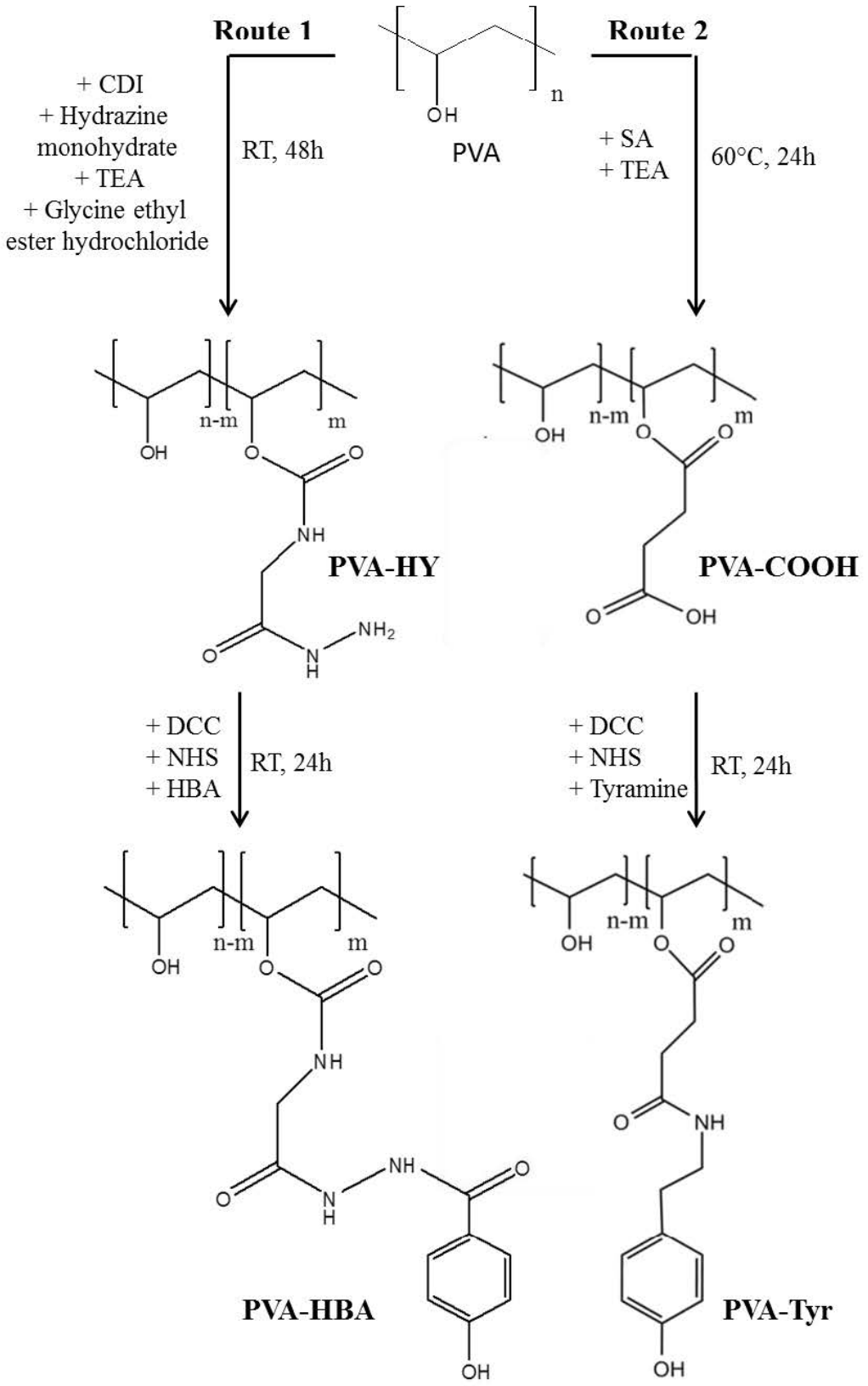

Figure 3.2: Synthesis routes to obtain phenolated PVA; Route 1: PVA-Hydroxy benzoic acid (PVA-HBA); Route 2: PVA-Tyramine (PVA-Tyr).

3.2.2.1. Synthesis of PVA-HY and PVA-HBA (Route 1)

PVA-HBA was synthesised through two steps as shown in Figure 3.2. Firstly, the hydroxyl groups of PVA were partially substituted with hydrazide groups (PVA-HY) following a protocol outlined by Alves et al [57]. In a typical experiment, 1 g of PVA was dissolved in 20 ml of dry DMSO under nitrogen atmosphere at 60ºC. The fully dissolved PVA solution was left to cool down to room temperature (RT). 0.507 g of CDI was then added to the PVA solution, with stirring under nitrogen atmosphere for 3 hours. Next, 0.087 g of glycine ethyl ester hydrochloride and 0.087 ml of TEA was added to the reaction mixture. After 20 hours, 2 ml of hydrazine monohydrate was added to the reaction solution and was further stirred at RT for 24 hours. The polymer solution was purified by dialysis (10 kDa molecular weight cut–off) against water, and then freeze-dried to obtain dried PVA-HY. The targeted amount of functionalisation was 7 hydrazide groups per PVA chain. Next, HBA was conjugated onto the hydrazide groups of PVA-HY using carboxyl-amine coupling chemistry. 0.06 g of HBA, 0.271 g of DCC and 0.151 g of NHS were dissolved in 10 ml of dry DMSO and allowed to stir at RT. After 24 hours, 1 g of PVA-HY dissolved in 10 ml of dry DMSO was added to the reaction mixture, and was left to react for another 24 hours at RT.

3.2.2.2. Synthesis of PVA-COOH and PVA-Tyr (Route 2)

PVA-Tyr was also synthesised through 2 steps (Figure 3.2). Firstly, carboxyl groups were conjugated onto the PVA backbone. 1g of PVA was dissolved in 10 ml of dry DMSO at 60 ºC under nitrogen purging. 0.045 g of SA and 0.061 ml of TEA were added to the reaction mixture, and stirred at 60ºC for

24 hours. The targeted conjugation was 7 carboxyl groups per PVA chain. The carboxylated PVA (PVA-COOH) was precipitated in a 10-fold excess of ethanol, re-dissolved in water and dialysed against water prior to being freeze dried. 1 g of dried PVA-COOH was dissolved in 10 ml of dry DMSO at 60ºC, and purged with nitrogen for 30 minutes. The solution was left to cool to RT prior to the addition of 0.271 g of DCC and 0.151 g of NHS. After 24 hours, 0.121 g of Tyr was added to the reaction mixture and was allowed to react for another 24 hours. The targeted amount of Tyr conjugated was also 7 Tyr/PVA chain. In order to obtain complete conversion of carboxyl to Tyr groups, a study was conducted to evaluate the amount of DCC and NHS needed to activate the pendent carboxyl moieties. The synthesised PVA-Tyr was precipitated in 10-fold excess of acetone, re-dissolved in water, and vacuum filtered to remove the by-product (dicyclohexylurea). The filtered PVA-Tyr solution was purified by dialysis against water, and then freeze-dried.

3.2.3. Quantification of functional group density in synthesised macromers using ^{1}H NMR

The synthesized polymers were analysed using ^{1}H NMR (300 MHz Bruker Advance DPX-300 spectrometer) to quantify the amount of functional groups conjugated to the PVA backbone. The percentage conjugation was calculated by comparing the area of the peaks corresponding to the functional groups to the area of the peaks associated to the PVA backbone. The PVA used in this thesis had a reported molecular weight of 13 – 23 kDa, and all calculations are done based on the average molecular weight of PVA (16 kDa). The average

number of functional groups attached per PVA chain (functional groups/chain) was then calculated by the following equation:

$$Functional\ groups/chain = \%\ conjugation\ x \frac{MW_{PVA}}{MW_{RU}} \quad (3.1)$$

Where, MW is molecular weight and RU is the repeating unit of PVA; MW_{PVA} = 16,000 g mol^{-1}, MW_{RU} = 44 g mol^{-1}

The efficiency of the reaction can then be calculated by the equation as follows:

$$Reaction\ efficiency = \frac{functional\ groups/chain_{achieved}}{functional\ groups/chain_{targeted}} x\ 100 \quad (3.2)$$

3.2.3.1. PVA-HY (Route 1)

^{1}H NMR done on PVA-HY showed no signals corresponding to the hydrazide (-C*H*$_2$CONHNH$_2$) groups, which was likely due to overlapping with protons of the PVA backbone. Hence, PVA-HY was reacted with formaldehyde to convert the hydrazide groups to hydrazone (Figure 3.3). Firstly, free formaldehyde was generated by dissolving paraformaldehyde in PBS at 50 °C. PVA-HY dissolved in PBS was then added to the reaction mixture and was stirred at room temperature for 24 hours. The reacted polymer (PVA-Hydrazone) was dialysed against water then freeze-dried. PVA-Hydrazone was then dissolved in D_2O, and characterised through ^{1}H NMR to determine the functional group density. The area of the proton peaks corresponding to the hydrazone groups was compared to the area of the protons in the PVA backbone (δ = 1.3 – 1.9ppm, labelled "a" in Figure 3.4), to determine the percentage conjugation. The number of hydrazide groups attached is equivalent to the number of hydrazone

moieties present on the PVA chain. ^{1}H NMR: C*H*$_2$ of hydrazone bond (δ = 6.2 - 6.5 ppm and 6.7 - 6.9 ppm), C*H* of PVA backbone (δ = 3.5 - 4 ppm) and C*H*$_2$ of PVA backbone (δ = 1.3 – 1.9 ppm).

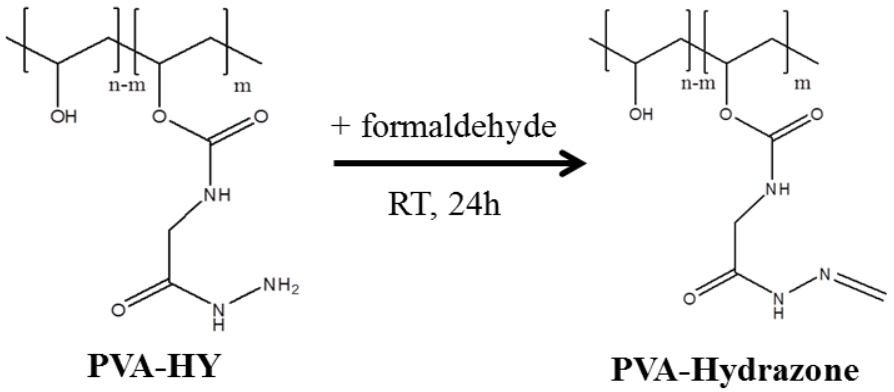

PVA-HY **PVA-Hydrazone**

Figure 3.3: Schematic of reacting PVA-HY with formaldehyde to form PVA-Hydrazone.

3.2.3.2. PVA-COOH and PVA-Tyr (Route 2)

Both PVA-COOH and PVA-Tyr were dissolved in D_2O and analysed using ^{1}H NMR. For PVA-COOH, the area of methylene proton peaks of the carboxyl moieties was compared to the area of proton peaks in the PVA backbone. ^{1}H NMR: C*H*$_2$ of carboxyl groups (δ = 2.5 – 2.6 ppm), C*H* of PVA backbone (δ = 3.5 - 4 ppm) and C*H*$_2$ of PVA backbone (δ = 1.3 – 1.9 ppm). Similarly for PVA-Tyr, the percentage conjugation of Tyr groups onto PVA backbone was calculated by comparing the area of the proton peaks corresponding to the aromatic moieties to the area of the protons in the PVA backbone (δ = 1.3 – 1.9 ppm, labelled "a" in Figure 3.7). ^{1}H NMR: C*H*$_2$ of aromatic groups (δ = 6.5 – 7.5 ppm), C*H* of PVA backbone (δ = 3.5 - 4 ppm) and C*H*$_2$ of PVA backbone (δ = 1.3 – 1.9 ppm).

3.2.4. L929 cell growth inhibition assay

Macromer samples (PVA, PVA-COOH and PVA-Tyr) were prepared at concentrations of 4 mg/mL (in DPBS) and diluted to 1 mg/mL with EMEM containing 10% FBS and 1% PS. Murine dermal fibroblasts (L929) were cultured in EMEM supplemented with 10% FBS and 1% PS. $5x10^4$ cells/mL were seeded onto 35 mm diameter tissue culture dishes. After 24 hours of incubation at 37 °C in a 5% CO_2 humidified atmosphere the media was discarded and 1 ml of sample solution was added to the cells. Following an additional 48 hours of incubation, the cells were trypsinised, and counted with a cell viability analyser (Vi-cell XR, Beckman Coulter). A series of ethanol solutions (4%, 5% and 7.5%) (v/v) was used as positive controls to confirm the validity of the assay. However, only 7.5% ethanol was showed in the results for comparison purposes. The negative control used was saline. The percentage cell growth inhibition was calculated by the following equation:

$$\%\ Cell\ growth\ inhibition = 1 - \frac{number\ of\ cells\ in\ sample\ dish}{number\ of\ cells\ in\ media\ control\ dish} \times 100 \quad (3.3)$$

3.2.5. Fabrication of PVA-Tyr hydrogels

Dried PVA-Tyr was dissolved in DPBS at 80 °C. Upon complete dissolution, the polymer solution was cooled to RT and the initiators, Ru and persulphate were added to the solution. The macromer solution was then placed into silicon moulds on a glass slide and covered with a cover slip. The samples were then irradiated under visible light (Blue wave 200, Dymax Co.) in a closed system. The light was irradiated through a light filter where only light of the

wavelength 400 – 450 nm was allowed to pass through. A variety of initiator combinations and irradiation conditions were studied. The total macromer content in the hydrogels was kept at 20 wt%.

3.2.5.1. Swelling and mass loss analysis

Directly after polymerisation, all samples were weighed for the initial wet mass ($m_{\text{initial, t0}}$) and three samples were immediately lyophilised to obtain their dry weights ($m_{\text{dry ,t0}}$). The actual macromer concentration was calculated based on the equation below:

$$\%\, macromer = \frac{m_{dry,\, t0}}{m_{initial,\, t0}}\ x\ 100 \tag{3.4}$$

These samples were then submerged in a sink of DPBS and incubated in an orbital shaker at 37 °C. Samples were removed from the incubator after 1 day, blotted dry and weighed (m_{swollen}). The swollen samples were then freeze-dried and weighed again (m_{dry}). The mass swelling ratio (q) and mass loss were calculated as follows:

$$q = \frac{m_{swollen}}{m_{\text{dry}}} \tag{3.5}$$

$$mass\ loss\ \% = \frac{m_{i,\, dry} - m_{dry}}{m_{i,\, dry}}\ x\ 100 \tag{3.6}$$

The sol fraction of the hydrogels is equal to the mass loss at 1 day, as it has been shown that in these types of PVA gels any polymer chains not attached to the network will diffuse out of the sample in this timeframe [9, 22, 202, 244].

3.2.5.2. Photo-kinetics of Ru/persulfate system

The light attenuation as a function of sample depth is given by the Beer-Lambert law [273]:

$$I = I_0 x\, e^{-\epsilon c z} \tag{3.7}$$

Where, I_0 = incident light intensity at the sample surface.

ϵ = molar absorption coefficient of the photoinitiator (1.46 x 10^4 $M^{-1}cm^{-1}$ for Ru^{2+} at 450 nm [274]).

c = photoinitiator concentration.

z = curing depth.

3.2.6. Statistical analysis

All samples for each swelling and mass loss study were prepared in triplicates, and each study was repeated three times. Two-way ANOVA was used to determine the significance for the sol fraction, mass loss and swelling ratio using Minitab 15 statistical analysis software.

3.3. Results and discussion

3.3.1. Synthesis of phenolated PVA

In this study, two routes of chemical synthesis were proposed to obtain phenolated PVA (Figure 3.2). Both routes were designed based on previous studies in the literature, where phenolic moieties were conjugated onto synthetic polymers such as PEG, PEO and PPO [270, 272]. The carboxyl-amine condensation reaction was utilised in both routes. It was also noted that the phenolated PVA proposed from both routes contain ester linkages (Figure 3.2), which are potentially hydrolytically degradable. However, the potential degradation behaviour of these macromers is not the focus of this chapter, and will be explored in Chapter 4.

3.3.1.1. Synthesis of PVA-HY and PVA-HBA (Route 1)

PVA-HY was successfully synthesised according to a protocol adapted from Alves et al [57]. Firstly, the hydroxyl groups of the PVA were activated with CDI. Glycine ester hydrochloride was then added to convert the hydroxyls into functional ester moieties. TEA was also included in the reaction to neutralise the hydrochloride salt, followed by the addition of hydrazide monohydrate to convert the esters into hydrazide groups. However, the conjugation of hydrazide groups onto the PVA backbone could not be confirmed with NMR, as the signals corresponding to the hydrazide groups were not detectable in the spectra (Figure 3.4A). This result agrees with the literature, where the peaks of the methylene groups of the conjugated hydrazide groups might overlap with the methylene protons of the PVA backbone [57]. Hence, PVA-HY was further reacted with formaldehyde to derivatise the hydrazide to hydrazone groups. This conversion

resulted in the appearance of peaks corresponding to the vinyl groups of PVA-Hydrazone in the 6.2 - 6.5 ppm and 6.7 - 6.9 ppm region (Figure 3.4B). The percentage conjugation was calculated based on the comparison of the area under these two peaks to the peaks of the PVA backbone. It was calculated that there were 7 hydrazide groups per PVA chain. This result showed a reaction efficiency of 100%, where the resultant number of functional groups attached was equivalent to the number of functional groups that were targeted.

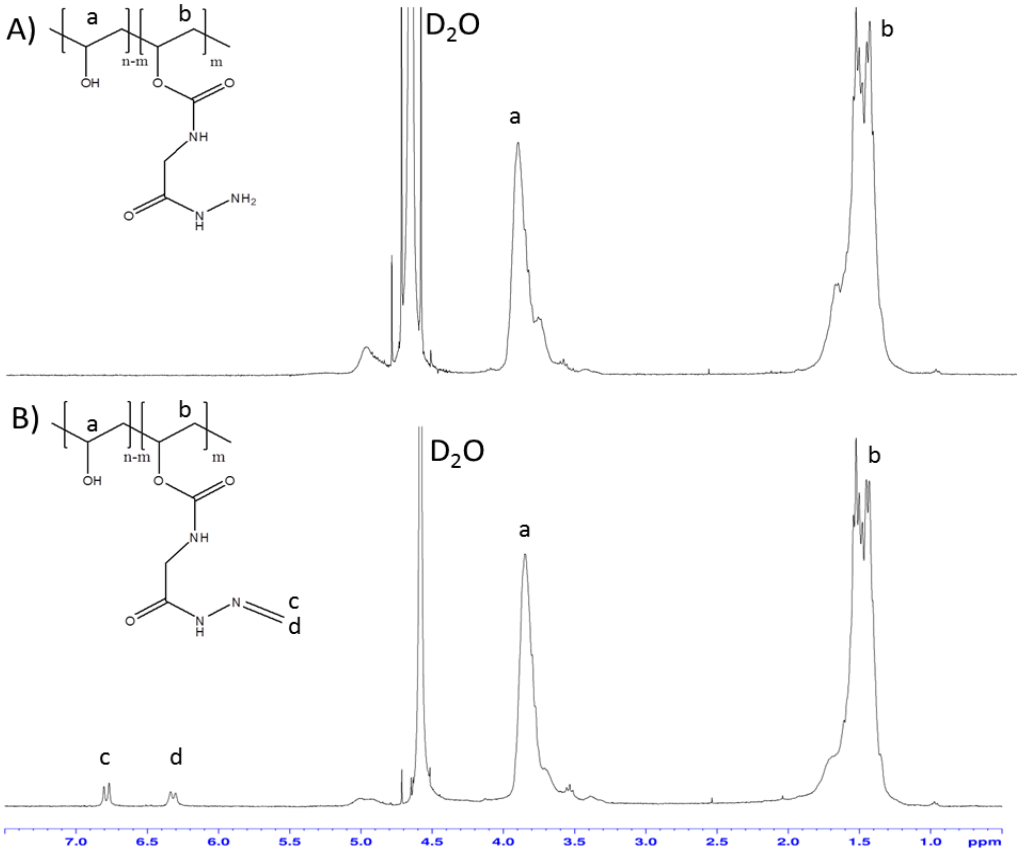

Figure 3.4: ^{1}H NMR spectra of macromers in D_2O: A) PVA-HY; B) PVA-Hydrazone.

After obtaining PVA-HY, HBA was conjugated onto the hydrazide groups using a conventional DCC/NHS coupling reaction. The carboxyl groups of HBA was firstly activated using DCC and stabilised using NHS. An insoluble by product, dicyclohexylurea was formed, as an indication of the successful

activation of the carboxyl groups. PVA-HY was then added to the activated HBA and left to react for 24 hours at RT. However, the reaction solution was observed to crosslink into a solid opague gel (Figure 3.5). It was hypothesised that during the formation of PVA-HBA, the newly formed carbonyl groups could react with remaining PVA-HY in the flask, forming hydrazone bonds that led to crosslinking of the solution (Figure 3.6) [57, 275]. Since the reaction was unsuccessful, further studies on Route 1 were discontinued.

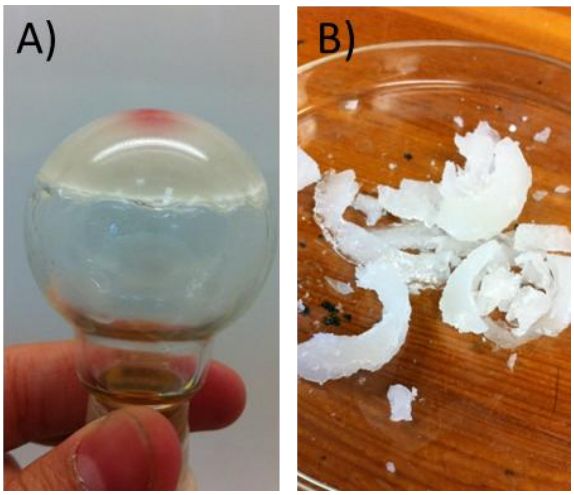

Figure 3.5: Solidification of PVA-HBA synthesis: A) Crosslinked reaction product in round bottom flask; B) Crosslinked reaction product in a petri dish.

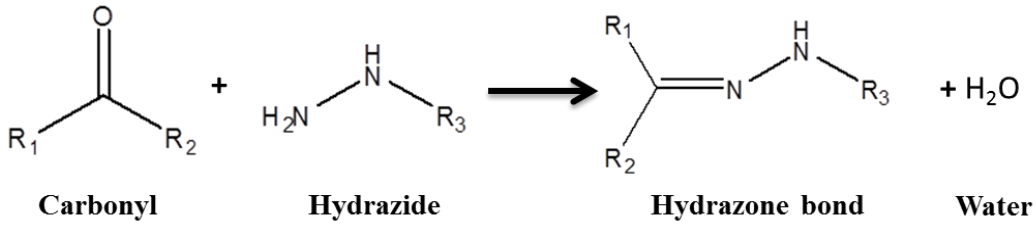

Figure 3.6: Schematic of hydrazone formation between carbonyl groups of PVA-HBA and hydrazide groups of PVA-HY (Adapted from [275]).

3.3.1.2. Synthesis of PVA-COOH and PVA-Tyr (Route 2)

The synthesis of PVA-Tyr was performed in two steps (Figure 3.2). Firstly, the hydroxyl groups of PVA were reacted with SA in the presence of TEA to obtain PVA-COOH. ^{1}H NMR spectra confirmed the conjugation of carboxyl groups onto PVA backbone (Figure 3.7A). The % conjugation was quantified to be 2%, where approximately 7 carboxyl groups were grafted on a PVA chain. This result yielded an efficiency of 100%, which is similar to reports in the literature [271, 276, 277]. The carboxyl groups were then treated with DCC and NHS to form activated ester moieties that were able to react with the amine group of Tyr. Similarly, ^{1}H NMR confirmed the successful functionalisation of Tyr groups, with the appearance of two peaks between 6.5 and 7.5 ppm, which were corresponding to the aromatic ring of Tyr (Figure 3.7B).

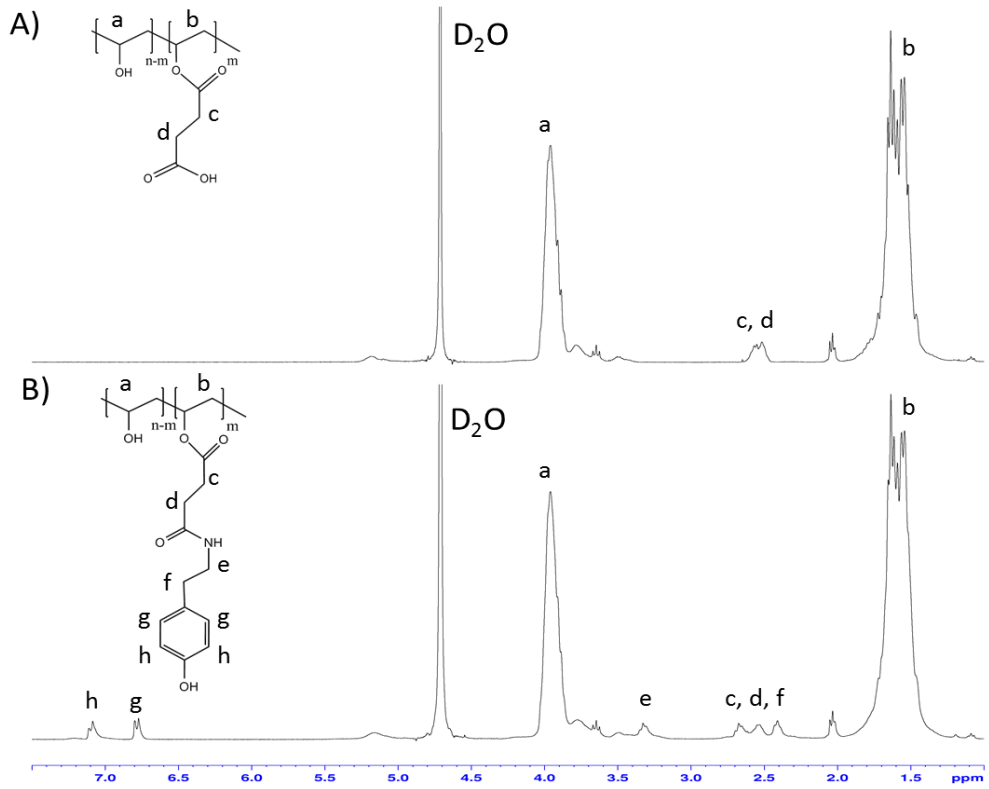

Figure 3.7: ^{1}H NMR spectra of macromers in D_2O: A) PVA-COOH; B) PVA-Tyr.

It has been previously reported in the literature that the carboxyl-amine coupling reaction was not 100% efficient, and excess DCC/NHS was required to drive the reaction [190, 271, 278]. By varying the feed ratio of DCC/NHS to the amount of carboxyl groups grafted on the PVA backbone, it was observed that in order to obtain complete conversion of carboxyl to Tyr groups, the number of moles of DCC/NHS required is 3 times equivalent to the number of moles of carboxyl groups on the PVA chain (Table 3.1). This result agrees with the literature, where excess amount of DCC/NHS was needed to conjugate Tyr groups onto PEO-PPO block copolymers [271]. Similarly, Benoit et al. also showed that carbodiimide/NHS was used in 10 times excess to couple aminated fluorescent labels to carboxyl groups of peptides [278].

Table 3.1: Number of Tyr/PVA chain and reaction efficiency (%), corresponding to the amount of DCC/NHS added to the reaction.

Moles equivalent of DCC/NHS to COOH on PVA backbone	**Number of Tyr/ PVA chain**	**Reaction efficiency (%)**
1:1	5	71.4
1.5:1	5.5	78.6
2:1	6	85.7
2.5:1	6.5	92.9
3:1	7	100
3.5:1	7	100
4:1	7	100

3.3.2. L929 cell growth inhibition assay

As the overall objective of this research is to use these systems as tissue engineering matrices, the cytotoxicity of the synthesised macromers (PVA-COOH and PVA-Tyr) is a vital piece of information, and was initially evaluated by the L929 cell growth inhibition assay. This assay showed relative low cell growth inhibition for the macromer samples as compared to the positive control (ethanol 7.5%, Figure 3.8). Statistical analysis showed that there were no significant differences between the negative control (saline), unmodified PVA, PVA-COOH and PVA-Tyr, in terms of inhibiting L929 cells growth (Figure 3.8).

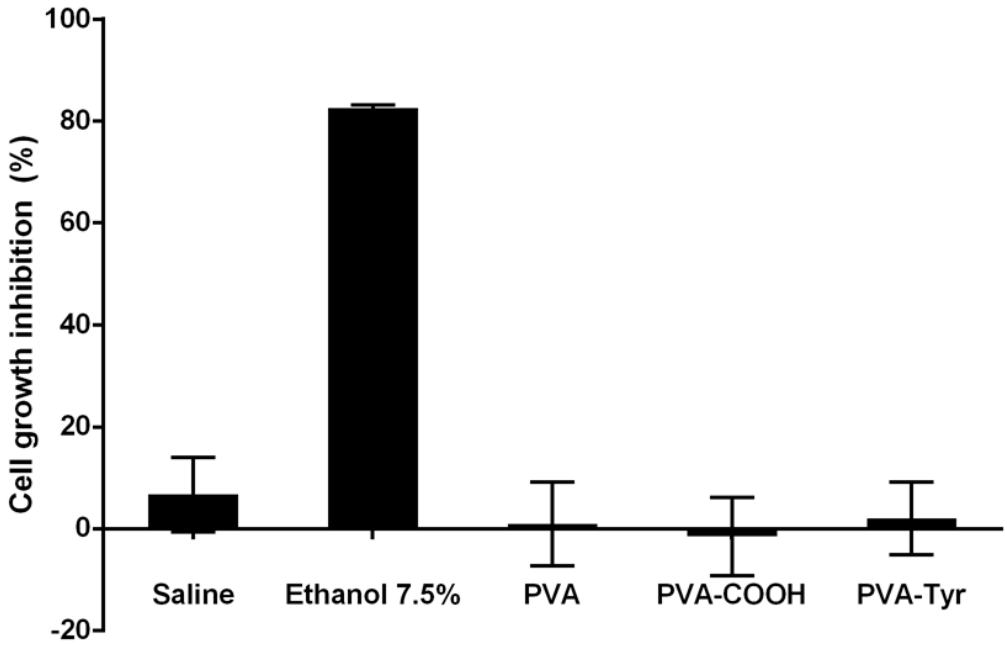

Figure 3.8: Cell growth inhibition of synthesised macromers. No significant differences ($p>0.05$) were observed between saline, PVA, PVA-COOH and PVA-Tyr.

Previous studies have shown that chemically grafting functional groups such as ester acrylates and methacrylates onto PVA resulted in a slight increase

in toxicity as compared to unmodified PVA [9, 72, 244]. However, this phenomenon was not observed for the macromers examined in this study, and might be due to the fact that both carboxyl and Tyr groups are known to be present in native biological molecules, such as proteins. Amino acids, which are basic building blocks of proteins, are known to be composed of carboxyl groups [255, 279] and Tyr is a derivative of tyrosine, which is also a naturally occurring amino acid [280]. Hence, it was hypothesised that the conjugation of these two groups onto PVA would not raise any significant toxicity issues.

3.3.3. Fabrication of PVA-Tyr hydrogels

The next step was to crosslink PVA-Tyr into hydrogels. It was hypothesised that the Tyr groups conjugated onto the PVA backbone could be crosslinked using a system that has only been previously applied to protein crosslinking. In brief, the Tyr groups will form covalent bonds (C-C or C-O-C) when exposed to visible light in the presence of Ru and persulphate (Figure 3.9). Several irradiation conditions have been used in the literature for this type of crosslinking. The light intensities ranged from 15 mW/cm^2 to 3000 mW/cm^2 whereas the irradiation time could be as short as 20 seconds to as long as 1.5 hours [252, 254, 263, 264]. Moreover, different types of persulphates have also been used as the electron acceptor component of this photo-crosslinking system [252, 264]. Hence, this section focuses on using different irradiation conditions to fabricate PVA-Tyr hydrogels.

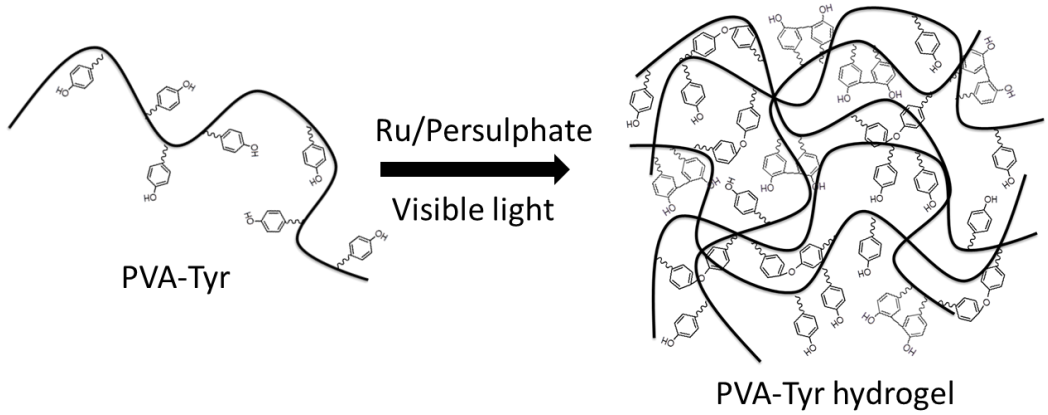

Figure 3.9: Schematic of PVA-Tyr crosslinking using Ru/Persulphate initiating system.

3.3.3.1. Comparison between APS and SPS

For this study, the irradiation conditions were kept constant at 15 mW/cm^2 and 3 minutes. As previously stated in the literature, two types of persulphates (APS and SPS) has been used in combination with Ru to crosslink proteins [252, 264]. However, the difference between these two persulphates, in terms of crosslinking efficiency, has never been reported. Hence in this study, both persulphates were used and compared. The concentration of 2 mM Ru/20 mM persulphate has been previously reported to successfully fabricate protein gels, and this was chosen as the starting point of this study [264].

Table 3.2: Sol fraction and mass swelling ratio, q of PVA-Tyr hydrogels fabricated

Ru (mM)	APS (mM)	SPS (mM)	Sol fraction (%)	Mass swelling ratio, *q*
2	20	-	no gel	
2	40	-	no gel	
2	60	-	53.5 ± 7.9	14.8 ± 3.8
2	80	-	49.7 ± 3.0	13.3 ± 1.5
2	-	20	25.6 ± 4.8	9.71 ± 0.5
2	-	40	16.8 ± 3.6	9.40 ± 0.2
2	-	60	17.8 ± 3.3	9.69 ± 0.3
2	-	80	23.5 ± 4.3	9.26 ± 1.1

No gel was formed using APS at 2 mM Ru/20 mM APS and 2 mM Ru/40 mM APS. However, substituting APS with SPS successfully fabricated PVA-Tyr gels at these concentrations. 2 mM Ru/20 mM SPS and 2 mM Ru/40 mM SPS created hydrogels with sol fraction of 25.6 ± 4.8% and 16.8 ± 3.6% respectively. This result demonstrated that APS and SPS were distinctly different in terms of catalysing this crosslinking reaction. The persulphate anion acts as an electron acceptor during the photo-oxidation of Ru^{2+}, allowing creation of tyrosyl radicals by Ru^{3+}, thus forming covalent crosslinks. Both APS and SPS have been reported to have similar electron accepting ability and there are no studies in the literature that compared the efficiency of these two persulfates in this crosslinking reaction. However, it was previously reported that phenolic amino acids such as histidine facilitates deprotonation of ammonium (NH_4^+) ions [281]. Therefore it was speculated that the presence of phenolic moieties such as tyramine in the system might cause deprotonation of NH_4^+, forming ammonia (NH_3) and protons (H^+),

It was then hypothesised that the protons (H^+) generated would affect the overall pH of the solution, thus decreasing the crosslinking efficiency. It was also previously reported in the literature that antioxidants such as ascorbic acid neutralise free radicals by donating H^+ ions to the free radicals [282]. Therefore, it was further speculated that the produced H^+ might have also quenched the radicals required to crosslink PVA-Tyr during the photo-oxidation.

On the other hand, increasing the concentration of both persulphates did not significantly affect the sol fraction of the PVA-Tyr gels. For APS, although PVA-Tyr hydrogels were only able to be successfully crosslinked at the higher concentrations of 60 mM and 80 mM, the fabricated gels had similar sol fractions of ~50% (Table 3.2). Similarly, increasing the concentration of SPS yielded hydrogels of similar sol fractions to each other, however these were in the range of 16 – 25% (Table 3.2), which is significantly lower than the APS gels. This result agrees with previous findings where the persulphate was just an electron acceptor and does not take part in the crosslink formation. Although there was speculation that the sulphate radicals dissociated from the persulphate might also contribute to the formation of tyrosyl radicals, a study conducted by Fancy et al. showed that quenching the sulphate radicals with ethanol did not affect the crosslinking process [252]. Moreover, these sol fraction values are similar to other chemically modified PVA with the same macromer content (20 wt%). For example, UV polymerised methacrylated PVA (PVA-MA) had a sol fraction around 20% [244], while acrylated PVA crosslinked through redox initiation had a sol fraction less than 30% [283].

The mass swelling ratio (q) showed that hydrogels with higher sol fraction had larger amount of water in the network. This result agrees with

previous findings where a less crosslinked network (higher sol fraction) allows more water to be entrapped in the network. The *q* of the PVA-Tyr gels fabricated using SPS was around 9, which was slightly higher than PVA-MA hydrogels (*q* = 6) [244]. This observation might be due to the difference in the crosslinking mechanism between the two systems. PVA-MA is a radical chain polymerization where upon photo-initiation radicals propagate through the methacrylate groups forming new kinetic chains. Whereas for the newly synthesised PVA-Tyr, the network was formed through the coupling of the Tyr groups [252, 254, 262]. This difference could result in larger mesh size in the PVA-Tyr hydrogels, hence the higher water content and increased *q*. Overall the initiator concentration 2 mM Ru/20 mM SPS was sufficient to produce hydrogels of good quality, and was chosen for all further experiments.

3.3.3.2. Irradiation conditions determination for crosslinking PVA-Tyr

It was previously reported in the literature, that light intensities ranging from 15 mW/cm^2 to 3000 mW/cm^2 were used to crosslink proteins. However, these irradiation conditions have only been applied to proteins and not synthetic polymers. In this section, a range of light intensities and exposure times was examined. From a biomedical stand point, weaker light intensity and shorter exposure time correlate to a smaller irradiation dosage, and are therefore theoretically safer for use in tissue engineering applications [284, 285]. Hence, the aim was to find minimal light intensity and exposure time that was required to form high quality PVA-Tyr hydrogels.

Fancy et al showed that an exposure time as short as 30 seconds was enough to crosslink fibrinogen and gelatin [254, 264]. This phenomenon was

also reflected in this study, where PVA-Tyr gels were successfully fabricated after 30 seconds. However, the minimum light intensity required was 10mW/cm^2, as no gel was formed with 5 mW/cm^2 (Table 3.3). Increasing the light intensity to 15 mW/cm^2 and 20 mW/cm^2 caused a decrease in sol fraction. This phenomenon has also been shown previously in the literature, where higher light intensities resulted in greater polymerisation rate, which lead to more crosslinks formed from acrylated and methacrylated macromers [286-288]. It was postulated that in this study that the rate of Ru^{3+} generation escalated with the light intensity, causing more di-tyrosine and ether crosslinks formation.

Table 3.3 Sol fraction (%) of PVA-Tyr gels irradiated for 30 seconds at different intensities

Intensity (mW/cm^2)	**Sol fraction (%)**
5	No gel
10	56.2 ± 4.4
15	30.1 ± 2.5
20	29.2 ± 3.1

According to Figure 3.10, there is a general trend where the sol fraction decreases with increasing exposure time for all intensities tested, reaching a plateau of around 16 - 22% sol fraction. The number of tyramine groups that are reported is a calculated average based on the assumption that the molecular weight of PVA is 16 kDa. Therefore, fractions of PVA may have no tyramine groups attached and other PVA chains will have more tyramine groups that reported. This variation is partially responsible for the sol fraction (16 ~ 22%).

This range of sol fractions is comparable to other studies done on similar polymers. For example, previous studies done on methacrylated PVA hydrogels using the same unmodified PVA as starting material and having similar number of functional groups/chain (7 methacrylates/PVA) have been reported to have sol fraction of ~20% [9, 200]. Lower light intensities require longer exposure time to achieve the minimal sol fraction, where both 5 mW/cm^2 and 10 mW/cm^2 required around 7.5 minutes to obtain completely crosslinked PVA-Tyr hydrogels. On the other hand, the sol fraction for PVA-Tyr gels fabricated from both 15 mW/cm^2 and 20 mW/cm^2 plateaued around 3 minutes. This result is due to higher light intensities provide more energy to activate Ru^{2+}, which subsequently generates tyrosyl radicals at a faster rate, thus leading to formation of the hydrogel network at a higher efficiency. Another explanation for the variation in sol fraction is related to the amount of light that is available for the polymerisation throughout the entire thickness of the sample. It has been reported that the amount of irradiated light varies with the depth of polymerisation [273]. In this study, it was calculated that for incident light intensity of 5 mW/cm^2 at the sample surface, only 0.27 mW/cm^2 remains at the bottom of the curing depth. Comparatively, 1.08 mW/cm^2 of light still remains at the bottom of the sample for 20 mW/cm^2 light intensity at the sample surface. Therefore, it was hypothesised that longer curing time may be required for the lower incident light intensities at the sample surface to achieve complete crosslinking of the PVA-Tyr gels.

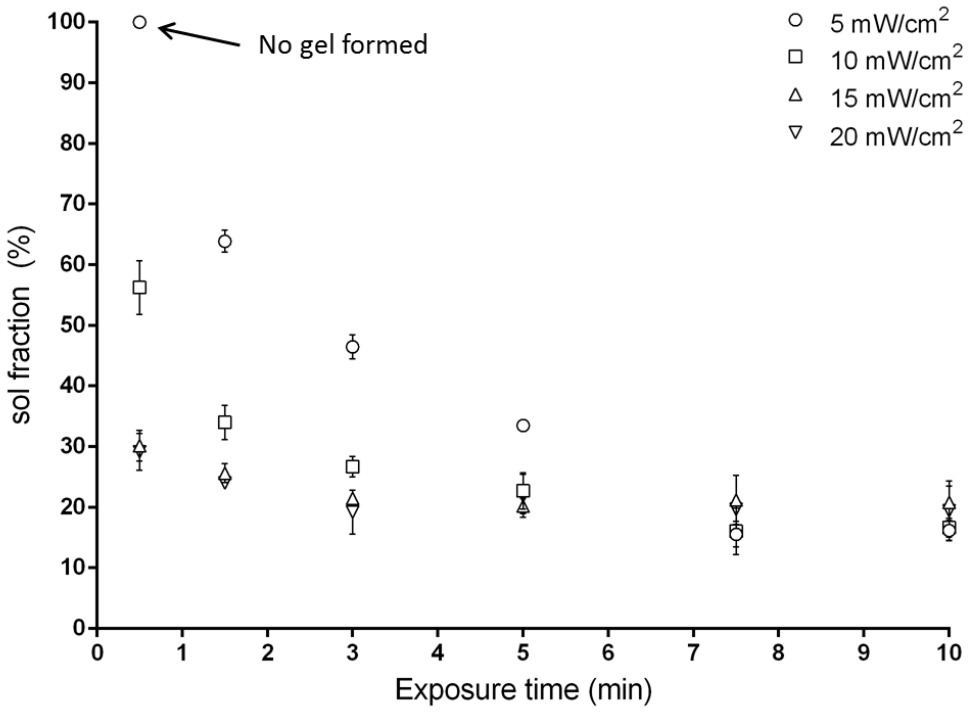

Figure 3.10: Sol fraction (%) of PVA-Tyr hydrogels as a function of exposure time (min) at different visible light intensities.

3.4. Conclusion

This chapter has demonstrated the synthesis of phenolated PVA using a conventional DCC/NHS system. The resulting PVA-Tyr could be crosslinked into hydrogels using the visible light initiated Ru/persulphate system that has previously only been used for protein-protein crosslinking. Comparison done between APS and SPS showed that the latter is more suitable to be used in combination with Ru to fabricate PVA-Tyr hydrogels. The initiators concentration of 2 mM Ru/20 mM SPS, and irradiation conditions of 15 mW/cm2 and 3 minutes, were studied to produce good quality PVA-Tyr gels. Moreover, it was also noted that the synthesised PVA-Tyr has ester linkages which may be hydrolysable. Hence, the next chapter will focus on evaluating the degradability of PVA-Tyr hydrogels, as well as understanding and tailoring the degradation of the gels.

Chapter 4

Understanding and Tailoring the Degradation of PVA-Tyramine Hydrogels

4.1. Introduction

A major consideration in cell encapsulation for tissue engineering applications is the hydrogel degradation behaviour. Degradation can be either enzymatic or hydrolytic, depending on the type of degradable linkages present in the crosslinked network. The majority of hydrogels designed to degrade via hydrolysis contain ester linkages located either in the crosslink or the backbone of the hydrogel. For example, polylactic acid (PLA), polyglycolic acid (PGA) and their copolymer, poly(DL-lactic acid-co-glycolic acid) (PLGA) have been incorporated into a range of hydrogels and are hydrolysable via their ester linkages [135, 289, 290]. Acrylated poly(ethylene glycol) (PEG) hydrogels that are known to be non-degradable have been shown to be hydrolysable when PLA was introduced between the PEG backbone and acrylate end groups [193, 291]. Hydrogels fabricated from PLA-PEG-PLA triblock copolymers had degradation rates that were dependent on the length of the PLA segments. Wang et al. showed that faster degradation occurred with increasing length of PLA segments [291]. Other hydrolytically degradable polymers such as poly(ε-caprolactone) (PCL) and poly(propylene furmarate) (PPF) were also copolymerised with PEG to form degradable hydrogels [292, 293]. Both Martens et al. and Mawad et al. reported that by incorporating ester groups into acrylate crosslinks conjugated onto PVA, the resultant hydrogels were hydrolytically degradable [72, 97, 294].

The mechanisms of ester bond hydrolysis have been extensively studied in the literature. It was found that at different conditions (i.e., neutral, acid and base) the esters undergo different hydrolysis mechanisms. In case of neutral hydrolysis, a water molecule extracts a hydrogen atom from another water molecule, releasing hydroxide ions, which eventually attacks the carbonyl carbon

of the esters [295]. Base-catalysed hydrolysis is very similar to neutral hydrolysis, where the abundant hydroxide nucleophiles present in the environment initiate the ester bond hydrolysis [296, 297]. On the other hand, during acid-catalysed hydrolysis, the ester carbonyl is firstly protonated to make it more electrophilic to react with water [298]. Although all three hydrolysis mechanisms are different, similar end products, a carboxylic acid and an alcohol, are obtained (Figure 4.1) [299]. Bergmann et al. showed that the rate of ester hydrolysis is pH dependent, where the rate increases with the acidity or alkalinity of the environment [300]. It has also been reported that heat can accelerate the hydrolysis rate by providing more energy to the reactants to overcome the activation energy required to initiate the hydrolysis reaction [295, 296].

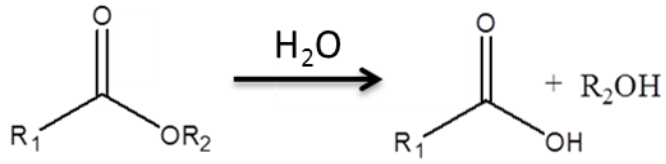

Figure 4.1: Hydrolysis of ester bonds.

The hydrolysis kinetic of the ester bonds also varies depending on the chemical structure of the ester [6, 301], as well as other factors such as polymer crystallinity and wettability [302]. It was reported that ester bonds associated with PLA degrades much more rapidly than ester linkages of PCL [1, 112]. Moreover, changes made to the polymer structure and size may also affect the degradation. For example, bulk PLA has been shown to degrade in both acidic and basic environments, whereas PLA brushes only degrade in basic conditions [303, 304]. Conversely, other studies of crosslinked polymers containing esters in the crosslink have demonstrated that their gels are non-degradable on the time

scales studied. Hennink et al. have reported that dextran hydrogels with high crosslinking density were resistive to hydrolysis despite having an ester group in the crosslinks [305]. Hydrogels formed from PVA conjugated with an ester containing methacrylate moiety were also not hydrolytically degradable [244, 306].

Another important parameter of the design of hydrogel matrices for tissue engineering application is the hydrogel degradation rate. It has been previously reported that the rate of degradation must match the secretion of newly synthesised ECM [1]. Typical mesh sizes of PEG and PVA gels used for cell encapsulation ranged from ~40 to 200 Å, which are significantly smaller than the size of a cell (e.g., mammalian stem cells are ~30 μm) [1, 19, 92, 202, 307]. As the gel degrades, the mesh size increases, thus allowing the migration of encapsulated cells and ECM secretion [77]. If degradation occurs too slowly, there will be an accumulation of ECM in the peri-cellular region [1, 18]. This accumulation may affect cell behaviour and the type of tissue produced due to masking of intracellular signals required for tissue growth [1, 18, 308]. On the other hand, if degradation occurs too quickly, the hydrogel will dissolve and cells will leach out of the scaffold [1]. The degradation rate of hydrogels can be tailored according to the number of degradable linkages, degree of crosslinking and the rate constant for hydrolysis [294]. Martens et al. successfully tailored the degradation of PVA ester acrylate gels from 1 to 12 to 35 days by varying the macromer concentration from 10 to 15 to 20 wt% respectively [294]. Moreover, increasing the crosslinking density of the PVA ester acrylate gels from 0.3 to 0.64 mol/L by fabricating the gels using macromers of different molecular weights also increased the degradation time from 12 to 45 days [294].

As noted in Chapter 3, the synthesised PVA-Tyr macromer has ester bonds which may be hydrolytically degradable. Therefore, this chapter will focus on understanding the degradation behaviour of the fabricated PVA-Tyr hydrogels. The aims were to determine if the gels were actually degradable, and if so, characterise the degradation profiles of PVA-Tyr hydrogels in various incubation conditions (pH and temperature), as well as tailoring the degradation rate by changing the hydrogel macromer content. Moreover, in order to use this system as cell encapsulation matrices, the cytotoxicity of the degradation products was also examined.

4.2. Experimental

4.2.1. Materials

Poly(vinyl alcohol) (PVA) (13-23 kDa, 98% hydrolysed), succinic anhydride (SA), triethylamine (TEA), 1,3-Dicyclohexylcarbodiimide (DCC), N-hydroxysuccinimide (NHS), tyramine (Tyr), sodium persulphate (SPS), 1,1-carbonyldiimidazole (CDI), tris(2,2-bipyridyl)dichlororuthenium(II) hexahydrate (Ru(II)bpy_3^{2+}), deuterium oxide (D_2O), molecular sieves (4 Å), Dulbecco's phosphate buffered saline (DPBS), dialysis tubing (10 kDa molecular weight cut-off), Eagle's minimum essential media (EMEM), trypsin, fetal bovine serum (FBS), and penicillin streptomycin (PS) were purchased from Sigma-Aldrich and used as received. Dimethyl sulfoxide (DMSO) was bought from Ajax Chemicals and was dried over 4 Å molecular sieves. Hydrogel disc moulds were made from silicone sheets (Silastic®Sheeting, reinforced medical grade silicone rubber, Dow Corning).

4.2.2. Macromer preparation

4.2.2.1. Synthesis of PVA-Tyr

PVA-Tyr was synthesised as outlined in Chapter 3. The PVA-Tyr used in this chapter was characterised to be 2% tyraminated (7 Tyr per PVA chain).

4.2.2.2. Fabrication of PVA-Tyr hydrogels

Dried PVA-Tyr was dissolved in DPBS at 80 °C. Upon complete dissolution, the polymer solution was cooled to RT. The initiators (Ru and SPS) were then added to the solution. The macromer solution was then scooped into

silicon moulds (5 mm diameter x 1mm thick) sandwiched between two cover slips. The samples were then irradiated under visible light of 400 – 450 nm (Blue wave 200, Dymax Co.).

4.2.3. Swelling and mass loss analysis

Directly after polymerisation, all samples were weighed for the initial wet mass ($m_{\text{initial, t0}}$) and three samples were immediately lyophilised to obtain their dry weights ($m_{\text{dry ,t0}}$). The actual macromer concentration was calculated based on the equation below:

$$\%\, macromer = \frac{m_{dry,\, t0}}{m_{initial,\, t0}}\ x\ 100 \tag{4.1}$$

These samples were then submerged in a sink of saline solution and incubated. Samples were removed from the incubator after 1 day, blotted dry and weighed (m_{swollen}). The swollen samples were then freeze-dried and weighed again (m_{dry}). The mass swelling ratio (q) and mass loss were calculated as follows:

$$q = \frac{m_{swollen}}{m_{\text{dry}}} \tag{4.2}$$

$$mass\ loss\,\% = \frac{m_{i,\, dry} - m_{dry}}{m_{i,\, dry}}\ x\ 100 \tag{4.3}$$

The sol fraction is given by the mass loss at 1 day, where previous studies conducted in the lab have shown that non-crosslinked polymers will dissolve out from the hydrogel network (incubated in 37 °C and DPBS) within this time frame [9, 244]. Images of the gels were taken using the Leica M80 stereo microscope at 0.75x magnification. The samples were monitored daily until

complete degradation was observed. The time required for complete degradation was measured.

The effective macromer percentage at day 1 was calculated by the equation below:

$$Effective\ macromer\ percentage = \frac{m_{dry,\ t=1}}{m_{swollen,\ t=1}}\ x\ 100 \quad (4.4)$$

The crosslinking density (ρ_x) was calculated using the equations below [202, 309]:

$$\frac{1}{\overline{M_c}} = \frac{2}{\overline{M_n}} - \frac{(\bar{v}/V_1)\left[ln(1-\upsilon_{2,s}) + \upsilon_{2,s} + \chi\upsilon_{2,s}^2\right]}{\upsilon_{2,r}\left[\left(\frac{\upsilon_{2,s}}{\upsilon_{2,r}}\right)^{\frac{1}{3}} - \frac{1}{2}\left(\frac{\upsilon_{2,s}}{\upsilon_{2,r}}\right)\right]} \quad (4.5)$$

$$(\bar{r}_0^2)^{1/2} = l\left(\frac{2\overline{M_c}}{M_r}\right)^{\frac{1}{2}} C_n^{1/2} \quad (4.6)$$

$$\xi = \upsilon_{2,s}^{-1/3}(\bar{r}_0^2)^{1/2} \quad (4.7)$$

$$\rho_x = \frac{1}{\bar{v}\,\overline{M_c}} \quad (4.8)$$

Where;

Mc: Number average molecular weight between crosslinks

Mn: Number average molecular weight in the absence of any crosslinking (16000 g/mol for PVA)

υ: The specific volume of the polymer (0.788 for PVA)

V_1: The molar volume of the solvent

$\upsilon_{2,s}$: The equilibrium polymer volume fraction

$\upsilon_{2,r}$: The polymer volume fraction after crosslinking but before swelling

$(r_0^2)^{1/2}$: End to end distance of the unperturbed (solvent free) state

χ: The polymer solvent interaction (0.49 for PVA in water)

l*:* The bond length (1.54 Å for PVA c-c bond)

M_r: Molecular weight of the repeating unit (44 for PVA)

C_n: The characteristic ratio (= 8.9 for PVA)

The assumptions associated with these equations are: tetrafunctional arrangement of the crosslinks, Gaussian distribution of the crosslinked polymer chains, and the formation of an ideal network (no cyclisation and chain interaction) [19, 110].

4.2.4. Recovery of PVA-Tyr macromers post hydrolytic degradation

20 wt% PVA-Tyr hydrogels were completely degraded at physiological conditions (pH = 7.4 and 37 °C). The degradation solution was then dialysed (10 kDa molecular weight cut-off) against water, freeze-dried, and characterised by ^{1}H NMR.

4.2.5. Effect of different incubation conditions on degradation of PVA-Tyr hydrogels

4.2.5.1. Effect of pH on hydrolytic degradation of PVA-Tyr hydrogels

Fabricated 20 wt% PVA-Tyr hydrogels were immersed in various pH saline solutions of (2, 6, 7.4, 10 and 12), then incubated at 37 °C. The mass loss and mass swelling ratios of the gels were calculated using equations 4.1 – 4.3. The pH was measured at time points 1, 3, 7, 10, 14 and 21 days. No changes in pH were observed, indicating that the degradation products did not affect the overall pH of the solution.

4.2.5.2. Effect of temperature on hydrolytic degradation of PVA-Tyr hydrogels

Fabricated 20 wt% PVA-Tyr hydrogels were immersed in DPBS (pH=7.4) and incubated at various temperatures (20, 30, 37, 50 and 60 °C). At the pre-determined time points, the mass loss and mass swelling ratios of the samples were calculated using equations 4.1 - 4.3.

4.2.6. Effect of varying macromer concentration on physical properties of PVA-Tyr hydrogels

4.2.6.1. Tailoring the degradation of PVA-Tyr hydrogels

PVA-Tyr hydrogels of 10, 15 and 20 wt% were fabricated as outlined in section 4.2.2.2. The sample names correspond to the nominal initial wt% of the gels (e.g., 10% PVA-Tyr). The gels were then immersed in DPBS (pH = 7.4) and incubated at 37 °C. Equations 4.1 – 4.3 were used to calculate the mass loss and mass swelling ratios corresponding to the fabricated samples.

4.2.6.2. Compression testing

The mechanical properties of the PVA-Tyr hydrogels were characterised using unconfined uniaxial compression testing at room temperature. Samples (5 mm diameter x 1 mm thick) were immersed in DPBS and incubated at 37 °C. At pre-determined time points (0, 1, 3, 7 and 10 days) the samples were removed from DPBS and compressed at a strain rate of 1mm/min using an Instron 5543 mechanical tester. The slope of the linear regression of the stress-strain curve generated within 5 - 15% strain was used to calculate the compressive modulus (K).

4.2.7. L929 cell growth inhibition assay

Degradation samples were prepared by immersing fabricated 20% PVA-Tyr hydrogels in media at 1.5 cm^2/mL. At various time points (1, 7 and 21 days), the degradation products were collected. The positive control used in this study was latex, and the negative control was saline. Murine dermal fibroblasts (L929) were cultured in EMEM supplemented with 10% FBS and 1% PS. $5x10^4$ cells/mL were seeded onto 35mm diameter tissue culture dishes. After 24 hours of incubation at 37 °C in a 5% CO_2 humidified atmosphere, the media was discarded and 1mLl of sample solution was added to the cells. Following an additional 48 hours of incubation, the cells were trypsinised, and counted with a cell viability analyser (Vi-cell XR, Beckman Coulter). The percentage cell growth inhibition was calculated by the following equation:

$$\%\ Cell\ growth\ inhibition = 1 - \frac{number\ of\ cells\ in\ sample\ dish}{number\ of\ cells\ in\ media\ control\ dish} \times 100 \quad (4.9)$$

4.2.8. Statistical analysis

All samples for each swelling and mass loss study were prepared in triplicates, and each study was repeated three times. Two-way ANOVA was used to determine the significance of the results using Minitab 15 statistical analysis software.

4.3. Results and discussion

4.3.1. Understanding the mechanism of PVA-Tyr hydrogels degradation

It was hypothesised that PVA-Tyr hydrogels would be hydrolytically degradable due to the presence of ester bonds in the macromer. By immersing the fabricated 20% PVA-Tyr hydrogels in PBS (pH = 7.4) at 37 °C, it was observed that the hydrogel degrades completely within 19 days (see section 4.3.2. for the full degradation profile). ^{1}H NMR was conducted to determine the degradation mechanism. Comparison of the degraded polymer spectra with the originally synthesised macromers clearly illustrates that the original PVA is regenerated. The signals corresponding to tyramine (indicated by arrows) conjugated onto PVA were below the NMR detection limit (less than 1% remains) in the degraded polymer spectra (Figure 4.2). This result further supports the hydrolytic degradation of the ester bonds which are directly next to the PVA backbone.

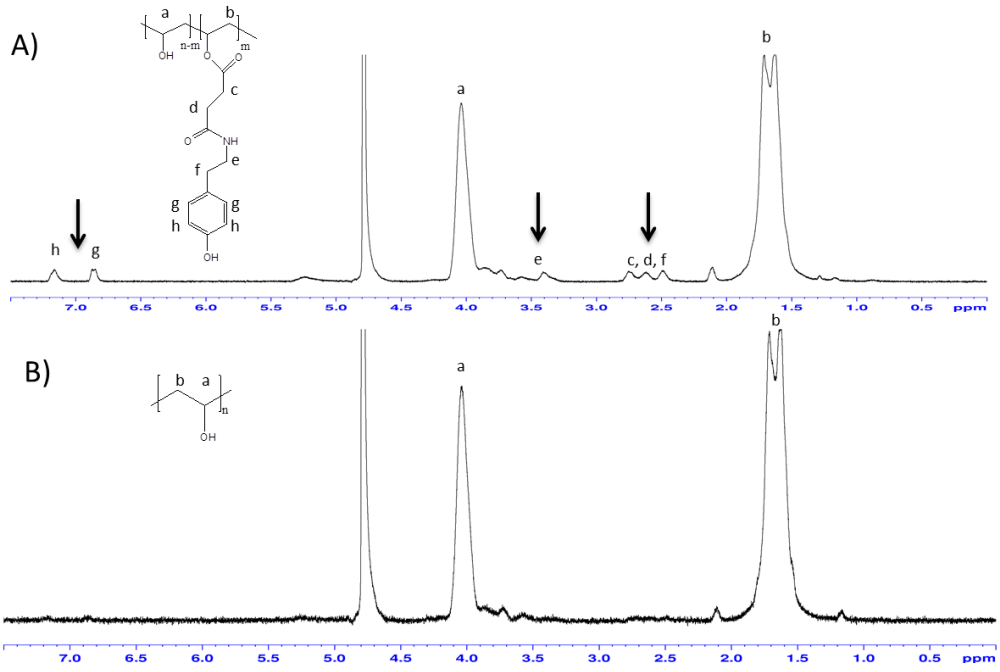

Figure 4.2: ^{1}H NMR spectra of macromers in D_2O: A) PVA-Tyr; B) Degradation products post dialysis against water (>10 kDa).

4.3.2. Degradation of PVA-Tyr hydrogels at different incubation conditions

4.3.2.1. Effect of pH on degradation profile of PVA-Tyr hydrogels

The behaviour of PVA-Tyr hydrogels at neutral, acidic and basic conditions was examined. Surprisingly, it was observed that the PVA-Tyr gels did not degrade in acidic environments (pH =2 and 6, Figure 4.3), and the mass loss remained constant in the range of ~20% to 30% throughout the study.

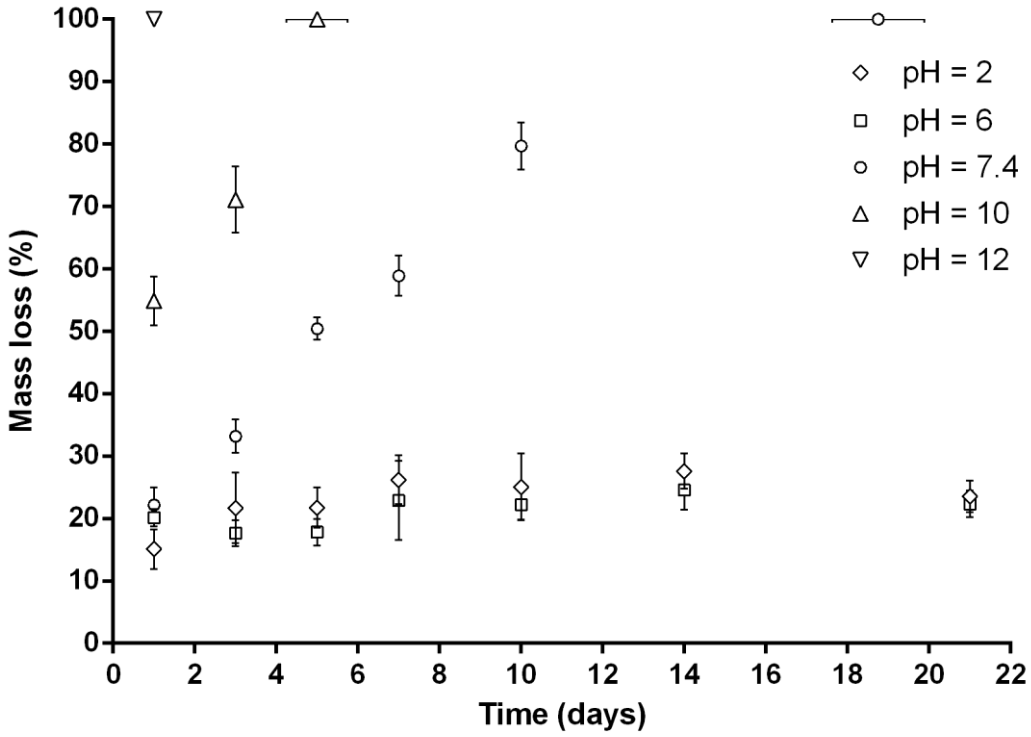

Figure 4.3: Mass loss profiles of PVA-Tyr gels at different pH. Temperature was kept constant at 37 °C. No significant differences ($p<0.05$) were observed between samples in pH 2 and 6 for all time points. The samples in pH 7.4, 10 and 12 were statistically different for all time points ($p>0.05$).

It was believed that this initial loss corresponds to the non-crosslinked macromers (sol fraction) diffusing out from the gel, and agrees with previous sol fraction values reported in Chapter 3 (25.6 ± 4.8%). At pH = 7.4, hydrogel

degradation occurred with a linear degradation profile where the gels completely dissociated within 18 days. In a basic environment the degradation was accelerated, where the samples were completely degraded within 5 and 1 day at pH = 10 and 12, respectively (Figure 4.3.).

This result was unexpected as it has been shown that increasing acidity *or* alkalinity resulted in faster hydrolysis rates for carboxylic ester and phosphoester groups [295, 300]. Conversely, the PVA-Tyr hydrogels in this study only degraded in pH $\geq$ 7.4. This observation suggests that although degradation occurred at the ester bonds present in the hydrogel network, other chemical groups around the ester bonds, such as the aromatics/phenols of the tyramine moieties might have affected the hydrolysis. Ghandehari et al. also showed that hydrogels containing azoaromatic crosslinks were stable in acidic environment but degradable in basic conditions [310]. It was speculated that these gels had low levels of ionisation in an acidic environment which hindered the accessibility of the degradable bonds, thus no degradation occurred [310]. Similarly, hydrogels containing weak acid groups such as carboxylic acid were also reported to be pH sensitive with higher ionisation levels in basic media compared to acidic media [310-313]. For example, hyaluronic acid hydrogels crosslinked through hydrazides were shown to be stable in acid but degradable in basic environments due to the different ionisation levels of pendant carboxyl groups in the network [312]. The higher ionisation level leads to greater water uptake into the gels, which subsequently cause faster degradation [312]. As the pendant phenol groups in PVA-Tyr are also weak acids, it was then hypothesised in this study that the lack of ionisation in acidic solutions was the cause of the non-degradable behaviour observed at pH < 7.4. This statement agrees with previous

work done by Riegelman et al. where the degree of ionisation of the phenol groups of phenylephrine and tyramine was shown to increase with pH [314]. Therefore it was speculated that more water was entrapped in the PVA-Tyr hydrogels in basic conditions due to the higher ionisation level. The increment in water uptake contributes to the faster degradation observed in this study.

Similarly, the mass swelling ratios (*q*) of PVA-Tyr hydrogels incubated in acidic saline remained constant over the time period of the study (Figure 4.4).

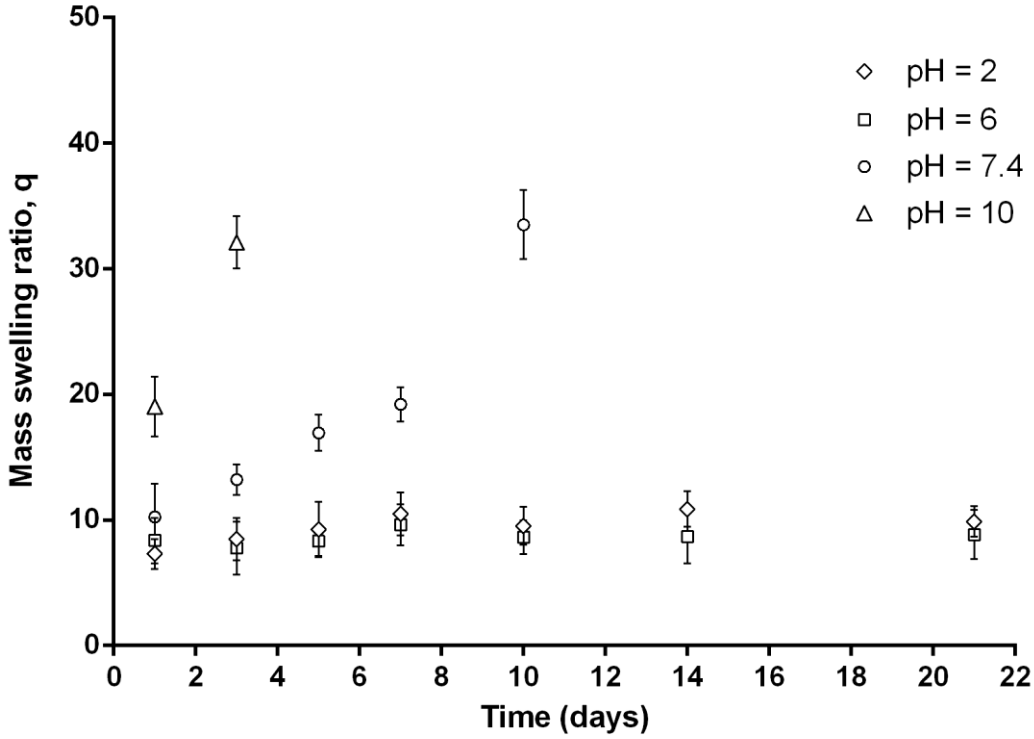

Figure 4.4: Mass swelling ratio, q of PVA-Tyr gels at different pH. The temperature was kept constant at 37 °C. No significant differences ($p<0.05$) were observed between samples in pH 2 and 6 for all time points. The samples in pH 7.4, and 10 were statistically different for all time points ($p>0.05$).

This result agrees with the mass loss study where no degradation occurred at pH = 2 and 6. At pH = 7.4 and 10, it was shown that the *q* increases over time

linearly as per the degradation profile. As the hydrogel is degrading, the crosslinks are being cleaved leading to formation of larger mesh sizes that allow more water to be imbibed in the network [315]. Similarly, the q in basic conditions (pH = 10) are significantly higher when compared to physiological conditions (pH = 7.4) at respective time points (Figure 4.4.). Once again, this observation is attributed to the faster degradation occurring in basic environments.

The pH sensitive degradation of PVA-Tyr hydrogels highlights the potential of using these hydrogels for oral specific drug delivery applications. For example, at gastric pH ~1.4, the hydrogels are non-degradable. However, at enteric pH ~7.4, degradation occurs and drugs loaded in the gels will be gradually released permitting sustained and localised drugs delivery [316].

4.3.2.2. Effect of temperature on degradation profile of PVA-Tyr hydrogels

Next, the effect of temperature on the degradation of PVA-Tyr hydrogels was examined. No sign of degradation was observed when the PVA-Tyr gels were kept at 20 °C, where mass loss values were consistent with the sol fraction percentage (~20% to 30%) for all the time points (Figure 4.5). When the temperature was increased to 30 °C, a slow degradation was noted. Further increasing the temperature to 37, 50 and 60 °C yielded linear degradation profiles where the gels were all completely degraded within 19, 3 and 1 day, respectively (Figure 4.5).

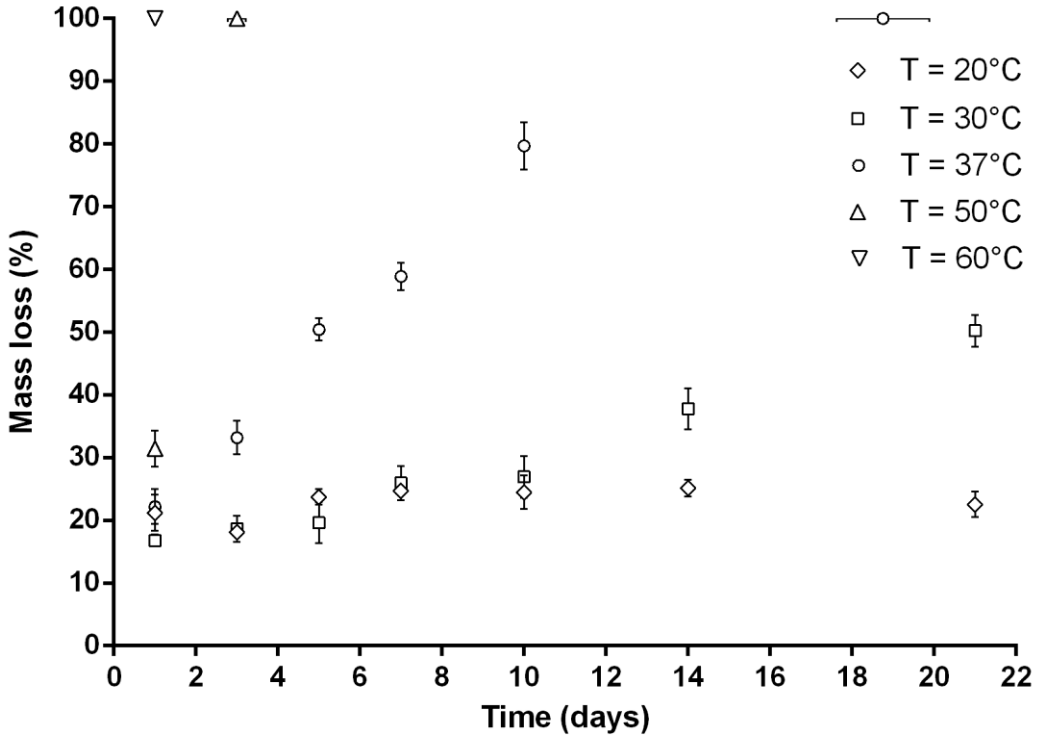

Figure 4.5: Mass loss profiles of PVA-Tyr gels at various temperatures. The pH was kept constant at 7.4. Statistical analysis was done on the regression of the degradation profiles. All samples were statistically different ($p<0.05$).

These observations agree with the literature where ester hydrolysis at neutral pH can be accelerated with heat. Xu et al. showed that PLA hydrogel brushes degraded more rapidly at higher temperature [303]. Comisar et al. also reported that hydrolysis rate constants of esters increase with temperature [298]. At elevated temperature, more thermal energy is provided to the system to facilitate the hydrolysis of ester bonds, hence the faster degradation rate achieved [296].

Again the swelling values correlate nicely with the mass loss data. The *q* of PVA-Tyr gels remained constant (~10) at 20 °C, which was the temperature where no degradation was observed (Figure 4.6). As degradation only started to

happen when heat was applied to the system, the increase in *q* over time was also only observed at elevated temperatures (30, 37, and 50 °C) (Figure 4.6).

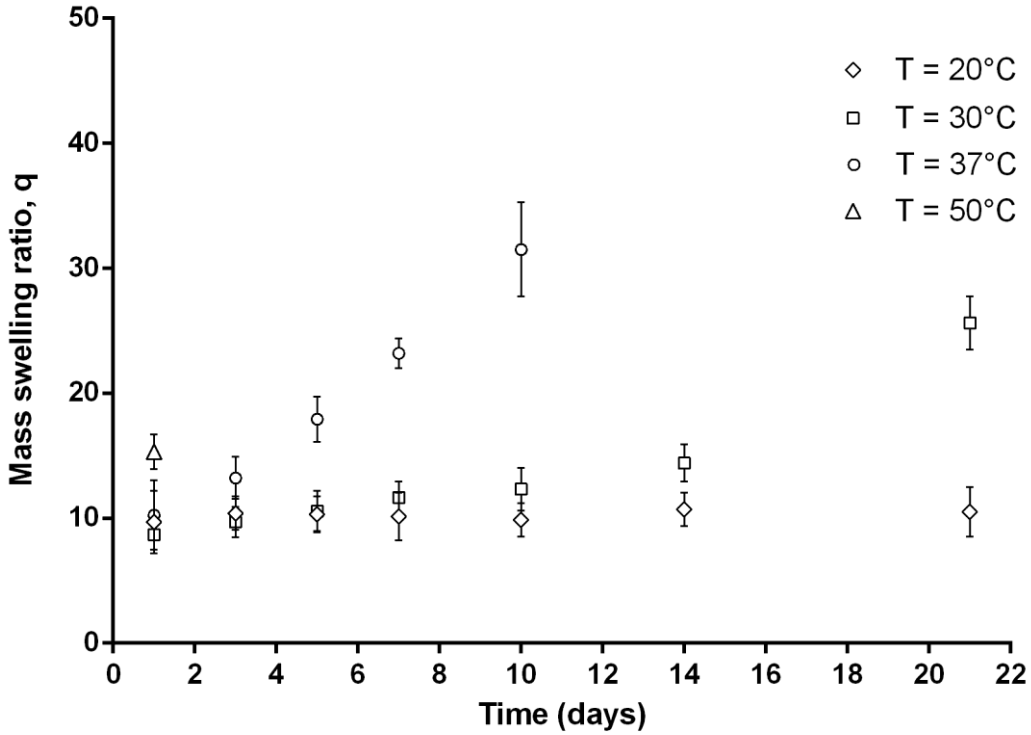

Figure 4.6: Mass swelling ratio, q of PVA-Tyr gels at different temperatures. The pH was kept constant at 7.4. Statistical analysis was done on the regression of the degradation profiles. All samples were statistically different ($p<0.05$).

4.3.3. Tailoring degradation of PVA-Tyr hydrogels by varying macromer concentration

It has been shown in other systems that the degradation rates of hydrogels can be tailored by altering the macromer content [89, 97, 294]. In this study, the degradation profiles of 10%, 15% and 20% PVA-Tyr hydrogels were examined. The pH (7.4), temperature (37 ºC) and concentration of initiators (2 mM Ru/20 mM SPS) were kept constant for all three macromer contents.

Firstly, the sol fraction of the fabricated hydrogels was evaluated. It was shown that 10% PVA-Tyr has the lowest sol fraction (15% sol fraction), followed by 15% PVA-Tyr (20% sol fraction) and 20% PVA-Tyr (22% sol fraction) (Table 4.1).

Table 4.1: Physical properties of 10%, 15% and 20% PVA-Tyr hydrogels

Sample name	**Sol fraction (%)**	**Effective macromer percentage (wt%)***	**Mass swelling ratio, *q***	**Crosslinking density, ρ_x (x10^4 mol/L)#**
10% PVA-Tyr	14.9 ± 2.7	12.2 ± 0.6	8.14 ± 0.56	2.95 ± 0.19
15% PVA-Tyr	19.1 ± 4.2	10.7 ± 1.0	9.46 ± 0.84	2.39 ± 0.17
20% PVA-Tyr	21.4 ± 3.4	10.0 ± 0.7	10.1 ± 0.77	2.11 ± 0.13

** As determined from the mass loss and swelling at 24 hours (Equation 4.4)*

 # Calculated from the equations 4.5 -4.8

This result does not agree with the literature, where sol fraction has generally been reported to decrease with increasing nominal macromer concentration [317]. Moeinzadeh showed that increasing the macromer concentration of poly(ethylene oxide-co-lactide-glycolide acrylate) hydrogels from 10 to 25 wt% successfully decreased the sol fraction from ~17 to ~7.6%. Kaihara et al. also indicated that acrylated PEG based hydrogels with higher macromer concentrations had lower sol fraction [318]. The effective macromer percentage, which is defined as the ratio of the mass of crosslinked macromers in the hydrogel to the total mass of the hydrogel (mass of crosslinked macromers and mass of water in the hydrogel) after equilibrium swelling (1 day) was also calculated (Equation 4.4). Interestingly, it was observed that the samples with the lowest nominal macromer

concentration (10% PVA-Tyr) ended up with the highest effective macromer percentage (~12 wt%), which was significantly different to both 15% and 20% PVA-Tyr gels (~10 wt% effective) after equilibrium swelling (Table 4.1). This observation indicates that after equilibrium swelling and sol fraction extraction, the total amount of macromers in the 10% PVA-Tyr gels was higher than both the 15% and 20% PVA-Tyr gels. Furthermore, the q of the fabricated samples was also shown to increase with higher nominal macromer concentration (Table 4.1), which agrees with the trend observed for the sol fraction and effective macromer percentage values. This result was further supported by the macroscopic images of PVA-Tyr hydrogels taken straight after polymerisation (before swelling, t = 0) and after 1 day of swelling. It was clearly seen that 10%, 15% and 20% PVA-Tyr gels had similar dimensions before swelling (Figure 4.7). After 1 day, 20% PVA-Tyr hydrogels were observed to swell the most, as compared to 15% and 10% PVA-Tyr gels (Figure 4.7).

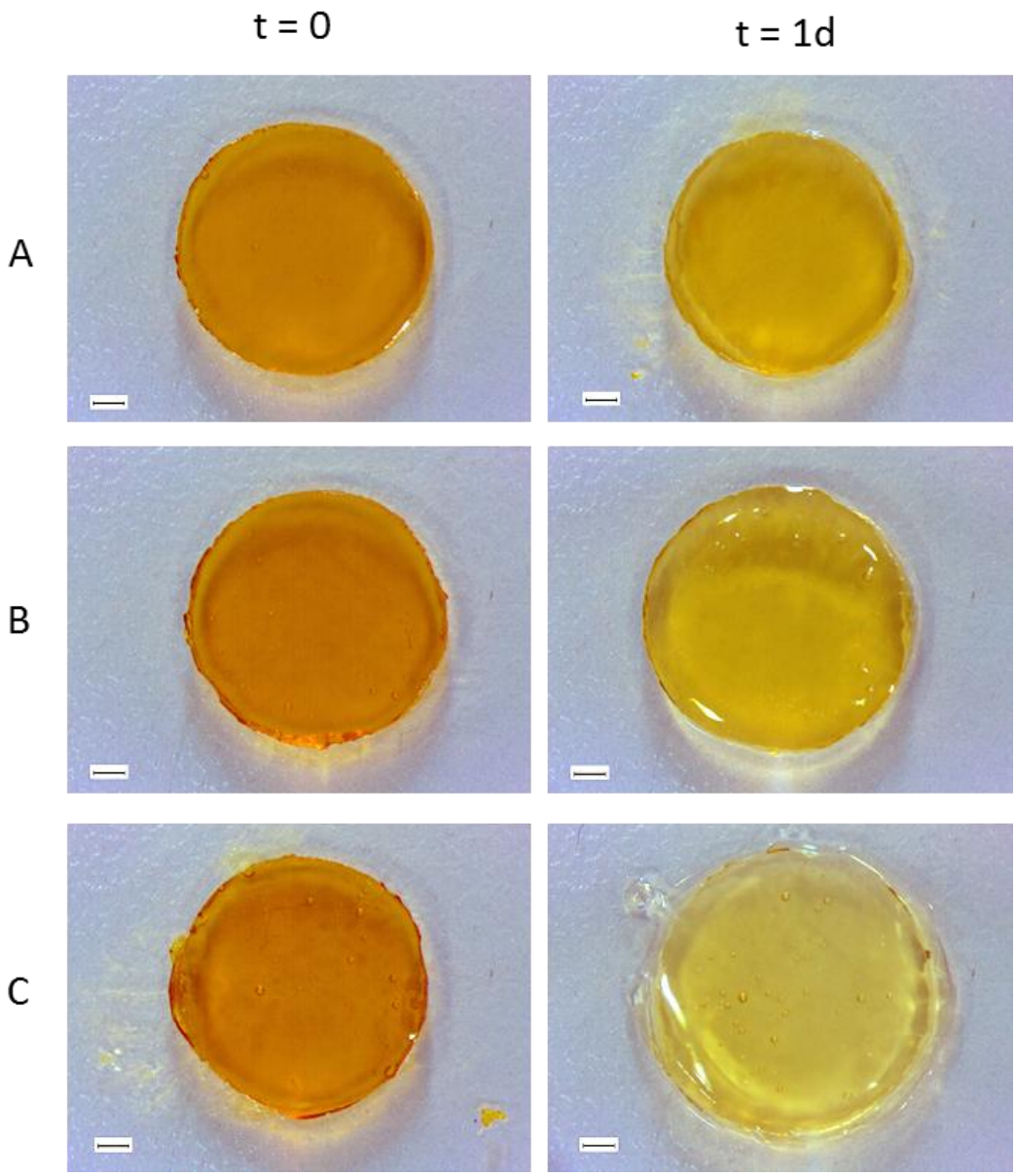

Figure 4.7: Macroscopic images of PVA-Tyr gels fabricated at t = 0 (before swelling) and 1 day (after swelling); A = 10% PVA-Tyr; B = 15% PVA-Tyr; C = 20% PVA-Tyr.

In order to better understand the structure of the network formed, the crosslinking density which is known to directly correlate to the swelling behaviour of the gels was calculated (Equations 4.5 - 4.8) [19, 88]. It was determined that 10% PVA-Tyr hydrogels which had the lowest mass swelling

ratio had the highest crosslinking density when compared to 15% PVA-Tyr and 20% PVA-Tyr gels (Table 4.1). In a tighter network (i.e., higher crosslinking density) the mobility of the polymeric chains are more restricted, and thus less water can be absorbed in the network [82, 87, 89]. Zustiak et al. showed that the swelling of PEG based hydrogels decreased with increasing crosslinking density [6]. Burdick et al. also reported that increasing crosslinking density of methacrylated hyaluronan hydrogels resulted in smaller mesh size and lower swelling [82]. Moreover, statistical analysis revealed that the crosslinking densities were significantly different for all three compositions. Once again, this result is contrary to previous studies published in the literature, where increasing macromer concentration lead to decreased sol fraction and swelling, as well as the formation of a more tightly crosslinked network [82, 89, 319].

The disagreement between the results obtained in this study and the literature may be explained by the relative initiator concentration present in the gels. As previously discussed in Chapter 3, the main component responsible for the crosslinking reaction is the Ru. As the concentration of Ru was kept at 2mM for all three nominal hydrogel macromer concentrations, the mol ratios of Ru to Tyr functional groups were actually highest in the 10% PVA-Tyr gels followed by 15% and 20% PVA-Tyr hydrogels. A sample calculation of the Ru to Tyr functional groups ratios for 1 g of 20% PVA-Tyr hydrogel is described here. The number of moles of Tyr functional groups can be calculated by the mass of PVA-Tyr (0.2 g) divided by the molecular weight of PVA-Tyr (16000 g/mol), and further multiplied by the number of Tyr groups per PVA chain (7). The ratio of Ru to Tyr functional groups is then given by dividing the number of moles of Ru with the number of moles of Tyr functional groups. The calculated values are

0.46, 0.31 and 0.23 for 10%, 15% and 20% PVA-Tyr hydrogels respectively. Hence, it can be speculated that at higher Ru:Tyr ratios the production of tyrosyl radicals required for crosslink formation is more efficient, which resulted in a more crosslinked network. Another explanation for the higher mass loss in the higher nominal macromer concentrations is the differences in the viscosity of the initial macromer solutions, which is known to impact on the reaction rate constant [320]. During fabrication, it was clearly seen that the PVA-Tyr macromer solutions' viscosity dramatically increased with macromer concentration (data not shown). This was not unexpected as it has previously been shown that PVA solutions with higher concentrations have higher viscosities [35, 110, 321, 322]. One hypothesis is that this increase in viscosity reduced the crosslinking efficiency by affecting the mobility of macromer chains and tyrosyl radicals produced during photo-polymerisation and thus limited the crosslinking reaction. Moreover, higher amounts of tyramine groups present in the higher nominal macromer concentrations can also lead to intramolecular cyclisation, where crosslinks might be formed between tyramine groups on the same PVA chain.

Mass loss studies revealed that 10%, 15% and 20% PVA-Tyr hydrogels were completely degraded in ~ 27, 22 and 19 days respectively (Figure 4.8). Once again, this phenomenon can be explained by the differences in the effective macromer fraction and the crosslinking density of the fabricated gels. Theoretically, the number of crosslinks formed is directly proportional to the crosslinking density [15, 87, 323, 324]. Furthermore, the swelling capacity of the gel also decreases due to the tighter network formed, causing the hydrolysable ester bonds to be less accessible to water molecules [89, 97, 100, 325]. Hence,

10% PVA-Tyr hydrogels which were determined to have the highest effective macromer concentration (~12%) and to be the most crosslinked gel would be expected to degrade at a slower rate compared to 15% and 20% PVA-Tyr (both ~10% effective gels). A study conducted by Burdick et al. showed that increasing the crosslinking density of methacrylated hyaluronan hydrogels resulted in longer degradation period [82]. Similarly, Martens et al. showed that increasing the crosslinking density of PVA ester acrylate gels also resulted in slower degradation [294]. Furthermore, Lee et al. revealed that tyraminated hyaluronan hydrogels had a slower degradation rate when the crosslinking density was increased [326].

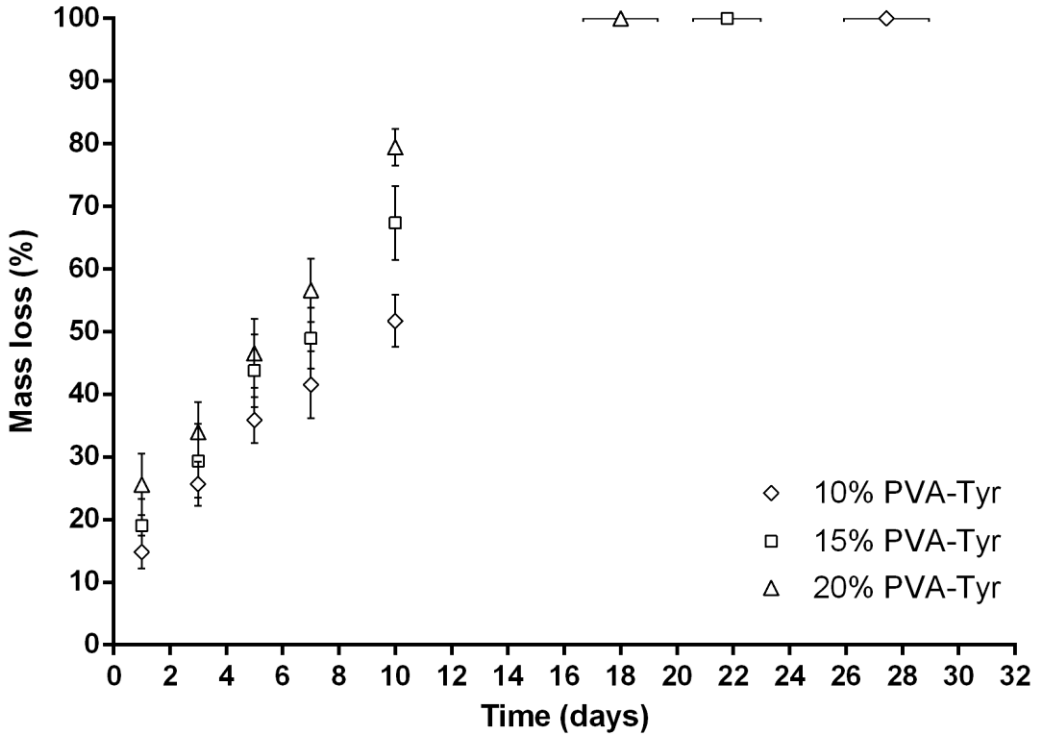

Figure 4.8: Mass loss profiles of 10%, 15% and 20% PVA-Tyr gels at physiological conditions. No statistical significance was observed at time points 1, 3, 5 and 7 days ($p>0.05$). 10%, 15% and 20% PVA-Tyr gels were significantly different at 10 days ($p<0.05$). The time to complete degradation was also statistically different for all three compositions ($p<0.05$).

Similarly, the mass swelling ratios of the gels followed the same trend as the mass loss profiles (Figure 4.9). During degradation, the crosslinks in the hydrogel are being cleaved, leading to a larger mesh and more water uptake (increase in mass swelling ratio). 10% PVA-Tyr gels were found to exhibit a lower mass swelling ratio at all the time points studied, followed by 15% and 20% PVA-Tyr samples. This result is in accordance to previous sections where 10% PVA-Tyr gels had the slowest degradation rate. Another possible explanation for this observation is the different mol content of charged tyramine groups present in the hydrogels of various macromer concentrations, as increasing the number of

ionic groups in hydrogels has been reported to increase their swelling capacities [327, 328]. Previous work done in our group has shown that incorporating charged molecules, such as heparin and chondroitin sulphate, into the hydrogel network caused an increase in swelling [9]. Durmaz et al. also showed that increasing the ionic group concentration in polyacrylamide gels from 0 to 80mol% resulted in a 27-fold increase in the volumetric swelling ratio [328]. This increment was explained by the overall increase of counter-ions in the gels, causing an additional osmotic pressure that swells the gel [327]. As 20% PVA-Tyr hydrogels have the highest concentration of tyramine groups in the network, the anionic repulsion between these moieties can also lead to a larger mesh and higher water content [329, 330].

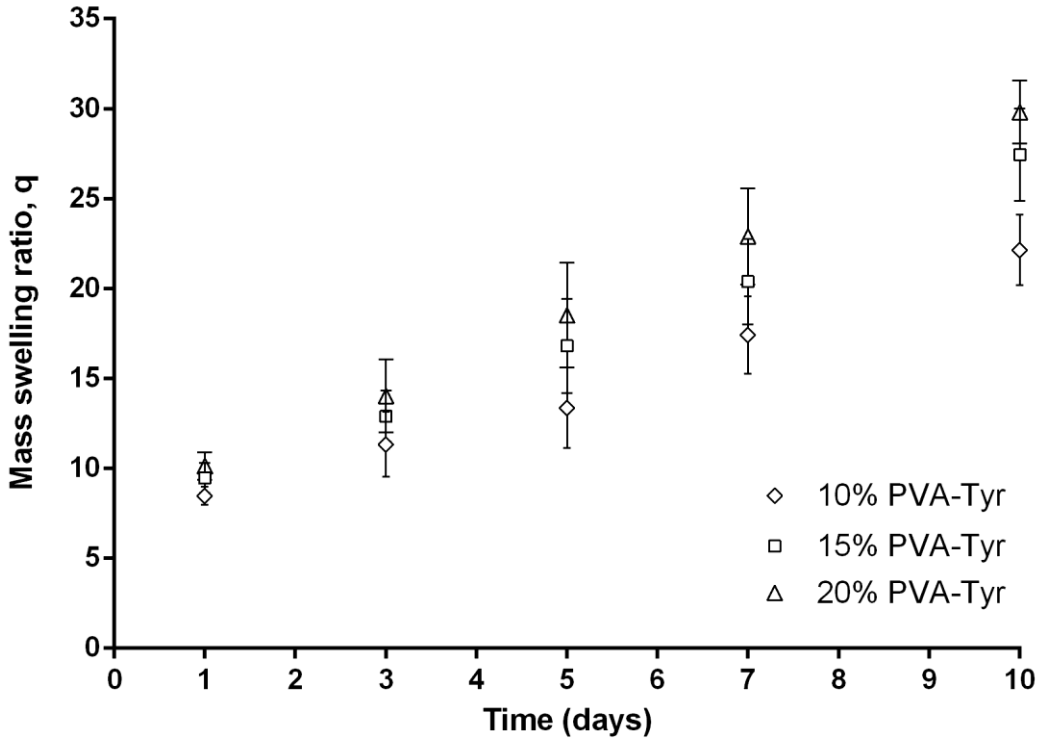

Figure 4.9: Mass swelling ratio, q of 10%, 15% and 20% PVA-Tyr gels at physiological conditions. No statistical difference was observed for time points 1, 3, 5 and 7 days ($p>0.05$). At 10 days, 10% PVA-Tyr was significantly different to 15% and 20% PVA-Tyr ($p<0.05$).

4.3.4. Mechanical properties of PVA-Tyr hydrogels with various macromer concentrations

Another important aspect of the hydrogel degradation behaviour is the change in mechanical properties during degradation. At t = 0, it was reflected that the compressive modulus of the fabricated hydrogels increased in relation to the nominal macromer concentration (Figure 4.10). 10%, 15% and 20% PVA-Tyr gels had compressive modulus of ~135, 233 and ~250 kPa respectively (Figure 4.10).

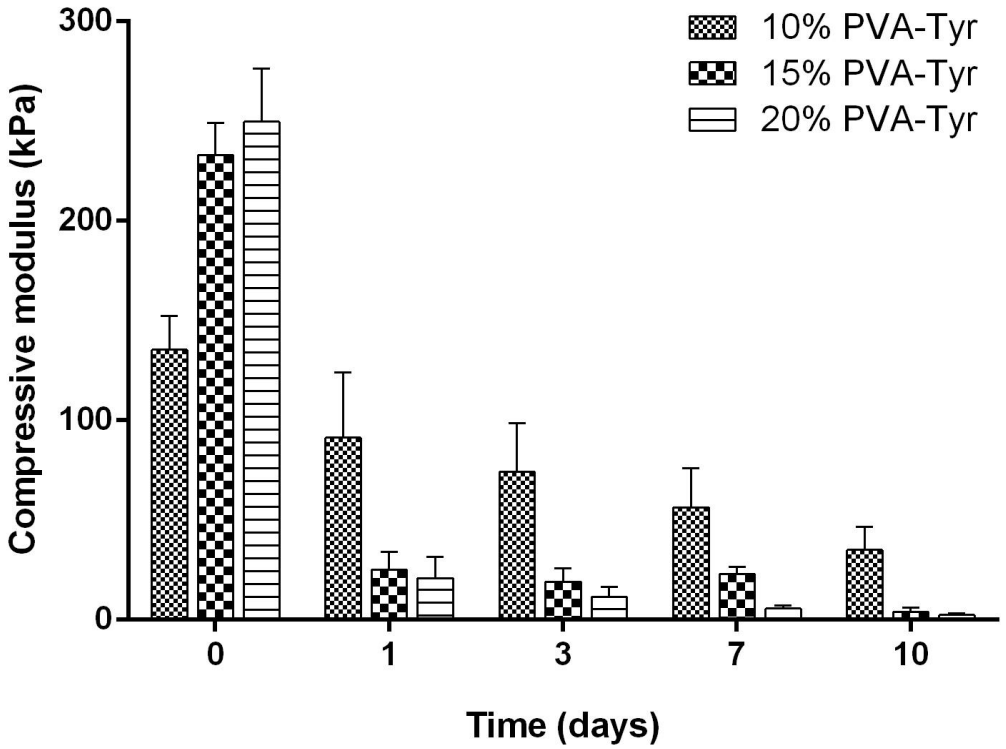

Figure 4.10: Compressive modulus of 10%, 15% and 20% PVA-Tyr hydrogels at various time points. 10% PVA-Tyr was statistically different to 15% and 20% PVA-Tyr at 0, 1 and 3 days ($p<0.05$). All three compositions were significantly different at 7 and 10 days ($p<0.05$).

This result was expected at this time point as all the macromer chains (crosslinked and non-crosslinked) were still present in the gel, and the effective macromer concentration and crosslinking density are not yet relevant. For example, in a 1 g macromer solution, 10% PVA-Tyr gels will theoretically have 0.1 g of macromer, followed by 15% (0.15 g) and 20% PVA-Tyr (0.2 g). As the total amount of macromer in the 10% PVA-Tyr is the least, it was expected that the compressive modulus would also be the lowest. This result is in agreement with a study conducted by Martens et al. where the modulus was shown to increase with the amount of macromer in the hydrogel [110]. After immersing the gels into DPBS for 1 day to extract the sol fraction and allow equilibrium

swelling, all the gels had a major decrease in the compressive modulus. This observation was due to the removal of non-crosslinked macromer chains (sol fraction) which leads to a decrease in the total amount of polymer chains in the final hydrogel network [110, 196, 325]. Moreover, at day 1 the 10% PVA-Tyr exhibited a compressive modulus of ~90 kPa which was much higher than 15% (~25 kPa) and 20% PVA-Tyr gels (~20 kPa). As shown and discussed in previous sections, this observation was now expected due to the higher *effective* macromer concentration and more tightly crosslinked network. The more efficient crosslinking process in 10% PVA-Tyr hydrogels was hypothesised to be due to the higher initiator to Tyr functional group ratio which led to formation of hydrogels of higher crosslinking densities. As a result, it was anticipated that the 10% PVA-Tyr hydrogels would have stronger mechanical properties compared to 15% and 20% PVA-Tyr hydrogels at day 1. Bryant et al. showed that increasing gel crosslinking density from 0.119 mol/L to 0.376 mol/L resulted in gels with 11-fold higher compressive modulus [86]. Moreover, all gels had a decrease in compressive modulus throughout the degradation period. This phenomenon agrees with the literature. It has been stated that during degradation, hydrolysis of network chains cause a decrease in the degree of crosslinking, which further reduces the gels' mechanical strength [82, 86, 331].

4.3.5. L929 cell growth inhibition assay

The toxicity of the PVA-Tyr hydrogels degradation products were assessed by the L929 cell growth inhibition assay. As the degradation of PVA-Tyr hydrogels has been confirmed to be due to hydrolysis of the ester bonds next to the PVA backbone (section 4.3.1), the degradation products were speculated to

be in the form of phenolic compounds. A separate study was conducted to recover and characterise the degradation products (<10kDa). However, the signals obtained in the NMR spectra were noisy and inconclusive (results not shown). Previous studies have also reported that phenolic compounds are toxic [332]. For example, polyphenolic compounds such as flavonoids were reported to inhibit protein kinases and were toxic to mammalian cell lines [333]. In this study, the degradation products of PVA-Tyr hydrogels were shown to have low toxicity (Figure 4.11).

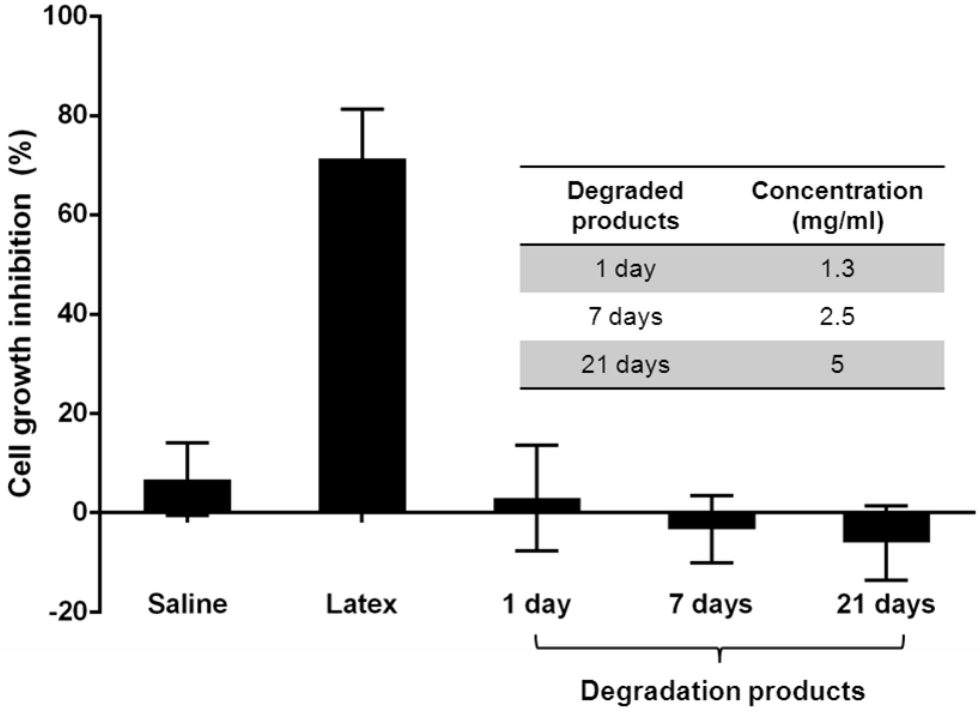

Figure 4.11: Cell growth inhibition of PVA-Tyr hydrogel degradation products. No statistical difference (p>0.05) was observed between saline and the degradation products.

The extracts at 1 day did not have a high concentration of degradation products (1.3 mg/ml), and were likely to consist of only the sol fraction and residual Ru/SPS with a small amount of degraded polymer. Higher amounts of degradation products were present in samples collected at 7 and 21 days (2.5

mg/ml and 5 mg/ml) respectively. Although there seem to be a trend where higher amount of degradation products promoted cell growth to a greater extent, no statistical significance was observed between these samples.

4.4. Conclusion

In conclusion, this chapter has demonstrated that the PVA-Tyr macromer synthesised from the conventional carboxyl-amine coupling reaction can be fabricated into hydrogels via the Ru/SPS crosslinking system, and are hydrolytically degradable due to the hydrolysis of ester bonds next to the PVA backbone. The fabricated hydrogels are pH sensitive, where degradation only occurred in neutral and basic conditions, but not an acidic environment. The degradation process can also be accelerated by increasing the temperature of the system. It was also highlighted that increasing the hydrogel nominal macromer concentration resulted in a decrease in the effective macromer fraction and crosslinking density, which further influenced the degradation rates and mechanical strength of the fabricated PVA-Tyr hydrogels. Most importantly, the degradation products collected from PVA-Tyr hydrogels were not cytotoxic. The results in this chapter have shown the potential of using PVA-Tyr hydrogels as tissue engineering matrices. However, the overall goal of this thesis was to create a system whereby non-chemically modified proteins could be covalently incorporated into a synthetic hydrogel system. Therefore the next chapter will look at incorporating tyrosine rich proteins into these hydrogel networks.

Chapter 5

Covalent Incorporation of Non-Chemically Modified Gelatin into PVA-Tyramine Hydrogels

---

This chapter was partly published in Biomaterials and permission was granted by the publisher for use in this thesis. The concepts and writing of this paper was largely under the control of Lim KS (90% input). The other authors contributed to the analysis and interpretation of the literature and assisted in the development of the arguments.

Paper citation:

Lim KS, Alves MH, Poole-Warren LA, Martens PJ. *Covalent incorporation of non-chemically modified gelatin into degradable PVA-tyramine hydrogels*. Biomaterials. 2013;34:7097-105.

5.1. Introduction

Synthetic hydrogels lack the biological functionality to support cell adhesion, migration and tissue organisation. Therefore, natural polymers including extracellular matrix (ECM) molecules [206, 242], growth factors [77, 334-336] and glycosaminoglycans [9, 22], have been incorporated into synthetic hydrogels for improved biological activity [50, 244]. Many approaches have been studied to incorporate proteins into synthetic hydrogels including physical blending and covalent incorporation.

Physical blending of proteins has been used to increase bio-functionality. However, rapid leaching of proteins from the gels typically occurs over relatively short incubation times [6, 156, 337]. Previous studies conducted by Leach et al reported that 60% of albumin physically trapped in poly(ethylene glycol) (PEG) hydrogels was released within 6h [337]. Zustiak et al also showed that proteins such as lysozyme and albumin diffused out of hydrolytically degradable PEG hydrogels within 24 hours, where the release rate was inversely proportional to the size of the proteins [6]. Thus covalently binding proteins within hydrogel networks has been one of the preferred approaches to achieve control over the amount of protein presented and to support stable and sustained bioactivity for cellular interactions [338-340].

The use of chemical crosslinking agents for the stabilisation of proteins and for their integration with synthetic polymers is a historical approach that although still used today, has significant issues associated with the toxicity of the crosslinking agents, such as aldehydes, epoxides and carbodiimides [7, 234, 340-342]. Another issue with this approach is the harsh conditions that are often

required, such as the use of acidic conditions and high temperatures for epoxide reactions with collagen [342].

More recently, covalent incorporation has been achieved via a number of approaches including modification of proteins with synthetic polymers, such as PEG, or functionalisation of biological molecules to allow covalent incorporation into hydrogel networks. Saik et al reported that covalent immobilisation of platelet-derived growth factor and fibroblast growth factor in PEG gels significantly improved endothelial cell migration in the 3D degradable hydrogels [232]. Proteins such as collagen and fibrinogen have also been chemically conjugated with PEG and used as a 2 dimensional (2D) cell culture platform for neural cells and fibroblasts [338, 339]. However, it was reported that grafting PEG on fibrinogen significantly affected its capacity to form fibrin clots as a result of the PEGylation process inducing fibrinogen denaturation and degradation [343]. This loss of functionality following protein modification is a significant limitation associated with the use of this PEGylation approach. The grafting of functional moieties such as acrylates and methacrylates onto proteins is another approach that allows for the covalent binding of biological and synthetic polymers. The added functional groups are able to co-polymerise the biological molecules with the synthetic polymers [9, 22, 244, 338, 344, 345]. Disadvantages of this approach include the potential disruption of the protein via the conditions typically used in organic synthesis and the inability to control the location and distribution of functional groups. Conjugation of functional groups onto the proteins can also disrupt the side chains required for protein activity [7, 343, 346, 347]. Therefore, new approaches that eliminate the use of harsh

chemicals and that do not require prior modification of the protein backbone would be beneficial.

This chapter proposes a new approach to incorporate proteins into synthetic hydrogels without the need of chemical modification. The PVA-Tyr hydrogels fabricated using the Ru/SPS photo-crosslinking system is hypothesised to have the ability to form covalent crosslinks with proteins via their tyrosine groups. Many extracellular matrix proteins of interest to the biomaterials field have tyrosine residues and thus could be crosslinked into PVA-Tyr hydrogels.

Gelatin, the product of collagen hydrolysis, was selected as the biological molecule for incorporation due to its water solubility, low immunogenicity and capacity to facilitate cell adhesion, migration, differentiation and proliferation [154, 348]. Gelatin based hydrogels have been used for encapsulation of many cell types including chondrocytes, fibroblasts, myoblasts and endothelial cells [156, 223, 349, 350]. Previous studies have shown that the addition of gelatin (2 to 10 wt%) into PEG hydrogels significantly improved fibroblasts viability and proliferation in the gels [223, 350]. However, as gelatin has a large molecular weight and low mechanical strength, it can affect the crosslinking efficiency of the resultant gel. It was reported that increasing gelatin concentration in PVA gels affected their physical properties [351-353]. Pal et al. showed that incorporation of 2.5 wt% of gelatin into 10 wt% PVA hydrogels produced composites with significantly lower crystallinity compared to pure PVA gels [353]. This reduction in crystallinity also affected the tensile strength and elastic modulus of the gels [353, 354]. A study conducted by You et al concluded that the degree of swelling of PVA/gelatin gels increased with the amount of gelatin incorporated [352]. Therefore, incorporating the minimal amount of gelatin for

the required cellular functions, without perturbing the physical and mechanical properties of the base synthetic polymer is desirable. In addition, for higher cost proteins and those more difficult to source in high quantities, it may be advantageous to understand the concentration limits of effectiveness for the biological components.

This chapter aims to covalently incorporate non-chemically modified gelatin into PVA-Tyr hydrogels. Furthermore, the minimum gelatin concentration required for producing a biological effect in the biosynthetic hydrogel will be explored.

5.2. Experimental

5.2.1. Materials

All materials were purchased from Sigma-Aldrich unless otherwise stated. Poly(vinyl alcohol) (PVA) (13-23 kDa, 98% hydrolysed), succinic anhydride (SA), triethylamine (TEA), 1,3-Dicyclohexylcarbodiimide (DCC), N-hydroxysuccinimide (NHS), tyramine (Tyr), sodium persulphate (SPS), tris(2,2-bipyridyl)dichlororuthenium(II) hexahydrate (Ru(II)bpy$_3^{2+}$), gelatin (porcine skin, type A, gel strength 300), deuterium oxide (D_2O), molecular sieves (4 Å), dialysis tubing (10 kDa molecular weight cut-off), Eagle's minimum essential media (EMEM), Dulbecco's phosphate buffered saline (DPBS), trypsin, fetal bovine serum (FBS), penicilin streptomycin (PS), L-Glutamine, Ham's Nutrient Mixture F12 (HAM-12), 4',6-diamidino-2-phenylindole (DAPI), bovine serum albumin (BSA), Tween 20, Triton X-100, paraformaldehyde, Adenosine 5'-triphosphate disodium salt solution (ATP), Calcein-AM and propidium iodide (PI), were used as received. Dimethyl sulfoxide (DMSO) was bought from Ajax Chemicals and was dried over 4Å molecular sieves. Hydrogel disc moulds were made from silicone sheets (Silastic®Sheeting, reinforced medical grade silicone rubber, Dow Corning). CellTiterGlo ATP assay kit was bought from Promega. EGM2-Bulletkit for culturing endothelial cells was purchased from Lonza. Rhodamine-phalloidin (Rh-phalloidin) was purchased from Molecular Probes, Australia.

5.2.2. Macromer preparation

5.2.2.1. Synthesis of PVA-Tyr

PVA-Tyr was synthesised and characterised as described in Chapter 3. The PVA-Tyr used in this chapter was quantified to have 2% conjugation, which corresponds to 7 Tyr per PVA chain.

5.2.2.2. Fabrication of PVA-Tyr/gelatin hydrogels

PVA-Tyr hydrogels were prepared as outlined in Chapter 3. The initiators concentration and irradiation conditions used were 2 mM Ru/20 mM SPS and 15 mW/cm^2 of visible light (Blue wave 200, Dymax Co., 400 – 450 nm). To prepare PVA/gelatin hydrogels, both PVA-Tyr and gelatin were dissolved separately then mixed at RT prior to addition of initiators. The samples were prepared according to the compositions listed in Table 5.1. The total macromer content in the hydrogels was kept at 20 wt%.

Table 5.1: Sample names and wt% of PVA-Tyr and gelatin used to fabricate samples.

Sample	**PVA-Tyr (wt%)**	**Gelatin (wt%)**
20% PVA-Tyr	20	-
0.01% gelatin	19.99	0.01
0.1% gelatin	19.9	0.1
1% gelatin	19	1

5.2.3. Swelling and mass loss analysis

Swelling and mass loss studies were performed as outlined in Chapter 3. The PVA-Tyr and PVA-Tyr/gelatin gels were prepared as discs (5 mm diameter, 1 mm thick). Hydrogel discs (5 mm diameter x 1 mm thick) were immediately weighed after polymerisation ($m_{initial}$). Three discs were immediately lyophilised to determine the actual macromer fraction (%macromer). The rest of the samples were then incubated in PBS (pH = 7.4) at 37 °C. Samples were removed from the incubator a different time points (1, 3, 5, 7, 10 days) and then monitored daily until complete degradation), blotted dry and weighed ($m_{swollen}$). The swollen samples were freeze-dried and weighed again (m_{dry}). The mass loss and mass swelling ratio (*q*) were calculated using equations detailed in Chapter 3 (Eqs. 3.3-3.5). The sol fraction is equal to the mass loss at 1 day.

5.2.4. Quantification of gelatin release from PVA-Tyr/gelatin hydrogel

Hydrogel disks used in this study were prepared in dimensions of 10 mm diameter and 1 mm thick. After fabrication, the samples were immersed in 5 ml of DPBS and incubated at 37 °C. At pre-determined time points (1, 3, 7, 10, 14, 21 days), the extracts were collected and fresh 5ml DPBS was added to the hydrogels. Coomassie Plus Protein Assay (ThermoFisher) was used to quantify the amount of gelatin present in the extracts as per manufacturer's protocol. In brief, 150 µl of working reagent was added to 150 µl of sample extract in a well plate, and incubated at RT for 15 minutes. The absorbance of the samples was then read at 570 nm using a plate reader (Tecan Infinite F200). Gelatin concentration in the extracts was calculated from a gelatin standard curve

constructed by reacting known amount of gelatin with the Coomassie working reagent. The percentage of gelatin release was then calculated according to the following equation:

$$Gelatin\,release\,(\%) = \frac{mass\ of\ gelatin\,released}{mass\ of\ gelatin\,originally\,in\,gel}\ x\ 100 \qquad (5.1)$$

5.2.5. Cell adhesion studies on PVA-gelatin hydrogels

Hydrogels were prepared in sterile conditions, and then soaked in media and incubated at 37 °C for 1 day to extract the sol fraction from the network. After sol fraction extraction, the media was discarded and hollow metal fences (Aix Scientifics) were placed on top of the hydrogels to ensure the cells were only seeded on the hydrogel surface. Three different kinds of cells were used to assess the bioactivity of the fabricated hydrogels.

Murine dermal fibroblasts (L929) were cultured in EMEM supplemented with 10% FBS and 1% PS. When required for experiments, cells were trypsinised and resuspended in DPBS. Cells were seeded onto the hydrogels at a concentration of 800 cells/mm^2 through the metal fences (12.57 mm^2). Media was added through the side path of the metal fences to surround the hydrogels. After 4 hours, live-dead assay was done to determine the amount of adhered cells on the gels. Tissue culture plate (TCP) was used as the positive control.

Primary human umbilical vein endothelial cells (HUVEC) were kindly donated by Professor Jennifer Gamble of the Centenary Insitute, Sydney. The HUVECs were cultured at low passage (3-5) in EGM-2, trypsinised, resuspended in DPBS, and seeded onto the hydrogels at a concentration of 800 cells/mm^2. TCP and gelatin coated TCP were used as positive controls. After 4 hours, the

samples were characterised using a live-dead assay. The cytoskeleton organisation of the adhered cells was also studied using actin filament staining.

Schwann cells 4.1/F7 from rat nerve sheaths (SCL) were cultured in HAM-12 supplemented with 2 mM L-Glutamine, 10% FBS and 1% PS. The SCLs were also trypsinised, resuspended in DPBS, and seeded onto the hydrogels at a concentration of 200 cells/mm^2. For this study, SCL adhesion and proliferation was studied. The time points were set as 4 hours, 1 and 3 days. At each time points, live-dead assay was done to determine the viability of SCLs attached on the gels. ATP assay was also performed to study the metabolic activity of the adhered SCLs.

5.2.5.1. Live-dead assay

The cells adhered samples were washed with DPBS then stained with 1µg/ml of Calcein-AM and PI. Calcein-AM stains live cells green, while PI stains dead cells red. After 10 minutes incubation with the stains, the gels were washed again with DPBS then imaged with the fluorescent microscope (Zeiss, Axioskop 2 MAT). ImageJ (version 1.46, National Institutes of Health) was used to count the adhered cells.

5.2.6. L929 cell encapsulation in PVA-Tyr/gelatin hydrogels

L929s were trypsinised and resuspended in DPBS. The initiators were added to the macromer solution at a final concentration of 2mM Ru and 20mM SPS, and the solution was gently mixed. The cell suspension was then added to the macromer solution to give a final density of 1x10^6 cells/mL, and the solution was gently mixed again to ensure even cell distribution. The solution was then

transferred into silicone moulds (7.5 mm diameter x 0.25 mm thick) sandwiched between two cover slips, then irradiated under 15 mW/cm^2 of visible light (Blue wave 200, Dymax Co., 400 – 450 nm) for 3 minutes. The samples were immediately immersed in media then placed in a humidified incubator (37 °C and 5% CO_2). Live-dead assay was performed on these samples to evaluate the viability of cells encapsulated in the gels.

5.2.7. Statistical analysis

All samples were prepared in triplicates and all experiments were repeated three times. Two-way ANOVA model constructed using Minitab 15 statistical analysis software was used to analyse the results.

5.3. Results and discussion

5.3.1. Fabrication of PVA-Tyr/gelatin hydrogels

It was hypothesised that non-chemically modified gelatin can be covalently incorporated into the PVA-Tyr network. The photo-crosslinking process used in this system should enable the formation of covalent bonds between tyrosine groups of gelatin and tyramine groups of PVA-Tyr (Figure 5.1). The successful formation of the biosynthetic gels was confirmed in mass loss and swelling studies, and the stable incorporation of gelatin was confirmed via analysis of the gelatin released.

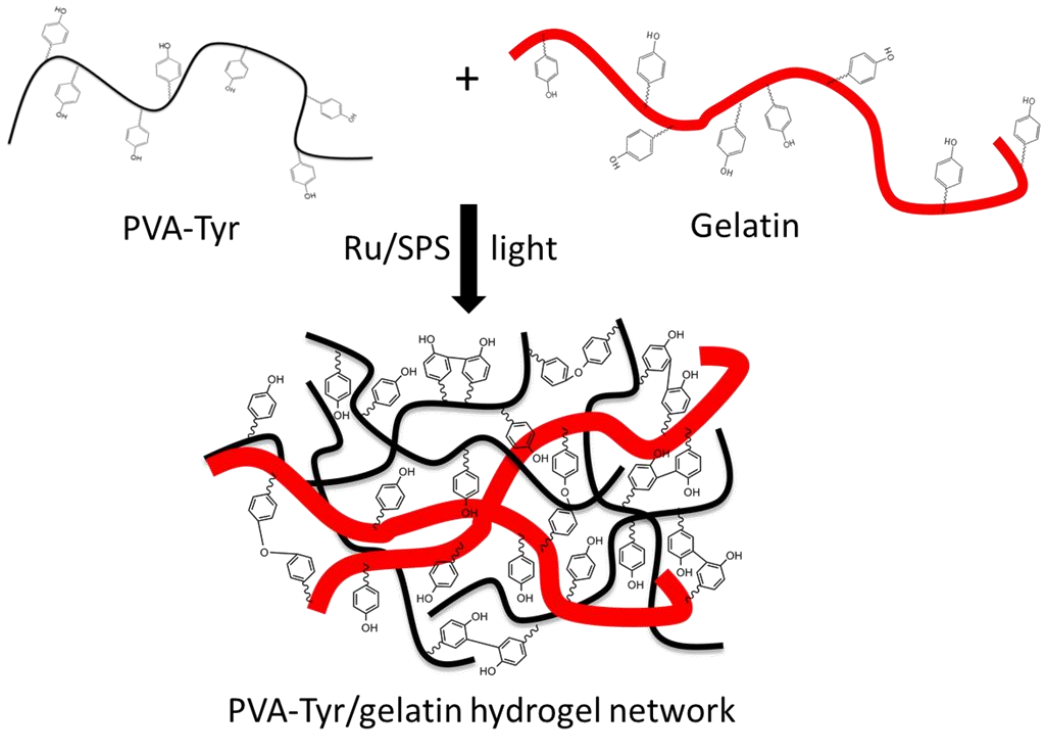

Figure 5.1: Schematic of co-polymerisation of PVA-Tyr and gelatin.

5.3.1.1. Mass loss and swelling studies conducted on PVA-Tyr/gelatin hydrogels

Physical properties of the fabricated hydrogels at 1 day post polymerisation were evaluated by swelling and mass loss analysis, and are summarised in Table 5.2. The incorporation of gelatin was shown to have no effect on the crosslinking efficiency ($p>0.05$), as both PVA-Tyr and PVA-Tyr/gelatin gels had sol fractions in the range of 26 to 28%. Gelatin, reported to be slightly anti-oxidative, had the potential to scavenge the radicals formed during the polymerisation process [355]. However, as the amount of gelatin incorporated was very low (0.01 wt% to 1 wt%), the radical scavenging effect was not significant in this study.

Table 5.2: Sol fraction (%) and mass swelling ratio of fabricated hydrogels after 1 day.

Sample	**Sol fraction (%)**	**Mass swelling ratio, *q***
20% PVA-Tyr	25.6 ± 4.9	9.1 ± 1.2
0.01% gelatin	26.7 ± 3.4	8.6 ± 0.8
0.1% gelatin	27.8 ± 3.6	8.8 ± 0.5
1% gelatin	27.8 ± 4.8	9.8 ± 1.8

Previous studies have shown that the incorporation of charged biological molecules such as chondroitin sulphate, heparin and sericin into PVA hydrogels, resulted in an increase in the mass swelling ratio [4, 6, 35]. Gelatin is also a positively charged molecule at pH 7.4 [36]. However, it was shown that there was no significant difference between the mass swelling ratios of pure PVA-Tyr

and PVA-Tyr/gelatin hydrogels. This result is most likely again due to the low amount of gelatin incorporated into the PVA hydrogel networks. This theory is supported by previous work where the incorporation of 2 wt% of sericin into PVA-MA gels significantly increased the mass swelling ratio, however no significant change was observed when the sericin amount was decreased to 1 wt% [6]. As the gelatin concentration used in this study was kept equal to or lower than 1 wt%, it was expected that the mass swelling ratio would not be affected.

PVA-Tyr hydrogels were found to be hydrolytically degradable, with a linear degradation profile (Chapter 4). In this study, the presence of gelatin did not significantly affect the degradation rate and all the gels were completely degraded in 3 weeks (Figure 5.2).

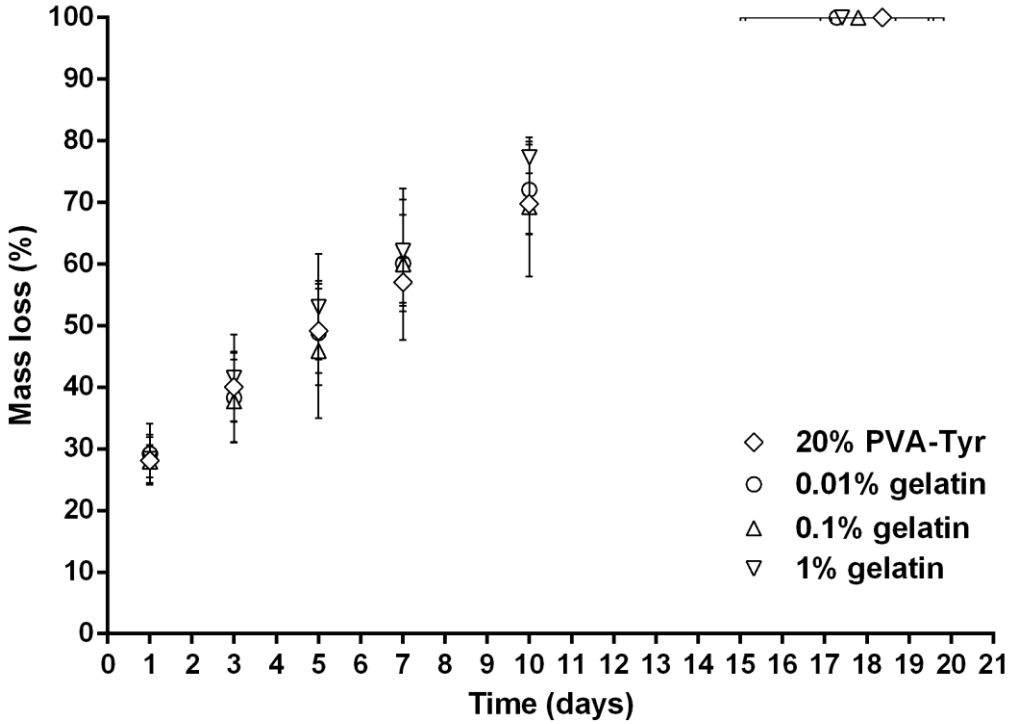

Figure 5.2: Mass loss profiles of fabricated PVA-Tyr and PVA-Tyr/gelatin hydrogels. Error bars represent standard deviation. No statistical difference ($p>0.05$) was observered between all samples at all time points.

The *q* of the gels also increased linearly, similar to the degradation profile, as shown in Figure 5.3. Once again, this is due to the fact that hydrogel degradation results in a looser network where more water is entrapped in the gel. Statistical analysis showed no difference between all the gels at each time point. This result again indicates that incorporation of gelatin (0.01% to 1%) did not affect the physical properties and degradation profile of the resultant gels.

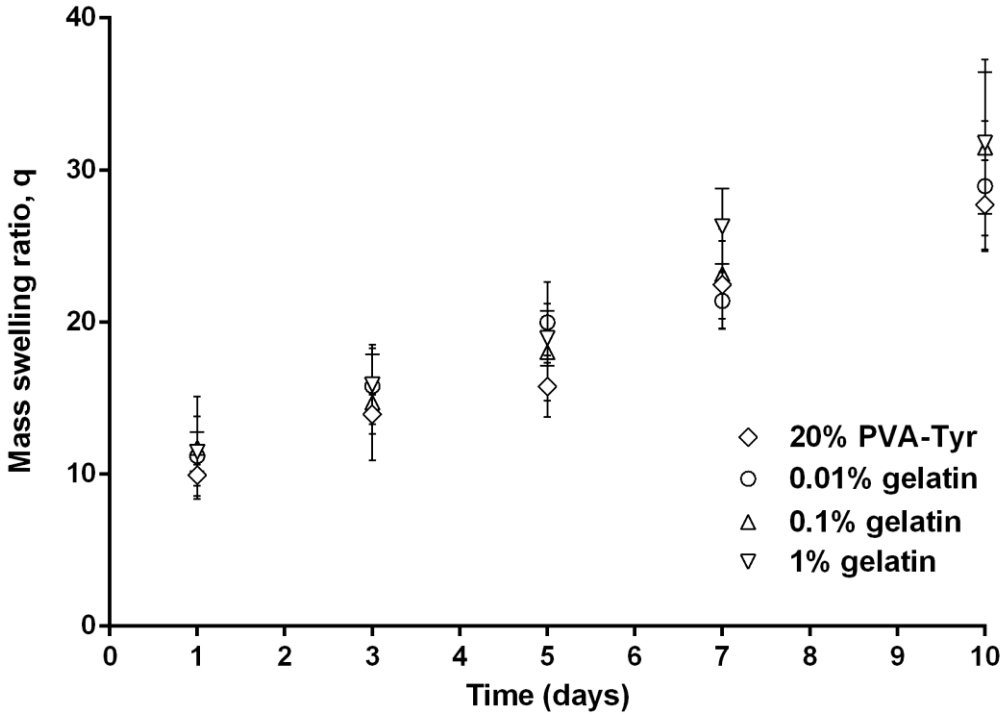

Figure 5.3: Mass swelling ratio (q) of fabricated PVA-Tyr and PVA-Tyr/gelatin hydrogels. Error bars represent standard deviation. No statistical difference ($p>0.05$) was observered between all samples at all time points.

5.3.2. Gelatin release from PVA-Tyr/gelatin hydrogels

A release study was conducted to evaluate the stability of gelatin integrated in the PVA-Tyr gels. As the amount of gelatin incorporated in 0.01% gelatin gels was below the detection limit for quantification, it was not included

in this study. Previous work on methacrylated gelatin crosslinked with non-degradable PVA-MA showed that uncrosslinked gelatin required 3 days to completely diffuse out of the network [200]. In this study, it was shown that amount of gelatin released from both 0.1% gelatin and 1% gelatin gels after 3 days was ~25% (Figure 5.4).

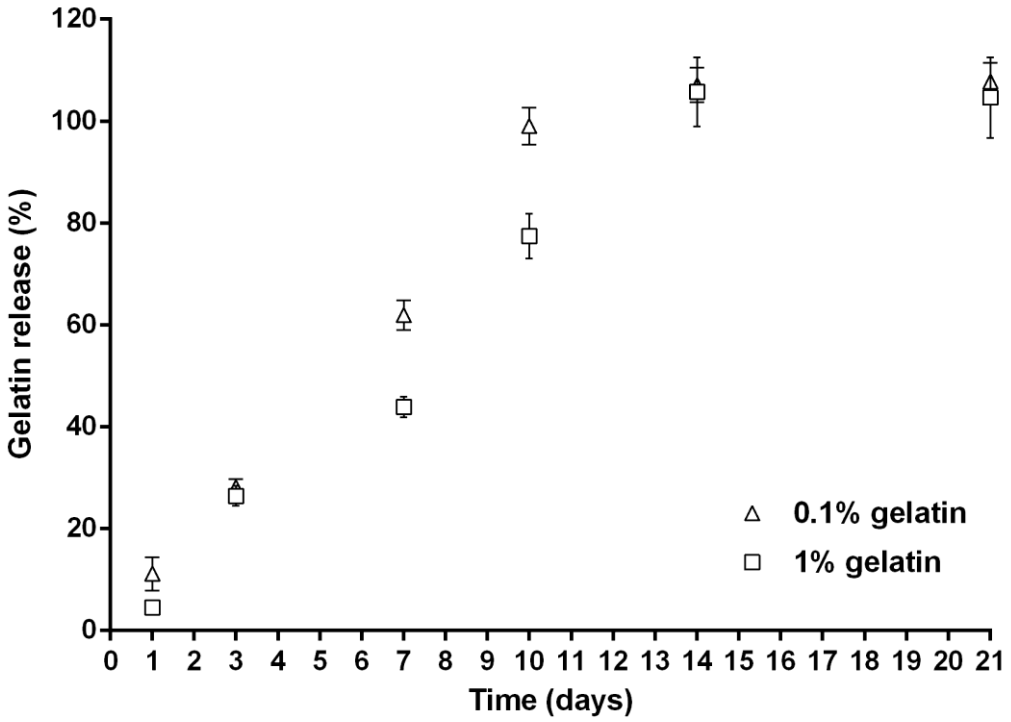

Figure 5.4: Gelatin release (%) from PVA-Tyr/gelatin gels. Error bars represent standard deviation. 0.1 and 1% gelatin were significantly different ($p<0.05$) at $t = 1, 7$ and 10 days.

This value agrees with previous studies in terms of the amount of gelatin that is incorporated in PVA-MA gels [200], and confirms that the non-chemically modified gelatin used in this study was covalently co-polymerised with the PVA-Tyr hydrogel. Moreover, as the hydrogels are hydrolytically degradable, the gelatin release study was conducted up to 21 days, which is when both gels were completely degraded. It was observed that the release of gelatin increased over

time similar to the mass loss profiles. However, 0.1% gelatin gels had a faster gelatin release profile than 1% gelatin. All incorporated gelatin was released after 10 days for 0.1% gelatin gels, as compared to 14 days for 1% gelatin gels. This might be due to formation of covalent crosslinks between the incorporated gelatin molecules. During the photo-crosslinking process, the tyrosine residues on gelatin can either react with the tyramine groups on PVA-Tyr, or can also crosslink with nearby tyrosine moieties on the gelatin molecules. As there is a higher amount of gelatin present in 1% gelatin gels, there is a higher probability for this to occur as compared in 0.1% gelatin gels. The crosslinking between gelatin will lead to a larger size and molecular weight, hence longer time is needed for the gelatin molecules to diffuse out of the hydrogel network.

5.3.3. Bioactivity of gelatin incorporated in PVA-Tyr hydrogels

5.3.3.1. L929s adhesion on PVA-Tyr and PVA-Tyr/gelatin hydrogels

Murine dermal fibroblasts (L929) were seeded on top of the fabricated PVA-Tyr/gelatin hydrogels at a density of 800 cells/mm^2. It was observed that all the cells were attached on the TCP control after 4 hours, whereas only a small number of cells were attached on pure PVA-Tyr hydrogels (see Figure 5.5). This lack of adherence on the pure PVA gels was expected as PVA-Tyr is a synthetic polymer with no biological components incorporated to support cell attachment. Previous studies have also confirmed that cells do not attach to hydrogels made out of pure PVA due to its highly hydrophilic nature [244, 325, 356].

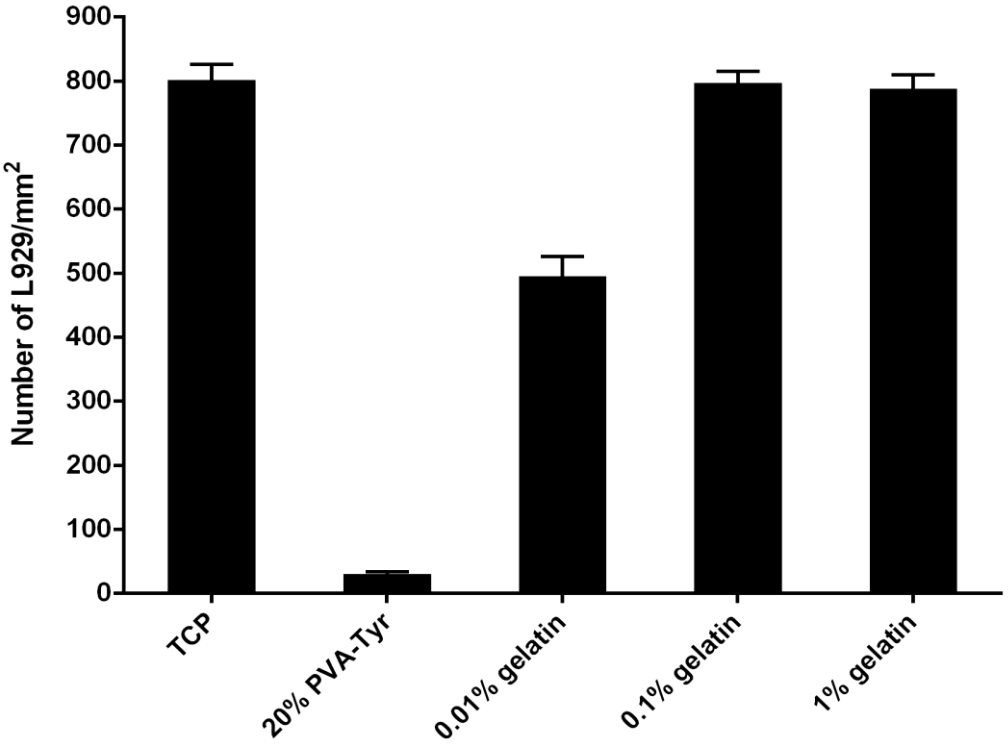

Figure 5.5: Number of attached L929s/mm^2 on PVA-Tyr and PVA-Tyr/gelatin hydrogels at 4 hours. Error bars represent standard error mean. 0.1% and 1% gelatin were not significantly different ($p>0.05$) to TCP. 20% PVA-Tyr was significantly different ($p<0.05$) to all other samples. 0.01% gelatin was significantly different ($p<0.05$) to all samples.

In this study, it was observed that gelatin at concentrations as low as 0.01% markedly increased the bioactivity of the hydrogels with approximately 60% seeding efficiency (500 cells/mm^2) achieved. When gelatin concentration was further increased to 0.1% and 1%, 100% seeding efficiency was observed. Statistical analysis showed that all PVA-Tyr/gelatin gels were significantly different to pure 20% PVA-Tyr gels. 0.01% gelatin was also statistically different to 0.1% gelatin and 1% gelatin samples. In previously reported studies, the lowest concentration of gelatin incorporated into synthetic polymeric gels was 1% [352]. You et al showed that incorporation of 1 – 3 wt% of gelatin into

PVA gels promoted significantly more fibroblasts attached onto the gel surfaces. However, the present study showed that the amount of protein required to augment bioactivity could be as small as 0.01%. Gelatin being a product of collagen degradation retained the functional peptide sequences required for cellular interaction. It has an abundance of arginine-glycine-aspartic acid (RGD) sequences which promotes cell adhesion [357]. These RGD ligands could bind to the integrin on cell surfaces, providing enhanced cellular attachment. This study also confirmed that the gelatin remained bioactive post integration into the PVA-Tyr gels and was able to promote cellular adhesion.

While cell counts are a good indication of cell survival, even more information can be gained from observing the morphology of the cells on the gels. Cells attached to TCP remained rounded at 4 hours, whereas the cells on the PVA-gelatin hydrogels were spread and appeared more similar to their natural morphology (see Figure 5.6). More interestingly, the cells on 0.01% gelatin gels were in the forms of cell aggregates, as compared to being evenly spread on 0.1% and 1% gelatin gels.

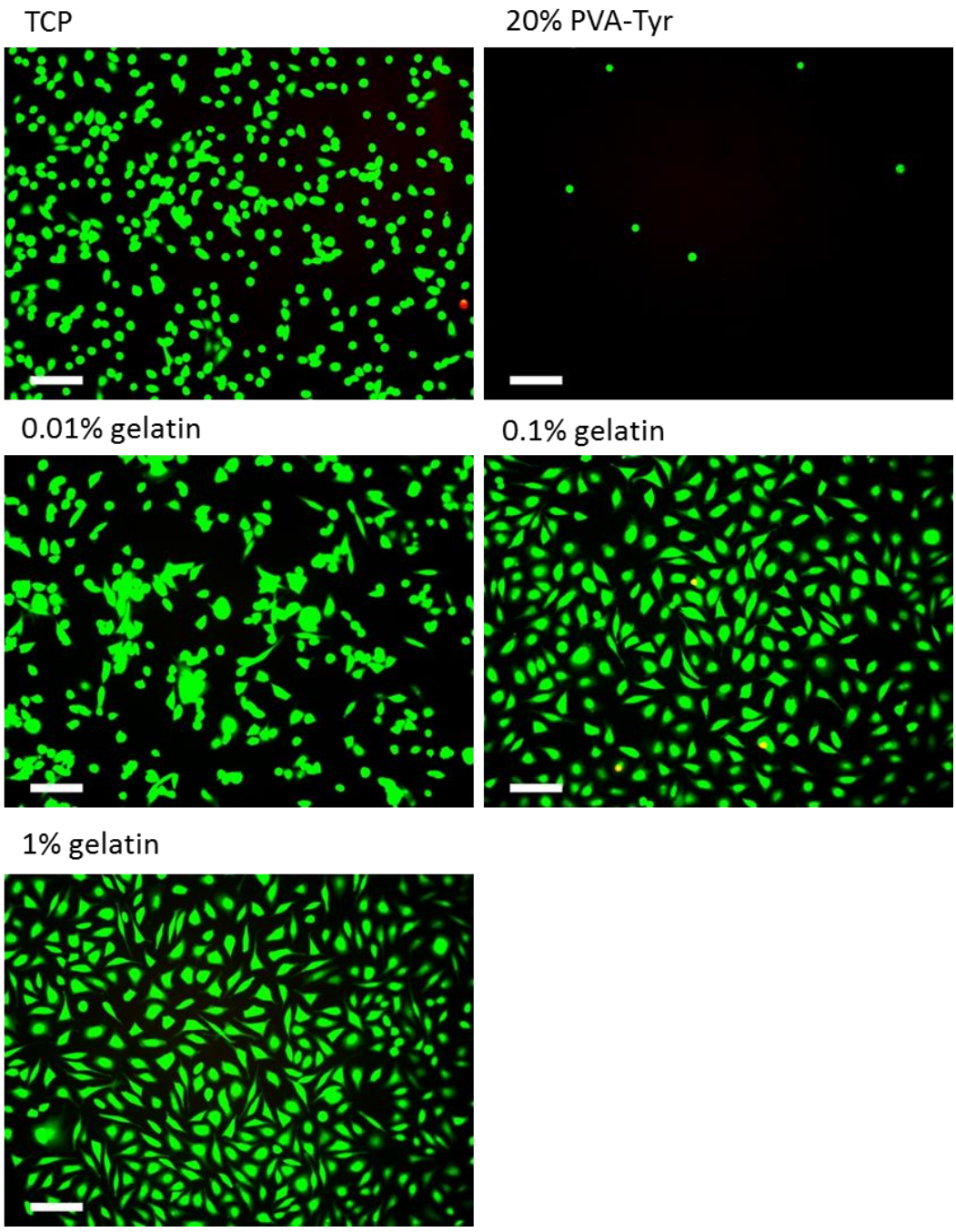

Figure 5.6: Live-dead images of attached L929s on PVA-Tyr and PVA-Tyr/gelatin hydrogels at 4 hours. Green = live; Red = dead. Scale bar = 100 µm.

5.3.3.2. HUVECs adhesion on PVA-Tyr and PVA-Tyr/gelatin hydrogels

The bioactivity of the incorporated gelatin was further evaluated by cell adhesion assay using primary human umbilical vein endothelial cells (HUVEC),

where are known to be sensitive to surface topology and rigidity. The HUVECs were also seeded onto the fabricated PVA-Tyr/gelatin hydrogels at 800cells/mm^2. It was observed that 60% of the seeded cells were attached on TCP after 4 hours (Figure 5.7).

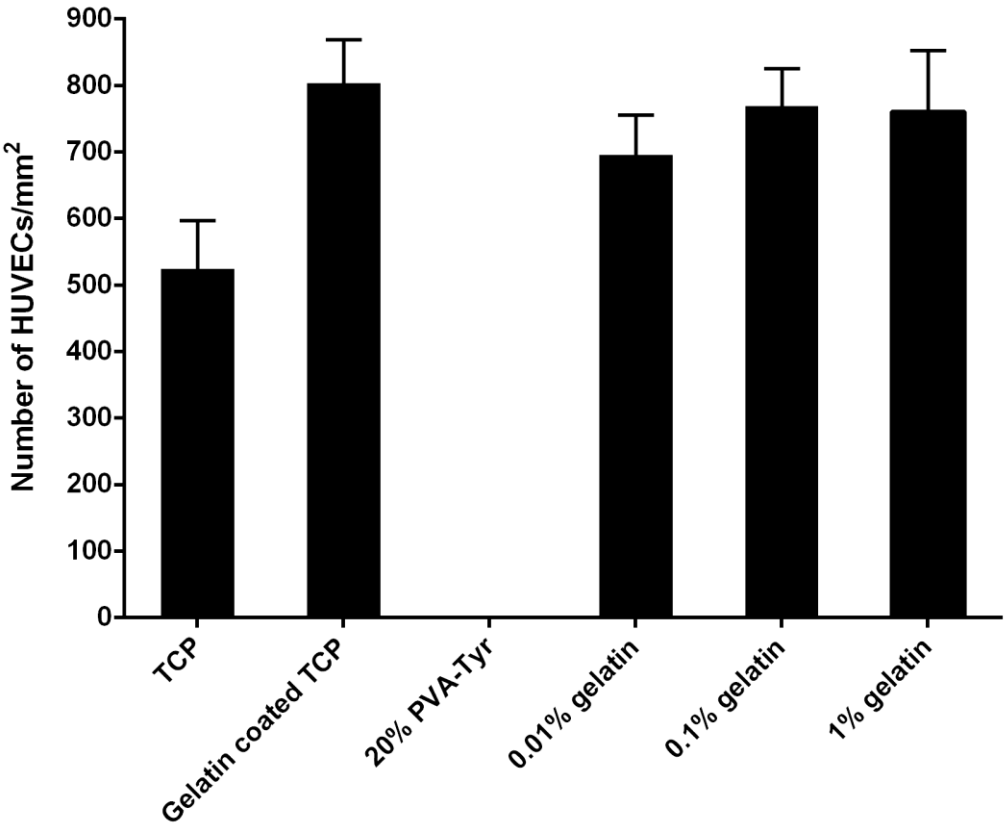

Figure 5.7: Number of attached HUVECs/mm^2 on PVA-Tyr and PVA-Tyr/gelatin hydrogels at 4 hours. Error bars represent standard error mean. TCP was significantly different ($p<0.05$) to gelatin coated TCP. 0.01%, 0.1% and 1% gelatin were significantly different ($p<0.05$) to TCP, and not statistically different ($p>0.05$) to gelatin coated TCP. 20% PVA-Tyr was significantly different ($p<0.05$) to all other samples.

However, when gelatin was used to coat TCP, all the seeded cells were attached on the plate surfaces. This result agrees with previous studies where ECM

proteins such as collagen, fibronectin and gelatin were required to facilitate HUVECs attachment, even when TCP was used [358]. Similarly, 20% PVA-Tyr did not support any cell adhesion. Incorporation of 0.01% - 1% gelatin significantly enhanced the amount of cells attached on the gel surfaces. Statistical analysis reported significant differences between all PVA-Tyr/gelatin samples and pure 20% PVA-Tyr gels. Moreover, there were no significant differences between all the PVA-Tyr/gelatin gels and the gelatin coated TCP samples. This result is slightly different to the L929 adhesion studies in section 5.3.3.1, where 0.01% gelatin was statistically different to 0.1% and 1% gelatin gels. This phenomenon might be due to the higher sensitivity and selectivity of HUVECs to the gelatin molecule [358]. Live-dead images clearly showed that the morphology of HUVECs attached onto TCP, gelatin coated TCP and PVA-Tyr/gelatin hydrogels is similar (Figure 5.8).

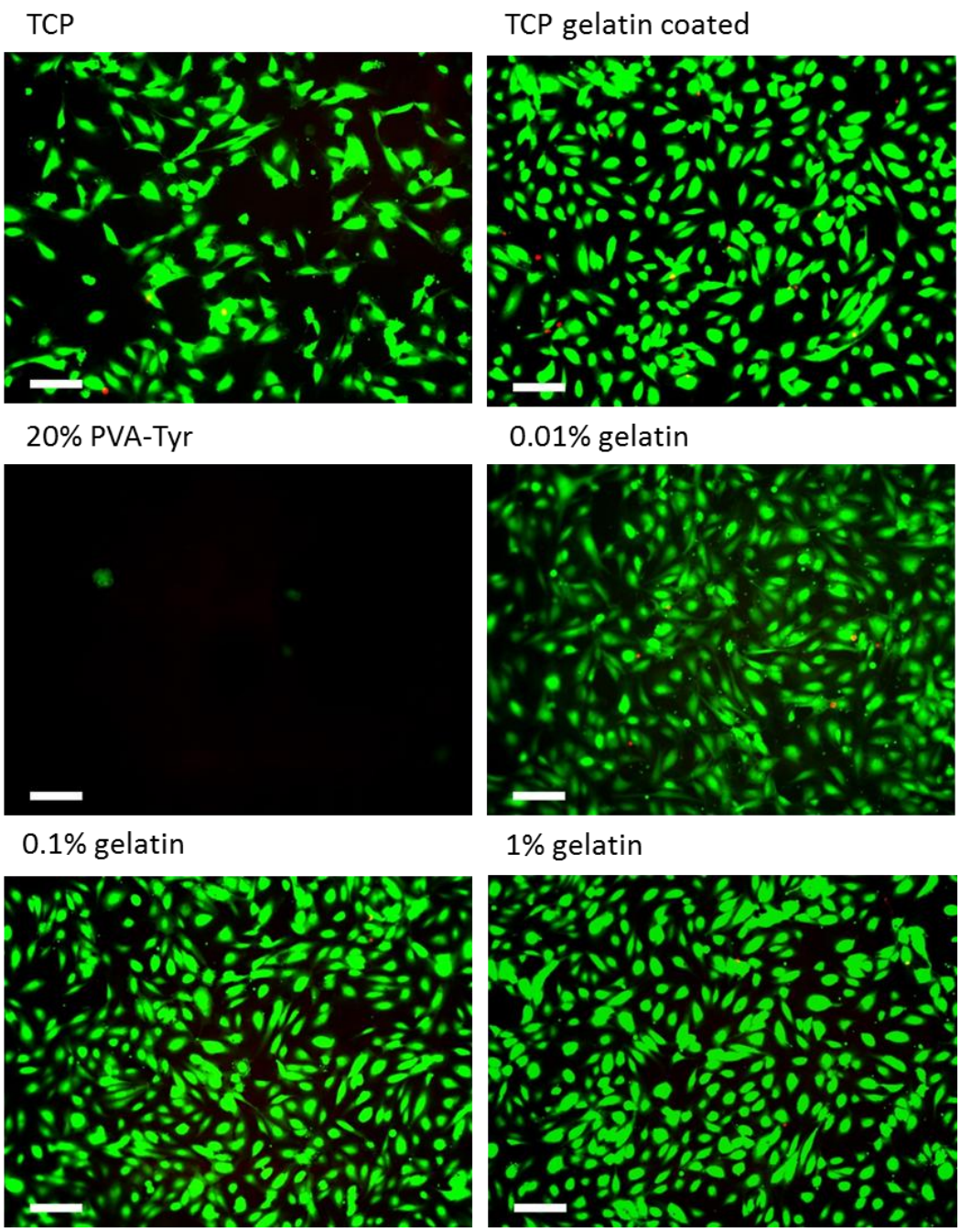

Figure 5.8: Live-dead images of attached HUVECs on TCP, PVA-Tyr and PVA-Tyr/gelatin hydrogels at 4 hours. Green = live; Red = dead. Scale bar = 100 µm.

Endothelial cells are responsible for the synthesis and regulation of ECM that acts as the border between blood vessels and other contact tissues. Hence, most endothelial cell cultures require the addition of at least one ECM adhesion protein to the cell culture supports (TCP). The ECM molecule allows initial

attachment of the endothelial cells prior to re-modelling and secretion of new ECM [358, 359]. Previous studies have shown that the presence of gelatin successfully promoted attachment of HUVECs on several synthetic hydrogels. Ohya et al. reported that grafting gelatin onto pNIPAAm hydrogel increased the hydrogel surface roughness, which further influenced endothelial cell adhesion [354]. Similarly, Zhu et al. and Saunder et al. showed that conjugating RGD sequences onto PEG and polyacrylamide hydrogels promoted HUVEC adhesion [360, 361]. As gelatin is known to be rich is RGD sequences, it was expected that incorporating this protein into PVA-Tyr gels would promote HUVEC attachment.

Incorporation of gelatin into the PVA gels allowed HUVECs to attach and spread in a similar manner as the positive controls (TCP and TCP gelatin coated). No difference was observed in terms of the cell elongation and the actin stress fibers alignment, where HUVECs attached on all samples showed ordered F-actin arrangement enveloping the cell nuclei. This study demonstrated that the gelatin incorporated into PVA-Tyr hydrogels was presented on the gel surfaces, and remained biologically active to support HUVECs attachment. Once again, gelatin concentration as minimal as 0.01% was enough to augment bio-functionality of PVA-Tyr gels.

5.3.3.3. SCLs adhesion and proliferation on PVA-Tyr and PVA-Tyr/gelatin hydrogels

Next, in order to further confirm the feasibility of this system as a cell culture platform that supports several types of cells, the bioactivity of the PVA-Tyr/gelatin gels was further evaluated using Schwann cells harvested from rat nerve sheath (SCL). The previous cell adhesion studies (i.e., L929s and HUVECs)

were only done for a short time period (4 hours). However these gels are degradable and the effect of gel degradation on cell proliferation was examined using the SCLs.

SCLs were seeded on the samples at a concentration of 200cells/mm^2. At 4 hours, very few cells were found to attach on pure PVA-Tyr gels, and no discernable proliferation was observed on the pure PVA-Tyr gels over the course of the study (Figure 5.9). In contrast to this, 85% of the seeded cells were adhered onto TCP and the PVA-Tyr/gelatin samples after 4 hours. These adhered cells were then shown to proliferate from 4 hours to 1 and 3 days. Statistical analysis showed no difference between the PVA-Tyr/gelatin gels at all-time points studied. However, TCP had significantly more cells attached compared to the PVA- Tyr/gelatin samples at the 3 day time point.

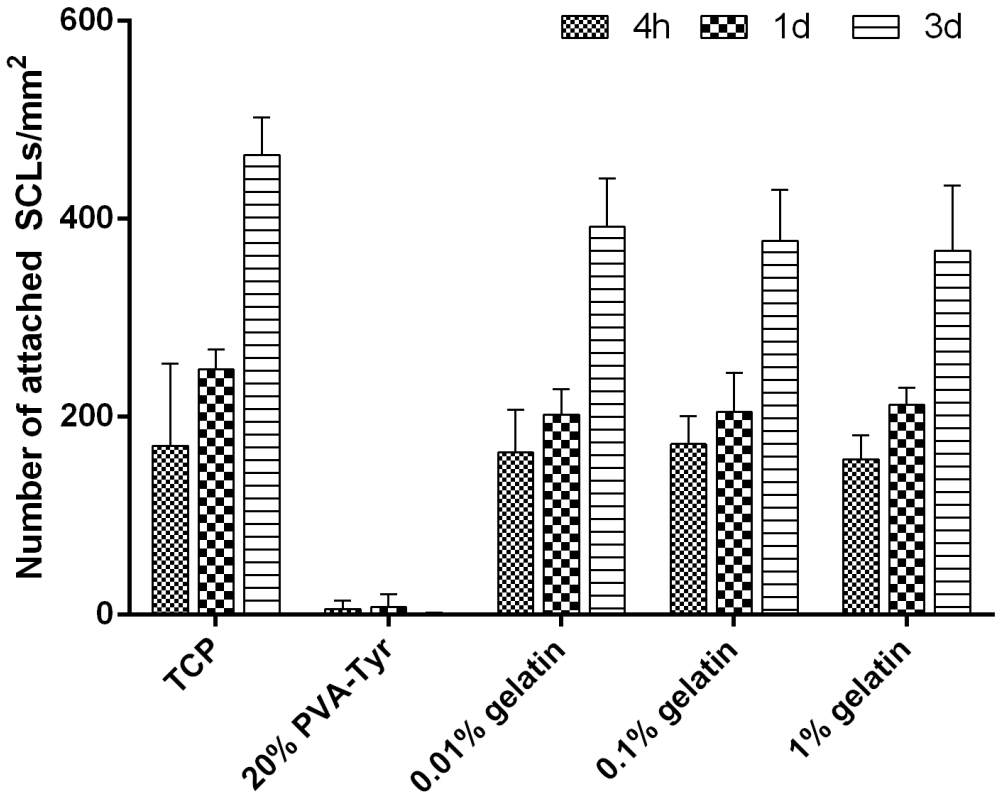

Figure 5.9: Number of attached SCLs/mm^2 on PVA-Tyr and PVA-Tyr/gelatin hydrogels at 4 hours, 1 day and 3 days. Error bars represent standard error mean. No significant differences ($p>0.05$) were observed between 0.01%, 0.1% and 1% gelatin samples at all time points. 20% PVA-Tyr was significantly different ($p<0.05$) to all other samples at all time points. 0.01%, 0.1% and 1% gelatin samples were significantly different ($p>0.05$) to TCP at t = 3 days.

The lack of cells on the PVA-Tyr/gelatin gels as compared to TCP might be due to the degradation of the PVA-Tyr/gelatin hydrogels. It was shown that the mechanical strength of the gels decreases as the hydrogel degrades (section 4.3.4, Chapter 4). Previous studies have shown that spreading and proliferation of mammalian cells can be influenced by multiple parameters such as external mechanical-stress field, hydrodynamic and compressive forces [21, 354, 361]. The substrate surface rigidity has been shown to heavily influence the behaviour

of anchorage dependant cells attached onto the surfaces, such as fibroblasts, endothelial cells and Schwann cells [93, 354, 361-363]. For example, Ohya et al reported that endothelial cells preferred to attach onto poly(N-isopropylacrylamide)-gelatin hydrogels with greater stiffness [354]. As mechanotransduction between the cell adhesion sites and the surface plays a huge role in cell spreading, migration and proliferation [21, 362, 364], it was hypothesised that the decrease in surface mechanics due to hydrogel degradation would also result in a decrease in the cell proliferation rate. This speculation agrees with previous findings reported by Cao et al., where Schwann cells were shown to proliferate faster on chitosan films with Young's modulus of ~22 MPa compared to ~16 MPa [363].

Live-dead images showed the morphology of cells attached on all the samples (Figure 5.10). It was observed that the SCLs were initially rounded at 4 hours, but became spindled shape at 1 and 3 days on every surface examined. In addition, almost all the attached cells were alive at all-time points on all surfaces (all cells stained green at 4 hours, 1 day and 3 days). This observation was particularly important due to the fact that during the degradation of the gels, degradation products are leached out into the environment and might be detrimental to the attached cells. However, these images suggest that the degradation products did not affect the cell viability. This study agrees with the cytotoxicity study conducted in Chapter 4, where the degradation products conducted from the gels did not exhibit any cell growth inhibitory effect on L929s.

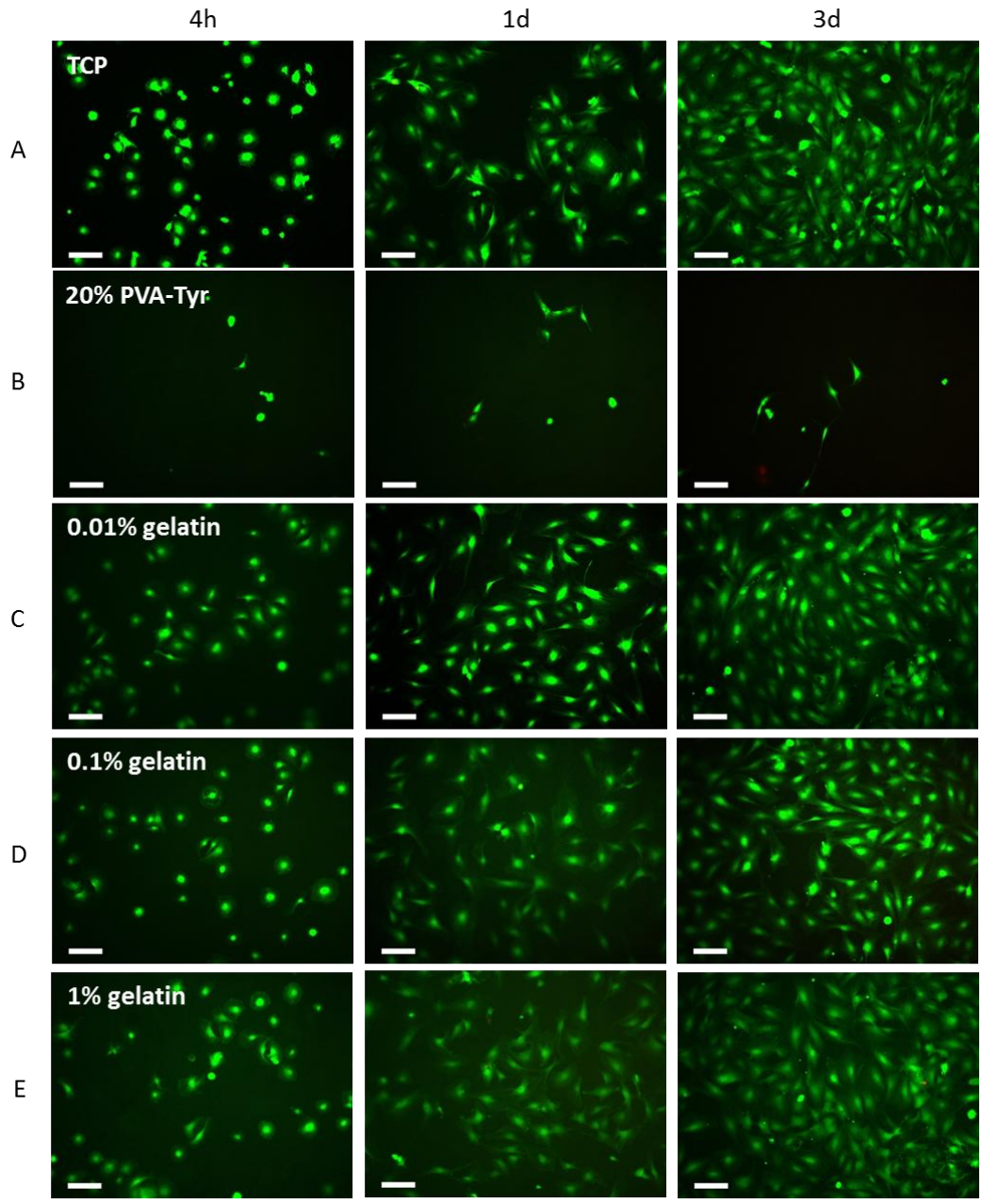

Figure 5.10: Live-dead images of attached SCLs on PVA-Tyr and PVA-Tyr/gelatin hydrogels at 4 hours, 1 and 3 days. A = TCP; B = 20% PVA-Tyr; C = 0.01% gelatin; D = 0.1% gelatin; E = 1% gelatin; Green = live; Red = dead. Scale bar = 100 µm.

5.3.4. Translating PVA-Tyr/gelatin hydrogels system as cell encapsulation matrices

As the overall objective of this thesis is to exploit PVA-Tyr hydrogels as cell encapsulation matrices, L929s were encapsulated within the PVA-Tyr/gelatin hydrogels. As observed in Figure 5.11, none of the cells encapsulated in the different PVA-Tyr/gelatin gels survived the photo-encapsulation process (all cells stained red).

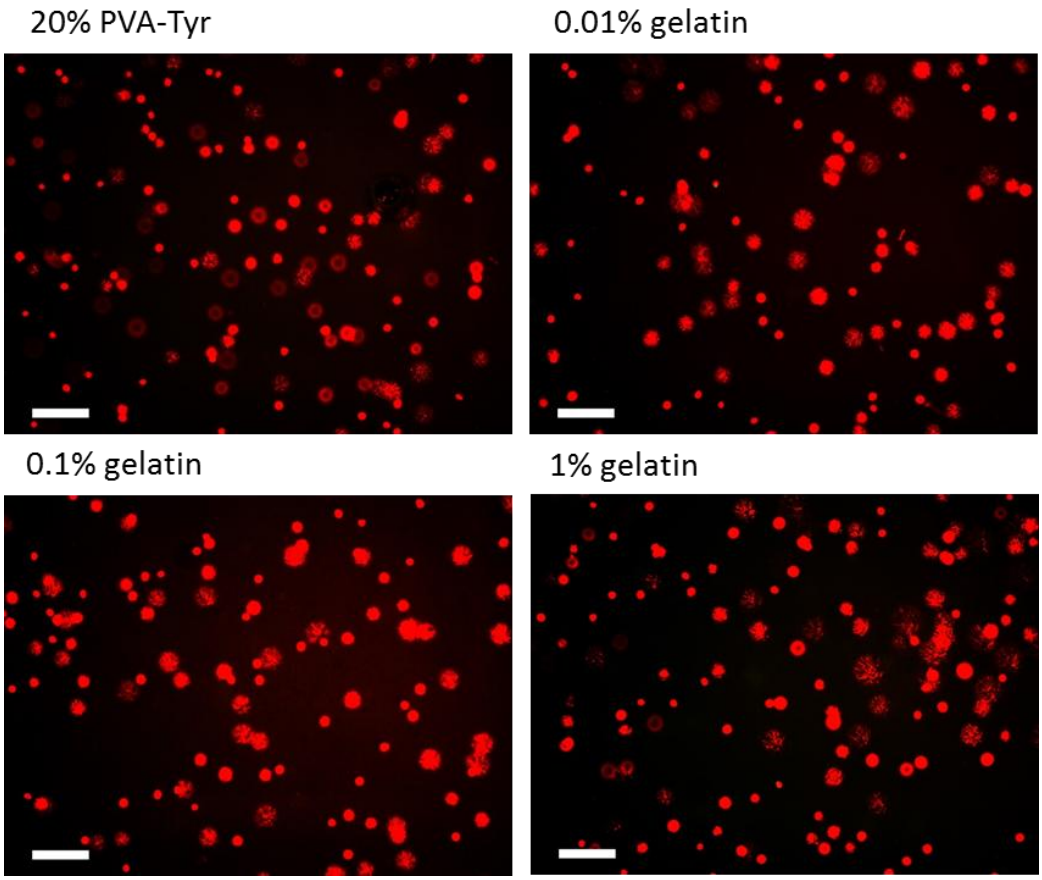

Figure 5.11: Live-dead images of L929s encapsulated in PVA-Tyr/gelatin hydrogels; Green = live; Red = dead. Scale bar = 100 µm.

This result was hypothesised to be due to the abundance of sulphate and tyrosyl radicals generated during the hydrogel formation. During the crosslinking process, the persulphates dissociate into sulphate anions and sulphate radicals

after accepting electrons from photoactivated Ru (Figure 5.12). At the same time, the photoactivated Ru^{3+} reacts with the phenolic moieites (tyramine of PVA-Tyr and tyrosine of gelatin) forming tyrosyl radicals. These free radicals may abstract electrons from the cells membranes causing peroxidation of the membrane lipids.

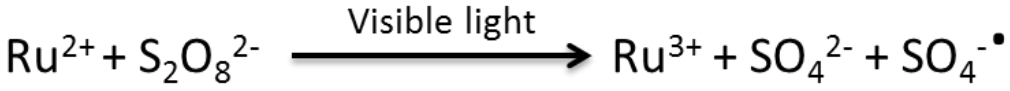

Figure 5.12: Generation of sulphate radicals during Ru/SPS photocrosslinking.

The cell membrane is made of a lipid bilayer that maintains the structural integrity of the cell, as well as the diffusion of proteins and nutrients across the membrane [365, 366]. It has been previously reported that free radicals and other reactive oxygen species produced in the body can disrupt the lipid bilayer through lipid peroxidation [366, 367]. Hence, it was speculated that the sulphate and tyrosyl radicals generated during crosslinking are also capable of damaging the cell membrane leading to cell death. Similarly, Lin et al. has also stated that free radicals generated from photoinitiators used in fabricating PEG hydrogels caused cellular damage during cell encapsulation [368, 369]. A study conducted by Farnsworth et al. showed that the radical initiated photopolymerisation process was exerting oxidative stress on chondrocytes encapsulated in PEG hydrogels [370]. Although the gelatin incorporated in the hydrogels is known to be anti-oxidative, its radical scavenging effect was not reflected in this study. This study showed that the Ru/SPS photopolymerisation process used to fabricate PVA-Tyr/gelatin hydrogels is not suitable to encapsulate cells, and further modification to the system is needed to promote cell survival during photoencapsulation.

5.4. Conclusion

The results from this chapter have demonstrated that non-chemically modified gelatin could be covalently crosslinked with PVA-Tyr through the native tyrosine groups present in the gelatin backbone. The incorporation of gelatin did not affect the mass loss and swelling profiles of the pure PVA-Tyr gels. The stable integration of gelatin was also reflected in the gelatin release study. Short cell adhesion assays using the L929s and HUVECs proved that the gelatin remained bioactive post crosslinking, and an amount as minimal as 0.01wt% was enough to augment bio-functionality of pure PVA-Tyr hydrogels. Furthermore, longer cell adhesion assays conducted using SCLs showed that the loss in surface mechanics and release of degradation products during gel degradation did not affect the viability and proliferation of SCLs on the PVA-Tyr/gelatin gels. However, cell encapsulation studies were not successful due to the generation of sulphate radicals that are detrimental to cells during the encapsulation. Hence, the next chapter will focus on promoting cell survival and viability within PVA-Tyr hydrogels.

Chapter 6

Promoting Cell Survival, Proliferation and Function in Degradable PVA-Tyramine Hydrogels

6.1. Introduction

Preliminary cell encapsulation studies in Chapter 5 showed that cells did not survive the photoencapsulation process. It was hypothesised that the sulphate and tyrosyl radicals (Figure 6.1) generated during the crosslinking reaction might impose oxidative stress to the cells, killing them in the process [252, 262].

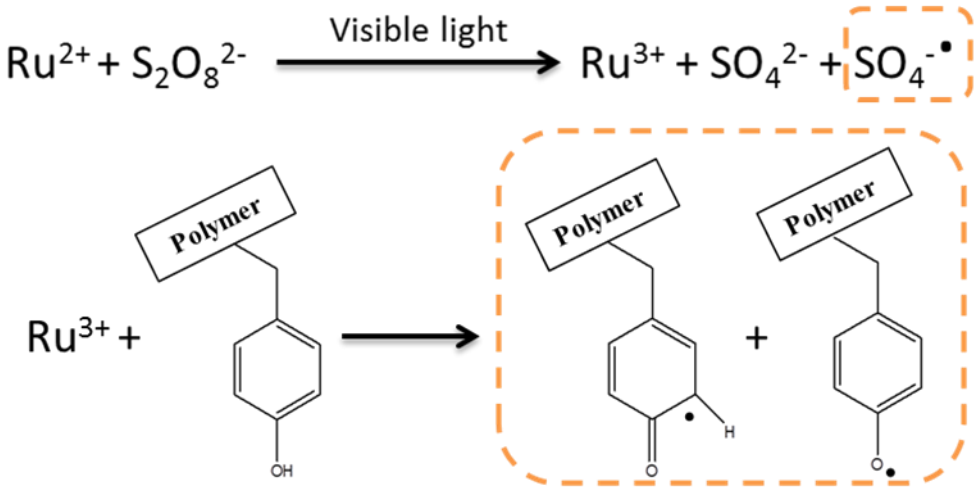

Figure 6.1: *Generation of sulphate and tyrosyl radicals (highlighted in boxes) during Ru/SPS photo-crosslinking.*

This hypothesis is in accordance with previous studies reported in the literature, where reduction in cell viability post encapsulation due to radicals was observed in photopolymerised hydrogels [82, 194, 371]. Nicodemus et al. demonstrated that the viability of chondrocytes decreased after encapsulation in photocrosslinked PEG hydrogels [194]. Lin et al. also showed a reduction in mouse insulinoma cells viability post photopolymerised into PEG hydrogels [369]. During the photoencapsulation process, the initiator molecules absorb photons of light and dissociate into radicals that react with functional groups on the hydrogel macromers to form covalent crosslinks [202, 370, 372]. The presence of radicals in the gel microenvironment creates a harsh environment for

cells, since the generated radicals can attack cells causing direct or indirect damage that may lead to cell death [369]. A study conducted by Burdick et al. indicated that the viability of fibroblasts encapsulated in photopolymerised hyaluronic acid gels decrease with increasing radical concentration [82]. These radicals can also react with oxygen, forming reactive oxygen species (ROS) that can trigger oxidative stress in cells [366].

Several photopolymerisation-induced ROS such as superoxide radical ($O_2^{\cdot\cdot}$), hydroxyl radical ($OH^{\cdot}$), singlet oxygen ($^1O_2$) and ozone (O_3), have been reported in the literature [366, 367]. In terms of cell encapsulation, these ROS can react with the lipid bilayer of cells, causing oxidative stress in the form of lipid peroxidation. It has been shown that lipid peroxidation disrupts the cell membrane integrity and permeability, which can lead to DNA damage, upregulation of tissue degrading enzymes, and generation of toxic products [365, 367]. Previous studies also demonstrated that chondrocytes encapsulated in photopolymerised PEG hydrogels had degenerated metabolic activity, reduced matrix synthesis, and upregulation of matrix metalloproteinase-13 (MMP-13) as effects of lipid peroxidation [370]. Therefore, the next step of this research was to incorporate antioxidants into these hydrogels to scavenge the radicals and ROS formed during the photoencapsulation process as an approach to protect the cells. In this chapter, the two antioxidative biomolecules of interest are ascorbic acid and silk sericin. These two molecules are water soluble and easily miscible with the PVA-Tyr macromer used in this thesis.

Ascorbic acid, also known as vitamin C occurs naturally in fruits and vegetables, and has important roles in growth, differentiation, and metabolism of plants [373, 374]. It was reported that ascorbic acid can react with oxygen more

rapidly than any other aqueous components to reduce the amount of ROS generated [375]. Moreover, it can also react with ROS directly, with and without enzyme catalysts, to form monodehydroascorbic or dehydroascorbic acid [374, 375]. These reduced forms can be regenerated back to ascorbic acid using enzyme complexes bound to the cell membrane [366, 373, 374]. Hence, ascorbic acid has been widely considered as the almost perfect antioxidant, due to its rapid ROS scavenging activity and most importantly, its ability to regenerate [366, 373].

On the other hand, silk sericin is a glue-like protein that coats silk fibers during cocoon formation [376]. It is secreted from the middle silk gland of a mature silkworm larva and is composed of random coil and β-sheet structures [244, 376]. Previous studies have shown that sericin has many biomedical advantages such as UV protective, cryoprotective, chemoprotective and most importantly, antioxidative [376-378]. Both Lim et al. and Dash et al. reported that sericin successfully protected keratinocytes from hydrogen peroxide and ultra-violet (UV) light induced oxidative stress [244, 379, 380]. It was also speculated that the high content of hydroxyl amino acid groups (serine and threonine) in sericin is responsible for its radical scavenging properties [379].

Although the antioxidative ability of sericin is well established, there are yet to be any studies comparing its radical scavenging efficiency to other conventional and well known antioxidants, such as ascorbic acid. However, it should be noted that there are many differences between ascorbic acid and sericin. For example, the molecular weight of ascorbic acid is 177Da, which is much smaller than sericin (150kDa) [244, 378, 381, 382]. Moreover, ascorbic acid is a simple organic molecule while sericin is a protein consisting of different primary

and secondary structures, as well as amino acid sequences that can facilitate several biological activities. Hence, it is of interest to compare these two molecules in this chapter.

Furthermore, previous studies have also reported that the presence of cell adhesive peptides or proteins is vital in promoting cell growth and proliferation within a 3D hydrogel network [227, 383-386]. Incorporating peptides or proteins containing the cell adhesive motif, Arginine-Glycine-Aspartic acid (RGD) into PEG hydrogels has been reported to significantly enhance chondrogenesis of encapsulated human mesenchymal stem cells as compared to pure PEG hydrogels [387]. Moreover, Yang et al. also showed that PEG hydrogels rich in RGD sequences successfully promoted osteogenesis of encapsulated marrow stromal cells [388]. As the two antioxidants, ascorbic acid and sericin are not known to possess any cell adhesive sequences, gelatin which is known to have abundance of RGD motifs will also be co-incorporated with the antioxidants into the PVA-Tyr gels [357].

While Chapter 5 demonstrated that the PVA-Tyr/gelatin gels had many advantages as pre-formed biomaterials (i.e., cells are placed *on* them after the polymerisation process), it was also shown that the encapsulation of cells was not feasible in these gels without further modification. This inability to encapsulate cells was hypothesised to be due to the abundance of radicals generated during the photopolymerisation procedure. Therefore, this chapter aims to promote cell survival during the photoencapsulation process by incorporating an antioxidative molecule (i.e., ascorbic acid or sericin) into the PVA-Tyr gels. The efficiency of these two antioxidants in terms of protecting cells from harmful radical generated during the crosslinking process will be evaluated. A secondary aim was to assess

the synergistic effect of integrating both the antioxidant and gelatin on the growth and proliferation of cells post encapsulation in PVA-Tyr hydrogels.

6.2. Experimental

6.2.1. Materials

All materials were purchased from Sigma-Aldrich unless otherwise stated. Poly(vinyl alcohol) (PVA) (13-23 kDa, 98% hydrolysed), succinic anhydride (SA), triethylamine (TEA), 1,3-dicyclohexylcarbodiimide (DCC), N-hydroxysuccinimide (NHS), tyramine (Tyr), sodium persulphate (SPS), tris(2,2-bipyridyl)dichlororuthenium(II) hexahydrate (Ru(II)bpy_3^{2+}), gelatin (porcine skin, type A, gel strength 300), molecular sieves (4Å), dialysis tubing (10 kDa molecular weight cut-off), Eagle's minimum essential media (EMEM), Dulbecco's phosphate buffered saline (DPBS), sodium carbonate, trypsin, fetal bovine serum (FBS), penicilin streptomycin (PS), ascorbic acid, bovine serum albumin (BSA), tween 20, triton X-100, paraformaldehyde, adenosine 5'-triphosphate disodium salt solution (ATP), calcein-AM and propidium iodide (PI), were used as received. Dimethyl sulfoxide (DMSO) was bought from Ajax Chemicals and was dried over 4 Å molecular sieves. Hydrogel disc moulds were made from silicone sheets (Silastic®Sheeting, reinforced medical grade silicone rubber, Dow Corning). CellTiterGlo ATP assay kit was bought from Promega. All primary antibodies were bought from Sapphire Bioscience. AlexaFluor-conjugated secondary antibodies were bought from Invitrogen, Australia. Rhodamine-phalloidin (Rh-phalloidin) and 4',6-diamidino-2-phenylindole (DAPI) were purchased from Molecular Probes, Australia.

6.2.2. Macromer preparation and hydrogel fabrication

PVA-Tyr used in this chapter was synthesised as described in Chapter 3 using conventional DCC/NHS chemistry and characterised to have 7 Tyr per PVA chain (2% conjugation). The macromer solution was also prepared as described in previous chapters. Dried and sterile PVA-Tyr was dissolved in sterile DPBS, then left to cool at RT overnight. The total macromer percentage was kept at 20 wt%.

6.2.3. Incorporation of antioxidants into PVA-Tyr hydrogels

Antioxidants (ascorbic acid or sericin) were also incorporated into the gels to promote survival of the encapsulated cells. Both ascorbic acid and sericin were dissolved separately then mixed with the PVA-Tyr solution at RT prior to addition of initiators. The concentration of initiators used was 2 mM Ru/20 mM SPS, and the samples were irradiated with 15mW/cm^2 of visible light (Blue wave 200, Dymax Co., 400 – 450 nm) for 3 minutes. The concentration of ascorbic acid tested was 2, 10 and 20 mM, whereas the concentration of sericin was 0.5 and 1 wt%. Ascorbic acid was used as received from the manufacturer, whereas sericin was isolated from silkworm cocoons as outlined in section 6.2.3.1. below.

6.2.3.1. Isolation of sericin from silkworm cocoons

Antheraea mylitta silkworm cocoons were kindly provided by Professor Subhas Kundu from the Indian Institute of Technology Kharagpur, India. The cocoons were cut into small pieces then boiled in excess 0.02 M sodium carbonate solution for 4 hours. The supernatant was dialysed against deionised

water for 3 days. Post dialysis, the sericin solution was sterile filtered and then lyophilised.

6.2.3.2. Mass loss and swelling studies

Mass loss and swelling studies were performed as per outlined in previous chapters to evaluate the physical properties of the antioxidants incorporated hydrogels. In brief, the fabricated hydrogels were weighed after crosslinking for $m_{initial}$. The samples were then incubated in PBS (pH = 7.4) at 37 ºC. After 1 day, the samples were removed and weighed for $m_{swollen}$, then freeze-dried for m_{dry}. The mass loss and mass swelling ratio (q) were calculated using equations detailed in Chapter 3 (Eqs 3.3-3.5). The sol fraction is the mass loss at 1 day [9, 244].

6.2.4. L929 cell encapsulation

L929s were encapsulated in the hydrogels as described in Chapter 5. Cell suspension was added to the macromer solution to give a final density of $1x10^6$ cells/mL, and the solution was gently mixed again to ensure even cell distribution. The solution was then transferred into silicone moulds (7.5 mm diameter x 0.25 mm thick) sandwiched between two cover slips, then irradiated under 15 mW/cm^2 of visible light (Blue wave 200, Dymax Co., 400 – 450 nm) for 3 minutes. The samples were immediately immersed in media then placed in a humidified incubator (37 °C and 5% CO_2). After 1 day, the media was discarded to remove the sol fraction and initiator residues. The samples were then replenished with fresh media every 3 days. Macroscopic images of the samples at different time points were taken using the Leica M80 stereo

microscope at 0.75x magnification. The sample names corresponding to the concentration of biological molecules incorporated in to the PVA-Tyr hydrogels were listed in Table 6.1.

Table 6.1: Sample names corresponding to the concentration of biological molecules incorporated into PVA-Tyr hydrogels.

Sample	PVA-Tyr (wt%)	Ascorbic acid (mM)	Sericin (wt%)	Gelatin (wt%)
2 mM Ascorbic acid	20	2	-	-
10 mM Ascorbic acid	20	10	-	-
20 mM Ascorbic acid	20	20	-	-
0.5% sericin	19.5	-	0.5	-
1% sericin	19	-	1	-
0.01% gelatin	18.99	-	1	0.01
0.1% gelatin	18.9	-	1	0.1
1% gelatin	18	-	1	1

6.2.4.1. Live-dead assay

The viability of the cells encapsulated in the gels was evaluated at time points 1, 3, 7, 14 and 21 days. At each respective time points, the samples were washed with DPBS then stained with 1 µg/ml of Calcein-AM and PI. After 10 minutes incubation with the stains, the gels were washed with DPBS again then imaged using fluorescence microscope (Zeiss, Axioshop 2 MAT) while hydrated. ImageJ (version 1.46, National Institutes of Health) was used to count the cells. The viability of the cells was calculated based on the following equation:

$$Viability\ (\%) = \frac{number\ of\ live\ cells}{number\ of\ live\ cells + dead\ cells}\ x\ 100 \quad (6.1)$$

Similarly, ImageJ was also used to quantify the live cell coverage area using the following equation:

$$Live\ cell\ coverage\ area\ (\%) = \frac{Pixels_{\ live\ cells}}{Pixels_{\ total\ image}}\ x\ 100 \quad (6.2)$$

6.2.4.2. Cytoskeleton organisation staining of L929s encapsulated in1% gelatin gels

The morphology and cytoskeletal organisation of L929s encapsulated in the hydrogels was studied through actin filament staining as described in Chapter 5. The cell encapsulated samples were firstly fixed in 4% formaldehyde then washed with blocking solution (3% (w/v) BSA and 0.5% (w/v) tween in DPBS). Next, the cells were then permeabilised with 0.25% (w/v) triton X-100, and then incubated for 1h with Rh-phalloidin (1:500 in blocking solution) and DAPI (1:500 in blocking solution). The samples were washed with DPBS post staining, followed by imaging using the confocal microscope (Olympus FV1000).

6.2.4.3. ATP assay

The metabolic activity of L929s encapsulated in the gels was evaluated using the CellTiterGlo luminescent cell viability assay. The samples were firstly washed with DPBS, and then incubated on an orbital shaker at RT in 100 µl DPBS and 100 µl CellTiterGlo reagent for 45 minutes. The luminescence of the samples was then measured using a microplate reader (Tecan Infinite200). The ATP concentrations of the samples were then calculated from a standard curve constructed using known concentrations of ATP.

6.2.4.4. Immunocytochemistry staining of ECM produced in hydrogels

Samples were firstly fixed in 4% formaldehyde solution overnight, followed by blocking with 3% (w/v) BSA and 0.5% (w/v) in DPBS at RT. Primary antibodies as shown in Table 6.2 were diluted in DPBS, added to the samples, and then incubated overnight at 4 ºC. Samples were then washed three times with DPBS, then incubated with AlexaFluor-conjugated secondaries (Molecular Probes/Invitrogen), diluted 1:200 with DPBS, in the dark at RT for 1 hour. Samples were once again washed with DPBS three times, and then counter-stained with Rh-phalloidin to visualise the F-actin, and DAPI to observe the cell nuclei. Post staining, the samples were washed with DPBS three times and then kept in the dark at RT until being imaged using confocal microscopy (Olympus FV1000 and Zeiss LSM780). Samples were viewed at 10x and 40x magnification.

Table 6.2: Host species and source of primary antibodies used for immunohistochemistry

Antigen	Host species	Source
Collagen IV	Rabbit	Abcam
Laminin	Rabbit	Abcam

6.2.4.5. Quantification of ECM produced in hydrogels

The amount of ECM produced in the hydrogels was quantified using Coomassie Plus Protein assay (ThermoFisher). The cells encapsulated samples were completely degraded in DPBS at 60 ºC for 2 days. 150 µl of sample was then added with 150 µl of Coomassie working reagent, and then incubated at RT for 15 minutes. The samples absorbance was read at 570 nm using a plate reader

(Tecan Infinite F200). The protein concentrations were calculated from a standard curve constructed using known concentrations of BSA. Blank samples without any cells encapsulated were used as controls.

6.2.3. Statistical analysis

All samples were prepared in triplicates and all experiments were repeated three times. Two-way ANOVA model constructed using Minitab 15 statistical analysis software was used to analyse the results.

6.3. Results and discussion

6.3.1. Incorporation of antioxidants into PVA-Tyr hydrogels

It was previously shown in Chapter 5 that the cells did not survive the photoencapsulation process. It was hypothesised that the sulphate and tyrosyl radicals generated during the encapsulation process may directly damage the cells, or react with oxygen to form ROS that are detrimental to the cells. Hence, two different types of antioxidants, ascorbic acid and sericin, were incorporated into PVA-Tyr hydrogels to address this problem. Ascorbic acid has been widely referred to as the gold standard for antioxidants, due to its high radical scavenging efficiency and ability to regenerate [366, 373]. On the other hand, silk sericin has been discovered in the past decade as an antioxidative protein with other biological attributes such as being cryoprotective and chemoprotective [244, 379, 380]. Hence, this section will focus on comparing the effect of ascorbic acid and sericin on the crosslinking efficiency of PVA-Tyr gels, as well as their ability to protect cells during the photopolymerisation process.

6.3.1.1. Mass loss and swelling studies

The incorporated antioxidants have the potential to scavenge both the harmful sulphate radicals, as well as the beneficial and needed tyrosyl radicals that are formed during the photopolymerisation process. The covalent bonds required to crosslink the hydrogel network will not be formed if the tryosyl radicals were scavenged (see Chapter 3). Therefore, mass loss and swelling studies were performed to evaluate the quality of the fabricated gels and determine if the polymerisation reaction was still able to efficiently crosslink the macromers. The concentration of ascorbic acid used was set at a maximum of

20mM, corresponding to the concentration of SPS. However, no gel was formed at this concentration. A study conducted by Fancy et al. showed that the key components for the crosslinks formation are the tyrosyl radicals, where quenching all the sulphate radicals did not affect the overall crosslinking efficiency [252, 262]. Therefore, it was hypothesised that ascorbic acid at 20mM was able to quench not only the sulphate radicals, but all the radicals generated including the tyrosyl radicals required for crosslinking. When the ascorbic acid concentration was decreased to 10 mM and 2 mM, PVA-Tyr gels were successfully formed. However, it was also observed that lower concentrations of ascorbic acid resulted in PVA-Tyr gels with lower sol fractions and mass swelling ratios (Table 6.3). This observation agrees with the literature where the radical scavenging activity of ascorbic acid is dose dependant [375, 389]. It was speculated that by lowering the concentration of ascorbic acid, the overall radical scavenging efficiency is also reduced. Therefore, tyrosyl radicals are still present in the system to allow formation of crosslinks.

Table 6.3: Sol fraction (%) and mass swelling ratio of antioxidants incorporated PVA-Tyr hydrogels.

Sample	**Sol fraction (%)**	**Mass swelling ratio, *q***
20 mM Ascorbic acid	No gel formed	
10 mM Ascorbic acid	54.7 ± 3.1	14.1 ± 0.7
2 mM Ascorbic acid	24.3 ± 1.8	8.9± 0.2
1% sericin	23.6 ± 1.9	9.6 ± 0.1
0.5% sericin	21.9 ± 3.1	9.1 ± 0.8

On the other hand, PVA-Tyr gels copolymerised with 1 wt% sericin produced gels with similar sol fraction and mass swelling ratio as pure PVA-Tyr gels (i.e., without any antioxidants incorporated) (sol fraction = 25.6 ± 4.9, q = 9.7 ± 0.5). More interestingly, the quality of the gels was not influenced by the concentration of sericin, as similar sol fractions were observed for gels with 0.5% (Table 6.3). This observation is in contrast to the results obtained with ascorbic acid, where higher concentrations of ascorbic acid lead to a reduction in crosslinking efficiency (higher sol fraction and q). This observed difference might be due to the composition of sericin. Amino acid analysis has shown that the sericin used in this study (*A. mylitta)* has a high tyrosine contents (3 mol%) [378]. Therefore, it is believed that despite being able to scavenge sulphate and tyrosyl radicals (from SPS and PVA-Tyr), the tyrosine groups on the sericin were also converted to new tyrosyl radicals at the same time. Hence, the newly generated tyrosyl radicals from sericin further ensured the formation of covalent bonds that were required to crosslink the network.

6.3.1.2. Viability of L929s encapsulated in PVA-Tyr/antioxidants gels

Next, the protective effects and efficiency of ascorbic acid and sericin in promoting the survival of L929s were evaluated through cell encapsulation studies. In this study, the addition of 2 mM ascorbic acid did not show any improvement in cell survival (Figure 6.2), where all the cells are stained red (viability = 0%). Previous mass loss results (section 6.3.1.1.) indicated that 2 mM of ascorbic acid was the only concentration that made high quality gels (i.e., low sol fraction), although this was hypothesised to be due to there not being enough ascorbic acid to quench all the radicals generated during the crosslinking process.

Therefore, it was expected that there were still large amounts of radicals present in the system and these were still able to damage the cells.

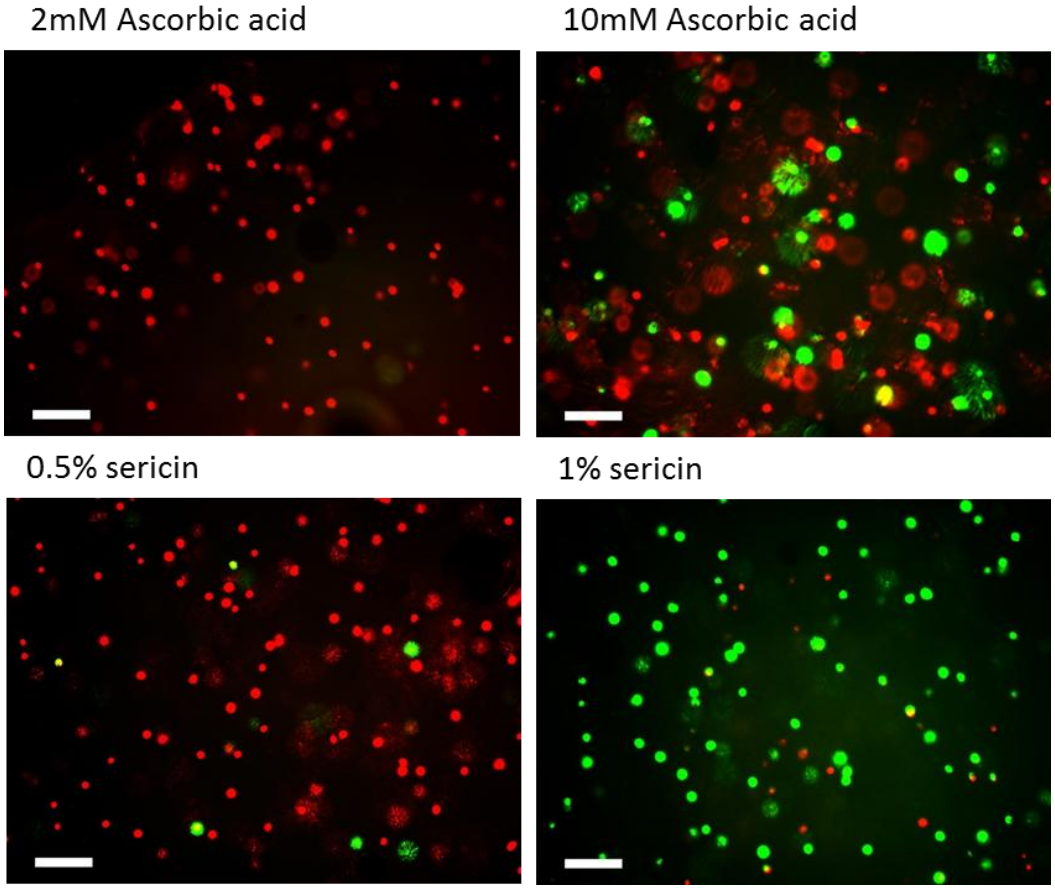

Figure 6.2: Live-dead images of L929s encapsulated in PVA-Tyr hydrogels incorporated with ascorbic acid or sericin; Green = live; Red = dead; Scale bar = 100 µm.

Increasing the ascorbic acid concentration to 10 mM, which was previously shown in the mass loss studies to have a profound effect on the quenching of radicals at the expense of the quality of the formed gel, significantly improved the cellular viability to 62 ± 17% (Figure 6.2 and Table 6.4). Similarly with sericin, incorporation of 0.5 wt% sericin showed improvement in cell survival over pure PVA-Tyr gels with a viability of 19.3 ± 9.0%, whereas 1% sericin gels had a viability of 90.4 ± 3.8%.

Table 6.4: Viability of L929s encapsulated in antioxidant incorporated PVA-Tyr gels

Sample	Viability (%)
2 mM Ascorbic acid	0
10 mM Ascorbic acid	62.0± 17.0
0.5% sericin	19.3 ± 9.0
1% sericin	90.4 ± 3.8

Ascorbic acid is a well-known naturally occurring biological molecule that scavenges transition metal radicals and ROS formed in the body. In this study, the concentration of ascorbic acid present in the system during the photoencapsulation process greatly affected the survival of the cells in the gels. Once again, this result agrees with previous studies where the antioxidant activity of ascorbic acid is dose dependant [389]. Rekha et al. showed that more 2,2-diphenyl-1-picrylhydrazyl (DPPH) radicals were scavenged with increasing concentrations of ascorbic acid [389]. Oh et al. reported that the amount of ROS in UV irradiated cells decrease with increasing concentration of ascorbic acid treatment [390]. In this study, although 10 mM of ascorbic acid was able to increase cell viability, it also caused a significant increase in the sol fraction of the hydrogel. This observation indicates that in spite of scavenging the harmful sulphate radicals to protect the cells, the added ascorbic acid was also quenching the tyrosyl radicals that are responsible for the hydrogel crosslinking. This non-specific quenching then led to a major decrease in the crosslinking efficiency and formation of hydrogels with higher sol fraction and mass swelling ratios.

On the other hand, sericin is an antioxidative protein that is present in silkworm cocoons. Previous studies has shown that this protein is able to protect cells from UV induced oxidative stress due to the abundance of hydroxyl amino acid groups present (serine and threonine) in the protein sequence [376, 379, 380, 391]. In this study it was shown that the more sericin that was incorporated into the hydrogels, the higher the cell viability with no effect on the quality of the gel that was formed. This result agrees with previous findings where the cytoprotective activity of sericin has been reported to be dosage dependant [244, 379, 380]. Dash et al demonstrated that 150 ng/ml of sericin significantly increased the cell viability of hydrogen peroxide treated fibroblasts compared to 30 ng/ml [379]. Lim et al also showed that oxidative stressed keratinocytes treated with 100 ng/ml of sericin had lower levels of oxidative damage markers (catalase and malonaldehyde) as compared to 50 ng/ml [244]. Most importantly in this study, the incorporation of sericin did not affect the hydrogel crosslinking efficiency. Once again, this phenomenon was speculated to be due to the high tyrosine content in sericin [376]. While scavenging the harmful radicals, the tyrosine groups of sericin are also being converted into new tyrosyl radicals. Since there was no overall loss in tyrosyl radical generation, the hydrogel crosslinking efficiency was also not affected.

Although ascorbic acid at a concentration of 10mM did improve the survival and viability of cells during the photoencapsulation process, it was also shown to reduce the crosslinking efficiency of the PVA-Tyr gels by scavenging the tyrosyl radicals required for the hydrogel formation. Conversely, incorporation of sericin (0.5 and 1 wt%) did not impair the physical properties of the PVA-Tyr/sericin gels formed, and was believed to be due to the abundance of

tyrosine groups present in sericin. Moreover, 1% sericin was also revealed to have the best cell protective effect. Therefore, all further cell encapsulation studies are conducted with 1% sericin incorporated in the gels to ensure cell survival without affecting the hydrogel crosslinking efficiency during the encapsulation process.

6.3.2. L929s encapsulation in PVA-Tyr/sericin/gelatin hydrogels

Previous studies have shown that cell adhesive sequences in forms of either peptides or proteins are important to promote cell growth and proliferation in 3D hydrogel networks [212, 383, 392]. In this study, sericin was incorporated into the PVA-Tyr gels as an antioxidant to protect the cells during the encapsulation process. However, no cell adhesive sequences have been found in this protein [244, 381]. Therefore, gelatin, which has an abundance of cell adhesive motifs (RGD), was also co-incorporated with sericin into PVA-Tyr hydrogels. It has been previously shown in Chapter 5 that gelatin could be covalently bound into PVA-Tyr gels, and successfully facilitated 2D cell adhesion on the gels but was not sufficient to protect the cells during the encapsulation process. Therefore, this section is focused on evaluating the effect of combining both sericin and gelatin in the gels on the behaviour of the encapsulated cells. It was hypothesised that the antioxidative sericin will scavenge the radicals detrimental to the cells during the photoencapsulation process itself, while gelatin will further enhance the cell growth and function in the gels over time. The concentration of sericin was kept constant at 1 wt%, whereas the concentration of gelatin was varied from 0.01, 0.1 to 1 wt%. The

sample names corresponding to the sample compositions were tabulated in Table 6.1 in section 6.2.4.

6.3.2.1. Cell viability and proliferation

All the L929s encapsulated in 1% sericin, 0.01% gelatin, 0.1% gelatin and 1% gelatin gels retained high viability for all time points (up to 21 days) as shown in Figures 6.3 and 6.4. The cells were able to proliferate and cell aggregates were noticeable at later time points (14 and 21 days, Figure 6.4). Cell proliferation leading to aggregation has been previously reported in the literature [386, 392-394]. Chen et al. showed that breast tumour cells (LCC6) formed multicellular spheroids when encapsulated in 2 wt% alginate hydrogels [395]. Aubin et al. also demonstrated that human liver carcinoma cells (HEP-G2) encapsulated in 5 wt% gelatin methacrylate hydrogels were able to aggregate after 5 days [396]. Fibroblasts encapsulated in pullulan methacrylate hydrogels also formed clusters post encapsulation, where the aggregate diameter was found to increase with time [397]. In this study, there was a marked difference observed between PVA-Tyr/sericin and PVA-Tyr/sericin/gelatin gels. Significantly sized cell aggregates were only visualised in gels with gelatin incorporated (Figure 6.4).

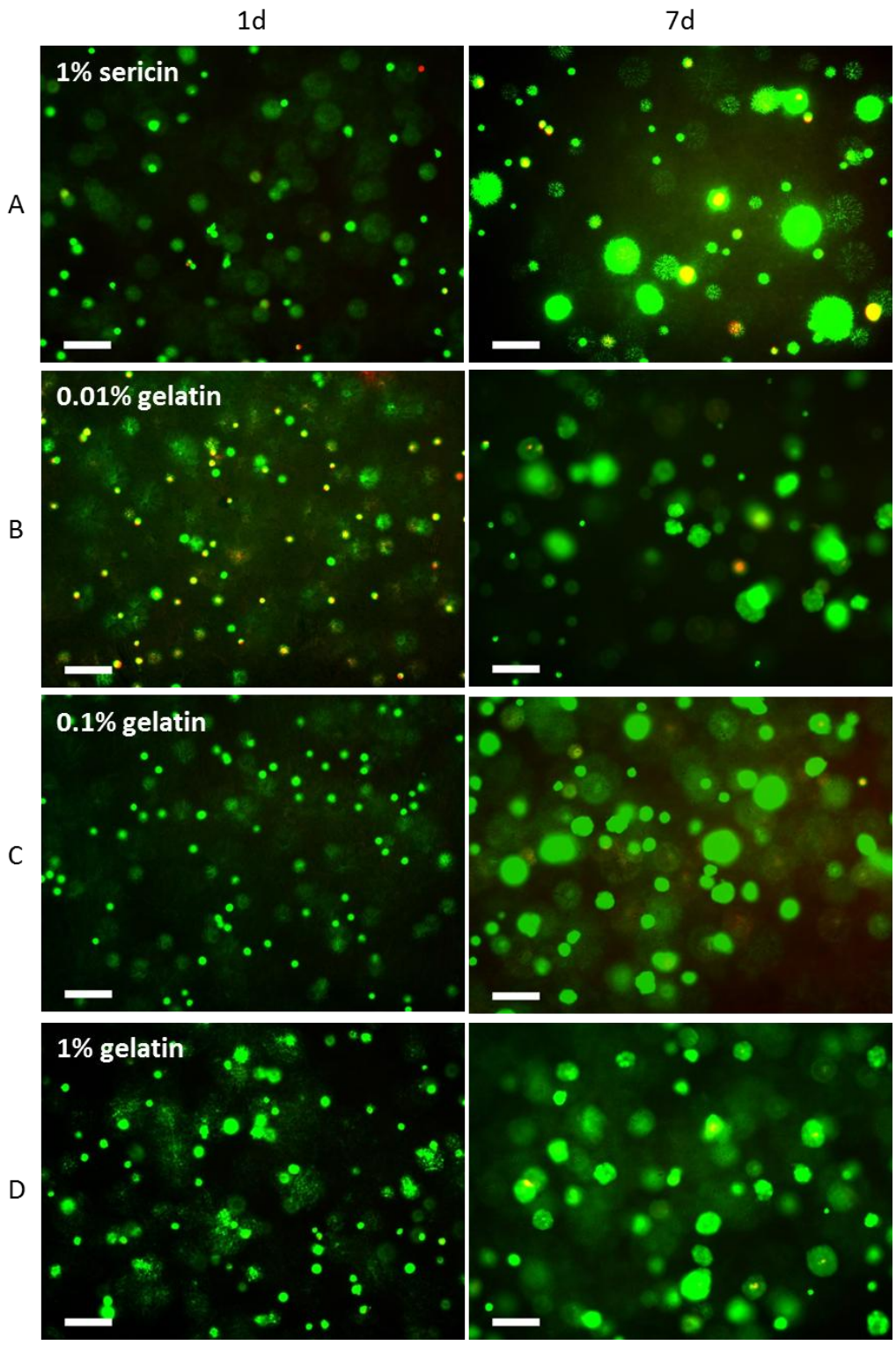

Figure 6.3: Live-dead images of L929s encapsulated in PVA-Tyr/sericin gels and PVA-Tyr/sericin/gelatin gels at 1 and 7 days; A = 1% sericin; B = 0.01% gelatin; C = 0.1% gelatin; D = 1% gelatin; 1wt% sericin was incorporated in all samples. Green = live; Red = dead; Scale bar = 100 µm.

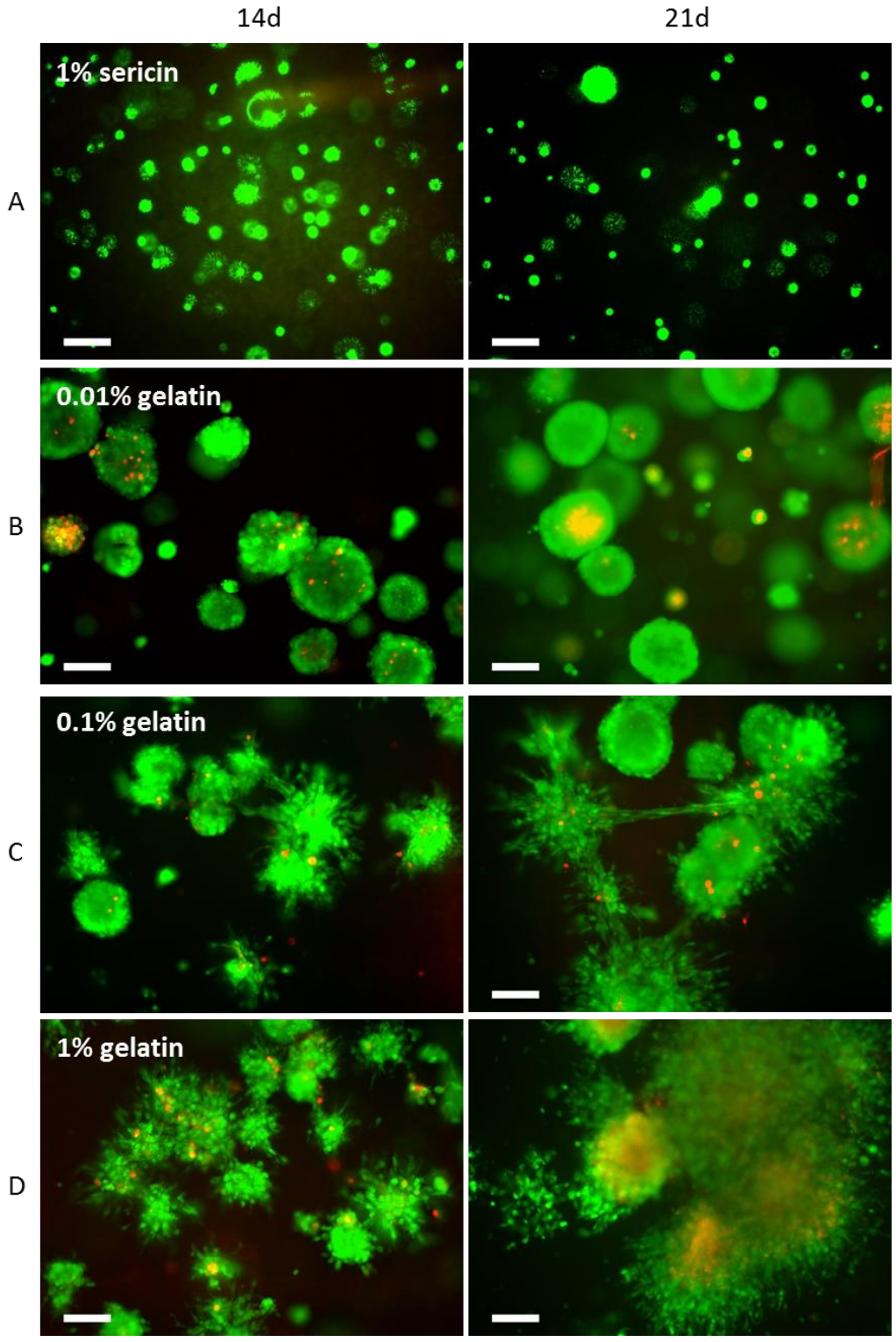

Figure 6.4: Live-dead images of L929s encapsulated in PVA-Tyr/sericin and PVA-Tyr/sericin/gelatin gels at 14 and 21 days; A = 1% sericin; B = 0.01% gelatin; C = 0.1% gelatin; D = 1% gelatin; 1wt% sericin was incorporated in all samples; Green = live; Red = dead; Scale bar = 100 µm.

This lack of cell proliferation and aggregation in the PVA-sericin gels is confirms our hypothesis where although sericin was able to protect the cells during the polymerisation, it was not able to promote cell proliferation and aggregation, due to the absence of cell adhesive sequences. A study conducted by Raza et al. reported that incorporation of cell adhesive peptide sequences into PEG gels greatly promoted formation of epithelial cell clusters [383]. Therefore, gelatin which has abundance of cell adhesive motifs (RGD) was believed to be capable of significantly enhancing the L929s proliferation and aggregation in these gels [357].

Moreover, the morphology of the cell clusters was also examined. At 14 and 21 days, cell spreading was only observed in 0.1% and 1% gelatin gels, and not in 0.01% gelatin gels (Figure 6.4). F-actin staining for cell aggregates in 1% gelatin gels showed that the encapsulated cells had elongated and spindled morphology (Figure 6.5).

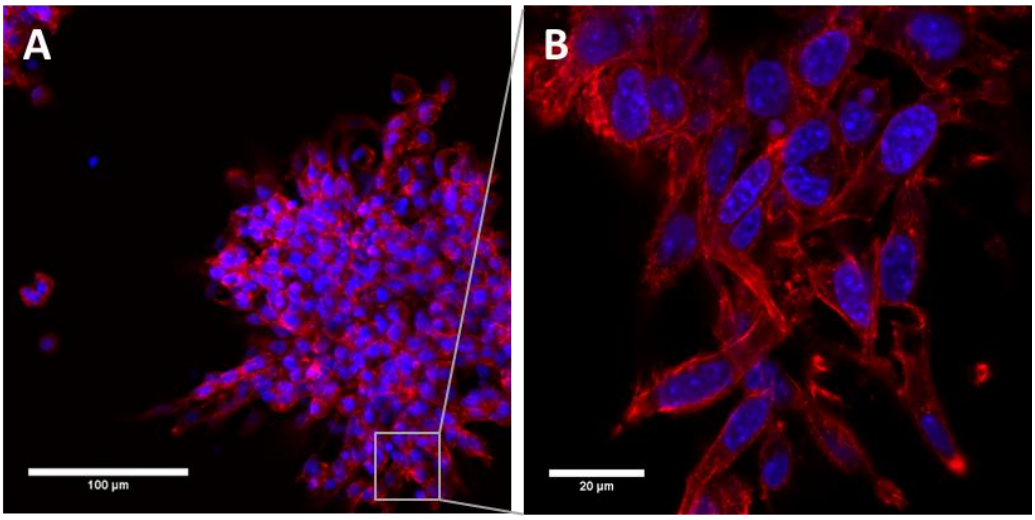

Figure 6.5: F-actin staining of L929s encapsulated in 1% gelatin (+18%PVA and 1% sericin) hydrogels at 21 days. A = image taken at 10x (scale bar = 100 µm); B = image taken at 40x (scale bar = 20 µm).

It was clearly visualised that the cells were forming tight cell-cell contact in the aggregates (Figure 6.5). Furthermore, the cell clusters in 0.01% gelatin gels remained individually separated at 21 days, while interconnected networks were formed between cell aggregates in 0.1% and 1% gelatin gels (Figure 6.4). This observation indicated that gelatin was required for cell spreading and network formation in the 3D hydrogel matrix. Once again, it was believed that the cell adhesion ligands present in gelatin was responsible for the migration of cells out from the clusters. The fact that the formation of interconnected networks happened only after 14 days, also indicated that a degree of gel degradation might be required for migratory activity of the encapsulated cells. It was hypothesised that as the hydrogel was degrading, the increase in average mesh size combined with the reduction in the mechanical rigidity of the gel allowed cell migration. It was previously reported that cells trapped in highly crosslinked networks were unable to translocate their integrins to fibrillar adhesions, which results in poor migratory action and matrix assembly [93, 94]. Fibroblasts encapsulated in highly crosslinked collagen gels were unable to stretch and proliferate [398]. Similarly, Peyton et al. reported that the spreading of smooth muscle cells in PEG-fibrinogen gels decreased with increasing gel stiffness [399]. Nichol et al. also showed that endothelial cells encapsulated in 15 wt% gelatin-methacrylate gels were unable to form cellular networks. However, when the gelatin-methacrylate concentration was reduced to 5 wt%, interconnected networks were observed after 2 days [154]. This result showed that higher scaffold rigidity may limit the cell movement in the 3D environment. This statement was also supported by Jeong et al. who demonstrated that

morphologies and movements of cells encapsulated in alginate hydrogels were greatly dependant on the substrate stiffness [398].

It should be noted that at 21 days the cell aggregates appeared to have a necrotic core (stained red in the middle, Figure 6.4). This phenomenon might be due to the compactness of the aggregates, where the core was unable to obtain nutrients and oxygen required to maintain viability and function. This result agrees with a study conducted by Skiles at al., where mouse insulinoma (MIN6) aggregates encapsulated in PEG hydrogels had a hypoxic core, where diffusion of oxygen across the cell aggregates was limited [400]. Overall, it was demonstrated in this study that the combination of gelatin concentration and gel degradation facilitated the spreading and migration of the encapsulated L929s.

Live-dead images were analysed to quantify the live cell coverage area as a measure of cell density in the gel. There was no significant difference between all the samples at 1 and 3 days. However, it was observed that starting from day 7 the gelatin containing gels had much larger cell coverage area (Figure 6.6). Addition of gelatin markedly improved the bioactivity of the gels as seen at 14 and 21 days. 0.01% gelatin, 0.1% gelatin and 1% gelatin samples were analysed to be significantly different to gels with no gelatin incorporation (1% sericin gels) at both 14 and 21 days (Figure 6.6). 1% gelatin samples were by far the best performing gels in terms of promoting cell proliferation (cell coverage area) and were statistically different to 0.01% gelatin and 0.1% gelatin at 7, 14 and 21 days. Once again, this result showed that although sericin was able to protect the cells from radical damage during the encapsulation process, it was unable to promote cell proliferation in the gel. A combination of both sericin and gelatin was required to maintain cell survival and growth in the PVA-Tyr gels.

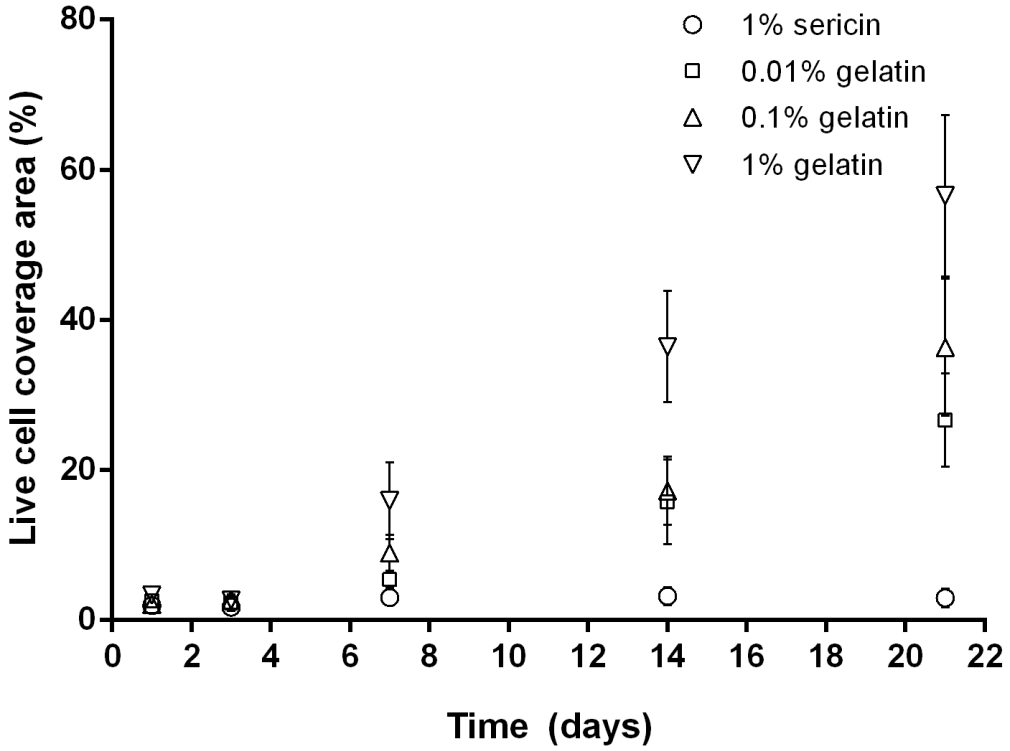

Figure 6.6: Live cell coverage area of L929s encapsulated in PVA-Tyr/sericin/gelatin gels. No significant differences ($p<0.05$) were observed between all samples at time points 1 and 3 days. 0.01%, 0.1% and 1% gelatin were significantly different ($p<0.05$) to 1% sericin at 14 and 21 days. 1% gelatin was statistically different ($p<0.05$) to 0.01% and 0.1% gelatin at 7, 14 and 21 days.

6.3.2.2. Metabolic activity of L929s encapsulated in PVA-Tyr/sericin/gelatin hydrogels

The metabolic activity of fibroblasts encapsulated in the PVA-Tyr/sericin/gelatin hydrogels was evaluated by measuring the quantity of ATP produced by the cells post encapsulation. It was shown that all the samples had similar ATP concentration 1 day post encapsulation, and thus had similar cell numbers (Figure 6.7).

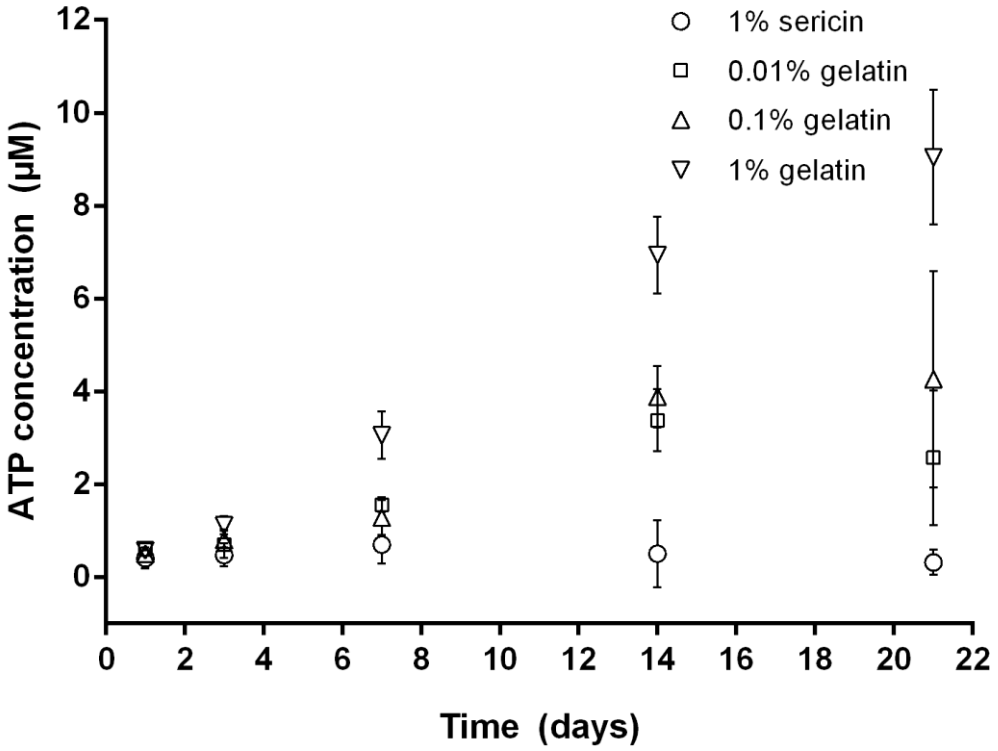

Figure 6.7: Metabolic activity of fibroblasts encapsulated in PVA-Tyr/sericin/gelatin hydrogels. No significant differences ($p<0.05$) were observed between all samples at time points 1 and 3 days. 0.01%, 0.1% and 1% gelatin were significantly different ($p<0.05$) to 1% sericin at 14 and 21 days. 1% gelatin was statistically different ($p<0.05$) to 0.01% and 0.1% gelatin at 7, 14 and 21 days.

However, L929s crosslinked in 1% sericin gels (no gelatin) produced a constant level of ATP for all time points (i.e., no increase in ATP means no increase in cell numbers). This result agreed with the live-dead assay (Figure 6.3 and 6.4) where the L929s in 1% sericin gels survived the photocrosslinking process, but did not show any significant growth and proliferation over time. On the other hand, PVA-Tyr hydrogels which contained both sericin and gelatin (0.01% gelatin, 0.1% gelatin and 1% gelatin) showed increased ATP levels over time. Once again, this phenomenon matched the live-dead assay, where PVA-

Tyr/sericin/gelatin gels showed significantly greater cell proliferation than PVA-Tyr/sericin samples. A previous study conducted by Desimone et al. showed that metabolic activity of fibroblasts encapsulated in collagen gels increased over a 14 days period [401]. As gelatin is derived from collagen and retains similar cellular interaction sequences with native collagen, it was expected that the presence of gelatin in PVA-Tyr gel would support the metabolic activity of encapsulated fibroblasts. Moreover, statistical analysis showed that 1% gelatin gels had significantly higher ATP compared to all other samples at 7, 14 and 21 days (Figure 6.7). This observation confirmed that the 1% gelatin gels are the most suitable for cell encapsulation studies, and all further experiments were conducted using this composition.

6.3.3. Characterisation of ECM produced in 1% gelatin encapsulated with L929s

Cells encapsulated in the PVA-Tyr/sericin/gelatin gels were hypothesised to secrete their own extracellular matrix while the gel degrades hydrolytically. Therefore, the next step was to evaluate the function of the encapsulated L929s in terms of ECM secretion, by characterising and identifying the ECM produced.

6.3.3.1. Macroscopic images of 1% sericin/1% gelatin gels encapsulated with L929s

Macroscopic images of the samples revealed that at 1 day, the appearance of samples with and without cells was very similar. However, cell clusters in forms of white spots were noticeable at later time points in cell containing samples (Figure 6.8). This result agreed with the live-dead assay where the

encapsulated fibroblasts agglomerated in the 1% gelatin gels. Most importantly, it was also shown that the samples without cells were almost completely degraded and the structural integrity of the network was severely compromised at 14 days (Figure 6.8). In contrast, the cell containing samples were still structurally intact. Similarly trends were observed at 21 days (i.e., 1% gelatin gels encapsulated with L929s were still physically intact whereas samples without cells were completely degraded, Figure 6.8).

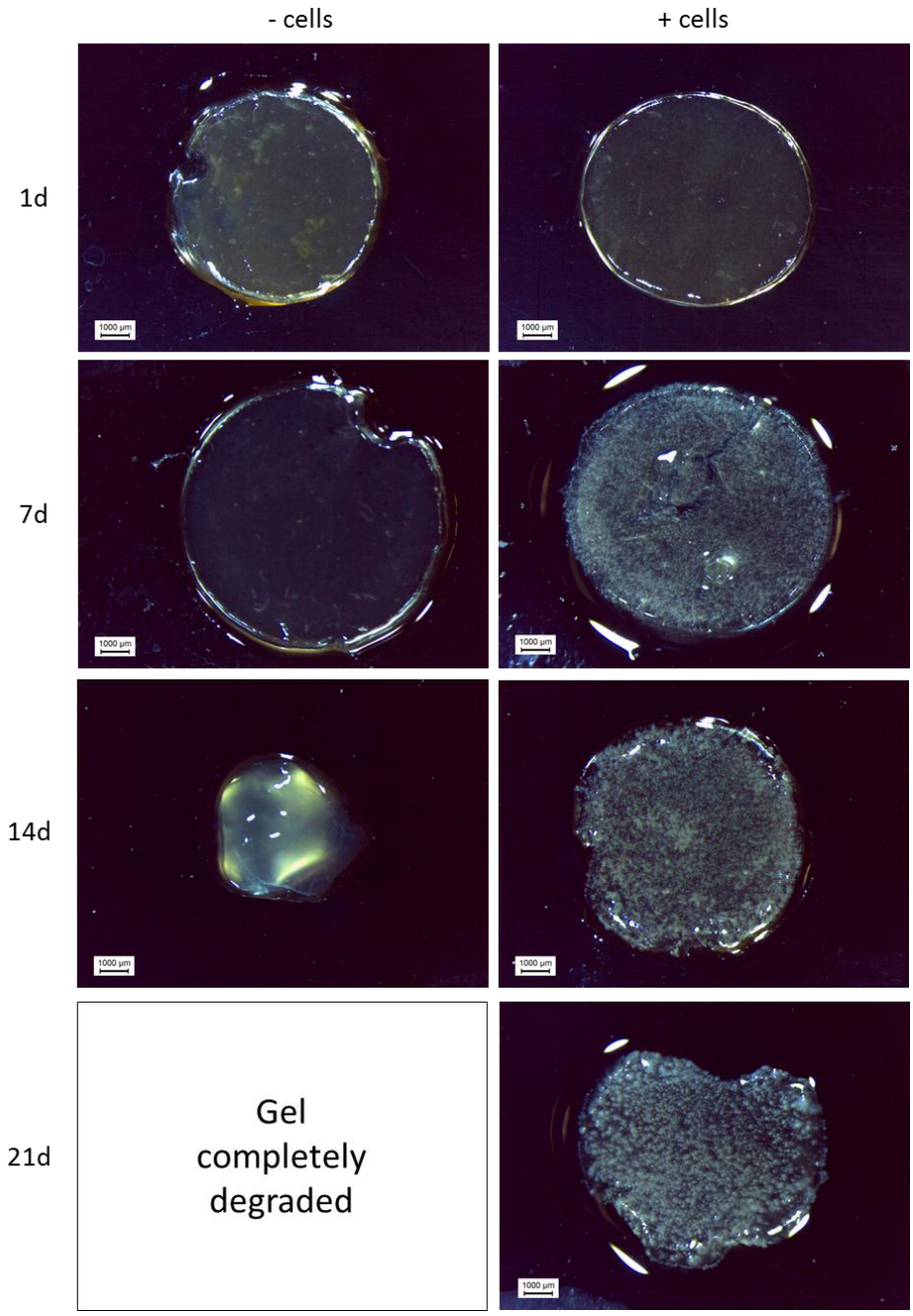

Figure 6.8: Macroscopic images of 1% gelatin hydrogels with and without L929s encapsulated at time points 1, 7, 14 and 21 days. 1wt% sericin was also incorporated in the sample. Scale bar = 1000 µm.

This observation clearly demonstrates that the hydrolytic degradation of the samples was slowed down in the presence of cells. This result agrees with previous studies conducted by Bryant et al., where the existence of cells in PEG-

PLA hydrogels decreased the degradation rate of the hydrolytically degradable hydrogels [111]. The incorporated proteins (sericin and gelatin) are also susceptible to enzymatic degradation via collagenases/gelatinases secreted by the cells. However, the concentration of the proteins incorporated was only 2 wt% (1 wt% sericin + 1 wt% gelatin) and the majority of polymer chains in the hydrogel are still PVA-Tyr. Therefore, the bulk degradation of these gels is speculated to be dictated by the hydrolysis of ester bonds on PVA-Tyr. It was also hypothesised that the encapsulated cells could secrete ECM in the hydrogels and the accumulation of ECM in the gel's microenvironment over time might be the key factor to the difference in the degradation rate observed. It was speculated that the presence of cells and increasing amount of ECM in the hydrogel would contribute to an overall lower water content, which would significantly decreased the rate of hydrolysis for the degradable ester bonds [1, 111]. A very preliminary study was conducted to quantify the total amount of ECM proteins in the hydrogel samples using the micro Coomassie assay. The mass of proteins was calculated from a standard curve generated using known amount of bovine serum albumin (BSA). It was clearly observed that the total amount of proteins in the samples with and without cells have distinctly different trends (see Appendix A). However, this assay was unable to differentiate if the proteins observed in the assay were ECM proteins secreted by the cells into the gel network, functional proteins in the cell body (cell surface and transport proteins), or the proteins that were original incorporated into the gel (i.e., gelatin and sericin). While the exact quantity and origin of the proteins in the gel could not be ascertained, the degradation studies indicated that proteins were being deposited (reduction in

degradation). Therefore, further studies were conducted to identify and locate the ECM produced in the gel through immunocytochemical analysis.

6.3.3.2. Immunocytochemical staining of ECM produced in 1% gelatin hydrogels

The fibroblasts used in this study were from dermal tissue and were previously reported to secrete a number of ECM proteins [402, 403]. The two ECM molecules of interest in this study are collagen IV and laminin. Collagen has an important role in maintaining skin structure, where specifically type IV collagen is a major compound of the basal lamina that interacts primarily with laminin. On the other hand, laminin is known to be a major constituent of the dermoepidermal basement membrane of blood vessels. It has also been shown to control a number of cellular functions, such as migration, differentiation and proliferation that may be responsible for re-epithelialisation and vascularisation during skin repair [404, 405].

In this study, both collagen IV and laminin were successfully immuno-stained in the gels at 21 days (Figure 6.9 and 6.10). This observation is a clear indication that the encapsulated L929s were able to secrete ECM in an attempt to remodel the hydrogel network. It was also noticed that both collagen IV and laminin were tightly associated within the cell aggregates. It appeared that although the cells were able to secrete ECM, the matrix molecules were not deposited into the acellular regions. Immunohistochemical staining (haematoxylin-eosin) was also performed on these samples to locate the ECM secreted but results were inconclusive (see Appendix B).

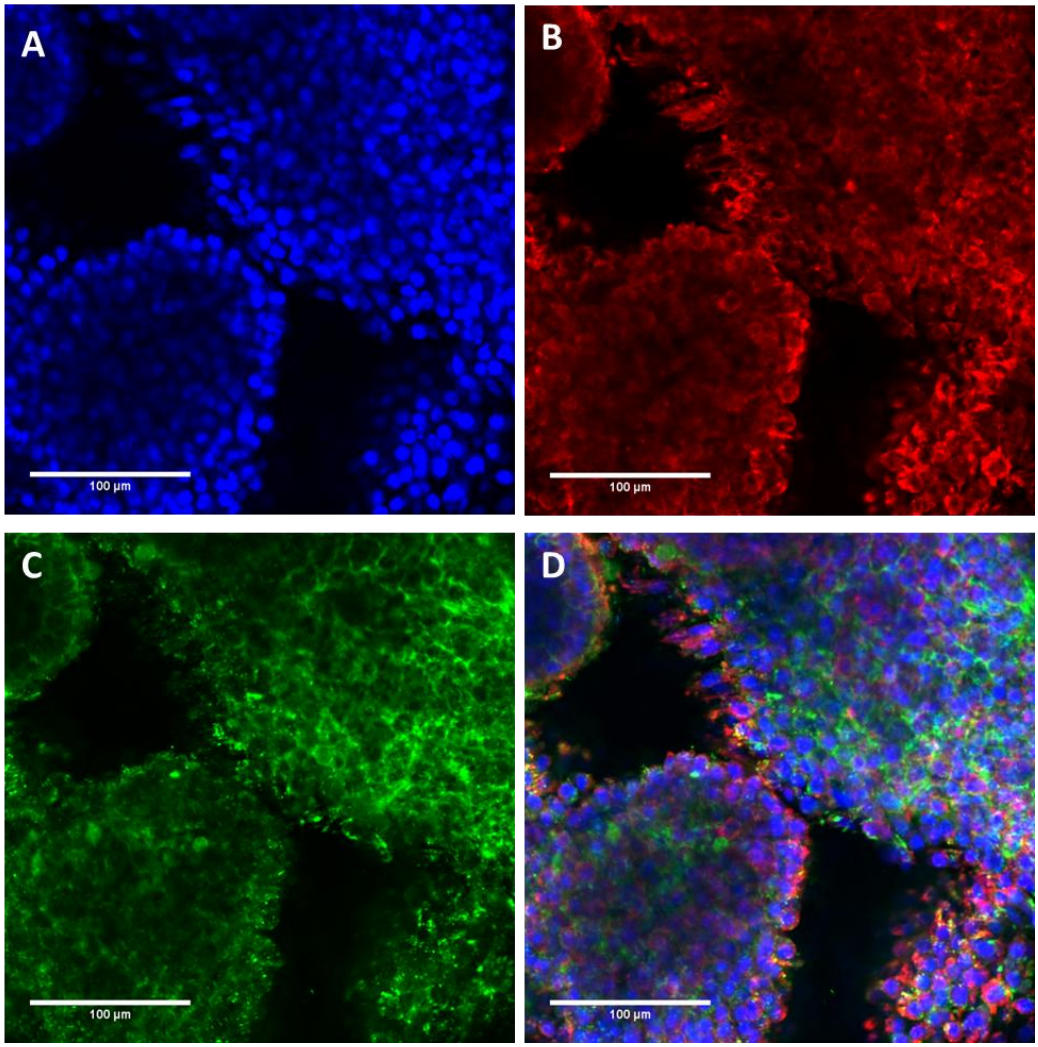

Figure 6.9: Immunocytochemical staining of L929s encapsulated in 1% gelatin hydrogel at 21 days; 1wt% sericin was also incorporated into the sample. A = Nuclei (blue); B = F-actin (red); C = Collagen IV (green); D=Overlay of A, B and C; Image was visualised at 40x; Scale bar = 100 µm.

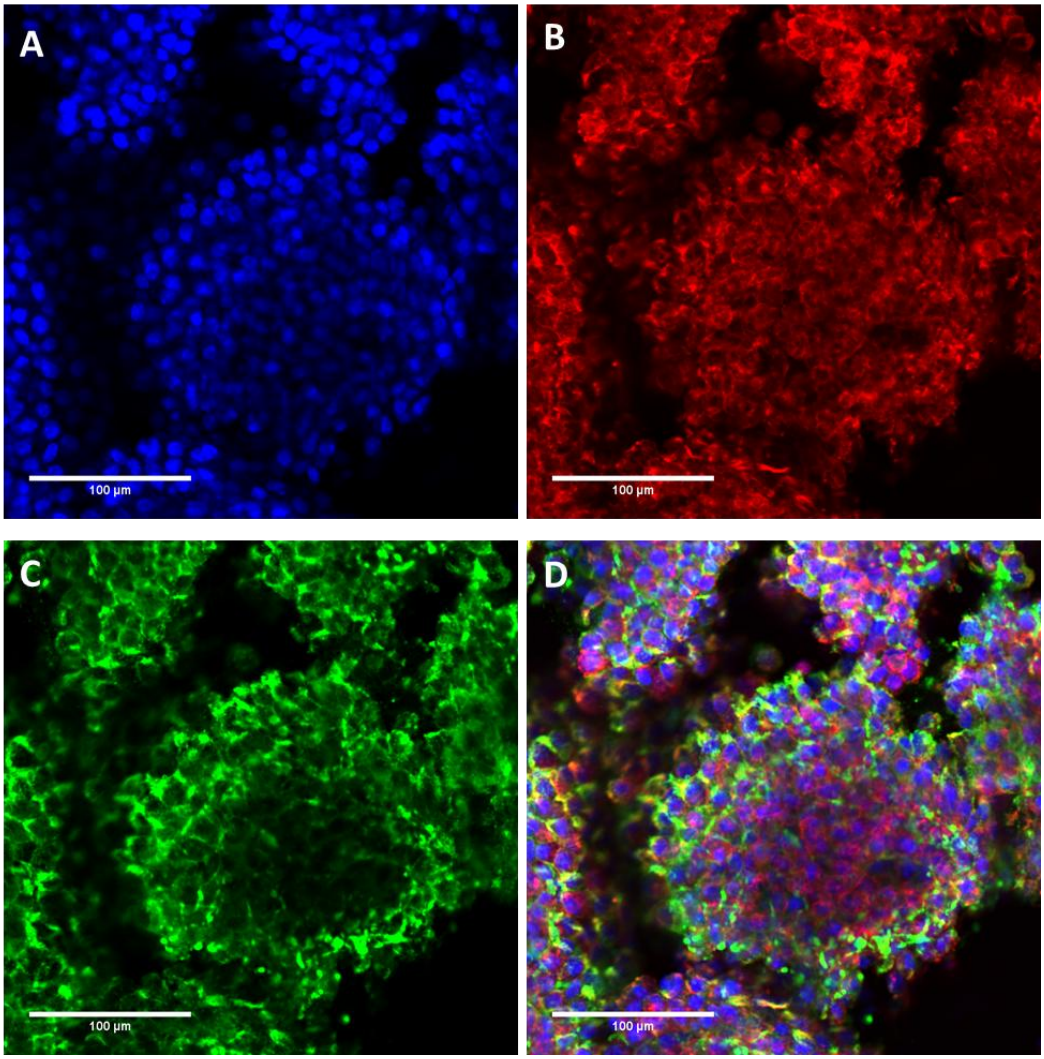

Figure 6.10: Immunocytochemical staining of L929s encapsulated in 1% gelatin hydrogel at 21 days; 1wt% sericin was also incorporated into the sample. A = Nuclei (blue); B = F-actin (red); C = laminin (green); D=Overlay of A, B and C; Image was visualised at 40x; Scale bar = 100 µm.

During tissue development, the ECM molecules are firstly secreted into the pericellular regions then further developed before diffusing into the extracellular regions [92, 111]. It was speculated that diffusivity of these ECM molecules is strictly related to the network structure and crosslinking density [111, 406]. Therefore, there is a possibility that although the gel was degraded, the remaining crosslinking was enough to restrict the mobility of the secreted ECM molecules

in the hydrogel network. Nicodemus et al. also stated that if degradation of the gel is too slow, the secreted ECM might be localised in the pericellular region [1]. It was then hypothesised that in this study that because the rate of hydrolytic degradation of the hydrogels did not match the rate of ECM secretion, ECM build-up in the pericellular region was noticed. Further studies are required to study the ECM secretion in PVA-Tyr gels with various degradation time frames. However, the fact that the encapsulated cells were able to survive, proliferate, migrate and secrete ECM in the PVA-Tyr gels highlights that this system can be potentially used as cell encapsulation matrices.

6.4. Conclusion

In conclusion, it was successfully shown in this chapter that L929s were able to survive the photoencapsulation process with the incorporation of antioxidative ascorbic acid and sericin into the PVA-Tyr hydrogels. Sericin was shown to be the better choice for this system when compared to ascorbic acid as it was able to quench the harmful radicals and protect the cells without affecting the hydrogel's crosslinking efficiency. However, the presence of gelatin in the gels was required to support cell spreading, growth, proliferation and metabolic activity. The PVA-Tyr gels incorporated with both 1wt% sericin and 1wt% gelatin were shown to have the greatest live cell coverage area and metabolic activity, and were the most suitable composition for cell encapsulation. Collagen IV and laminin were identified in the cells encapsulated samples, where both proteins were localised on the cell aggregates. Overall, the PVA-Tyr gels showed great promise as tissue engineering matrices for cell encapsulation purposes.

Chapter 7

Conclusions and Future Recommendations

7.1. Introduction

Synthetic hydrogels have been examined for decades as potential long term cell encapsulation matrices. Although these gels have good mechanical stability and tailorable physical properties, there has been little success with long term cell encapsulation studies, as cells tend to lose viability and function over time. This issue is due to the lack of biological recognition sites in the synthetic hydrogel which are vital for cellular signalling and function.

Therefore, this thesis aimed to address this challenge by using biosynthetic hydrogels based on PVA and bioactive proteins to encapsulate cells. To date, several approaches have been researched for successful covalent incorporation of biological molecules into synthetic polymeric networks. However, a common issue with these techniques was the need to chemically modify the biological molecules prior to encapsulation, which may have affected their bioactivity and capability to promote cell viability and function in the hydrogels. Therefore, the major research aim of this thesis was to evaluate the feasibility of covalently incorporating biological molecules into synthetic hydrogels without any prior chemical modification. It was hypothesised that by using a photocrosslinking system that has previously been used to crosslink native proteins, proteins can be covalently integrated into synthetic hydrogel networks. In addition, cells encapsulated within these biosynthetic hydrogels would have better viability and function over time compared to pure synthetic hydrogels.

7.2. Thesis conclusions

7.2.1. Development of a phenolated PVA system that can be crosslinked using the Ruthenium/persulphate system.

In this thesis, a visible light initiated crosslinking system (Ruthenium/persulphate) that had only been previously used for crosslinking proteins through their tyrosine (phenol) moieties was employed. It was proposed that by grafting similar phenol moieties onto PVA, these phenol moieties could form covalent crosslinks with the tyrosine groups of the proteins using the same photopolymerisation system. It was demonstrated that phenol moieites in the form of tyramine, were successfully conjugated onto PVA (PVA-Tyr) using a conventional carboxyl-amine coupling reaction. The synthesised PVA-Tyr was able to be crosslinked into hydrogels using the photocrosslinking system that had never been applied to synthetic polymers. It was also noted that the carboxyl-amine reaction employed to synthesise the PVA-Tyr introduced ester bonds into the macromers. The fabricated PVA-Tyr hydrogels were characterised to degrade hydrolytically via these ester linkages present in the network. Most interestingly, the hydrogel's degradation was pH and temperature sensitive, which highlights the potential of using these gels for other biomedical applications such as oral specific drug delivery carriers. In an attempt to tailor the physical properties of the PVA-Tyr hydrogels, it was shown that varying the initial macromer concentration successfully varied the effective macromer fraction and crosslinking density of the hydrogels. The degradation rates of the gels were dependant on the crosslinking density. Moreover, the PVA-Tyr macromers and degradation products collected from the hydrogel were evaluated to be non-cytotoxic.

7.2.2. Covalent incorporation of non-chemically modified proteins into PVA hydrogels

Non-chemically modified gelatin was successfully covalently bound to the PVA-Tyr network, where ~75% of gelatin was still present in the hydrogel after 3 days. It was also shown that incorporating minimal concentrations of gelatin (0.01, 0.1 and 1wt%) did not affect the base characteristics (mass loss, swelling and degradation profile) of the PVA-Tyr hydrogels, and gelatin retained its bioactivity. The retention of the gelatin bioactivity was assessed by the cell adhesion studies using three different cell types. The key finding was that gelatin concentration as low as 0.01wt% (which has never been shown in the literature) successfully facilitated cell adhesion on the gel surfaces. It was also once again confirmed that the degradation products of the PVA-Tyr hydrogels did not affect the viability of adhered cells which showed that these gels have great potential as 2D cell culture platforms.

7.2.3. Encapsulation of cells within biosynthetic PVA/protein hydrogels.

Initial 3D fibroblasts encapsulation studies in pure PVA-Tyr and PVA-Tyr/gelatin gels revealed that the radicals formed during the photocrosslinking process were detrimental to cells. Therefore, antioxidants were incorporated into the gels to overcome this drawback. It was shown that the antioxidative silkworm cocoon protein, sericin, successfully protected the cells from radical damage without affecting the physical properties of the PVA-Tyr gels, unlike the gold standard for antioxidants, ascorbic acid. However, having just sericin as the sole biological analogue in the PVA-Tyr gels was insufficient to promote cell growth and proliferation. Combination of both sericin and gelatin in the gels successfully

facilitated cell proliferation. Cell clusters were formed at higher time points where interconnected networks between clusters were observed. Increasing the concentration of gelatin also increased the overall live cell coverage area and ATP levels in the gels. The cells were able to stay viable and metabolically active over 21 days. Lastly, extracellular matrix (ECM) molecules such as collagen IV and laminin secreted by the encapsulated cells were also identified in the gels. Overall, the PVA-Tyr hydrogel system developed in this thesis has shown great potential as cell encapsulation matrices.

In conclusion, this thesis has reported the fabrication of biosynthetic hydrogels where the biological molecules were covalently incorporated into the synthetic network without any chemical modification process. The resultant biosynthetic hydrogels were shown to improve viability and proliferation of encapsulated cells compared to pure synthetic hydrogels. The major outcomes from this work are summarised below:

1. Novel PVA-Tyr was synthesised and crosslinked using a visible light initiated polymerisation system that has only been traditionally applied to proteins.
2. The PVA-Tyr hydrogels were characterised to be hydrolytically degradable where degradation was dependent on pH and temperature.
3. Manipulating the hydrogel's initial macromer concentration successfully produced hydrogels of varied effective macromer fraction, crosslinking density and degradation period.
4. Non-chemically modified gelatin was covalently incorporated into the network at low concentrations without interfering with the base PVA-Tyr

hydrogels' physical properties, and successfully facilitated 2D cell adhesion on the gels' surface.

5. Both sericin and gelatin was required for 3D cell encapsulation studies, where cells were shown to be more viable and metabolically active in PVA-Tyr/proteins gels compared to pure PVA-Tyr gels.

7.3. Future recommendations

7.3.1. Further modulation of hydrogel degradation period

The degradation time of the PVA-Tyr hydrogels was shown to vary between 17 to 27 days by changing the initial macromer concentration. In order to have a larger range of degradation period, future studies can investigate the effect of tailoring the functional group density on the degradation rate of PVA-Tyr gels. It has been reported in the literature that increasing number of functional groups conjugated onto synthetic polymer backbones successfully fabricated hydrogels of higher crosslinking density and longer degradation time. For example, Mawad et al. showed that increasing the number of ester acrylate groups on PVA from three to seven also increased the total degradation time from ~50 to 120 days for ~10wt% hydrogels [72]. Similar, increasing the number of functional groups from five to ten in PVA-Hydrazone hydrogels also significantly slowed down degradation (50% vs 80% degradation after 100 days for ten and five functional groups respectively) [57]. It is thus recommended that by using this approach, PVA-Tyr hydrogels with tunable degradation period can also be fabricated.

7.3.2. Adaptation of this system to encapsulate other cell types

Throughout this thesis, the developed biosynthetic hydrogels was only used to encapsulate L929 fibroblasts and showed good viability as well as metabolic activity for a long period of time. Therefore, future studies should focus on encapsulating different types of cells into these hydrogels. In particular, gelatin which was used in this system has been showed to support viability and function of Schwann cells, chondrocytes, endothelial cells, cardiomyocytes and

mesenchymal stem cells [121, 156, 396, 407]. Therefore, further extending the cell encapsulation studies to these cells would be of interest. Preliminary studies have shown that rat pheochromocytoma cells (PC12s), Schwann cells, and cardiomyoctes have been successfully encapsulated in the PVA-Tyr gels (with sericin and gelatin), and showed good viability and function over 2 weeks (results not shown). However, further characterisation needs to be done to evaluate the function of the encapsulated cells.

Moreover, co-encapsulation of different kinds of cells in the PVA-Tyr gels can also be examined. In this thesis, although the encapsulated L929 fibroblasts were shown form cell aggregates with good viability and metabolic activity after a period of time, the core of the cell clusters also appeared to be necrotic. Endothelial cells can be co-encapsulated with the fibroblasts to overcome this problem. Eckermann et al. showed that cell spheroids formed by co-culturing fibroblasts and endothelial cells have no necrotic core after 14 days of culture, where tubular endothelial cells structures were visualised in the clusters [408]. It was believed that the microvascular structures formed by the endothelial cells were able to supply oxygen and nutrients to the core of the spheroids preventing cell death [408].

To date, many co-culture studies are done on 2D cell culture platforms. However, 3D cell culture matrices are more suitable as mimics of the native body environment to provide a better understanding of cellular interactions with tissues *in vivo* [409]. In the body, complex communication pathways between multiple cells of different kinds are required for tissue repair and development. Therefore, the PVA-Tyr system developed in this thesis can also be potentially

used as 3D cell co-culture platforms. It can be used to study the effect of co-culture and paracrine signalling on cellular function and differentiation.

7.3.3. Incorporation of other biological molecules

The major advantage of the PVA-Tyr system used in this thesis was its ability to form covalent crosslinks with biological molecules through their tyrosine moieties. Therefore, any biological molecules that may improve cell function can also be covalently incorporated into the PVA-Tyr hydrogels, as long as they contain tyrosine residues. For example, growth factors such as fibroblast growth factor (FGF) and vascular endothelial growth factor (VEGF) have been reported to contain tyrosine residues. Moreover, FGF has also been shown to promote fibroblast proliferation, whereas vascular endothelial growth factor (VEGF) induces endothelial cell proliferation and migration [410-412]. Therefore, it is recommended that growth factors can be incorporated into the PVA-Tyr gels in the future to enhance proliferation and function of the encapsulated cells.

7.3.4. Further assessment of biological properties

The biological properties of the biosynthetic hydrogels fabricated in this thesis were assessed by *in vitro* culture of the samples and assays to evaluate viability and metabolic activity. Although these assays are fundamental to assess the potential of the system as cell encapsulation matrices, other assays can also be employed to further evaluate the functionality of encapsulated cells. For example, the photocrosslinking technique used in this system generates radicals that may induce oxidative damage to the encapsulated cells. The radicals and

subsequent reactive oxygen species formed can be quantified using the carboxy-2,7-difluorodihydrofluorescein diacetate dye, as a measure of the level of oxidative stress exerted to the cells [370].

In addition to *in vitro* studies, animal studies are also important to determine the performance of these PVA-Tyr gels *in vivo*. As the *in vivo* environment is complex and unpredictable, it is not possibly to predict the behaviour of cells, or rather the biomaterial *in vivo* by *in vitro* assays only. Therefore, it is recommended that future studies should focus on *in vivo* studies to evaluate the host tissue responses of the PVA-Tyr gels.

Appendices

Appendix A - Quantification of total protein mass in 1% gelatin hydrogels using micro Coomassie assay (with and without L929s encapsulated).

Micro Coomassie assay (Thermo Fisher Scientific) was employed to quantify the total amount of ECM deposited by cells in the 1% gelatin gels (+18 wt% PVA-Tyr and 1 wt% sericin). In brief, samples were harvested at respective time points (1, 3, 7, 14, 21 days) then allowed to degrade completely in 5ml DPBS at 60°C for 2 days. 150µl of sample was then added with 150µl of Coomassie working reagent, and incubated at room temperature for 15min. The samples' absorbance was read at 570nm using a plate reader (Tecan Infinite F200). The protein concentrations were calculated from a standard curve constructed using known concentrations of bovine serum albumin (BSA).

It was observed that in the samples without cells, the total mass of protein in the gel decreased over time (Figure A.1). This result was thought to be the release of sericin and gelatin from the gels over time, and matches the protein release study conducted in Chapter 5. However, when cells were encapsulated in the gels, a distinctly different trend was observed (Figure A.1). The mass of protein in the gels remained constant from 3 to 14 days then increased from 14 to 21 days. It was also noted that the data point for 21 days has huge standard deviations. Since the bulk of the hydrogel was already degraded at 21 days, the hydrogels were weak and flimsy, and posed technical difficulties in harvesting the samples, hence the huge error bars. Moreover, the total mass of proteins quantified in the gels was also not selective to the secreted ECM as cells also possess membrane surface bound proteins and transport proteins. Therefore, the

mass of ECM deposited into the gels by the encapsulated cells was unable to be determined from this study.

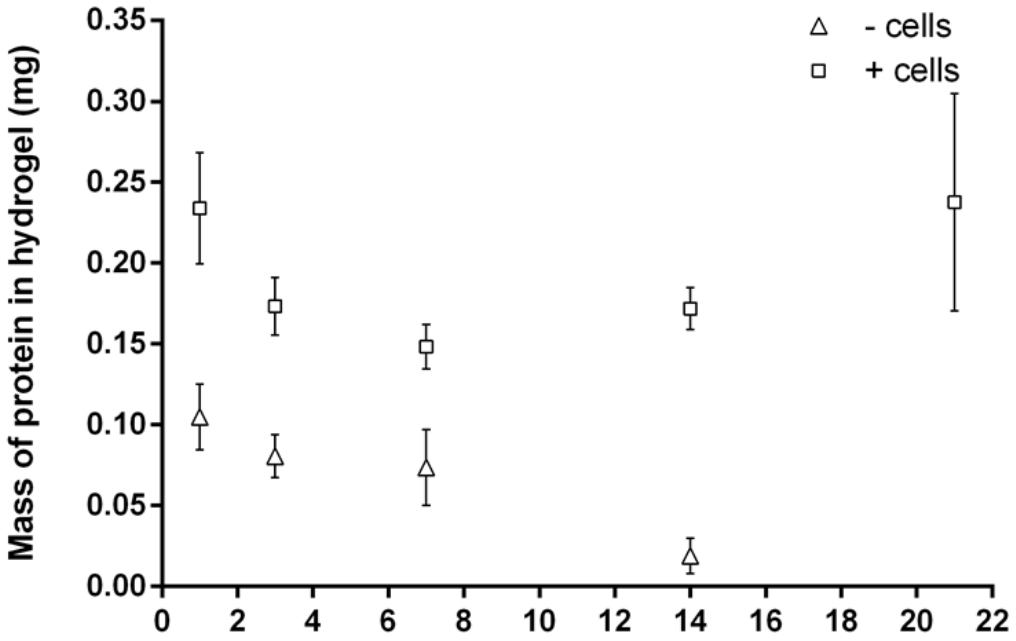

Figure A.1: Mass of protein in 1% gelatin (+18wt% PVA-Tyr and 1wt% sericin) hydrogels with and without cells.

Appendix B - Haematoxylin and Eosin (H&E) staining of sectioned 1% gelatin hydrogels encapsulated with L929s

1% gelatin hydrogels (+18wt% PVA-Tyr and 1wt% sericin) containing L929 fibroblasts were fixed for 24 hours at room temperature in 10% neutral buffered formalin (Confix "Clear" pH 7.0). Formalin-fixed specimens were then cryo-sectioned (~10μm) and mounted on positively charged silane slides. Sections were stained in Harris haematoxylin (Surgipath Medical) for 4 minutes, washed in water, differentiated in 1% acid alcohol for 2 seconds and washed again in water. Sections were then placed in Scott's Blueing solution (Fronine) for 20 seconds, washed and then counterstained in Eosin (Surgipath Medical) for 3 minutes and dehydrated, cleared and mounted with Ultramount (Fronine).

H&E stained images revealed the presence of large pores in the gels (indicated by arrows) (Figure A.2). It was believed that these artefacts were being generated during the cryo-sectioning process due to the smearing of the gel sample on the sectioning blade. It was further hypothesised that this smearing effect caused the removal of cells and ECM deposited in the gels. However, further studies are needed to confirm this hypothesis.

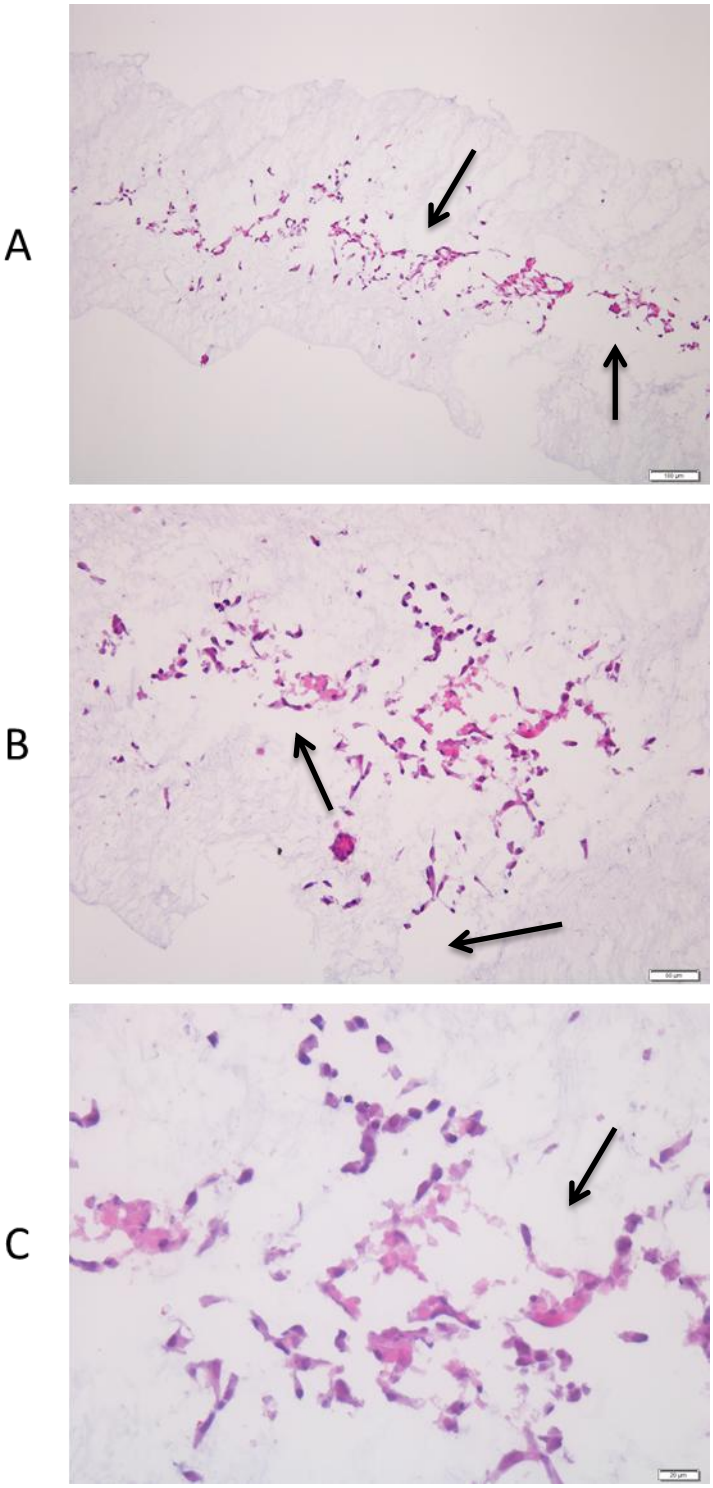

Figure A.2: Haemotoxylin and eosin staining of cryo-sectioned 1% gelatin hydrogels (+18wt% PVA-Tyr and 1wt% sericin) at 21 days: A = 2.5x (Scale bar = 100µm); B = 10x (Scale bar = 50µm); C = 20x (Scale bar = 20µm).

References

1. Nicodemus, G. and S.J. Bryant, *Cell encapsulation in biodegradable hydrogels for tissue engineering applications.* Tissue Engineering, Part B, 2008. **14**(2): p. 149-65.
2. Selimović, Š., J. Oh, H. Bae, M. Dokmeci, and A. Khademhosseini, *Microscale Strategies for Generating Cell-Encapsulating Hydrogels.* Polymers, 2012. **4**(3): p. 1554-1579.
3. Drury, J.L. and D.J. Mooney, *Hydrogels for tissue engineering: scaffold design variables and applications.* Biomaterials, 2003. **24**(24): p. 4337-4351.
4. Helary, C., I. Bataille, A. Abed, C. Illoul, A. Anglo, L. Louedec, D. Letourneur, A. Meddahi-Pellé, and M.M. Giraud-Guille, *Concentrated collagen hydrogels as dermal substitutes.* Biomaterials, 2010. **31**(3): p. 481-490.
5. Nafea, E.H., A. Marson, L.A. Poole-Warren, and P.J. Martens, *Immunoisolating semi-permeable membranes for cell encapsulation: focus on hydrogels.* J Control Release, 2011. **154**(2): p. 110-22.
6. Zustiak, S.P. and J.B. Leach, *Characterization of protein release from hydrolytically degradable poly(ethylene glycol) hydrogels.* Biotechnology and Bioengineering, 2011. **108**(1): p. 197-206.
7. Gonen-Wadmany, M., R. Goldshmid, and D. Seliktar, *Biological and mechanical implications of PEGylating proteins into hydrogel biomaterials.* Biomaterials, 2011. **32**(26): p. 6025-6033.
8. Fry, A.K., K.F. Schilke, J. McGuire, and K.E. Bird, *Synthesis and anticoagulant activity of heparin immobilized "end-on" to polystyrene microspheres coated with end-group activated polyethylene oxide.* J Biomed Mater Res B Appl Biomater, 2010. **94**(1): p. 187-95.
9. Nilasaroya, A., L.A. Poole-Warren, J.M. Whitelock, and P. Jo Martens, *Structural and functional characterisation of poly(vinyl alcohol) and heparin hydrogels.* Biomaterials, 2008. **29**(35): p. 4658-4664.
10. Jin, R., L. Moreira Teixeira, A. Krouwels, P. Dijkstra, C. Van Blitterswijk, M. Karperien, and J. Feijen, *Synthesis and characterization of hyaluronic acid–poly (ethylene glycol) hydrogels via Michael addition: An injectable biomaterial for cartilage repair.* Acta Biomaterialia, 2010. **6**(6): p. 1968-1977.
11. Tae, G., Y.-J. Kim, W.-I. Choi, M. Kim, P.S. Stayton, and A.S. Hoffman, *Formation of a Novel Heparin-Based Hydrogel in the Presence of Heparin-Binding Biomolecules.* Biomacromolecules, 2007. **8**(6): p. 1979-1986.
12. Gonen-Wadmany, M., L. Oss-Ronen, and D. Seliktar, *Protein-polymer conjugates for forming photopolymerizable biomimetic hydrogels for tissue engineering.* Biomaterials, 2007. **28**(26): p. 3876-3886.
13. *Organ and Tissue Donation Facts*. 2014 [cited 2014 23rd January]; Available from: http://www.donatelife.gov.au/.
14. Brown, R.A. and J.B. Phillips, *Cell Responses to Biomimetic Protein Scaffolds Used in Tissue Repair and Engineering*, in *International Review of Cytology*, W.J. Kwang, Editor. 2007, Academic Press. p. 75-150.

15. Peppas, N.A., J.Z. Hilt, A. Khademhosseini, and R. Langer, *Hydrogels in Biology and Medicine: From Molecular Principles to Bionanotechnology*. Advanced Materials, 2006. **18**(11): p. 1345-1360.
16. Hoffman, A.S., *Hydrogels for biomedical applications.* Advanced Drug Delivery Reviews, 2002. **54**(1): p. 3-12.
17. Bryant, S., G. Nicodemus, and I. Villanueva, *Designing 3D Photopolymer Hydrogels to Regulate Biomechanical Cues and Tissue Growth for Cartilage Tissue Engineering.* Pharmaceutical Research, 2008. **25**(10): p. 2379-2386.
18. Bryant, S.J. and K.S. Anseth, *Hydrogel properties influence ECM production by chondrocytes photoencapsulated in poly(ethylene glycol) hydrogels.* Journal of Biomedical Materials Research, 2002. **59**(1): p. 63-72.
19. Nafea, E., *UV Photopolymerised Biosynthetic PVA Hydrogels with Tailored Permselectivity for Cell Immunoisolation*, in *Graduate School of Biomedical Engineering*. 2012, University of New South Wales: Australia.
20. Berger, J., M. Reist, J. Mayer, O. Felt, N. Peppas, and R. Gurny, *Structure and interactions in covalently and ionically crosslinked chitosan hydrogels for biomedical applications.* European Journal of Pharmaceutics and Biopharmaceutics, 2004. **57**(1): p. 19-34.
21. Ohya, S., Y. Nakayama, and T. Matsuda, *Thermoresponsive artificial extracellular matrix for tissue engineering: Hyaluronic acid bioconjugated with poly(N-isopropylacrylamide) grafts.* Biomacromolecules, 2001. **2**(3): p. 856-863.
22. Young, C.J., L.A. Poole-Warren, and P.J. Martens, *Combining submerged electrospray and UV photopolymerization for production of synthetic hydrogel microspheres for cell encapsulation.* Biotechnology and Bioengineering, 2012. **109**(6): p. 1561-1570.
23. Habib Nafea, E., L.A. Poole-Warren, and P.J. Martens, *Correlation of macromolecular permeability to network characteristics of multivinyl poly(vinyl alcohol) hydrogels.* Journal of Polymer Science Part B: Polymer Physics, 2014. **52**(1): p. 63-72.
24. Risbud, M., A. Hardikar, and R. Bhonde, *Chitosan-polyvinyl pyrrolidone hydrogels as candidate for islet immunoisolation: in vitro biocompatibility evaluation.* Cell Transplant, 2000. **9**(1): p. 25-31.
25. Gulrez, S.K., S. Al-Assaf, and G.O. Phillips, *Hydrogels: methods of preparation, characterisation and applications.* Progress in molecular and environmental bioengineering—from analysis and modeling to technology applications. InTech, Winchester, 2011: p. 117-150.
26. Gold, G.T., D.M. Varma, D. Harbottle, M.S. Gupta, S.S. Stalling, P.J. Taub, and S.B. Nicoll, *Injectable redox-polymerized methylcellulose hydrogels as potential soft tissue filler materials.* Journal of Biomedical Materials Research Part A, 2014: p. n/a-n/a.
27. Maia, F.R., A.H. Lourenço, P.L. Granja, R.M. Gonçalves, and C.C. Barrias, *Effect of Cell Density on Mesenchymal Stem Cells Aggregation in RGD-Alginate 3D Matrices under Osteoinductive Conditions.* Macromolecular Bioscience, 2014: p. n/a-n/a.
28. Augst, A.D., H.J. Kong, and D.J. Mooney, *Alginate hydrogels as biomaterials.* Macromolecular Bioscience, 2006. **6**(8): p. 623-633.

29. Kong, H.-J., K.Y. Lee, and D.J. Mooney, *Decoupling the dependence of rheological/mechanical properties of hydrogels from solids concentration.* Polymer, 2002. **43**(23): p. 6239-6246.
30. Chu, C.-H., H. Kumagai, and K. Nakamura, *Application of polyelectrolyte complex gel composed of xanthan and chitosan to the immobilization of corynebacterium glutamicum.* Journal of Applied Polymer Science, 1996. **60**(7): p. 1041-1047.
31. Argin-Soysal, S., P. Kofinas, and Y.M. Lo, *Effect of complexation conditions on xanthan–chitosan polyelectrolyte complex gels.* Food Hydrocolloids, 2009. **23**(1): p. 202-209.
32. Takigami, M., H. Amada, N. Nagasawa, T. Yagi, T. Kasahara, S. Takigami, and M. Tamada, *Preparation and properties of CMC gel.* Transactions-materials Research Society of Japan 2007. **32**(3): p. 713.
33. Barbucci, R., A. Magnani, and M. Consumi, *Swelling Behavior of Carboxymethylcellulose Hydrogels in Relation to Cross-Linking, pH, and Charge Density.* Macromolecules, 2000. **33**(20): p. 7475-7480.
34. Hellio, D. and M. Djabourov, *Physically and Chemically Crosslinked Gelatin Gels.* Macromolecular Symposia, 2006. **241**(1): p. 23-27.
35. Hassan, C. and N. Peppas, *Structure and Applications of Poly(vinyl alcohol) Hydrogels Produced by Conventional Crosslinking or by Freezing/Thawing Methods*, in *Biopolymers · PVA Hydrogels, Anionic Polymerisation Nanocomposites*. 2000, Springer Berlin Heidelberg. p. 37-65.
36. Giannouli, P. and E.R. Morris, *Cryogelation of xanthan.* Food Hydrocolloids, 2003. **17**(4): p. 495-501.
37. Mirzaei B, E., A. Ramazani S. A, M. Shafiee, and M. Danaei, *Studies on Glutaraldehyde Crosslinked Chitosan Hydrogel Properties for Drug Delivery Systems.* International Journal of Polymeric Materials and Polymeric Biomaterials, 2013. **62**(11): p. 605-611.
38. Wu, X., L. Black, G. Santacana-Laffitte, and C.W. Patrick, Jr., *Preparation and assessment of glutaraldehyde-crosslinked collagen-chitosan hydrogels for adipose tissue engineering.* J Biomed Mater Res A, 2007. **81**(1): p. 59-65.
39. Mirzaei B, E., A. Ramazani SA, M. Shafiee, and M. Danaei, *Studies on glutaraldehyde crosslinked chitosan hydrogel properties for drug delivery systems.* International Journal of Polymeric Materials and Polymeric Biomaterials, 2013. **62**(11): p. 605-611.
40. Monteiro Jr, O.A.C. and C. Airoldi, *Some studies of crosslinking chitosan–glutaraldehyde interaction in a homogeneous system.* International Journal of Biological Macromolecules, 1999. **26**(2–3): p. 119-128.
41. Bo, J., *Study on PVA hydrogel crosslinked by epichlorohydrin.* Journal of Applied Polymer Science, 1992. **46**(5): p. 783-786.
42. Dogan, A.K., M. Gumusderelioglu, and E. Aksoz, *Controlled release of EGF and bFGF from dextran hydrogels in vitro and in vivo.* J Biomed Mater Res B Appl Biomater, 2005. **74**(1): p. 504-10.
43. Fangkangwanwong, J., R. Yoksan, and S. Chirachanchai, *Chitosan gel formation via the chitosan–epichlorohydrin adduct and its subsequent mineralization with hydroxyapatite.* Polymer, 2006. **47**(18): p. 6438-6445.

44. Fürst, W. and A. Banerjee, *Release of glutaraldehyde from an albumin-glutaraldehyde tissue adhesive causes significant in vitro and in vivo toxicity.* The Annals of thoracic surgery, 2005. **79**(5): p. 1522-1528.
45. Thampi, P., D. Nair, S. Venugopal, and U. Ramachandra, *Pathological Effects of Processed Bovine Pericardial Scaffolds—A Comparative In Vivo Evaluation.* Artificial organs, 2013. **37**(7): p. 600-605.
46. Vermonden, T., R. Censi, and W.E. Hennink, *Hydrogels for Protein Delivery.* Chemical Reviews (Washington, DC, United States), 2012. **112**(5): p. 2853-2888.
47. Friedman, M., J.F. Cavins, and J.S. Wall, *Relative Nucleophilic Reactivities of Amino Groups and Mercaptide Ions in Addition Reactions with α,β-Unsaturated Compounds1,2.* Journal of the American Chemical Society, 1965. **87**(16): p. 3672-3682.
48. Ranu, B.C. and S. Banerjee, *Ionic liquid as catalyst and reaction medium. The dramatic influence of a task-specific ionic liquid,[bmIm] OH, in michael addition of active methylene compounds to conjugated ketones, carboxylic esters, and nitriles.* Organic Letters, 2005. **7**(14): p. 3049-3052.
49. Metters, A. and J. Hubbell, *Network formation and degradation behavior of hydrogels formed by Michael-type addition reactions.* Biomacromolecules, 2005. **6**(1): p. 290-301.
50. Lutolf, M.P. and J.A. Hubbell, *Synthesis and Physicochemical Characterization of End-Linked Poly(ethylene glycol)-co-peptide Hydrogels Formed by Michael-Type Addition.* Biomacromolecules, 2003. **4**(3): p. 713-722.
51. Lutolf, M.P., N. Tirelli, S. Cerritelli, L. Cavalli, and J.A. Hubbell, *Systematic Modulation of Michael-Type Reactivity of Thiols through the Use of Charged Amino Acids.* Bioconjugate Chemistry, 2001. **12**(6): p. 1051-1056.
52. Lutolf, M.P., G.P. Raeber, A.H. Zisch, N. Tirelli, and J.A. Hubbell, *Cell-Responsive Synthetic Hydrogels.* Advanced Materials, 2003. **15**(11): p. 888-892.
53. Rizzi, S.C., M. Ehrbar, S. Halstenberg, G.P. Raeber, H.G. Schmoekel, H. Hagenmüller, R. Müller, F.E. Weber, and J.A. Hubbell, *Recombinant Protein-co-PEG Networks as Cell-Adhesive and Proteolytically Degradable Hydrogel Matrixes. Part II: Biofunctional Characteristics.* Biomacromolecules, 2006. **7**(11): p. 3019-3029.
54. Vernon, B., N. Tirelli, T. Bachi, D. Haldimann, and J.A. Hubbell, *Water-borne, in situ crosslinked biomaterials from phase-segregated precursors.* J Biomed Mater Res A, 2003. **64**(3): p. 447-56.
55. Lutolf, M.P. and J.A. Hubbell, *Synthetic biomaterials as instructive extracellular microenvironments for morphogenesis in tissue engineering.* Nature Biotechnology, 2005. **23**(1): p. 47-55.
56. Lutolf, M.P., J.L. Lauer-Fields, H.G. Schmoekel, A.T. Metters, F.E. Weber, G.B. Fields, and J.A. Hubbell, *Synthetic matrix metalloproteinase-sensitive hydrogels for the conduction of tissue regeneration: Engineering cell-invasion characteristics.* Proceedings of the National Academy of Sciences of the United States of America, 2003. **100**(9): p. 5413-5418.
57. Alves, M.H., C.J. Young, K. Bozzetto, L.A. Poole-Warren, and P.J. Martens, *Degradable, click poly(vinyl alcohol) hydrogels:*

Characterization of degradation and cellular compatibility. Biomedical Materials, 2012. **7**(2).

58. Shu, X.Z., Y. Liu, Y. Luo, M.C. Roberts, and G.D. Prestwich, *Disulfide cross-linked hyaluronan hydrogels.* Biomacromolecules, 2002. **3**(6): p. 1304-1311.
59. Shu, X.Z., Y. Liu, F.S. Palumbo, Y. Luo, and G.D. Prestwich, *In situ crosslinkable hyaluronan hydrogels for tissue engineering.* Biomaterials, 2004. **25**(7-8): p. 1339-1348.
60. Malkoch, M., R. Vestberg, N. Gupta, L. Mespouille, P. Dubois, A.F. Mason, J.L. Hedrick, Q. Liao, C.W. Frank, K. Kingsbury, and C.J. Hawker, *Synthesis of well-defined hydrogel networks using click chemistry.* Chem Commun (Camb), 2006(26): p. 2774-6.
61. Crescenzi, V., L. Cornelio, C. Di Meo, S. Nardecchia, and R. Lamanna, *Novel Hydrogels via Click Chemistry: Synthesis and Potential Biomedical Applications.* Biomacromolecules, 2007. **8**(6): p. 1844-1850.
62. Ossipov, D.A. and J. Hilborn, *Poly(vinyl alcohol)-Based Hydrogels Formed by "Click Chemistry".* Macromolecules, 2006. **39**(5): p. 1709-1718.
63. Moses, J.E. and A.D. Moorhouse, *The growing applications of click chemistry.* Chemical Society Reviews, 2007. **36**(8): p. 1249-1262.
64. Demko, Z.P. and K.B. Sharpless, *A click chemistry approach to tetrazoles by Huisgen 1, 3-dipolar cycloaddition: Synthesis of 5-sulfonyl tetrazoles from azides and sulfonyl cyanides.* Angewandte Chemie International Edition, 2002. **41**(12): p. 2110-2113.
65. van Dijk, M., C.F. van Nostrum, W.E. Hennink, D.T. Rijkers, and R.M. Liskamp, *Synthesis and characterization of enzymatically biodegradable PEG and peptide-based hydrogels prepared by click chemistry.* Biomacromolecules, 2010. **11**(6): p. 1608-14.
66. Letelier, M.E., S. Sánchez-Jofré, L. Peredo-Silva, J. Cortés-Troncoso, and P. Aracena-Parks, *Mechanisms underlying iron and copper ions toxicity in biological systems: Pro-oxidant activity and protein-binding effects.* Chemico-Biological Interactions, 2010. **188**(1): p. 220-227.
67. Kozlowski, H., A. Janicka-Klos, J. Brasun, E. Gaggelli, D. Valensin, and G. Valensin, *Copper, iron, and zinc ions homeostasis and their role in neurodegenerative disorders (metal uptake, transport, distribution and regulation).* Coordination Chemistry Reviews, 2009. **253**(21–22): p. 2665-2685.
68. DeForest, C.A., B.D. Polizzotti, and K.S. Anseth, *Sequential click reactions for synthesizing and patterning three-dimensional cell microenvironments.* Nature Materials, 2009. **8**(8): p. 659-664.
69. Clark, M. and P. Kiser, *In situ crosslinked hydrogels formed using Cu(I)-free Huisgen cycloaddition reaction.* Polymer International, 2009. **58**(10): p. 1190-1195.
70. Maia, J., L. Ferreira, R. Carvalho, M.A. Ramos, and M.H. Gil, *Synthesis and characterization of new injectable and degradable dextran-based hydrogels.* Polymer, 2005. **46**(23): p. 9604-9614.
71. Ito, T., Y. Yeo, C.B. Highley, E. Bellas, and D.S. Kohane, *Dextran-based in situ cross-linked injectable hydrogels to prevent peritoneal adhesions.* Biomaterials, 2007. **28**(23): p. 3418-3426.

72. Mawad, D., P.J. Martens, R.A. Odell, and L.A. Poole-Warren, *The effect of redox polymerisation on degradation and cell responses to poly (vinyl alcohol) hydrogels.* Biomaterials, 2007. **28**(6): p. 947-955.
73. Desai, E.S., M.Y. Tang, A.E. Ross, and R.A. Gemeinhart, *Critical factors affecting cell encapsulation in superporous hydrogels.* Biomed Mater, 2012. **7**(2): p. 024108.
74. Betz, M.W., P.C. Modi, J.F. Caccamese, D.P. Coletti, J.J. Sauk, and J.P. Fisher, *Cyclic acetal hydrogel system for bone marrow stromal cell encapsulation and osteodifferentiation.* J Biomed Mater Res A, 2008. **86**(3): p. 662-70.
75. Hong, Y., H. Song, Y. Gong, Z. Mao, C. Gao, and J. Shen, *Covalently crosslinked chitosan hydrogel: Properties of in vitro degradation and chondrocyte encapsulation.* Acta Biomaterialia, 2007. **3**(1): p. 23-31.
76. Fedorovich, N.E., J. Alblas, J.R. De Wijn, W.E. Hennink, A.B.J. Verbout, and W.J.A. Dhert, *Hydrogels as extracellular matrices for skeletal tissue engineering: State-of-the-art and novel application in organ printing.* Tissue Engineering, 2007. **13**(8): p. 1905-1925.
77. West, J.L. and J.A. Hubbell, *Polymeric biomaterials with degradation sites for proteases involved in cell migration.* Macromolecules, 1999. **32**(1): p. 241-244.
78. Nguyen, K.T. and J.L. West, *Photopolymerizable hydrogels for tissue engineering applications.* Biomaterials, 2002. **23**(22): p. 4307-4314.
79. Williams, C.G., A.N. Malik, T.K. Kim, P.N. Manson, and J.H. Elisseeff, *Variable cytocompatibility of six cell lines with photoinitiators used for polymerizing hydrogels and cell encapsulation.* Biomaterials, 2005. **26**(11): p. 1211-1218.
80. Bryant, S.J., C.R. Nuttelman, and K.S. Anseth, *Cytocompatibility of UV and visible light photoinitiating systems on cultured NIH/3T3 fibroblasts in vitro.* Journal of Biomaterials Science, Polymer Edition, 2000. **11**(5): p. 439-457.
81. Mann, B.K., A.S. Gobin, A.T. Tsai, R.H. Schmedlen, and J.L. West, *Smooth muscle cell growth in photopolymerized hydrogels with cell adhesive and proteolytically degradable domains: Synthetic ECM analogs for tissue engineering.* Biomaterials, 2001. **22**(22): p. 3045-3051.
82. Burdick, J.A., C. Chung, X. Jia, M.A. Randolph, and R. Langer, *Controlled degradation and mechanical behavior of photopolymerized hyaluronic acid networks.* Biomacromolecules, 2005. **6**(1): p. 386-391.
83. Cruise, G.M., O.D. Hegre, F.V. Lamberti, S.R. Hager, R. Hill, D.S. Scharp, and J.A. Hubbell, *In vitro and in vivo performance of porcine islets encapsulated in interfacially photopolymerized poly(ethylene glycol) diacrylate membranes.* Cell Transplantation, 1999. **8**(3): p. 293-306.
84. Cruise, G.M., D.S. Scharp, and J.A. Hubbell, *Characterization of permeability and network structure of interfacially photopolymerized poly(ethylene glycol) diacrylate hydrogels.* Biomaterials, 1998. **19**(14): p. 1287-1294.
85. Shih, H. and C.-C. Lin, *Visible-Light-Mediated Thiol-Ene Hydrogelation Using Eosin-Y as the Only Photoinitiator.* Macromolecular Rapid Communications, 2013. **34**(3): p. 269-273.
86. Bryant, S.J., K.S. Anseth, D.A. Lee, and D.L. Bader, *Crosslinking density influences the morphology of chondrocytes photoencapsulated in PEG*

hydrogels during the application of compressive strain. J Orthop Res, 2004. **22**(5): p. 1143-9.

87. Peppas, N.A., Y. Huang, M. Torres-Lugo, J.H. Ward, and J. Zhang, *Physicochemical foundations and structural design of hydrogels in medicine and biology*. 2000. p. 9-29.
88. Gehrke, S.H., J.P. Fisher, M. Palasis, and M.E. Lund, *Factors Determining Hydrogel Permeability.* Annals of the New York Academy of Sciences, 1997. **831**(1): p. 179-184.
89. Martens, P.J., S.J. Bryant, and K.S. Anseth, *Tailoring the Degradation of Hydrogels Formed from Multivinyl Poly(ethylene glycol) and Poly(vinyl alcohol) Macromers for Cartilage Tissue Engineering.* Biomacromolecules, 2003. **4**(2): p. 283-292.
90. Villanueva, I., D.S. Hauschulz, D. Mejic, and S.J. Bryant, *Static and dynamic compressive strains influence nitric oxide production and chondrocyte bioactivity when encapsulated in PEG hydrogels of different crosslinking densities.* Osteoarthr. Cartil, 2007.
91. Bryant, S.J. and K.S. Anseth, *The effects of scaffold thickness on tissue engineered cartilage in photocrosslinked poly(ethylene oxide) hydrogels.* Biomaterials, 2001. **22**(6): p. 619-626.
92. Bryant, S.J. and K.S. Anseth, *Controlling the spatial distribution of ECM components in degradable PEG hydrogels for tissue engineering cartilage.* Journal of Biomedical Materials Research - Part A, 2003. **64**(1): p. 70-79.
93. Pelham, R.J. and Y.-l. Wang, *Cell locomotion and focal adhesions are regulated by substrate flexibility.* Proceedings of the National Academy of Sciences, 1997. **94**(25): p. 13661-13665.
94. Pelham, R.J., Jr. and Y.-L. Wang, *Cell Locomotion and Focal Adhesions Are Regulated by the Mechanical Properties of the Substrate.* Biological Bulletin, 1998. **194**(3): p. 348-350.
95. Cushing, M.C. and K.S. Anseth, *Hydrogel cell cultures.* Science, 2007. **316**(5828): p. 1133-1134.
96. Benoit, D.S.W. and K.S. Anseth, *Heparin functionalized PEG gels that modulate protein adsorption for hMSC adhesion and differentiation.* Acta Biomaterialia, 2005. **1**(4): p. 461-470.
97. Martens, P.J., C.N. Bowman, and K.S. Anseth, *Degradable networks formed from multi-functional poly(vinyl alcohol) macromers: comparison of results from a generalized bulk-degradation model for polymer networks and experimental data.* Polymer, 2004. **45**(10): p. 3377-3387.
98. Rice, M.A. and K.S. Anseth, *Encapsulating chondrocytes in copolymer gels: Bimodal degradation kinetics influence cell phenotype and extracellular matrix development.* Journal of Biomedical Materials Research - Part A, 2004. **70**(4): p. 560-568.
99. Bryant, S.J. and K.S. Anseth, *Hydrogel properties influence ECM production by chondrocyte photoencapsulated in poly(ethylene glycol) hydrogels.* J Biomed Mater Res, 2001. **59**: p. 63-72.
100. Bryant, S.J., R.J. Bender, K.L. Durand, and K.S. Anseth, *Encapsulating chondrocytes in degrading PEG hydrogels with high modulus: Engineering gel structural changes to facilitate cartilaginous tissue production.* Biotechnology and Bioengineering, 2004. **86**(7): p. 747-755.

101. Söntjens, S.H.M., D.L. Nettles, M.A. Carnahan, L.A. Setton, and M.W. Grinstaff, *Biodendrimer-based hydrogel scaffolds for cartilage tissue repair.* Biomacromolecules, 2006. **7**(1): p. 310-316.
102. Williams, C.G., T.K. Kim, A. Taboas, A. Malik, P. Manson, and J. Elisseeff, *In vitro chondrogenesis of bone marrow-derived mesenchymal stem cells in a photopolymerizing hydrogel.* Tissue Engineering, 2003. **9**(4): p. 679-688.
103. Benoit, D.S.W., A.R. Durney, and K.S. Anseth, *Manipulations in hydrogel degradation behavior enhance osteoblast function and mineralized tissue formation.* Tissue Engineering, 2006. **12**(6): p. 1663-1673.
104. Fisher, J.P., S. Jo, A.G. Mikos, and A.H. Reddi, *Thermoreversible hydrogel scaffolds for articular cartilage engineering.* Journal of Biomedical Materials Research - Part A, 2004. **71**(2): p. 268-274.
105. Wang, D.A., S. Varghese, B. Sharma, I. Strehin, S. Fermanian, J. Gorham, D.H. Fairbrother, B. Cascio, and J.H. Elisseeff, *Multifunctional chondroitin sulphate for cartilage tissue-biomaterial integration.* Nature Materials, 2007. **6**(5): p. 385-392.
106. Wang, D.A., C.G. Williams, Q. Li, B. Sharma, and J.H. Elisseeff, *Synthesis and characterization of a novel degradable phosphate-containing hydrogel.* Biomaterials, 2003. **24**(22): p. 3969-3980.
107. Smeds, K.A. and M.W. Grinstaff, *Photocrosslinkable polysaccharides for in situ hydrogel formation.* Journal of Biomedical Materials Research, 2001. **54**(1): p. 115-121.
108. Halstenberg, S., A. Panitch, S. Rizzi, H. Hall, and J.A. Hubbell, *Biologically engineered protein-graft-poly(ethylene glycol) hydrogels: A cell adhesive and plasmin-degradable biosynthetic material for tissue repair.* Biomacromolecules, 2002. **3**(4): p. 710-723.
109. Park, H., J.S. Temenoff, Y. Tabata, A.I. Caplan, and A.G. Mikos, *Injectable biodegradable hydrogel composites for rabbit marrow mesenchymal stem cell and growth factor delivery for cartilage tissue engineering.* Biomaterials, 2007. **28**(21): p. 3217-3227.
110. Martens, P., J. Blundo, A. Nilasaroya, R.A. Odell, J. Cooper-White, and L.A. Poole-Warren, *Effect of Poly(vinyl alcohol) Macromer Chemistry and Chain Interactions on Hydrogel Mechanical Properties.* Chem. Mater., 2007. **19**(10): p. 2641-2648.
111. Bryant, S.J., K.L. Durand, and K.S. Anseth, *Manipulations in hydrogel chemistry control photoencapsulated chondrocyte behavior and their extracellular matrix production.* Journal of Biomedical Materials Research Part A, 2003. **67A**(4): p. 1430-1436.
112. Sawhney, A.S., C.P. Pathak, and J.A. Hubbell, *Bioerodible hydrogels based on photopolymerized poly(ethylene glycol)-co-poly(α-hydroxy acid) diacrylate macromers.* Macromolecules, 1993. **26**(4): p. 581-587.
113. Balakrishnan, B. and A. Jayakrishnan, *Self-cross-linking biopolymers as injectable in situ forming biodegradable scaffolds.* Biomaterials, 2005. **26**(18): p. 3941-3951.
114. Yeo, Y., W. Geng, T. Ito, D.S. Kohane, J.A. Burdick, and M. Radisic, *Photocrosslinkable hydrogel for myocyte cell culture and injection.* Journal of Biomedical Materials Research - Part B Applied Biomaterials, 2007. **81**(2): p. 312-322.

115. Flynn, L., G.D. Prestwich, J.L. Semple, and K.A. Woodhouse, *Adipose tissue engineering with naturally derived scaffolds and adipose-derived stem cells.* Biomaterials, 2007. **28**(26): p. 3834-3842.
116. Shu, X.Z., K. Ghosh, Y. Liu, F.S. Palumbo, Y. Luo, R.A. Clark, and G.D. Prestwich, *Attachment and spreading of fibroblasts on an RGD peptide-modified injectable hyaluronan hydrogel.* Journal of Biomedical Materials Research - Part A, 2004. **68**(2): p. 365-375.
117. Chung, C., J. Mesa, G.J. Miller, M.A. Randolph, T.J. Gill, and J.A. Burdick, *Effects of auricular chondrocyte expansion on neocartilage formation in photocrosslinked hyaluronic acid networks.* Tissue Engineering, 2006. **12**(9): p. 2665-2673.
118. Yeh, J., Y. Ling, J.M. Karp, J. Gantz, A. Chandawarkar, G. Eng, J. Blumling Iii, R. Langer, and A. Khademhosseini, *Micromolding of shape-controlled, harvestable cell-laden hydrogels.* Biomaterials, 2006. **27**(31): p. 5391-5398.
119. Bryant, S.J., J.A. Arthur, and K.S. Anseth, *Incorporation of tissue-specific molecules alters chondrocyte metabolism and gene expression in photocrosslinked hydrogels.* Acta Biomaterialia, 2005. **1**(2): p. 243-252.
120. Li, Q., C.G. Williams, D.D.N. Sun, J. Wang, K. Leong, and J.H. Elisseeff, *Photocrosslinkable polysaccharides based on chondroitin sulfate.* Journal of Biomedical Materials Research - Part A, 2004. **68**(1): p. 28-33.
121. Hoshikawa, A., Y. Nakayama, T. Matsuda, H. Oda, K. Nakamura, and K. Mabuchi, *Encapsulation of chondrocytes in photopolymerizable styrenated gelatin for cartilage tissue engineering.* Tissue Engineering, 2006. **12**(8): p. 2333-2341.
122. Kim, J., I.S. Kim, T.H. Cho, K.B. Lee, S.J. Hwang, G. Tae, I. Noh, S.H. Lee, Y. Park, and K. Sun, *Bone regeneration using hyaluronic acid-based hydrogel with bone morphogenic protein-2 and human mesenchymal stem cells.* Biomaterials, 2007. **28**(10): p. 1830-1837.
123. Almany, L. and D. Seliktar, *Biosynthetic hydrogel scaffolds made from fibrinogen and polyethylene glycol for 3D cell cultures.* Biomaterials, 2005. **26**(15): p. 2467-2477.
124. Rice, M.A. and K.S. Anseth, *Controlling cartilaginous matrix evolution in hydrogels with degradation triggered by exogenous addition of an enzyme.* Tissue Engineering, 2007. **13**(4): p. 683-691.
125. He, X. and E. Jabbari, *Material properties and cytocompatibility of injectable MMP degradable poly(lactide ethylene oxide fumarate)hydrogel as a carrier for marrow stromal cell.* Biomacromolecules, 2007. **8**(3): p. 780-792.
126. Ali, S., J.E. Saik, D.J. Gould, M.E. Dickinson, and J.L. West, *Immobilization of Cell-Adhesive Laminin Peptides in Degradable PEGDA Hydrogels Influences Endothelial Cell Tubulogenesis.* Biores Open Access, 2013. **2**(4): p. 241-9.
127. Lei, Y. and T. Segura, *DNA delivery from matrix metalloproteinase degradable poly(ethylene glycol) hydrogels to mouse cloned mesenchymal stem cells.* Biomaterials, 2009. **30**(2): p. 254-265.
128. Kraehenbuehl, T.P., P. Zammaretti, A.J. Van der Vlies, R.G. Schoenmakers, M.P. Lutolf, M.E. Jaconi, and J.A. Hubbell, *Three-dimensional extracellular matrix-directed cardioprogenitor*

differentiation: Systematic modulation of a synthetic cell-responsive PEG-hydrogel. Biomaterials, 2008. **29**(18): p. 2757-2766.

129. Adelöw, C., T. Segura, J.A. Hubbell, and P. Frey, *The effect of enzymatically degradable poly(ethylene glycol) hydrogels on smooth muscle cell phenotype.* Biomaterials, 2008. **29**(3): p. 314-326.
130. Raeber, G.P., M.P. Lutolf, and J.A. Hubbell, *Mechanisms of 3-D migration and matrix remodeling of fibroblasts within artificial ECMs.* Acta Biomaterialia, 2007. **3**(5): p. 615-629.
131. Lim, F. and A.M. Sun, *Microencapsulated islets as bioartificial endocrine pancreas.* Science, 1980. **210**(4472): p. 908-910.
132. Francis Suh, J.K. and H.W.T. Matthew, *Application of chitosan-based polysaccharide biomaterials in cartilage tissue engineering: A review.* Biomaterials, 2000. **21**(24): p. 2589-2598.
133. Young, C., *Fabrication and Characterisation of Poly(vinyl alcohol) and Heparin Biosynthetic Hydrogel Microspheres for Cell Microencapsulation*, in *Graduate School of Biomedical Engineering*. 2012, University of New South Wales: Australia.
134. Young, C., K. Rozario, C. Serra, L. Poole-Warren, and P. Martens, *Poly (vinyl alcohol)-heparin biosynthetic microspheres produced by microfluidics and ultraviolet photopolymerisation.* Biomicrofluidics, 2013. **7**(4): p. 044109.
135. Kim, M.S., J.H. Kim, B.H. Min, H.J. Chun, D.K. Han, and H.B. Lee, *Polymeric Scaffolds for Regenerative Medicine.* Polymer Reviews (Philadelphia, PA, United States), 2011. **51**(1): p. 23-52.
136. Khattak, S.F., K.-s. Chin, S.R. Bhatia, and S.C. Roberts, *Enhancing oxygen tension and cellular function in alginate cell encapsulation devices through the use of perfluorocarbons.* Biotechnology and Bioengineering, 2007. **96**(1): p. 156-166.
137. Tan, W.H. and S. Takeuchi, *Monodisperse Alginate Hydrogel Microbeads for Cell Encapsulation.* Advanced Materials (Weinheim, Germany), 2007. **19**(18): p. 2696-2701.
138. Orive, G., R.M. Hernández, A.R. Gascón, R. Calafiore, T.M. Chang, P. De Vos, G. Hortelano, D. Hunkeler, I. Lacík, and A.J. Shapiro, *Cell encapsulation: promise and progress.* Nature Medicine (New York, NY, United States), 2003. **9**(1): p. 104-107.
139. Bhattarai, N., J. Gunn, and M. Zhang, *Chitosan-based hydrogels for controlled, localized drug delivery.* Advanced Drug Delivery Reviews, 2010. **62**(1): p. 83-99.
140. Mao, J.S., Y.L. Cui, X.H. Wang, Y. Sun, Y.J. Yin, H.M. Zhao, and K.D. Yao, *A preliminary study on chitosan and gelatin polyelectrolyte complex cytocompatibility by cell cycle and apoptosis analysis.* Biomaterials, 2004. **25**(18): p. 3973-3981.
141. Shu, X.Z. and K.J. Zhu, *Controlled drug release properties of ionically cross-linked chitosan beads: The influence of anion structure.* International Journal of Pharmaceutics, 2002. **233**(1-2): p. 217-225.
142. Shen, E.C., C. Wang, E. Fu, C.Y. Chiang, T.T. Chen, and S. Nieh, *Tetracycline release from tripolyphosphate-chitosan cross-linked sponge: A preliminary in vitro study.* Journal of Periodontal Research, 2008. **43**(6): p. 642-648.

143. Crompton, K.E., J.D. Goud, R.V. Bellamkonda, T.R. Gengenbach, D.I. Finkelstein, M.K. Horne, and J.S. Forsythe, *Polylysine-functionalised thermoresponsive chitosan hydrogel for neural tissue engineering.* Biomaterials, 2007. **28**(3): p. 441-449.
144. Yeo, Y., J.A. Burdick, C.B. Higliley, R. Marini, R. Langer, and D.S. Kohane, *Peritoneal application of chitosan and UV-cross-linkable chitosan.* Journal of Biomedical Materials Research - Part A, 2006. **78**(4): p. 668-675.
145. Chenite, A., C. Chaput, D. Wang, C. Combes, M.D. Buschmann, C.D. Hoemann, J.C. Leroux, B.L. Atkinson, F. Binette, and A. Selmani, *Novel injectable neutral solutions of chitosan form biodegradable gels in situ.* Biomaterials, 2000. **21**(21): p. 2155-2161.
146. Kim, K.S., S.J. Park, J.A. Yang, J.H. Jeon, S.H. Bhang, B.S. Kim, and S.K. Hahn, *Injectable hyaluronic acid-tyramine hydrogels for the treatment of rheumatoid arthritis.* Acta Biomaterialia, 2011. **7**(2): p. 666-674.
147. Hascall, V.C., A.K. Majors, C.A. de la Motte, S.P. Evanko, A. Wang, J.A. Drazba, S.A. Strong, and T.N. Wight, *Intracellular hyaluronan: a new frontier for inflammation?* Biochimica et Biophysica Acta (BBA)-General Subjects, 2004. **1673**(1): p. 3-12.
148. Longaker, M.T., E.S. Chiu, N.S. Adzick, M. Stern, M.R. Harrison, and R. Stern, *Studies in fetal wound healing. V. A prolonged presence of hyaluronic acid characterizes fetal wound fluid.* Annals of surgery, 1991. **213**(4): p. 292.
149. West, D.C., I.N. Hampson, F. Arnold, and S. Kumar, *Angiogenesis induced by degradation products of hyaluronic acid.* Science, 1985. **228**(4705): p. 1324-1326.
150. Ushida, T., K. Furukawa, K. Toita, and T. Tateishi, *Three-Dimensional Seeding of Chondrocytes Encapsulated in Collagen Gel Into PLLA Scaffolds.* Cell Transplant, 2002. **11**(5): p. 489-494.
151. Awad, H.A., M.Q. Wickham, H.A. Leddy, J.M. Gimble, and F. Guilak, *Chondrogenic differentiation of adipose-derived adult stem cells in agarose, alginate, and gelatin scaffolds.* Biomaterials, 2004. **25**(16): p. 3211-3222.
152. Gamez Sazo, R.E., K. Maenaka, W. Gu, P.M. Wood, and M.B. Bunge, *Fabrication of growth factor- and extracellular matrix-loaded, gelatin-based scaffolds and their biocompatibility with Schwann cells and dorsal root ganglia.* Biomaterials, 2012. **33**(33): p. 8529-39.
153. Ponticiello, M.S., R.M. Schinagl, S. Kadiyala, and F.P. Barry, *Gelatin-based resorbable sponge as a carrier matrix for human mesenchymal stem cells in cartilage regeneration therapy.* Journal of Biomedical Materials Research, 2000. **52**(2): p. 246-255.
154. Nichol, J.W., S.T. Koshy, H. Bae, C.M. Hwang, S. Yamanlar, and A. Khademhosseini, *Cell-laden microengineered gelatin methacrylate hydrogels.* Biomaterials, 2010. **31**(21): p. 5536-5544.
155. Chang, C.J., *The effect of pulse-released nerve growth factor from genipin-crosslinked gelatin in schwann cell-seeded polycaprolactone conduits on large-gap peripheral nerve regeneration.* Tissue Eng Part A, 2009. **15**(3): p. 547-57.

156. Nikkhah, M., N. Eshak, P. Zorlutuna, N. Annabi, M. Castello, K. Kim, A. Dolatshahi-Pirouz, F. Edalat, H. Bae, Y. Yang, and A. Khademhosseini, *Directed endothelial cell morphogenesis in micropatterned gelatin methacrylate hydrogels.* Biomaterials, 2012. **33**(35): p. 9009-9018.
157. Laurens, N., P. Koolwijk, and M.P. de Maat, *Fibrin structure and wound healing.* J Thromb Haemost, 2006. **4**(5): p. 932-9.
158. Janmey, P.A., J.P. Winer, and J.W. Weisel, *Fibrin gels and their clinical and bioengineering applications.* Journal of The Royal Society Interface, 2009. **6**(30): p. 1-10.
159. Janmey, P.A. and J.D. Ferry, *Gel formation by fibrin oligomers without addition of monomers.* Biopolymers, 1986. **25**(7): p. 1337-1344.
160. Ahmed, T.A., E.V. Dare, and M. Hincke, *Fibrin: a versatile scaffold for tissue engineering applications.* Tissue Engineering Part B: Reviews, 2008. **14**(2): p. 199-215.
161. Weisel, J.W., *The mechanical properties of fibrin for basic scientists and clinicians.* Biophysical Chemistry, 2004. **112**(2-3): p. 267-76.
162. Yuan Ye, K., K.E. Sullivan, and L.D. Black, *Encapsulation of cardiomyocytes in a fibrin hydrogel for cardiac tissue engineering.* J Vis Exp, 2011(55).
163. Willerth, S.M., K.J. Arendas, D.I. Gottlieb, and S.E. Sakiyama-Elbert, *Optimization of fibrin scaffolds for differentiation of murine embryonic stem cells into neural lineage cells.* Biomaterials, 2006. **27**(36): p. 5990-6003.
164. Catelas, I., N. Sese, B.M. Wu, J.C. Dunn, S. Helgerson, and B. Tawil, *Human mesenchymal stem cell proliferation and osteogenic differentiation in fibrin gels in vitro.* Tissue Eng, 2006. **12**(8): p. 2385-96.
165. Kneser, U., A. Voogd, J. Ohnolz, O. Buettner, L. Stangenberg, Y. Zhang, G. Stark, and D. Schaefer, *Fibrin gel-immobilized primary osteoblasts in calcium phosphate bone cement: in vivo evaluation with regard to application as injectable biological bone substitute.* Cells Tissues Organs, 2005. **179**(4): p. 158-169.
166. Flanagan, T.C., C. Cornelissen, S. Koch, B. Tschoeke, J.S. Sachweh, T. Schmitz-Rode, and S. Jockenhoevel, *The in vitro development of autologous fibrin-based tissue-engineered heart valves through optimised dynamic conditioning.* Biomaterials, 2007. **28**(23): p. 3388-3397.
167. Wright, B. and C.J. Connon, *Chapter 7 Alginate Hydrogels for the 3D Culture and Therapeutic Delivery of Cells*, in *Hydrogels in Cell-Based Therapies*. 2014, The Royal Society of Chemistry. p. 135-170.
168. Fu, S., A. Thacker, D. Sperger, R. Boni, S. Velankar, E. Munson, and L. Block, *Rheological Evaluation of Inter-grade and Inter-batch Variability of Sodium Alginate.* AAPS PharmSciTech, 2010. **11**(4): p. 1662-1674.
169. Peng, Y., V. Glattauer, J.A. Werkmeister, and J.A. Ramshaw, *Evaluation for collagen products for cosmetic application.* J Cosmet Sci, 2004. **55**(4): p. 327-41.
170. Alsberg, E., K.W. Anderson, A. Albeiruti, R.T. Franceschi, and D.J. Mooney, *Cell-interactive alginate hydrogels for bone tissue engineering.* Journal of Dental Research, 2001. **80**(11): p. 2025-2029.
171. Kuo, C.K. and P.X. Ma, *Ionically crosslinked alginate hydrogels as scaffolds for tissue engineering: Part 1. Structure, gelation rate and mechanical properties.* Biomaterials, 2001. **22**(6): p. 511-521.

172. Lee, C.R., A.J. Grodzinsky, and M. Spector, *The effects of cross-linking of collagen-glycosaminoglycan scaffolds on compressive stiffness, chondrocyte-mediated contraction, proliferation and biosynthesis.* Biomaterials, 2001. **22**(23): p. 3145-3154.
173. Lee, C.R., A.J. Grodzinsky, and M. Spector, *Modulation of the contractile and biosynthetic activity of chondrocytes seeded in collagen-glycosaminoglycan matrices.* Tissue Eng, 2003. **9**(1): p. 27-36.
174. Park, S.H., S.R. Park, S.I. Chung, K.S. Pai, and B.H. Min, *Tissue-engineered cartilage using fibrin/hyaluronan composite gel and its in vivo implantation.* Artificial organs, 2005. **29**(10): p. 838-845.
175. Kim, D.Y., J. Pyun, J.W. Choi, J.H. Kim, J.S. Lee, H. Shin, H.J. Kim, H.N. Lee, B.H. Min, and H.E. Cha, *Tissue-engineered allograft tracheal cartilage using fibrin/hyaluronan composite gel and its in vivo implantation.* The Laryngoscope, 2010. **120**(1): p. 30-38.
176. Park, S.H., J.H. Cui, S.R. Park, and B.H. Min, *Potential of fortified fibrin/hyaluronic acid composite gel as a cell delivery vehicle for chondrocytes.* Artificial organs, 2009. **33**(6): p. 439-447.
177. Park, S.-H., B.H. Choi, S.R. Park, and B.-H. Min, *Chondrogenesis of rabbit mesenchymal stem cells in fibrin/hyaluronan composite scaffold in vitro.* Tissue Engineering Part A, 2011. **17**(9-10): p. 1277-1286.
178. Jockenhoevel, S., G. Zund, S.P. Hoerstrup, K. Chalabi, J.S. Sachweh, L. Demircan, B.J. Messmer, and M. Turina, *Fibrin gel – advantages of a new scaffold in cardiovascular tissue engineering.* European Journal of Cardio-Thoracic Surgery, 2001. **19**(4): p. 424-430.
179. Galler, K.M., A.C. Cavender, U. Koeklue, L.J. Suggs, G. Schmalz, and R.N. D'Souza, *Bioengineering of dental stem cells in a PEGylated fibrin gel.* Regenerative medicine, 2011. **6**(2): p. 191-200.
180. Molla, A., M.B. Donati, and J. Vermylen, *The antigenic determinant of fibrin(ogen) measured with agglutination inhibition immunoassays.* J Clin Pathol, 1974. **27**(6): p. 473-9.
181. Lynn, A., I. Yannas, and W. Bonfield, *Antigenicity and immunogenicity of collagen.* Journal of Biomedical Materials Research Part B: Applied Biomaterials, 2004. **71**(2): p. 343-354.
182. Humphrey, J.H., *Antigenic properties of hyaluronic acid.* Biochemical Journal, 1943. **37**(4): p. 460-3.
183. Cooperman, L. and D. Michaeli, *The immunogenicity of injectable collagen. I. A 1-year prospective study.* Journal of the American Academy of Dermatology, 1984. **10**(4): p. 638-646.
184. Steffen, C., R. Timpl, and I. Wolff, *Immunogenicity and specificity of collagen: V. Demonstration of three different antigenic determinants on calf collagen.* Immunology, 1968. **15**(1): p. 135.
185. Cooperman, L. and D. Michaeli, *The immunogenicity of injectable collagen. II. A retrospective review of seventy-two tested and treated patients.* Journal of the American Academy of Dermatology, 1984. **10**(4): p. 647-651.
186. Furthmayr, H., W. Beil, and R. Timpl, *Different antigenic determinants in the polypeptide chains of human collagen.* FEBS Letters, 1971. **12**(6): p. 341-344.
187. Yamamoto, S., T. Yoshimine, T. Fujita, R. Kuroda, T. Irie, K. Fujioka, and T. Hayakawa, *Protective effect of NGF atelocollagen mini-pellet on*

the hippocampal delayed neuronal death in gerbils. Neuroscience Letters, 1992. **141**(2): p. 161-5.

188. Vizarova, K., D. Bakos, M. Rehakova, and V. Macho, *Modification of layered atelocollagen by ultraviolet irradiation and chemical cross-linking: structure stability and mechanical properties.* Biomaterials, 1994. **15**(13): p. 1082-6.
189. Speer, D.P., M. Chvapil, C.D. Eskelson, and J. Ulreich, *Biological Effects of Residual Glutaraldehyde in Glutaraldehye-Tanned Collagen Biomaterials* Journal of Biomedical Materials Research, 1980. **14**(6): p. 753-764.
190. Zhu, J., *Bioactive modification of poly(ethylene glycol) hydrogels for tissue engineering.* Biomaterials, 2010. **31**(17): p. 4639-4656.
191. Revzin, A., R.J. Russell, V.K. Yadavalli, W.-G. Koh, C. Deister, D.D. Hile, M.B. Mellott, and M.V. Pishko, *Fabrication of poly (ethylene glycol) hydrogel microstructures using photolithography.* Langmuir, 2001. **17**(18): p. 5440-5447.
192. Mellott, M.B., K. Searcy, and M.V. Pishko, *Release of protein from highly cross-linked hydrogels of poly (ethylene glycol) diacrylate fabricated by UV polymerization.* Biomaterials, 2001. **22**(9): p. 929-941.
193. Metters, A.T., K.S. Anseth, and C.N. Bowman, *Fundamental studies of a novel, biodegradable PEG-b-PLA hydrogel.* Polymer, 2000. **41**(11): p. 3993-4004.
194. Nicodemus, G.D., I. Villanueva, and S.J. Bryant, *Mechanical stimulation of TMJ condylar chondrocytes encapsulated in PEG hydrogels.* Journal of Biomedical Materials Research - Part A, 2007. **83**(2): p. 323-331.
195. Nuttelman, C.R., M.C. Tripodi, and K.S. Anseth, *In vitro osteogenic differentiation of human mesenchymal stem cells photoencapsulated in PEG hydrogels.* Journal of Biomedical Materials Research - Part A, 2004. **68**(4): p. 773-782.
196. Nuttelman, C.R., M.C. Tripodi, and K.S. Anseth, *Synthetic hydrogel niches that promote hMSC viability.* Matrix Biology, 2005. **24**(3): p. 208-218.
197. Stosich, M.S. and J.J. Mao, *Adipose tissue engineering from human adult stem cells: Clinical implications in plastic and reconstructive surgery.* Plastic and Reconstructive Surgery, 2007. **119**(1): p. 71-83.
198. Schmedlen, R.H., K.S. Masters, and J.L. West, *Photocrosslinkable polyvinyl alcohol hydrogels that can be modified with cell adhesion peptides for use in tissue engineering.* Biomaterials, 2002. **23**(22): p. 4325-4332.
199. Alves, M.H., B.E. Jensen, A.A. Smith, and A.N. Zelikin, *Poly(vinyl alcohol) physical hydrogels: new vista on a long serving biomaterial.* Macromolecular Bioscience, 2011. **11**(10): p. 1293-313.
200. Nafea, E.H., L.A. Poole-Warren, and P.J. Martens, *Structural and functional characterization of biosynthetic PVA-gelatin hydrogels designed for cell based therapy*, in *World Congress on Medical Physics and Biomedical Engineering May 26-31, 2012, Beijing, China*, M. Long, Editor. 2013, Springer Berlin Heidelberg. p. 91-94.
201. Paradossi, G., F. Cavalieri, E. Chiessi, C. Spagnoli, and M.K. Cowman, *Poly(vinyl alcohol) as versatile biomaterial for potential biomedical*

applications. Journal of Materials Science: Materials in Medicine, 2003. **14**(8): p. 687-691.

202. Martens, P. and K.S. Anseth, *Characterization of hydrogels formed from acrylate modified poly(vinyl alcohol) macromers.* Polymer, 2000. **41**(21): p. 7715-7722.
203. Rafat, M., L.S. Rotenstein, J.-O. You, and D.T. Auguste, *Dual functionalized PVA hydrogels that adhere endothelial cells synergistically.* Biomaterials, 2012. **33**(15): p. 3880-3886.
204. Stammen, J.A., S. Williams, D.N. Ku, and R.E. Guldberg, *Mechanical properties of a novel PVA hydrogel in shear and unconfined compression.* Biomaterials, 2001. **22**(8): p. 799-806.
205. Anseth, K.S., A.T. Metters, S.J. Bryant, P.J. Martens, J.H. Elisseeff, and C.N. Bowman, *In situ forming degradable networks and their application in tissue engineering and drug delivery.* Journal of Controlled Release, 2002. **78**(1-3): p. 199-209.
206. Lin, C.-C. and K. Anseth, *PEG Hydrogels for the Controlled Release of Biomolecules in Regenerative Medicine.* Pharmaceutical Research, 2009. **26**(3): p. 631-643.
207. Ma, G., B. Miao, and C. Song, *Thermosensitive PCL - PEG - PCL hydrogels: Synthesis, characterization, and delivery of proteins.* Journal of Applied Polymer Science, 2010. **116**(4): p. 1985-1993.
208. Park, J.S., D.G. Woo, B.K. Sun, H.-M. Chung, S.J. Im, Y.M. Choi, K. Park, K.M. Huh, and K.-H. Park, *in vitro and in vivo test of PEG/PCL-based hydrogel scaffold for cell delivery application.* Journal of Controlled Release, 2007. **124**(1): p. 51-59.
209. Wang, Y.C., Y.Y. Yuan, J.Z. Du, X.Z. Yang, and J. Wang, *Recent progress in polyphosphoesters: from controlled synthesis to biomedical applications.* Macromolecular Bioscience, 2009. **9**(12): p. 1154-1164.
210. Reichert, J.C., A. Heymer, A. Berner, J. Eulert, and U. Noth, *Fabrication of polycaprolactone collagen hydrogel constructs seeded with mesenchymal stem cells for bone regeneration.* Biomed Mater, 2009. **4**(6): p. 065001.
211. Nuttelman, C.R., D.S.W. Benoit, M.C. Tripodi, and K.S. Anseth, *The effect of ethylene glycol methacrylate phosphate in PEG hydrogels on mineralization and viability of encapsulated hMSCs.* Biomaterials, 2006. **27**(8): p. 1377-1386.
212. Kutty, J.K., E. Cho, J. Soo Lee, N.R. Vyavahare, and K. Webb, *The effect of hyaluronic acid incorporation on fibroblast spreading and proliferation within PEG-diacrylate based semi-interpenetrating networks.* Biomaterials, 2007. **28**(33): p. 4928-4938.
213. Chen, W.Y.J. and G. Abatangelo, *Functions of hyaluronan in wound repair.* Wound Repair and Regeneration, 1999. **7**(2): p. 79-89.
214. Yu, F., X. Cao, Y. Li, L. Zeng, B. Yuan, and X. Chen, *An injectable hyaluronic acid/PEG hydrogel for cartilage tissue engineering formed by integrating enzymatic crosslinking and Diels-Alder "click chemistry".* Polymer Chemistry, 2014. **5**(3): p. 1082-1090.
215. Bryant, S.J., K.A. Davis-Arehart, N. Luo, R.K. Shoemaker, J.A. Arthur, and K.S. Anseth, *Synthesis and characterization of photopolymerized multifunctional hydrogels: water soluble poly(vinyl alcohol) and*

chondroitin sulfate macromers for chondrocyte encapsulation. Macromolecules, 2004. **37**(18): p. 6726-6733.

216. Kim, M., J.Y. Lee, C.N. Jones, A. Revzin, and G. Tae, *Heparin-based hydrogel as a matrix for encapsulation and cultivation of primary hepatocytes.* Biomaterials, 2010. **31**(13): p. 3596-603.
217. Benoit, D.S.W., A.R. Durney, and K.S. Anseth, *The effect of heparin-functionalized PEG hydrogels on three-dimensional human mesenchymal stem cell osteogenic differentiation.* Biomaterials, 2007. **28**(1): p. 66-77.
218. Singh, R.K., D. Seliktar, and A.J. Putnam, *Capillary morphogenesis in PEG-collagen hydrogels.* Biomaterials, 2013. **34**(37): p. 9331-40.
219. Francisco, A.T., R.J. Mancino, R.D. Bowles, J.M. Brunger, D.M. Tainter, Y.T. Chen, W.J. Richardson, F. Guilak, and L.A. Setton, *Injectable laminin-functionalized hydrogel for nucleus pulposus regeneration.* Biomaterials, 2013. **34**(30): p. 7381-8.
220. Francisco, A.T., P.Y. Hwang, C.G. Jeong, L. Jing, J. Chen, and L.A. Setton, *Photocrosslinkable laminin-functionalized polyethylene glycol hydrogel for intervertebral disc regeneration.* Acta Biomater, 2014. **10**(3): p. 1102-11.
221. Dikovsky, D., H. Bianco-Peled, and D. Seliktar, *The effect of structural alterations of PEG-fibrinogen hydrogel scaffolds on 3-D cellular morphology and cellular migration.* Biomaterials, 2006. **27**(8): p. 1496-1506.
222. Rufaihah, A.J., S.R. Vaibavi, M. Plotkin, J. Shen, V. Nithya, J. Wang, D. Seliktar, and T. Kofidis, *Enhanced infarct stabilization and neovascularization mediated by VEGF-loaded PEGylated fibrinogen hydrogel in a rodent myocardial infarction model.* Biomaterials, 2013. **34**(33): p. 8195-8202.
223. Hutson, C.B., J.W. Nichol, H. Aubin, H. Bae, S. Yamanlar, S. Al-Haque, S.T. Koshy, and A. Khademhosseini, *Synthesis and characterization of tunable poly(ethylene glycol): gelatin methacrylate composite hydrogels.* Tissue Eng Part A, 2011. **17**(13-14): p. 1713-23.
224. Eid, K., E. Chen, L. Griffith, and J. Glowacki, *Effect of RGD coating on osteocompatibility of PLGA-polymer disks in a rat tibial wound.* Journal of Biomedical Materials Research, 2001. **57**(2): p. 224-231.
225. Gobin, A.S. and J.L. West, *Cell migration through defined, synthetic ECM analogs.* The FASEB journal : official publication of the Federation of American Societies for Experimental Biology, 2002. **16**(7): p. 751-753.
226. Palecek, S.P., J.C. Loftust, M.H. Ginsberg, D.A. Lauffenburger, and A.F. Horwitz, *Integrin-ligand binding properties govern cell migration speed through cell-substratum adhesiveness.* Nature, 1997. **385**(6616): p. 537-540.
227. Guarnieri, D., A. De Capua, M. Ventre, A. Borzacchiello, C. Pedone, D. Marasco, M. Ruvo, and P.A. Netti, *Covalently immobilized RGD gradient on PEG hydrogel scaffold influences cell migration parameters.* Acta Biomaterialia, 2010. **6**(7): p. 2532-2539.
228. Qiong Liu, S., Q. Tian, L. Wang, J.L. Hedrick, J.H. Po Hui, Y. Yan Yang, and P.L.R. Ee, *Injectable biodegradable polyethylene glycol/ RGD peptide hybrid hydrogels for in vitro chondrogenesis of human mesenchymal stern cells.* Macromolecular Rapid Communications, 2010. **31**(13): p. 1148-1154.

229. Weber, L.M. and K.S. Anseth, *Hydrogel encapsulation environments functionalized with extracellular matrix interactions increase islet insulin secretion.* Matrix Biology, 2008. **27**(8): p. 667-673.
230. Barker, T.H., *The role of ECM proteins and protein fragments in guiding cell behavior in regenerative medicine.* Biomaterials, 2011. **32**(18): p. 4211-4214.
231. Leslie-Barbick, J.E., J.J. Moon, and J.L. West, *Covalently-Immobilized Vascular Endothelial Growth Factor Promotes Endothelial Cell Tubulogenesis in Poly(ethylene glycol) Diacrylate Hydrogels.* Journal of Biomaterials Science, Polymer Edition, 2009. **20**(12): p. 1763-1779.
232. Saik, J.E., D.J. Gould, E.M. Watkins, M.E. Dickinson, and J.L. West, *Covalently immobilized platelet-derived growth factor-BB promotes angiogenesis in biomimetic poly(ethylene glycol) hydrogels.* Acta Biomaterialia, 2011. **7**(1): p. 133-143.
233. Dikovsky, D., H. Bianco-Peled, and D. Seliktar, *Proteolytically Degradable Photo-Polymerized Hydrogels Made From PEG–Fibrinogen Adducts.* Advanced Engineering Materials, 2010. **12**(6): p. B200-B209.
234. Gaudet, I. and D. Shreiber, *Characterization of Methacrylated Type-I Collagen as a Dynamic, Photoactive Hydrogel.* Biointerphases, 2012. **7**(1-4): p. 1-9.
235. Brinkman, W.T., K. Nagapudi, B.S. Thomas, and E.L. Chaikof, *Photo-cross-linking of type I collagen gels in the presence of smooth muscle cells: mechanical properties, cell viability, and function.* Biomacromolecules, 2003. **4**(4): p. 890-5.
236. Poshusta, A.K. and K.S. Anseth, *Photopolymerized biomaterials for application in the temporomandibular joint.* Cells Tissues Organs, 2001. **169**(3): p. 272-8.
237. Browning, M.B., B. Russell, J. Rivera, M. Höök, and E.M. Cosgriff-Hernandez, *Bioactive Hydrogels with Enhanced Initial and Sustained Cell Interactions.* Biomacromolecules, 2013. **14**(7): p. 2225-2233.
238. Park, S., S.H. Nam, and W.G. Koh, *Preparation of collagen-immobilized poly(ethylene glycol)/poly(2-hydroxyethyl methacrylate) interpenetrating network hydrogels for potential application of artificial cornea.* Journal of Applied Polymer Science, 2011.
239. Dong, C.M., X. Wu, J. Caves, S.S. Rele, B.S. Thomas, and E.L. Chaikof, *Photomediated crosslinking of C6-cinnamate derivatized type I collagen.* Biomaterials, 2005. **26**(18): p. 4041-9.
240. Ghandehari, H., R. Sharan, W. Rubas, and W.M. Killing, *Molecular modeling of arginine-glycine-aspartic acid (RGD) analogs: relevance to transepithelial transport.* J Pharm Pharm Sci, 2001. **4**(1): p. 32-41.
241. Barker, T.H., G.M. Fuller, M.M. Klinger, D.S. Feldman, and J.S. Hagood, *Modification of fibrinogen with poly(ethylene glycol) and its effects on fibrin clot characteristics.* J Biomed Mater Res, 2001. **56**(4): p. 529-35.
242. Lee, H.J., J.S. Lee, T. Chansakul, C. Yu, J.H. Elisseeff, and S.M. Yu, *Collagen mimetic peptide-conjugated photopolymerizable PEG hydrogel.* Biomaterials, 2006. **27**(30): p. 5268-5276.
243. Lee, K., E.A. Silva, and D.J. Mooney, *Growth factor delivery-based tissue engineering: general approaches and a review of recent developments.* Journal of The Royal Society Interface, 2011. **8**(55): p. 153-170.

244. Lim, K.S., J. Kundu, A. Reeves, L.A. Poole-Warren, S.C. Kundu, and P.J. Martens, *The influence of silkworm species on cellular interactions with novel pva/silk sericin hydrogels.* Macromolecular Bioscience, 2012. **12**(3): p. 322-332.
245. Lee, D., O. Redfern, and C. Orengo, *Predicting protein function from sequence and structure.* Nature Reviews Molecular Cell Biology, 2007. **8**(12): p. 995-1005.
246. Bernardes, J.S. and C.E. Pedreira, *A review of protein function prediction under machine learning perspective.* Recent Patents on Biotechnology, 2013. **7**(2): p. 122-41.
247. Kluger, R. and A. Alagic, *Chemical cross-linking and protein–protein interactions—a review with illustrative protocols.* Bioorganic Chemistry, 2004. **32**(6): p. 451-472.
248. Moosavi, S., M. Rahgozar, and A. Rahimi, *Protein function prediction using neighbor relativity in protein–protein interaction network.* Computational Biology and Chemistry, 2013. **43**(0): p. 11-16.
249. Tang, X. and J. Bruce, *Chemical Cross-Linking for Protein–Protein Interaction Studies*, in *Mass Spectrometry of Proteins and Peptides*, M. Lipton and L. Paša-Tolic, Editors. 2009, Humana Press. p. 283-293.
250. Sutherland, B.W., J. Toews, and J. Kast, *Utility of formaldehyde cross-linking and mass spectrometry in the study of protein-protein interactions.* Journal of Mass Spectrometry, 2008. **43**(6): p. 699-715.
251. Sinz, A., *Chemical cross-linking and mass spectrometry to map three-dimensional protein structures and protein–protein interactions.* Mass Spectrometry Reviews, 2006. **25**(4): p. 663-682.
252. Fancy, D.A. and T. Kodadek, *Chemistry for the analysis of protein–protein interactions: rapid and efficient cross-linking triggered by long wavelength light.* Proc Natl Acad Sci U S A, 1999. **96**(11): p. 6020-6024.
253. Leavell, M.D., P. Novak, C.R. Behrens, J.S. Schoeniger, and G.H. Kruppa, *Strategy for selective chemical cross-linking of tyrosine and lysine residues.* Journal of the American Society for Mass Spectrometry, 2004. **15**(11): p. 1604-11.
254. Elvin, C.M., T. Vuocolo, A.G. Brownlee, L. Sando, M.G. Huson, N.E. Liyou, P.R. Stockwell, R.E. Lyons, M. Kim, G.A. Edwards, G. Johnson, G.A. McFarland, J.A.M. Ramshaw, and J.A. Werkmeister, *A highly elastic tissue sealant based on photopolymerised gelatin.* Biomaterials, 2010. **31**(32): p. 8323-8331.
255. Tanaka, T., M. Inoue, J. Sakamoto, and N. Sone, *Intra- and Inter-Complex Cross-Linking of Subunits in the Quinol Oxidase Super-Complex from Thermophilic Bacillus PS3.* Journal of Biochemistry (Tokyo, Japan), 1996. **119**(3): p. 482-486.
256. Partis, M.D., D.G. Griffiths, G.C. Roberts, and R.B. Beechey, *Cross-linking of protein by ω-maleimido alkanoylN-hydroxysuccinimido esters.* Journal of Protein Chemistry, 1983. **2**(3): p. 263-277.
257. Burke, M. and E. Reisler, *Effect of nucleotide binding on the proximity of the essential sulfhydryl groups of myosin. Chemical probing of movement of residues during conformational transitions.* Biochemistry, 1977. **16**(25): p. 5559-5563.

258. Nitao, L.K. and E. Reisler, *Probing the Conformational States of the SH1−SH2 Helix in Myosin: A Cross-Linking Approach†.* Biochemistry, 1998. **37**(47): p. 16704-16710.
259. Li, L., B.S. Lollar, H. Li, U.G. Wortmann, and G. Lacrampe-Couloume, *Ammonium stability and nitrogen isotope fractionations for –NH3(aq)–NH3(gas) systems at 20–70°C and pH of 2–13: Applications to habitability and nitrogen cycling in low-temperature hydrothermal systems.* Geochimica et Cosmochimica Acta, 2012. **84**(0): p. 280-296.
260. Joshi, S. and R. Burrows, *ATP synthase complex from bovine heart mitochondria. Subunit arrangement as revealed by nearest neighbor analysis and susceptibility to trypsin.* Journal of Biological Chemistry, 1990. **265**(24): p. 14518-14525.
261. Juris, A., V. Balzani, F. Barigelletti, S. Campagna, P. Belser, and A. von Zelewsky, *Ru(II) polypyridine complexes: photophysics, photochemistry, eletrochemistry, and chemiluminescence.* Coordination Chemistry Reviews, 1988. **84**(0): p. 85-277.
262. Fancy, D.A., C. Denison, K. Kim, Y. Xie, T. Holdeman, F. Amini, and T. Kodadek, *Scope, limitations and mechanistic aspects of the photo-induced cross-linking of proteins by water-soluble metal complexes.* Chemistry & Biology, 2000. **7**(9): p. 697-708.
263. Shen, H.R., J.D. Spikes, C.J. Smith, and J. Kopeček, *Photodynamic cross-linking of proteins V. Nature of the tyrosine-tyrosine bonds formed in the FMN-sensitized intermolecular cross-linking of N-acetyl-L-tyrosine.* Journal of Photochemistry and Photobiology A: Chemistry, 2000. **133**(1-2): p. 115-122.
264. Elvin, C.M., A.G. Brownlee, M.G. Huson, T.A. Tebb, M. Kim, R.E. Lyons, T. Vuocolo, N.E. Liyou, T.C. Hughes, J.A.M. Ramshaw, and J.A. Werkmeister, *The development of photochemically crosslinked native fibrinogen as a rapidly formed and mechanically strong surgical tissue sealant.* Biomaterials, 2009. **30**(11): p. 2059-2065.
265. Elvin, C.M., S.J. Danon, A.G. Brownlee, J.F. White, M. Hickey, N.E. Liyou, G.A. Edwards, J.A.M. Ramshaw, and J.A. Werkmeister, *Evaluation of photo-crosslinked fibrinogen as a rapid and strong tissue adhesive.* J Biomed Mater Res A, 2010. **93**(2): p. 687-695.
266. Sando, L., M. Kim, M.L. Colgrave, J.A.M. Ramshaw, J.A. Werkmeister, and C.M. Elvin, *Photochemical crosslinking of soluble wool keratins produces a mechanically stable biomaterial that supports cell adhesion and proliferation.* Journal of Biomedical Materials Research - Part A, 2010. **95**(3 A): p. 901-911.
267. Elvin, C.M., A.G. Carr, M.G. Huson, J.M. Maxwell, R.D. Pearson, T. Vuocolo, N.E. Liyou, D.C.C. Wong, D.J. Merritt, and N.E. Dixon, *Synthesis and properties of crosslinked recombinant pro-resilin.* Nature, 2005. **437**(7061): p. 999-1002.
268. Sando, L., S. Danon, A.G. Brownlee, R.J. McCulloch, J.A.M. Ramshaw, C.M. Elvin, and J.A. Werkmeister, *Photochemically crosslinked matrices of gelatin and fibrinogen promote rapid cell proliferation.* Journal of Tissue Engineering and Regenerative Medicine, 2011. **5**(5): p. 337-346.
269. Vuocolo, T., R. Haddad, G.A. Edwards, R.E. Lyons, N.E. Liyou, J.A. Werkmeister, J.A.M. Ramshaw, and C.M. Elvin, *A Highly Elastic and*

Adhesive Gelatin Tissue Sealant for Gastrointestinal Surgery and Colon Anastomosis. Journal of Gastrointestinal Surgery, 2012. **16**(5): p. 744-752.

270. Park, K.M., I. Jun, Y.K. Joung, H. Shin, and K.D. Park, *In situ hydrogelation and RGD conjugation of tyramine-conjugated 4-arm PPO-PEO block copolymer for injectable bio-mimetic scaffolds.* Soft Matter, 2011. **7**(3): p. 986-992.
271. Park, K.M., Y.M. Shin, Y.K. Joung, H. Shin, and K.D. Park, *In situ forming hydrogels based on tyramine conjugated 4-Arm-PPO-PEO via enzymatic oxidative reaction.* Biomacromolecules, 2010. **11**(3): p. 706-712.
272. Menzies, D.J., A. Cameron, T. Munro, E. Wolvetang, L. Grøndahl, and J.J. Cooper-White, *Tailorable Cell Culture Platforms from Enzymatically Cross-Linked Multifunctional Poly(ethylene glycol)-Based Hydrogels.* Biomacromolecules, 2012. **14**(2): p. 413-423.
273. Burdick, J.A., A.J. Peterson, and K.S. Anseth, *Conversion and temperature profiles during the photoinitiated polymerization of thick orthopaedic biomaterials.* Biomaterials, 2001. **22**(13): p. 1779-1786.
274. Muller, P. and K. Brettel, *[Ru(bpy)3]2+ as a reference in transient absorption spectroscopy: differential absorption coefficients for formation of the long-lived 3MLCT excited state.* Photochemical & Photobiological Sciences, 2012. **11**(4): p. 632-636.
275. Bulpitt, P. and D. Aeschlimann, *New strategy for chemical modification of hyaluronic acid: Preparation of functionalized derivatives and their use in the formation of novel biocompatible hydrogels.* Journal of Biomedical Materials Research, 1999. **47**(2): p. 152-169.
276. Guzman-Villanueva, D., H.D.C. Smyth, D. Herrera-Ruiz, and I.M. El-Sherbiny, *A novel aerosol method for the production of hydrogel particles.* J Nanomater, 2011. **2011**.
277. Atassi, M.Z. and T. Manshouri, *Synthesis of tolerogenic monomethoxypolyethylene glycol and polyvinyl alcohol conjugates of peptides.* Journal of Protein Chemistry, 1991. **10**(6): p. 623-627.
278. Benoit, D.S.W. and K.S. Anseth, *The effect on osteoblast function of colocalized rgd and phsrn epitopes on peg surfaces.* Biomaterials, 2005. **26**(25): p. 5209-5220.
279. Wong, L.S., F. Khan, and J. Micklefield, *Selective Covalent Protein Immobilization: Strategies and Applications.* Chemical Reviews (Washington, DC, United States), 2009. **109**(9): p. 4025-4053.
280. Holmes, J.C. and N.O. Fowler, *Cardiac Effects of Tyramine.* Circulation Research, 1962. **11**(3): p. 364-369.
281. Zheng, L., D. Kostrewa, S. Bernèche, F.K. Winkler, and X.-D. Li, *The mechanism of ammonia transport based on the crystal structure of AmtB of Escherichia coli.* Proceedings of the National Academy of Sciences of the United States of America, 2004. **101**(49): p. 17090-17095.
282. Sivaranjani, N., S.V. Rao, and G. Rajeev, *Role of reactive oxygen species and antioxidants in atopic dermatitis.* J Clin Diagn Res, 2013. **7**(12): p. 2683-5.
283. Martens, P., M. Grant, A. Nilasaroya, J. Whitelock, and L. Poole-Warren, *Characterisation of redox initiators for producing poly(vinyl alcohol) hydrogels.* Macromolecular Symposia, 2008. **266**(1): p. 59-62.

284. Neto, V.F., J. Lencart, A.G. Dias, J.A. Santos, A. Ramos, and C. Relvas, *The effect of megavoltage radiation on polymeric materials to be used in biomedical devices.* Journal of Nanoscience and Nanotechnology, 2012. **12**(8): p. 6779-84.
285. Michael, B., *Non-DNA-Targeted Effects and Low-Dose Radiation Risk,* in *Radiation Health Risk Sciences*, M. Nakashima, et al., Editors. 2009, Springer Japan. p. 29-33.
286. Lecamp, L., B. Youssef, C. Bunel, and P. Lebaudy, *Kinetic studies of photoinitiated polymerization of a dimethacrylate oligomer.* Nuclear Instruments and Methods in Physics Research Section B: Beam Interactions with Materials and Atoms, 1999. **151**(1-4): p. 285-289.
287. Jančovičová, V., M. Mikula, B. Havlínová, and Z. Jakubíková, *Influence of UV-curing conditions on polymerization kinetics and gloss of urethane acrylate coatings.* Progress in Organic Coatings, 2013. **76**(2–3): p. 432-438.
288. Ghorpade, R.V., S.M. Bhosle, S. Ponrathnam, C.R. Rajan, N.N. Chavan, and R. Harikrishna, *Photopolymerization kinetics of 2-phenylethyl (meth)acrylates studied by photo DSC.* Journal of Polymer Research, 2012. **19**(2): p. 1-8.
289. Jilek, S., E. Walter, H.P. Merkle, and B. Corthesy, *Modulation of allergic responses in mice by using biodegradable poly(lactide-co-glycolide) microspheres.* J Allergy Clin Immunol, 2004. **114**(4): p. 943-50.
290. Kim, M.S., K.S. Seo, H. Hyun, S.K. Kim, G. Khang, and H.B. Lee, *Sustained release of bovine serum albumin using implantable wafers prepared by MPEG-PLGA diblock copolymers.* International Journal of Pharmaceutics, 2005. **304**(1-2): p. 165-77.
291. Wang, D.K., S. Varanasi, D.J.T. Hill, F. Rasoul, A.L. Symons, and A.K. Whittaker, *The influence of composition on the physical properties of PLA-PEG-PLA-co-Boltorn based polyester hydrogels and their biological performance.* Journal of Materials Chemistry, 2012. **22**(14): p. 6994-7004.
292. Chao, G.T., Z.Y. Qian, M.J. Huang, B. Kan, Y.C. Gu, C.Y. Gong, J.L. Yang, K. Wang, M. Dai, X.Y. Li, M.L. Gou, M.J. Tu, and Y.Q. Wei, *Synthesis, characterization, and hydrolytic degradation behavior of a novel biodegradable pH-sensitive hydrogel based on polycaprolactone, methacrylic acid, and poly(ethylene glycol).* Journal of Biomedical Materials Research Part A, 2008. **85A**(1): p. 36-46.
293. Suggs, L.J., E.Y. Kao, L.L. Palombo, R.S. Krishnan, M.S. Widmer, and A.G. Mikos, *Preparation and characterization of poly(propylene fumarate-co-ethylene glycol) hydrogels.* Journal of Biomaterials Science, Polymer Edition, 1998. **9**(7): p. 653-666.
294. Martens, P., T. Holland, and K.S. Anseth, *Synthesis and characterization of degradable hydrogels formed from acrylate modified poly(vinyl alcohol) macromers.* Polymer, 2002. **43**(23): p. 6093-6100.
295. da Silva, P.L., L. Guimarães, and J.R. Pliego, *Revisiting the Mechanism of Neutral Hydrolysis of Esters: Water Autoionization Mechanisms with Acid or Base Initiation Pathways.* The Journal of Physical Chemistry B, 2013. **117**(21): p. 6487-6497.
296. Simanenko, Y.S., I.A. Belousova, V.A. Savelova, A.F. Popov, and L.N. Vakhitova, *The Effect of Temperature on the Rate of Alkaline Hydrolysis*

of Esters in Concentrated Aqueous Solutions of Et4NCl. Theoretical and Experimental Chemistry, 2004. **40**(1): p. 17-24.
297. Bender, M.L. and B.W. Turnquest, *General Basic Catalysis of Ester Hydrolysis and Its Relationship to Enzymatic Hydrolysis1*. Journal of the American Chemical Society, 1957. **79**(7): p. 1656-1662.
298. Comisar, C.M., S.E. Hunter, A. Walton, and P.E. Savage, *Effect of pH on Ether, Ester, and Carbonate Hydrolysis in High-Temperature Water*. Industrial & Engineering Chemistry Research, 2007. **47**(3): p. 577-584.
299. da Silva, P.L., L. Guimaraes, and J.R. Pliego, Jr., *Revisiting the mechanism of neutral hydrolysis of esters: water autoionization mechanisms with acid or base initiation pathways.* J Phys Chem B, 2013. **117**(21): p. 6487-97.
300. Bergmann, F., R. Segal, A. Shimoni, and M. Wurzel, *The pH-dependence of enzymic ester hydrolysis.* Biochemical Journal, 1956. **63**(4): p. 684.
301. Carvalho, J., S. Moreira, J. Maia, and F.M. Gama, *Characterization of dextrin-based hydrogels: rheology, biocompatibility, and degradation.* J. Biomed Mater Res A, 2010. **93**(1): p. 389-399.
302. Janorkar, A.V., A.T. Metters, and D.E. Hirt, *Modification of Poly(lactic acid) Films: Enhanced Wettability from Surface-Confined Photografting and Increased Degradation Rate Due to an Artifact of the Photografting Process.* Macromolecules, 2004. **37**(24): p. 9151-9159.
303. Xu, L., K. Crawford, and C.B. Gorman, *Effects of Temperature and pH on the Degradation of Poly(lactic acid) Brushes.* Macromolecules, 2011. **44**(12): p. 4777-4782.
304. Jung, J.H., M. Ree, and H. Kim, *Acid- and base-catalyzed hydrolyses of aliphatic polycarbonates and polyesters.* Catalysis Today, 2006. **115**(1–4): p. 283-287.
305. Hennink, W.E., S.J. De Jong, G.W. Bos, T.F.J. Veldhuis, and C.F. Van Nostrum, *Biodegradable dextran hydrogels crosslinked by stereocomplex formation for the controlled release of pharmaceutical proteins.* International Journal of Pharmaceutics, 2004. **277**(1-2): p. 99-104.
306. Cavalieri, F., F. Miano, P. D'Antona, and G. Paradossi, *Study of gelling behavior of poly(vinyl alcohol)-methacrylate for potential utilizations in tissue replacement and drug delivery.* Biomacromolecules, 2004. **5**(6): p. 2439-2446.
307. Hoogduijn, M.J., J.C.v.d. Beukel, L.C.M. Wiersma, and J. Ijzer, *Morphology and size of stem cells from mouse and whale: observational study*. BMJ, 2013. **347**.
308. Guilak, F., L.G. Alexopoulos, M.L. Upton, I. Youn, J.B. Choi, L. Cao, L.A. Setton, and M.A. Haider, *The pericellular matrix as a transducer of biomechanical and biochemical signals in articular cartilage*. 2006. p. 498-512.
309. Canal, T. and N.A. Peppas, *Correlation between mesh size and equilibrium degree of swelling of polymeric networks.* J Biomed Mater Res, 1989. **23**(10): p. 1183-93.
310. Ghandehari, H., P. Kopečkové, and J. Kopeček, *In vitro degradation of pH-sensitive hydrogels containing aromatic azo bonds.* Biomaterials, 1997. **18**(12): p. 861-872.

311. Akala, E.O., P. Kopečková, and J. Kopeček, *Novel pH-sensitive hydrogels with adjustable swelling kinetics.* Biomaterials, 1998. **19**(11–12): p. 1037-1047.
312. Vercruysse, K.P., D.M. Marecak, J.F. Marecek, and G.D. Prestwich, *Synthesis and in Vitro Degradation of New Polyvalent Hydrazide Cross-Linked Hydrogels of Hyaluronic Acid.* Bioconjugate Chemistry, 1997. **8**(5): p. 686-694.
313. Qiu, Y. and K. Park, *Environment-sensitive hydrogels for drug delivery.* Advanced Drug Delivery Reviews, 2001. **53**(3): p. 321-339.
314. Riegelman, S., L.A. Strait, and E.Z. Fischer, *Acid dissociation constants of phenylalkanolamines.* Journal of Pharmaceutical Sciences, 1962. **51**(2): p. 129-133.
315. Meyvis, T.K.L., S.C. De Smedt, J. Demeester, and W.E. Hennink, *Influence of the Degradation Mechanism of Hydrogels on Their Elastic and Swelling Properties during Degradation.* Macromolecules, 2000. **33**(13): p. 4717-4725.
316. Dong, L.-c. and A.S. Hoffman, *A novel approach for preparation of pH-sensitive hydrogels for enteric drug delivery.* Journal of Controlled Release, 1991. **15**(2): p. 141-152.
317. Moeinzadeh, S., S.N. Khorasani, J. Ma, X. He, and E. Jabbari, *Synthesis and Gelation Characteristics of Photo-Crosslinkable Star Poly(ethylene oxide-co-lactide-glycolide acrylate) Macromonomers.* Polymer (Guildf), 2011. **52**(18): p. 3887-3896.
318. Kaihara, S., S. Matsumura, and J.P. Fisher, *Synthesis and characterization of cyclic acetal based degradable hydrogels.* European Journal of Pharmaceutics and Biopharmaceutics, 2008. **68**(1): p. 67-73.
319. Bian, L., C. Hou, E. Tous, R. Rai, R.L. Mauck, and J.A. Burdick, *The influence of hyaluronic acid hydrogel crosslinking density and macromolecular diffusivity on human MSC chondrogenesis and hypertrophy.* Biomaterials, 2013. **34**(2): p. 413-421.
320. Olea, A.F. and J.K. Thomas, *Rate constants for reactions in viscous media: correlation between the viscosity of the solvent and the rate constant of the diffusion-controlled reactions.* Journal of the American Chemical Society, 1988. **110**(14): p. 4494-4502.
321. Modarress, H., M.M. Nia, and R. Mostafa, *Viscosity Measurements and Modelling of Aqueous Polyvinyl Alcohol Mixtures.* Iranian Polymer Journal, 2005. **14**(2): p. 181-184.
322. Kadajji, V.G. and G.V. Betageri, *Water Soluble Polymers for Pharmaceutical Applications.* Polymers, 2011. **3**(4): p. 1972-2009.
323. Asmussen, E. and A. Peutzfeldt, *Influence of selected components on crosslink density in polymer structures.* Eur J Oral Sci, 2001. **109**(4): p. 282-5.
324. Peppas, N.A., Hydrogels in Medicine and Pharmacy, 1987.
325. Nuttelman, C.R., S.M. Henry, and K.S. Anseth, *Synthesis and characterization of photocrosslinkable, degradable poly(vinyl alcohol)-based tissue engineering scaffolds.* Biomaterials, 2002. **23**(17): p. 3617-3626.
326. Lee, F., J.E. Chung, and M. Kurisawa, *An injectable hyaluronic acid-tyramine hydrogel system for protein delivery.* Journal of Controlled Release, 2009. **134**(3): p. 186-193.

327. Flory, P.J., *Principles of polymer chemistry*. 1953: Cornell University Press.
328. Durmaz, S. and O. Okay, *Acrylamide/2-acrylamido-2-methylpropane sulfonic acid sodium salt-based hydrogels: synthesis and characterization.* Polymer, 2000. **41**(10): p. 3693-3704.
329. Sitte, H.H., S. Huck, H. Reither, S. Boehm, E.A. Singer, and C. Pifl, *Carrier-mediated release, transport rates, and charge transfer induced by amphetamine, tyramine, and dopamine in mammalian cells transfected with the human dopamine transporter.* Journal of Neurochemistry, 1998. **71**(3): p. 1289-97.
330. Lee, B.-D. and M.-J. Lee, *Prediction of Hydroxyl Substitution Site (s) of Phenol, Monochlorophenols and 4-Chloronitrobenzene by Atomic Charge Distribution Calculations.* Bull. Korean Chem. Soc, 2009. **30**(4): p. 787.
331. Behravesh, E., M.D. Timmer, J.J. Lemoine, M.A.K. Liebschner, and A.G. Mikos, *Evaluation of the in Vitro Degradation of Macroporous Hydrogels Using Gravimetry, Confined Compression Testing, and Microcomputed Tomography.* Biomacromolecules, 2002. **3**(6): p. 1263-1270.
332. Margesin, R., P. Bergauer, and S. Gander, *Degradation of phenol and toxicity of phenolic compounds: a comparison of cold-tolerant Arthrobacter sp. and mesophilic Pseudomonas putida.* Extremophiles, 2004. **8**(3): p. 201-207.
333. Nemeikaitė-Čėnienė, A., A. Marozienė, R. Vidžiūnaitė, and N. Čėnas, *Prooxidant cytotoxicity, apoptosis induction, and protective effects of polyphenolic antioxidants.* Chem Technol, 2009. **3**: p. 12-15.
334. Whitaker, M.J., R.A. Quirk, S.M. Howdle, and K.M. Shakesheff, *Growth factor release from tissue engineering scaffolds.* Journal of Pharmacy and Pharmacology, 2001. **53**(11): p. 1427-1437.
335. Zisch, A.H., M.P. Lutolf, M. Ehrbar, G.P. Raeber, S.C. Rizzi, N. Davies, H. Schmökel, D. Bezuidenhout, V. Djonov, P. Zilla, and J.A. Hubbell, *Cell-demanded release of VEGF from synthetic, biointeractive cell-ingrowth matrices for vascularized tissue growth.* The FASEB Journal, 2003.
336. Zisch, A.H., U. Schenk, J.C. Schense, S.E. Sakiyama-Elbert, and J.A. Hubbell, *Covalently conjugated VEGF-fibrin matrices for endothelialization.* Journal of Controlled Release, 2001. **72**(1-3): p. 101-113.
337. Leach, J.B. and C.E. Schmidt, *Characterization of protein release from photocrosslinkable hyaluronic acid-polyethylene glycol hydrogel tissue engineering scaffolds.* Biomaterials, 2005. **26**(2): p. 125-135.
338. Scott, R., L. Marquardt, and R.K. Willits, *Characterization of poly(ethylene glycol) gels with added collagen for neural tissue engineering.* Journal of Biomedical Materials Research Part A, 2010. **93A**(3): p. 817-823.
339. Sargeant, T.D., A.P. Desai, S. Banerjee, A. Agawu, and J.B. Stopek, *An in situ forming collagen–PEG hydrogel for tissue regeneration.* Acta Biomaterialia, 2012. **8**(1): p. 124-132.
340. Rafat, M., F. Li, P. Fagerholm, N.S. Lagali, M.A. Watsky, R. Munger, T. Matsuura, and M. Griffith, *PEG-stabilized carbodiimide crosslinked*

collagen–chitosan hydrogels for corneal tissue engineering. Biomaterials, 2008. **29**(29): p. 3960-3972.

341. Bax, D.V., R.S. Tipa, A. Kondyurin, M.J. Higgins, K. Tsoutas, A. Gelmi, G.G. Wallace, D.R. McKenzie, A.S. Weiss, and M.M.M. Bilek, *Cell patterning via linker-free protein functionalization of an organic conducting polymer (polypyrrole) electrode.* Acta Biomaterialia, 2012. **8**(7): p. 2538-2548.
342. Huang, L.L.H., P.C. Lee, L.W. Chen, and K.H. Hsieh, *Comparison of epoxides on grafting collagen to polyurethane and their effects on cellular growth.* Journal of Biomedical Materials Research, 1998. **39**(4): p. 630-636.
343. Barker, T.H., G.M. Fuller, M.M. Klinger, D.S. Feldman, and J.S. Hagood, *Modification of fibrinogen with poly(ethylene glycol) and its effects on fibrin clot characteristics.* Journal of Biomedical Materials Research, 2001. **56**(4): p. 529-535.
344. Jeyanthi, R. and K. Panduranga Rao, *In vivo biocompatibility of collagen poly(hydroxyethyl methacrylate) hydrogels.* Biomaterials, 1990. **11**(4): p. 238-243.
345. Potorac, S., M. Popa, V. Maier, G. Lisa, and L. Verestiuc, *New hydrogels based on maleilated collagen with potential applications in tissue engineering.* Materials Science and Engineering: C, 2012. **32**(2): p. 236-243.
346. Endrizzi, B.J., H. Gang, P.F. Kiser, and R.J. Stewart, *Specific covalent immobilization of proteins through dityrosine cross-links.* Langmuir, 2006. **22**(26): p. 11305-11310.
347. Nilasaroya, A., P.J. Martens, and J.M. Whitelock, *Enzymatic degradation of heparin-modified hydrogels and its effect on bioactivity.* Biomaterials, 2012. **33**(22): p. 5534-5540.
348. Skardal, A., J. Zhang, L. McCoard, X. Xu, S. Oottamasathien, and G.D. Prestwich, *Photocrosslinkable hyaluronan-gelatin hydrogels for two-step bioprinting.* Tissue Eng. Part A, 2010. **16**(8): p. 2675-85.
349. Ramon-Azcon, J., S. Ahadian, R. Obregon, G. Camci-Unal, S. Ostrovidov, V. Hosseini, H. Kaji, K. Ino, H. Shiku, A. Khademhosseini, and T. Matsue, *Gelatin methacrylate as a promising hydrogel for 3D microscale organization and proliferation of dielectrophoretically patterned cells.* Lab on a Chip, 2012. **12**(16): p. 2959-2969.
350. Fu, Y., K. Xu, X. Zheng, A.J. Giacomin, A.W. Mix, and W.J. Kao, *3D cell entrapment in crosslinked thiolated gelatin-poly(ethylene glycol) diacrylate hydrogels.* Biomaterials, 2012. **33**(1): p. 48-58.
351. Pawde, S.M. and K. Deshmukh, *Characterization of polyvinyl alcohol/gelatin blend hydrogel films for biomedical applications.* Journal of Applied Polymer Science, 2008. **109**(5): p. 3431-3437.
352. You, S.J., W.S. Ahn, H.S. Jang, M.I. Kang, H.J. Chun, Y.M. Lim, and Y.C. Nho, *Preparation and characterization of gelatin-poly(vinyl alcohol) hydrogels for three-dimensional cell culture.* J. Ind. Eng. Chem., 2007. **13**(1): p. 116-120.
353. Pal, K., A.K. Banthia, and D.K. Majumdar, *Preparation and characterization of polyvinyl alcohol-gelatin hydrogel membranes for biomedical applications.* AAPS PharmSciTech, 2007. **8**(1): p. 21.

354. Ohya, S., S. Kidoaki, and T. Matsuda, *Poly(N-isopropylacrylamide) (PNIPAM)-grafted gelatin hydrogel surfaces: interrelationship between microscopic structure and mechanical property of surface regions and cell adhesiveness.* Biomaterials, 2005. **26**(16): p. 3105-11.
355. Kittiphattanabawon, P., S. Benjakul, W. Visessanguan, and F. Shahidi, *Gelatin hydrolysate from blacktip shark skin prepared using papaya latex enzyme: antioxidant activity and its potential in model systems.* Food Chemistry, 2012. **135**(3): p. 1118-1126.
356. Burdick, J.A. and K.S. Anseth, *Photoencapsulation of osteoblasts in injectable RGD-modified PEG hydrogels for bone tissue engineering.* Biomaterials, 2002. **23**(22): p. 4315-4323.
357. Grover, C.N., J.H. Gwynne, N. Pugh, S. Hamaia, R.W. Farndale, S.M. Best, and R.E. Cameron, *Crosslinking and composition influence the surface properties, mechanical stiffness and cell reactivity of collagen-based films.* Acta Biomaterialia, 2012. **8**(8): p. 3080-3090.
358. Smeets, E.F., E.J. von Asmuth, C.J. van der Linden, J.F. Leeuwenberg, and W.A. Buurman, *A comparison of substrates for human umbilical vein endothelial cell culture.* Biotech Histochem, 1992. **67**(4): p. 241-50.
359. Huber, A.R. and S.J. Weiss, *Disruption of the subendothelial basement membrane during neutrophil diapedesis in an in vitro construct of a blood vessel wall.* Journal of Clinical Investigation, 1989. **83**(4): p. 1122-36.
360. Zhu, J., P. He, L. Lin, D.R. Jones, and R.E. Marchant, *Biomimetic Poly(ethylene glycol)-Based Hydrogels as Scaffolds for Inducing Endothelial Adhesion and Capillary-Like Network Formation.* Biomacromolecules, 2012. **13**(3): p. 706-713.
361. Saunders, R.L. and D.A. Hammer, *Assembly of Human Umbilical Vein Endothelial Cells on Compliant Hydrogels.* Cell Mol Bioeng, 2010. **3**(1): p. 60-67.
362. Harris, A.K., P. Wild, and D. Stopak, *Silicone rubber substrata: A new wrinkle in the study of cell locomotion.* Science, 1980. **208**(4440): p. 177-179.
363. Cao, W., M. Cheng, Q. Ao, Y. Gong, N. Zhao, and X. Zhang, *Physical, mechanical and degradation properties, and schwann cell affinity of cross-linked chitosan films.* J Biomater Sci Polym Ed, 2005. **16**(6): p. 791-807.
364. Zamir, E., M. Katz, Y. Posen, N. Erez, K.M. Yamada, B.Z. Katz, S. Lin, D.C. Lin, A. Bershadsky, Z. Kam, and B. Geiger, *Dynamics and segregation of cell-matrix adhesions in cultured fibroblasts.* Nature Cell Biology, 2000. **2**(4): p. 191-196.
365. Greenberg, M.E., X.-M. Li, B.G. Gugiu, X. Gu, J. Qin, R.G. Salomon, and S.L. Hazen, *The Lipid Whisker Model of the Structure of Oxidized Cell Membranes.* Journal of Biological Chemistry, 2008. **283**(4): p. 2385-2396.
366. El-Beltagi, H.S. and H.I. Mohamed, *Reactive Oxygen Species, Lipid Peroxidation and Antioxidative Defense Mechanism*. 2013. Vol. 41. 2013.
367. Halliwell, B. and S. Chirico, *Lipid peroxidation: its mechanism, measurement, and significance.* The American Journal of Clinical Nutrition, 1993. **57**(5): p. 715S-724S.

368. Lin, C.-C. and K.S. Anseth, *Glucagon-Like Peptide-1 Functionalized PEG Hydrogels Promote Survival and Function of Encapsulated Pancreatic β-Cells.* Biomacromolecules, 2009. **10**(9): p. 2460-2467.
369. Lin, C.-C., A. Raza, and H. Shih, *PEG hydrogels formed by thiol-ene photo-click chemistry and their effect on the formation and recovery of insulin-secreting cell spheroids.* Biomaterials, 2011. **32**(36): p. 9685-9695.
370. Farnsworth, N., C. Bensard, and S.J. Bryant, *The role of the PCM in reducing oxidative stress induced by radical initiated photoencapsulation of chondrocytes in poly(ethylene glycol) hydrogels.* Osteoarthritis Cartilage, 2012. **20**(11): p. 1326-35.
371. Nicodemus, G.D., S.C. Skaalure, and S.J. Bryant, *Gel structure has an impact on pericellular and extracellular matrix deposition, which subsequently alters metabolic activities in chondrocyte-laden PEG hydrogels.* Acta Biomaterialia, 2011. **7**(2): p. 492-504.
372. Anseth, K.S., C.M. Wang, and C.N. Bowman, *Kinetic evidence of reaction diffusion during the polymerization of multi(meth)acrylate monomers.* Macromolecules, 1994. **27**(3): p. 650-655.
373. Arrigoni, O. and M.C. De Tullio, *Ascorbic acid: much more than just an antioxidant.* Biochimica et Biophysica Acta (BBA) - General Subjects, 2002. **1569**(1–3): p. 1-9.
374. Foyer, C., P. Descourvieres, and K. Kunert, *Protection against oxygen radicals: an important defence mechanism studied in transgenic plants.* Plant, Cell and Environment, 1994. **17**(5): p. 507-523.
375. Niki, E., *Action of ascorbic acid as a scavenger of active and stable oxygen radicals.* The American Journal of Clinical Nutrition, 1991. **54**(6): p. 1119S-1124S.
376. Kundu, S.C., B.C. Dash, R. Dash, and D.L. Kaplan, *Natural protective glue protein, sericin bioengineered by silkworms: Potential for biomedical and biotechnological applications.* Progress in Polymer Science, 2008. **33**: p. 998-1012.
377. Aramwit, P., S. Damrongsakkul, S. Kanokpanont, and T. Srichana, *Properties and antityrosinase activity of sericin from various extraction methods.* Biotechnology and Applied Biochemistry, 2010. **55**(2): p. 91-98.
378. Mondal, M., K. Trivedy, and S. Nirmal Kumar, *The silk proteins, sericin and fibroin in silkworm, Bombyx mori Linn., - a review.* Caspian Journal of Environmental Sciences, 2007. **5**(2): p. 63-76.
379. Dash, R., C. Acharya, P. Bindu, and S. Kundu, *Antioxidant potential of silk protein sericin against hydrogen peroxide-induced oxidative stress in skin fibroblasts.* BMB reports, 2008. **41**: p. 236.
380. Dash, R., M. Mandal, S. Ghosh, and S. Kundu, *Silk sericin protein of tropical tasar silkworm inhibits UVB-induced apoptosis in human skin keratinocytes.* Molecular and Cellular Biochemistry, 2008. **311**(1): p. 111-119.
381. Mandal, B.B., B. Ghosh, and S.C. Kundu, *Non-mulberry silk sericin/poly (vinyl alcohol) hydrogel matrices for potential biotechnological applications.* International Journal of Biological Macromolecules, 2011. **49**(2): p. 125-133.
382. Temenoff, J.S., H. Shin, D.E. Conway, P.S. Engel, and A.G. Mikos, *In vitro cytotoxicity of redox radical initiators for cross-linking of*

oligo(poly(ethylene glycol) fumarate) macromers. Biomacromolecules, 2003. **4**(6): p. 1605-1613.
383. Raza, A., C.S. Ki, and C.-C. Lin, *The influence of matrix properties on growth and morphogenesis of human pancreatic ductal epithelial cells in 3D.* Biomaterials, 2013. **34**(21): p. 5117-5127.
384. Hersel, U., C. Dahmen, and H. Kessler, *RGD modified polymers: Biomaterials for stimulated cell adhesion and beyond.* Biomaterials, 2003. **24**(24): p. 4385-4415.
385. Tran, N.Q., Y.K. Joung, E. Lih, K.M. Park, and K.D. Park, *RGD-conjugated in Situ forming hydrogels as cell-adhesive injectable scaffolds.* Macromolecular Research, 2011. **19**(3): p. 300-306.
386. Turturro, M.V., M.C. Christenson, J.C. Larson, D.A. Young, E.M. Brey, and G. Papavasiliou, *MMP-Sensitive PEG Diacrylate Hydrogels with Spatial Variations in Matrix Properties Stimulate Directional Vascular Sprout Formation.* PLoS One, 2013. **8**(3): p. e58897.
387. Liu, S.Q., Q. Tian, L. Wang, J.L. Hedrick, J.H.P. Hui, Y.Y. Yang, and P.L.R. Ee, *Injectable Biodegradable Poly(ethylene glycol)/RGD Peptide Hybrid Hydrogels for in vitro Chondrogenesis of Human Mesenchymal Stem Cells.* Macromolecular Rapid Communications, 2010. **31**(13): p. 1148-1154.
388. Yang, F., C.G. Williams, D.A. Wang, H. Lee, P.N. Manson, and J. Elisseeff, *The effect of incorporating RGD adhesive peptide in polyethylene glycol diacrylate hydrogel on osteogenesis of bone marrow stromal cells.* Biomaterials, 2005. **26**(30): p. 5991-5998.
389. Rekha, C., G. Poornima, M. Manasa, V. Abhipsa, J. Pavithra Devi, V.K.H. T., and P.K.T. R., *Ascorbic Acid, Total Phenol Content and Antioxidant Activity of Fresh Juices of Four Ripe and Unripe Citrus Fruits.* Chemical Science Transactions, 2012. **1**(2): p. 303 - 310.
390. Oh, C., M. Li, E.-H. Kim, J.S. Park, J.-C. Lee, and S.W. Ham, *ChemInform Abstract: Antioxidant and Radical Scavenging Activities of Ascorbic Acid Derivatives Conjugated with Organogermanium.* ChemInform, 2011. **42**(16): p. no-no.
391. Dash, R., S. Mukherjee, and S.C. Kundu, *Isolation, purification and characterization of silk protein sericin from cocoon peduncles of tropical tasar silkworm, Antheraea mylitta.* International Journal of Biological Macromolecules, 2006. **38**(3): p. 255-258.
392. Kutty, J.K. and K. Webb, *Vibration stimulates vocal mucosa-like matrix expression by hydrogel-encapsulated fibroblasts.* Journal of Tissue Engineering and Regenerative Medicine, 2010. **4**(1): p. 62-72.
393. Hunt, N.C., R.M. Shelton, and L. Grover, *An alginate hydrogel matrix for the localised delivery of a fibroblast/keratinocyte co-culture.* Biotechnology Journal, 2009. **4**(5): p. 730-737.
394. Hunt, N.C., A.M. Smith, U. Gbureck, R.M. Shelton, and L.M. Grover, *Encapsulation of fibroblasts causes accelerated alginate hydrogel degradation.* Acta Biomaterialia, 2010. **6**(9): p. 3649-3656.
395. Chen, M.W., M. Gupta, and K. Cheung, *Alginate-based microfluidic system for tumor spheroid formation and anticancer agent screening.* Biomedical Microdevices, 2010. **12**(4): p. 647-654.
396. Aubin, H., J.W. Nichol, C.B. Hutson, H. Bae, A.L. Sieminski, D.M. Cropek, P. Akhyari, and A. Khademhosseini, *Directed 3D cell alignment*

and elongation in microengineered hydrogels. Biomaterials, 2010. **31**(27): p. 6941-6951.

397. Bae, H., A.F. Ahari, H. Shin, J.W. Nichol, C.B. Hutson, M. Masaeli, S.H. Kim, H. Aubin, S. Yamanlar, and A. Khademhosseini, *Cell-laden microengineered pullulan methacrylate hydrogels promote cell proliferation and 3D cluster formation.* Soft Matter, 2011. **7**(5): p. 1903-1911.
398. Jeong, J.H., Y. Liang, M. Jang, C. Cha, C. Chu, H. Lee, W. Jung, J.W. Kim, S.A. Boppart, and H. Kong, *Stiffness-modulated water retention and neovascularization of dermal fibroblast-encapsulating collagen gel.* Tissue Eng Part A, 2013. **19**(11-12): p. 1275-84.
399. Peyton, S.R., P.D. Kim, C.M. Ghajar, D. Seliktar, and A.J. Putnam, *The effects of matrix stiffness and RhoA on the phenotypic plasticity of smooth muscle cells in a 3-D biosynthetic hydrogel system.* Biomaterials, 2008. **29**(17): p. 2597-2607.
400. Skiles, M.L., S. Sahai, and J.O. Blanchette, *Tracking Hypoxic Signaling within Encapsulated Cell Aggregates.* 2011(58): p. e3521.
401. Desimone, M.F., C. Helary, G. Mosser, M.-M. Giraud-Guille, J. Livage, and T. Coradin, *Fibroblast encapsulation in hybrid silica-collagen hydrogels.* Journal of Materials Chemistry, 2010. **20**(4): p. 666-668.
402. McDougall, S., J. Dallon, J. Sherratt, and P. Maini, *Fibroblast migration and collagen deposition during dermal wound healing: mathematical modelling and clinical implications.* Philosophical Transactions of the Royal Society A: Mathematical, Physical and Engineering Sciences, 2006. **364**(1843): p. 1385-1405.
403. Watt, F.M. and H. Fujiwara, *Cell-extracellular matrix interactions in normal and diseased skin.* Cold Spring Harb Perspect Biol, 2011. **3**(4).
404. Woodley, D.T., J.R. Stanley, M.J. Reese, and E.J. O'Keefe, *Human Dermal Fibroblasts Synthesize Laminin.* J Investig Dermatol, 1988. **90**(5): p. 679-683.
405. Eckes, B., R. Nischt, and T. Krieg, *Cell-matrix interactions in dermal repair and scarring.* Fibrogenesis Tissue Repair, 2010. **3**: p. 4.
406. Canal, T. and N.A. Peppas, *Correlation between mesh size and equilibrium degree of swelling of polymeric networks.* Journal of Biomedical Materials Research, 1989. **23**(10): p. 1183-1193.
407. Kwack, K., S. Won, Y.-Y. Cha, S.-J. Park, H.J. Kim, S.K. Lee, and H. Kang, *Effects of gelatin on proliferation of cord blood derived mesenchymal stem cells.* The FASEB Journal, 2008. **22**(1_MeetingAbstracts): p. 819.6.
408. Eckermann, C.W., K. Lehle, S.A. Schmid, D.N. Wheatley, and L.A. Kunz-Schughart, *Characterization and modulation of fibroblast/endothelial cell co-cultures for the in vitro preformation of three-dimensional tubular networks.* Cell Biol Int, 2011. **35**(11): p. 1097-110.
409. Hamilton, S.K., N.C. Bloodworth, C.S. Massad, T.M. Hammoudi, S. Suri, P.J. Yang, H. Lu, and J.S. Temenoff, *Development of 3D hydrogel culture systems with on-demand cell separation.* Biotechnology Journal, 2013. **8**(4): p. 485-495.
410. Tischer, E., R. Mitchell, T. Hartman, M. Silva, D. Gospodarowicz, J. Fiddes, and J. Abraham, *The human gene for vascular endothelial growth*

factor. Multiple protein forms are encoded through alternative exon splicing. Journal of Biological Chemistry, 1991. **266**(18): p. 11947-11954.

411. Abraham, J.A., J.L. Whang, A. Tumolo, A. Mergia, J. Friedman, D. Gospodarowicz, and J.C. Fiddes, *Human basic fibroblast growth factor: nucleotide sequence and genomic organization.* EMBO Journal, 1986. **5**(10): p. 2523-8.
412. Neufeld, G., T. Cohen, S. Gengrinovitch, and Z. Poltorak, *Vascular endothelial growth factor (VEGF) and its receptors.* FASEB Journal, 1999. **13**(1): p. 9-22.